Thesis presented to obtain the degree of

Docteur de l'Université Louis Pasteur

STRASBOURG I

&

Doktor der Naturwissenschaften

Der Albert-Ludwigs Universität

FREIBURG

NEUROSCIENCES

Effets *in vitro* et *in vivo* d'une application combinée de 3,4-methylènedioxymethamphetamine (MDMA, ecstasy) et d'éthanol : étude des auto- et hétérorécepteurs présynaptiques du sous-type 5-HT_{1B} et de leur surexpression par transfection virale de gène.

Effects of combined applications of ethanol and 3,4-methylenedioxymethamphetamine (MDMA, ecstasy) *in vitro* and *in vivo*: focus on presynaptic 5-HT_{1B} auto- and heteroreceptors and their possible overexpression using HSV-1-mediated gene transfer.

RIEGERT Céline

Defended in public on December 12th, 2007

Referees:

Dr CASSEL JC	LINC, Strasbourg	Thesis Director
Prof Dr FISCHBACH KF	Faculty of Biology, Freiburg	Thesis co-Director
Prof Dr JACKISCH R	Pharmacology, Freiburg	Thesis co-Director
Dr LARMET Y	ULP, Strasbourg	Internal referee
Dr MORMEDE P	INRA, Bordeaux	External referee
Prof Dr AKTORIES K	Pharmacology, Freiburg	External referee

A mes parents

A ma sœur, ma petite

Special thanks to…

I first would like to thank Dr. Larmet (Strasbourg) and Dr. Mormede (Bordeaux) as well as Prof. Dr. Fischbach (Freiburg) and Prof. Dr. Aktories (Freiburg) for accepting to be members of the jury of my thesis. My special thanks also to Prof. Dr. Fischbach for accepting to be my thesis director at the Faculty of Biology at the University of Freiburg.
I would like to thank the neuroscience association Neurex for their three years of financial support and interest in my work. This work was additionally funded by the European Doctoral College and the University of Freiburg.

I would also like to thank Prof. Will and Dr. Kelche as well as Prof. Starke and Prof. Hein for welcoming me in their lab, respectively, in Strasbourg and Freiburg. They offered me all the facilities necessary to realize this work.

My very special thanks go to Dr. Cassel, director of this project, for his engagement. His patience and comprehensiveness, strong experience and extremely accurate view on scientific research were indispensable for me during the last five years we worked together.

I don't forget the co-director of my project, Prof. Dr. Jackisch for our every-day collaboration in the lab. I am very grateful for his numerous advices and his will to share his long experience in the neuroscience research as well as for his great help in all aspects of my work.

I would like to acknowledge Prof. Neumaier and all his team for our collaboration on the 'virus project'.

I would also like to thank Dr. Leemhuis for his help on the confocal microscope. He allowed me to have beautiful pictures of neurons!

I also take the opportunity to thank all the co-workers from the 'anatomy lab' from Prof. Dr. Frotcher. Special thanks go to Ulrich, Imre, Margot, Shanting and Sandra who shared with me their "cell culture lab" and a lot of essential advices.

I would also like to thank all the persons of the group of Dr. Ort for offering a place in their lab for the microinjections of the viral vector.

A special thank goes to all the persons in the different animal houses for the care they gave to all the ‘small-cute-rats’…

I would also like to thank all my collaborators of the ex-LN2C in Strasbourg: Alexandra(s), Alex, Anne, Brigitte, Catherine, Chantal, Christophe, Ekatarina, Erwan, Hélène, Karin, Monique, Olivier, Patrick, Rodrigue, Sarah... I really enjoyed the time spent during my DEA and my PhD. I especially thank Sami Ben Hamida for his participation to the last experiment of this work, and the great time we had in Freiburg even during the very long “injections days”. My very special thank goes to Julie Koenig with whom I started my work. Our discussions always had positive issues in scientific or non-scientific life. Of course, the time in the lab wouldn’t have been the same without our laughing and relaxing moments…I wish you the very best for your future life, a lot of success in science and a lot of happiness in your personal life!

I don’t forget my "lab girls" from Freiburg, Anja, Sanni, Katha and Franzi. I really enjoyed our every-day life in the lab and all the moments spent there. The four years of my time in Freiburg wouldn’t have been the same without our discussions, jokes and ice creams!

Je tiens également à remercier mes amis, ceux qui, en dehors du laboratoire m’ont soutenu dans les moments difficiles et m’ont permis de garder un équilibre indispensable. Merci tout particulièrement à Julie & David, Oliv, Dricky, Cris, Lolotte, Pacal !

Je n’oublie pas mes parents, sans qui je ne serai pas là aujourd’hui. Leur soutien de tous les moments m’a été indispensable pour atteindre mon but. Je ne vous remercierai jamais assez de tout ce que vous avez fait pour moi ! Ma petite sœur également, Camille à qui je souhaite tout le courage nécessaire pour la fin de ses études !! Je te souhaite de trouver ta voie et d’être heureuse.
Antoine, ton soutien quotidien, ta patience, ta motivation aussi, m’ont sans aucun doute permis d’achever ce travail. J’ai hâte de vivre "la vraie vie", celle qui nous attend, avec toi !

European Doctoral College:

« Melle RIEGERT Céline a été membre de la promotion Copernic du Collège Doctoral Européen des universités de Strasbourg pendant la préparation de sa thèse de 2003 à 2007. Elle a bénéficié des aides spécifiques du CDE et a suivi un enseignement hebdomadaire sur les affaires européennes dispensé par des spécialistes internationaux.
Ses travaux de recherche ont été effectués dans le cadre d'une convention de cotutelle avec l'université Albert Ludwigs de Freiburg (Allemagne) et l'Université Louis Pasteur de Strasbourg (France) ».

« Ms RIEGERT Céline was a member of the European Doctoral College of the Universities of Strasbourg during the preparation of her PhD, from 2003 to 2007, class name Copernic. She has benefited from specific financial supports offered by the College and, along with her mainstream research, has followed a special course on topics of general European interests presented by international experts. This PhD research project has been led with the collaboration of two universities: the University Albert Ludwigs of Freiburg (Germany) and the Louis Pasteur University in Strasbourg (France). »

List of publications:

Riegert C., Wedekind F., Ben Hamida S., Rutz S., Rothmaier AK., Cassel JC. and Jackisch R. 2007. Effects of Ethanol and 3,4-methylenedioxymethamphetamine (MDMA) alone or in combination on spontaneous and evoked overflow of dopamine, serotonin and acetylcholine in striatal slices of the rat. *International Journal of Neuropsychopharmacology (in press).*

Riegert C., Rothmaier AK., Leemhuis J., Sexton T., Neumaier JF, Cassel JC. and Jackisch R. 2007. Increased expression of 5-HT_{1B} receptor by Herpes simplex virus gene transfer in septal neurons: new *in vitro* and *in vivo* models to study 5-HT_{1B} receptor function. *Brain Research Bulletin (in press).*

Rutz S., **Riegert C.**, Rothmaier AK. and Jackisch R. 2007. Presynaptic modulation of 5-HT release in the rat septal region. *Neuroscience*. 146: 643-658.

Ehret A., Birthelmer A., Rutz S., **Riegert C.**, Rothmaier AK. and Jackisch R. 2007. Agonist-mediated regulation of presynaptic receptor function during development of rat septal neurons in culture. *J. Neurochem*. 102(4): 1071-1082.

Birthelmer A., Ehret A., **Riegert C.**, Rothmaier AK., Leemhuis J. and Jackisch R. 2007. Modulation of electrically-evoked serotonin release in cultured rat raphe neurons. *J. Neurochem*. 100(6): 1613-1625.

Rutz S., **Riegert C.**, Rothmaier AK., Buhot MC., Cassel JC. and Jackisch R. 2006. Presynaptic serotonergic modulation of 5-HT and acetylcholine release in the hippocampus and the cortex of 5-HT_{1B}-receptor knock-out mice. *Brain Res Bull*. 70: 81-93.

Cassel JC., **Riegert C.**, Rutz S., Koenig J., Rothmaier AK., Cosquer B., Lazarus C., Birthelmer A., Jeltsch H., Jones BC. and Jackisch R. 2005. Ethanol, 3,4-methylenedioxymethamphetamine (Ecstasy) and their combination: long-term behavioural, neurochemical and neuropharmacological effects in the rats. *Neuropsychopharmacology*. 30: 1870-1882.

Riegert C., Galani R., Heilig S., Lazarus C., Cosquer B., Cassel JC. 2004. Electrolytic lesions of the ventral subiculum weakly alter spatial memory but potentiate amphetamine-induced locomotion. *Behav Brain Res*. 152: 23-34.

Birthelmer A., Lazaris A., **Riegert C.**, Marques Pereira P., Koenig J., Jeltsch H., Jackisch R., Cassel JC. 2003. Does the release of acetylcholine in septal slices originate from intrinsic cholinergic neurons bearing $p75^{NTR}$ receptors ? A study using 192 IgG-saporin lesions in rats. *Neuroscience*. 122 (4): 1059-1071.

Poster presentations:

5th Forum of European Neuroscience In Vienna (Austria), July 8-12, 2006, Overexpression of $5\text{-}HT_{1B}$ receptor in septal neurons *in vivo* and *in vitro* using Herpes simplex virus gene transfer and its effect on the modulation of neurotransmitter release. **Riegert C.**, Rothmaier AK., Sexton T., Leemhuis J., Neumaier J., Jackisch R. and Cassel JC.FENS Abstr. Vol 3, A009.10, 2006.

Frühjahrstagung der DGPT, Mainz (Germany), April 4-6, 2006, Presynaptic modulation of 5-HT release in the septal nuclei of the rat brain. Rutz S., Rothmaier AK., **Riegert C.**, Jackisch R. Naunyn-Schmiedeberg's Arch. Pharmacol. 372, suppl 1, p78 [2006].

Frühjahrstagung der DGPT, Mainz (Germany), March 15-17, 2005, Ethanol, 3,4-methylenedioxymethamphetamine (MDMA, ecstasy) and their combination: long-term behavioural, neurochemical and neuropharmacological effects in the rat. Cassel JC., **Riegert C.**, Rutz S., Koenig J., Rothmaier K., Cosquer B., Lazarus C., Birthelmer A., Jeltsch H., Jones BC., Jackisch R. Naunyn-Schmiedeberg's Arch. Pharmacol. 371, suppl 1, p75 [2005].

Abbreviations:

[^{3}H]	Tritium
5-HT	5-hydroxytryptamine, Serotonin
5-HT$_{1B}$	Serotonergic receptor type 1B
5-HIAA	5-hydroxyindole acetic acid
ACh	Acetylcholine
ANOVA	Analyse of variance
ChAT	Cholinacetyltranferase
CNS	Central nervous system
DA	Dopamin
DB or DBB	Diagonal band or diagonal band of Broca
DIV	Days *in vitro*
DMEM	Dulbecco's modified Eagle's medium
FR	Fractional rate
GABA	γ-amino-butiric acid
GAD	Glutamate decarboxylase
GFAP	Glial fibrillary acidic protein
GFP	Green fluorescent protein
HSV-1	Herpes simplex virus type 1
KH-buffer	Kreb's Henseleit buffer
MDMA	3,4-methylenedioxymethamphetamine
min	minute
MS	Medial septum
n	number of slices or cell cultures
N	number of rats
NDS	Normal donkey serum
NGS	Normal goat serum
PB	Phosphate buffer
PBS	Phosphate buffer saline
PFA	Paraformaldehyde
SEM	standard error of the mean
SERT	serotonin transporter

Table of contents:

1. INTRODUCTION

1.1. OUTLINE OF THE THESIS

Since many years, the serotonin 1B (5-HT_{1B}) receptor has been widely studied as it may be implicated in various physiological processes, but also in more complex behaviours. For instance, the 5-HT_{1B} receptor plays a modulatory role not only in the regulation of the release of serotonin (5-HT) itself but also in that of other transmitters, as it was shown that, for example, also cholinergic, GABAergic or glutamatergic neurons express this receptor. On a more integrated point of view, the 5-HT_{1B} receptor has been involved in behavioural sensitisation to cocaine, depression, and anxiety as well as in learning and memory, particularly in spatial memory. The main topic of this work (**Part 1**) was to characterize – for the first time – a gene transfer technique to study the role of the 5-HT_{1B} receptor in the modulation of the release of ACh in the rat hippocampus. This technique has already been successful in studies on depression and anxiety.

On the other hand, the serotonergic system has also been implicated in the effects of drugs such as, for instance 3,4-methylenedioxymethamphetamine (MDMA or ecstasy). In particular, the 5-HT_{1B} receptor has been shown to mediate some of the effects of this drug, especially as regards locomotor activity. As the recreational use of MDMA is largely increasing and as its combination with other drugs of abuse (for instance ethanol [EtOH]) is frequent, it was also our aim in this study to further characterize some aspects of the actions of MDMA and its combination with EtOH in the brain both after long-term pre-treatment with these drugs *in vivo* (**Part 2**) or after acute application to brain slices *in vitro* (**Part 3**). Finally, as the first part of this work provided convincing data on the possibility to increase the expression of the 5-HT_{1B} receptor in selected brain areas by virally-mediated gene, we used this technique in the raphé region of the rat brain to study the possible role of the 5-HT_{1B} autoreceptor in the well-known locomotor effects induced by MDMA alone or in combination with EtOH (**Part 4**).

The next sections will expose in detail all informations necessary to understand the methods used and results obtained throughout this work.

1.2. ANATOMICAL STRUCTURES OF INTEREST AND RELATED NEUROTRANSMITTER SYSTEMS

As regards our topics of interest, the next paragraphs will focus on the anatomy of the medial septal region, the raphé region, the striatum and the hippocampus in the rat. In

connections with these structures, overview of respectively, the cholinergic, serotonergic and dopaminergic systems will be added.

1.2.1. The medial septal region and cholinergic system

When the medial interventricular wall of the telencephalon was first studied in the early 20th century, it was given the name “septum” because of the Latin translation for “wall”. It was rather quickly shown that this structure, which is part of the cerebral nuclei (sub-cortical nature), was bi-directionally connected with the hippocampus. In a morphofunctional context, the septal region has been attached to the limbic system and is involved in a variety of physiological and behavioural processes related to higher cognitive functions (e.g., learning and memory), emotions, fear, aggression and stress, as well as autonomic regulation (e.g., water/food intake, fever, hibernation, osmoregulation and humoral immune responses).

In a larger view, the septal region belongs to the basal forebrain (BF), which comprises a complex of cholinergic nuclei. The classically defined nuclei belonging to the BF include, in a rostral to caudal order, the medial septum, the vertical and horizontal limbs of the diagonal band of Broca, the ventral pallidum, the magnocellular preoptic area, the substantia innominata and the magnocellular basal nucleus [groups Ch1-Ch4, according to (Mesulam et al., 1983).

Based on their anatomical location within the septal region, four groups of nuclei were described (Risold, 2004). The lateral septal, the septofimbrial and the septohippocampal nuclei form the *lateral group*. The medial septal complex (MSDB complex) or *medial group* is composed of the medial septal nucleus and the nucleus of the diagonal band (DB also known as diagonal band of Broca or DBB). The nucleus of the diagonal band can be further subdivided into a (dorsal) vertical limb (VDB) and a (ventral) horizontal limb (HDB). Hereafter, the medial septal nucleus will be abbreviated medial septum or MS. The *posterior group* is made of the triangular nucleus and the bed nuclei of the anterior commissure and of the stria medullaris. Finally, the bed nuclei of the stria terminalis (BST) form the *ventral group*. In view of **Part 1** of the present work, only the medial group will be further described. Figure1 shows the localization of the MSDB complex at a level of 0.7 mm anterior to Bregma (Paxinos and Watson, 1998). Some nuclei, situated more caudally, do not appear on this drawing.

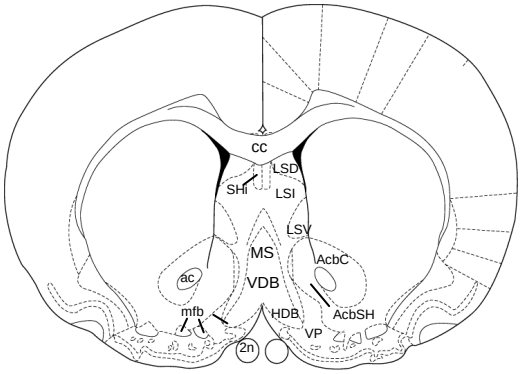

Figure1. Drawing of a frontal section through the MS and DB (MSDB complex) at a level of 0.7 mm anterior to Bregma. Abbreviations are as follows: 2n: optic nerve; ac: anterior commissure; AcbC: accumbens nucleus core; AcbSH: accumbens nucleus shell; cc: corpus callosum; HDB: horizontal limb of the diagonal band; LSD: lateral septal nucleus; LSI: lateral septal nucleus, intermediate part; LSV: lateral septal nucleus, ventral part; mfb: medial forebrain bundle; MS: medial septum; Shi: septohippocampal nucleus; VDB: vertical limb of the diagonal band; VP: ventral pallidum. Adapted from (Jakab and Leranth, 1995).

Cytoarchitecture of the MSDB complex

The MSDB region contains the largest neurons of the septum of which five types may be differentiated. As early suggested (Lewis and Shute, 1967) using acetylcholinesterase as a marker, the best known neuronal type of the MSDB complex is composed of cholinergic neurons. They were definitively identified in the early 80's especially thanks to new antibodies against choline acetyltransferase (ChAT), a specific marker for the cholinergic neurons (Wainer and Rye, 1984). Due to its chronotopic development, the septum has a laminar organization and the majority of the ChAT-positive neurons are present in the lateral zone of the MS although some scattered ChAT-positive neurons are intermingled with GABAergic neurons in the midline MS region. It was shown that two types of cholinergic neurons could be found in the MSDB. The first type displays relatively large, ovoid or round cellular bodies (20-30 µm), containing a small nucleus and an abundant amount of cytoplasm. The second type, also ovoid or round, displays medium-sized somata (15-20 µm), containing a rather large nucleus and a small amount of cytoplasm. This transmitter is sometimes associated to others like glutamate, nitric oxyde or neuropeptides such as, for instance, galanin (Semba, 2000).

The second important group of MSDB neurons is formed by GABAergic neurons (Gritti et al., 1993). Most of the studies performed to identify these neurons used immunohistochemistry for GABA or glutamic acid decarboxylase (GAD). These studies have shown that GABAergic neurons are large and multipolar, particularly in the MS and DB. However, they do not form a homogeneous population, as some of them that

are smaller, seem to be local interneurons while others project to the cortex or the hippocampus. It was also reported that GABAergic neurons of the MS express peptides and/or other proteins, such as calcium-binding proteins or trophic factors, revealing another aspect of neurochemical heterogeneity. Indeed, in the rat MS and DB, 34% of neurons have been shown to be parvalbumin (PARV)-positive (Kiss et al., 1990). While it was considered that PARV was a good marker for GABAergic neurons (Freund, 1989), more recent studies showed that the colocalization between GABAergic and PARV-positive neurons is not perfect (Brauer et al., 1991): in fact, all PARV-positive neurons are GABAergic but not all GABAergic neurons are PARV-positive. Neurons expressing NGF- (nerve growth factor) mRNA are also present in the rat basal forebrain and all of them are GABAergic (Lauterborn et al., 1995). Despite the co-distribution of ChAT- and GAD-immunoreactive neurons, the co-expression of these two markers in single BF neurons has been shown to be either absent or rather infrequent (Gritti et al., 1993).

Finally, the MSDB complex also contains GnRH (gonadotropin-releasing hormone, also known as LHRH or luteinizing hormone releasing hormone) neurons. In mammals, GnRH is involved in the regulation of luteinizing hormone and follicule stimulation hormone secretion and probably in the facilitation of reproductive behaviour. It was shown that the GnRH neurons are more scattered through the region (Hiatt et al., 1992).

In addition to these three main groups, some neuropeptide and calcium-binding protein containing neurons were also found in the MSDB complex. As regards neuropeptides (Gall and Moore, 1984; Köhler and Eriksson, 1984), the MS-LS border zone contains thin bands of neurons positive for substance P and neurotensin. The ventrolateral portion of the HDB harbors some somatostatin-positive neurons. Moreover, the MSDB region contains a small number of neurons immunopositive for Met-enkephalin, calcitonin-gene-related peptide (CGRP), dynorphin B, vasoactive intestinal peptide (VIP), cholecystokinin (CCK), neuropeptide Y (Senut et al., 1989) and δ-sleep inducing peptide (Vallet et al., 1990). Three types of calcium-binding proteins, parvalbumine, calbindin D28k and calretinin, were found in the MS. Calbindin D-28k has been shown to be expressed by non-cholinergic and non-GABAergic neurons (Geula et al., 1993; Smith et al., 1994). This small population is located in the MS-LS border zone; more medially located MS areas and DB regions contain only a few scattered calbindin D-28k-positive neurons. The calretinin-positive neurons were also found in the MS-LS border zone. These neurons are multipolar.

Connections of the MSDB complex

Connections of the medial septal complex are characterized by massive telencephalic outputs as well as bi-directional connections with the brainstem as shown by a number of retrograde and anterograde tracing studies.

Efferents of the MSDB complex

Ascending efferents from the medial septal complex innervate primarily the cortex and the hippocampal formation. These efferents reach many neocortical areas and are mainly of a cholinergic nature even if it is today widely accepted that a large part of GABAergic as well as neuropeptidergic (especially galanin containing) neurons also send their axons to cortical areas (Semba, 2000). Thus, corticopetal projections, intensively investigated using the anterograde tracer *Phaseolus vulgaris* leucoagglutinin (PHA-L), innervate all fields of the entorhinal, pyriform, infralimbic, cingulate, medial prefrontal, olfactory, and insular areas, as well as, to a lesser extent, occipital, somatosensory and orbital areas of the cerebral cortex (Gaykema et al., 1990). The interesting question, in view of the function of neuronal networks, is that of the postsynaptic target neurons of the BF in the cortex. It is suggested that cholinergic afferents target pyramidal cells as well as both excitatory and inhibitory interneurons. On the contrary, the main targets of GABAergic projections from the BF seem to be GABAergic interneurons [for a detailed review, see (Semba, 2000)].

Fibers of the septohippocampal pathway originate in the MS and vertical limb of the DB and remain mainly on the ipsilateral side. They reach the hippocampus via three known routes. The large majority of septohippocampal fibers travel through the fimbria-fornix. The second route involves DB efferents that course over the corpus callosum to form the cingular bundle (Swanson and Cowan, 1979). Finally, the third route, that seems to represent 10% of these cholinergic fibers, arises primarily in the DB and follows a ventral path (Gage et al., 1983). The topographical organization of these fibers has been clearly demonstrated. Indeed, it was shown that lateral cells in the MS mostly send their axons in ventral (temporal) hippocampal fields, while medial neurons project in the dorsal (septal) hippocampus (Gaykema et al., 1990). Acetylcholine is a major neurotransmitter in this pathway (Mesulam et al., 1983) but many medial septal complex cells projecting to the cortex are GABAergic (Semba, 2000). Retrograde tracing studies combined to immunohistochemistry showed that 35-45% (Rye et al., 1984) or 23-77% (Amaral and Kurz, 1985) of the septohippocampal fibers are cholinergic. Using PARV as a marker of GABAergic neurons, it was also shown that approximately 30% of these fibers use GABA as a transmitter (Köhler et al., 1984).

Several peptides are also involved, such as galanin (Melander et al., 1985), substance P, enkephalin and neurotensin (Semba, 2000) as well as possibly glutamate. The types of postsynaptic target neurons of the septohippocampal pathway are similar to those in the neocortex. Indeed, cholinergic projections end on principal neurons, i.e. pyramidal (glutamatergic) neurons in the hippocampus and on granule cells in the dentate gyrus (Frotscher and Leranth, 1985), as well as on interneurons (especially GABAergic interneurons containing neuropeptide Y). The same scheme is found for the GABAergic projections that end primarily on GABAergic basket interneurons (Freund and Antal, 1988).

Descending efferents of the medial septal complex travel through the ventral medial forebrain bundle to reach the brainstem (Semba et al., 1989) and seem to be largely non-cholinergic. Some of them arch dorsally and innervate several nuclei of the thalamus and hypothalamus. Moreover, some projections were found to reach the amygdala and olfactory bulb. These descending projections have cholinergic, GABAergic but also non-cholinergic and non-GABAergic components. Today, these projections are considered as important as the ascending ones to account for the functions associated with the medial septal complex. For a summary of the efferents of the MS, see Figure 2.

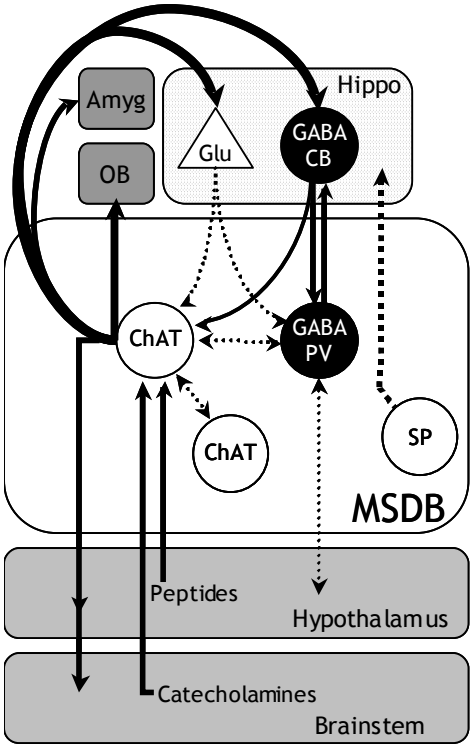

Figure 2. Simplified diagram of the bi-directional connections of neurochemically identified neurons of the medial septum (MS) with other brain regions, in particular, telencephalic, hypothalamic and brain stem areas. Dashed lines represent putative connections (based on indirect evidence). Structures involved primarily in cognitive functions, like the hippocampus, are shown with light gray shading. Medium gray shading indicates structures principally involved in autonomic and behavioural state control functions (hypothalamus, brainstem). Finally, the darker gray shading shows structures mainly involved in motivational and emotional processes (amygdala, olfactory bulb). With, Amyg: amygdala; CB: Calbindin D-28k; ChAT: cholineacetyltransferase; GABA: γ-aminobutyric acid; Glu: glutamate; MSDB: medial septum / diagonal band complex; OB: olfactory bulb; PV: parvalbumine; SP: substance P. Adapted from (Jakab and Leranth, 1995) and (Semba, 2000).

Afferents of the medial septal complex

Firstly, the medial septal complex receives **ascending projections** from the brainstem that travel through the medial forebrain bundle. These projections originate in the hypothalamus (Cullinan and Zaborszky, 1991), the interpedoncular nucleus, the ventral tegmental area, the laterodorsal tegmental nucleus and the locus coeruleus (Vertes, 1988). Of special interest for the present thesis is also an important serotonergic input originating from the raphé nuclei. Finally, the MS receives spinal axons that were demonstrated to originate in the deep dorsal horn and lateral reticulated area. In addition, the lateral spinal nucleus and the area around the central canal were also shown to contain some of the septal projection neurons. A small percentage of the neurons were also located in the superficial dorsal horn, the intermediate zone and the ventral horn. All levels of the spinal cord contribute to the spino-septal projections that may be involved in affective responses to somatosensory stimulation (Dutar et al., 1985).

Descending projections to the medial septal complex originate mainly in the hippocampus (Gaykema et al., 1991). For instance, Alonso and Köhler have demonstrated that the MS is mostly innervated by nonpyramidal cells in stratum oriens of the CA1-CA3 region (Alonso and Kohler, 1982). This projection exhibits both excitatory and inhibitory (apparently mediated via GABA) activities (Schwerdtfeger and Buhl, 1986) and innervate both PARV-containing and cholinergic septohippocampal neurons with a clear preference for the PARV-positive neurons. Together with the ascending efferents of the MSDB discussed above, these findings provide evidence for the existence of a septo-hippocampo-septal loop. Projections from other cortical areas such as the entorhinal and prefrontal cortex also reach the medial septal complex (Alonso and Kohler, 1984). PHA-L-labeled fibers of infralimbic and prelimbic cortical origin were also shown to form contacts with ChAT-positive neurons in the MS (Luiten et al., 1988). Projections originating in the lateral group were also shown to reach the medial septal complex. In the late 70s, the first experiments, using anterograde

transport of ^{3}H-labeled amino acids, concluded that dense projections from the lateral septal nucleus ended in the medial septal complex (Swanson and Cowan, 1979). Later, this view was minimized by other experiments using multiple injections of PHA-L in the lateral group, and showed topographically organized outputs in the medial septal complex (Risold and Swanson, 1997).

The cholinergic system

Synthesis and degradation of acetylcholine

Acetylcholine (ACh) is synthesized in the cytoplasm of cholinergic nerve endings from acetyl-CoA and choline. The reaction is catalyzed by the cytoplasmic and highly specific cholinergic enzyme, choline acetyltransferase (ChAT). ACh is then pumped into the vesicles by the vesicular ACh transporter (VAT), which is also specific for cholinerghic neurons (Figure 3). As choline cannot be produced in the neurons, it has to be taken up from the extracellular space. To achieve this, cholinergic neurons are equipped on their membranes with a high-affinity presynaptic choline transporter ("carrier"). After its release, ACh, in the extracellular compartment, is quickly hydrolyzed to choline and acetate by the specific acetylcholinesterase (AChE) and choline is avidly taken up again in the nerve ending. It is this presynaptic uptake of choline that is the main regulator of ACh synthesis. AChE is one the quickest and most efficient enzymes known in biology, as one molecule of AChE can hydrolyse 10.000 molecules of ACh per second.

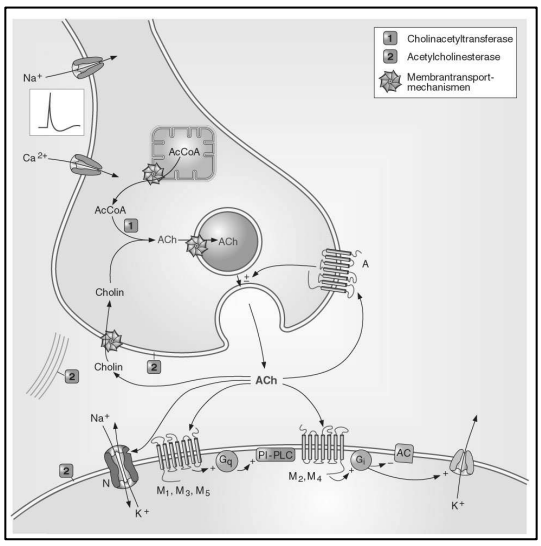

Figure 3. Simplified scheme of the cholinergic neurotransmission. A: presynaptic autoreceptor; AC: adenylyl cyclase; AcCoA: acetyl-coenzyme A; ACh: acetylcholine; M: Muscarinic receptors; N: nicotinic receptor; PI-PLC: phospholipase C (phosphatidylinositol specific). From (Starke, 2005)

Cholinergic receptors

Following exocytosis, ACh can bind to two classes of receptors: **(1)** Muscarinic ACh receptors, which include 5 subtypes [M_1 - M_5 (Bonner et al., 1987)] that are all G-protein-coupled receptors (metabotropic). As shown in Figure 3, M_1, M_3 and M_5 receptors are coupled to G_q proteins therefore stimulating phospholipase C (PLC), resulting in the production of inositol triphosphate (IP_3) and diacylglycerol (DAG) as second messengers. Conversely, the inhibitory M_2 and M_4 types are coupled to G_i protein. These receptors either reduce the formation of the second messenger cAMP by inhibition of adenylate cyclase, or hyperpolarize the postsynaptic cell by opening K^+ channels, or reduce the availability of cytoplasmic Ca^{2+} by closure of Ca^{2+} channels. **(2)** Nicotinic ACh receptors are either of the muscular (mAChR) or the neuronal (nAChR) type. Both belong to the class of ligand-gated ion channels (ionotropic receptors). After activation, their ion channels open and allow the influx of sodium (Na^+) and Ca^{2+}, which leads to a depolarisation of the cell.

In addition to these postsynaptic receptors, it is known that hippocampal cholinergic transmission is also under the control of presynaptic autoreceptors that regulate the release of ACh. After numerous contradictory results obtained in the last two decades, it appears that ACh release is controlled by M_2 and/or M_4 receptors (Vizi and Kiss, 1998). It has also been suggested that the release of ACh is under a facilitatory control of presynaptic nAChRs (Wilkie et al., 1996; Wonnacott, 1997). Moreover, nAChR (as heteroreceptors) have been implicated in the presynaptic control of several other neurotransmitters as for instance, GABA, Glycine, DA, noradrenaline, glutamate of 5-HT (McGehee and Role, 1996).

1.2.2. The raphé nuclei and the serotonergic system

It has been shown that the serotonergic system is one of the most widespread transmitter systems in the CNS, thus influencing almost every part of mammalian physiology, such as cardiovascular regulation, respiration, the gastrointestinal system, pain sensitivity and thermoregulation. Serotonin (5-hydroxytryptamine, 5-HT) is also involved in more centrally controlled functions such as the maintenance of circadian rhythm, appetite, aggression, sensorimotor activity, sexual behaviour, mood, cognition or learning and memory. In addition, personality dysfunctions like addictive behaviours, aggression, psychopathic and sociopathic behaviour, attention-deficit hyperactivity and autism are also associated with altered serotonergic transmission (Sari, 2004). Finally,

accumulating evidence suggests a role for 5-HT in synaptic plasticity and brain development (Sodhi and Sanders-Bush, 2004).

The neurons that produce 5-HT are located in a restricted zone of the brainstem. Most are found in the raphé nuclei, on the midline of the rhombencephalon, with a smaller number in the reticular formation. The 5-HT-containing neurons are known as the B1-B9 cell groups and they cluster as two main groups: the caudal division (B1-B5, corresponding to the raphé pallidus, magnus, obscursus and pontis), and the rostral division (B6-B9, corresponding to the dorsal and median raphé nuclei). Serotonergic neurons originating mainly in the dorsal and median raphé nuclei send their axons through the entire brain and even spinal cord. It was shown that dorsal raphé nucleus (DRN) projects fibers mainly in the frontal cortex, substantia nigra, dorsal striatum, globus pallidus. Conversely, the median raphé nucleus (MRN) provides 5-HT fibers mainly to the septal nuclei and dorsal hippocampus, the ventral hippocampus receiving a mixed DRN/MRN innervation (Conrad et al., 1974; Jacobs and Azmitia, 1992; McQuade and Sharp, 1997). The total number of serotonergic neurons is small – around 20,000 neurons in the rat – but they provide a relatively dense innervation to all brain areas and spinal cord by way of an extensive and diffuse collateralization of their axons.

Synthesis and degradation of serotonin

The precursor of 5-HT is the essential amino acid tryptophan that is transported into neurons. First, tryptophan is hydroxylated to 5-hydroxytryptophan (5-HTP) by the cytoplasmic enzyme, tryptophan hydroxylase. 5-HTP is then decarboxylated by an L-amino acid-decarboxylase to form 5-HT, which is subsequently stored into the vesicles using a specific carrier-mediated transport. To inactivate serotonergic transmission in the synaptic cleft, the released 5-HT is transported back into the presynaptic neurons with specific reuptake carriers in the membrane of serotonergic nerve endings. 5-HT is then either transported back into the vesicles (“recycling”) or metabolized by monoamine oxidase (MAO-A or MAO-B) and aldehyde dehydrogenase to 5-hydroxyindole acetic acid (5-HIAA), which is finally excreted in urine (Figure 4).

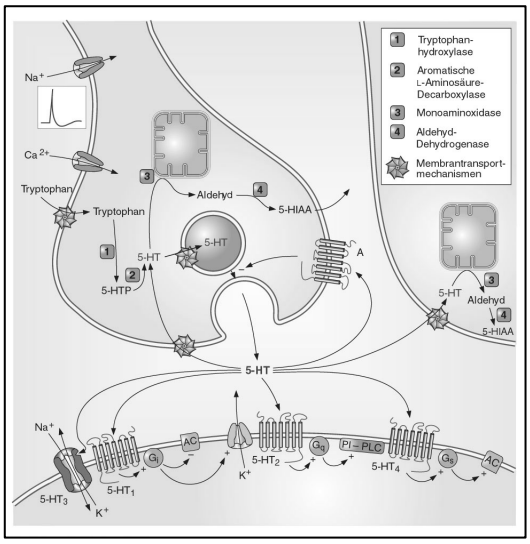

Figure 4. Simplified scheme of the serotonergic neurotransmission. A: presynaptic autoreceptor; AC: adenylyl cyclase; 5-HT: 5-hydroxytryptamine, serotonin; 5-HTP: 5-hydroxytryptophan; 5-HIAA: 5-hydroxindol acetic acid; PI-PLC: phospholipase C (phosphatidylinositol specific). From (Starke, 2005)

Serotonergic receptors

Serotonin receptors constitute a large family of several subtypes acting via different signal transduction cascades. Seven families (5-HT_1-5-HT_7) were defined depending on the pharmacological profiles, cDNA primary sequences and coupling mechanisms (Hoyer et al., 1994). Except for the 5-HT_3 receptor, that is a ligand-gated ion channel, all other subtypes belong to the superfamily of G-protein-coupled receptors containing a seven-transmembrane domain structure. The 5-HT_3 receptor opens cationic channels (Na^+/Ca^{2+} influx; K^+ efflux). The 5-HT_1 family (5-HT_{1A}, 5-HT_{1B}, 5-HT_{1D}, 5-HT_{1E} and 5-HT_{1F} subtypes) has been shown to be negatively coupled to adenylate cyclase ($G_{i/o}$ proteins) thus inhibiting the production of the second messenger cAMP. All subtypes of the 5-HT_2 family (5-HT_{2A}, 5-HT_{2B} and 5-HT_{2C}), act via $G_{q/11}$ proteins and thus are positively coupled to phospholipase C. Their activation leads to increased accumulation of IP_3 and intracellular Ca^{2+}. The 5-HT_4, 5-HT_6 and 5-HT_7 subtypes are coupled to G_s proteins and hence activate the cAMP synthesis. As regards the 5-HT_5 subtype (5-HT_{5A} and 5-HT_{5B}), their location (5-HT_{5A} could be expressed predominantly in astrocytes) and pharmacology remain uncertain. All subtypes are summarized in Table 1 and are extensively detailed in the review from (Barnes and Sharp, 1999).

Current classification of Serotonin Receptors

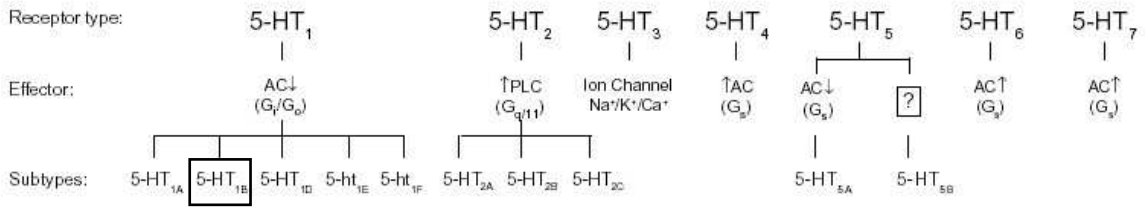

Table 1. Overview of the different types and subtypes of serotonergic receptors and their effectors. The receptor of primary interest for the present thesis, the 5-HT_{1B} is highlighted by a red box.

1.2.3. The striatum and dopaminergic system

Localisation and connections of the striatum

The caudate nucleus and the putamen, separated by the capsula interna, form a functional unit known as the striatum. The striatum is the main input structure of the basal ganglia, which also comprise the globus pallidus (external and internal parts), the subthalamic nucleus and the substantia nigra. This so-called “extrapyramidal” system, which connects the cortex via the thalamus back to the cortex, is mainly responsible for the regulation of motor responses, particularly via modulation of the “pyramidal” motor impulses. Moreover, in view of its complex interactions with the cortex, the striatum was suggested to be involved in special types of learning and cognitive integrations. Finally, the nucleus accumbens is thought to link the basal ganglia with the limbic system, thus functioning as a linkage of motor system with emotional aspects. Both the motor functions of the striatum, but also its possible role in cognitive and emotional processes are in the present thesis of special interest for the *in vivo* effects of MDMA.

Despite several distinct cell types constituting the striatum, more than 90% of them are the so-called GABAergic medium spiny projection neurons, which may also release different co-transmitters (substance P, dynorphin or enkephalin acting as release modulators). The remaining cells are local inhibitory interneurons such as the large aspiny cholinergic and the medium aspiny GABAergic neurons.

The main afference of the striatum, the corticostriatal connection, is composed of axons arising from virtually all cortical regions, but preferentially from the motor, sensory and prefrontal associative areas. These afferents, originating from pyramidal neurons of the cortical lamina V are excitatory and release glutamate as a neurotransmitter. Another afference of the striatum originates in the substantia nigra pars compacta and is well-known as the “nigrostriatal pathway”. Composed of

dopaminergic fibers, this pathway either inhibits or stimulates GABAergic neurons of the striatum via dopamine D_2 or D_1 receptors, respectively (as well as indirectly via D_2 receptors on cholinergic interneurons). Finally, the third main afference of the striatum originates in the posterior ventro-lateral nucleus of the thalamus and is also glutamatergic.

The striatum sends inhibitory GABAergic efferents to the substantia nigra (pars reticulata and pars compacta), but the main target region is the globus pallidus, pars external (Gpe) and internal (Gpi). The Gpi is considered as the output structure of the basal ganglia and sends inhibitory GABAergic fibers to the anterior ventro-lateral nucleus of the thalamus, which in turn stimulates the motor areas of the cortex. This way is considered as the “direct loop” of the basal ganglia. The “indirect loop” travels through the subthalamic nucleus (which is inhibited by the GPe) that in turn, sends excitatory axons to the Gpi. Again, the Gpi sends its GABAergic fibers to the anterior ventro-lateral nucleus of the thalamus. The thalamus itself serves as a sort of “filter” which, depending on the physiological or pathophysiological (e.g. Parkinson or Huntington disease) state of the basal ganglia, acts more or less excitatory to the pyramidal motor neurons in the cortex.

The dopaminergic system

First thought to be only a precursor for adrenaline and noradrenaline, DA was shown in 1957 to act as a neurotransmitter. Besides the occurrence of DA in the amacrine cells of the retina, four important systems in the CNS use DA as transmitter:

(1) The *nigrostriatal pathway* connects the substantia nigra (pars compacta) to the striatum (caudate-putamen). The DA released in the striatum inhibits cholinergic interneurons and affects the function of striatal GABAergic output neurons (see above). Degeneration of this pathway with subsequent loss of dopaminergic control in the striatum leads to the symptoms of Parkinsos’s disease;

(2) The *mesolimbic pathway*, originating in the ventral tegmental area (VTA) and terminating in the nucleus accumbens links the midbrain to the limbic system. It was shown that this pathway is activated during pleasurable feelings (“reward system”), playing a major role in the effects of addictive drugs such as ethanol, nicotine and amphetamines (like MDMA);

(3) The *mesocortical DA pathway* also originates in the VTA but ends in the prefrontal cortex (PFC) where it regulates complex cognitive processes such as selective attention and working memory;

(4) The *tubero-infundibular pathway* originating in the hypothalamus, controls via dopaminergic fibers the release of the hormone prolactin in the anterior pituitary.

In the first step of DA synthesis, axoplasmatic tyrosine hydroxylase hydroxylates the amino acid tyrosine to 3,4-dihydroxyphenylalanine (DOPA). DOPA is then decarboxylated by the axoplasmatic DOPA decarboxylase to DA, which is then packaged via a reserpine-sensitive carrier into release vesicles (Figure 5).

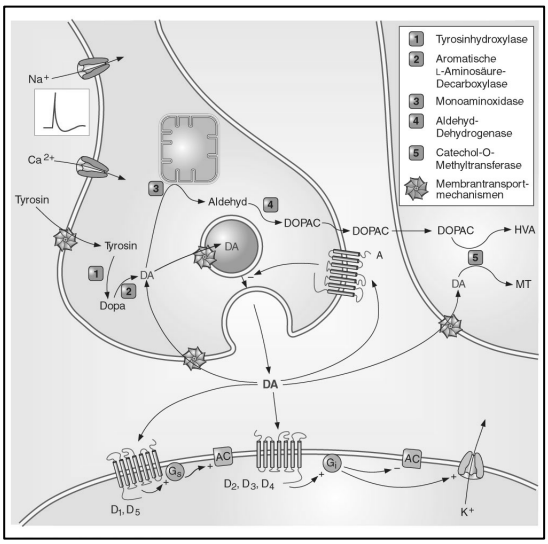

Figure 5. Simplified scheme of the dopaminergic neurotransmission. A: presynaptic autoreceptor; AC: adenylyl cyclase; D: DA receptors; DA: Dopamine; Dopa: 3,4-dihydroxyphenylalanine; DOPAC: 3,4-dihydroxyphenylacetic acid; HVA: Homovanillic acid; MT: Methoxythyramine. From (Starke, 2005)

Following release, DA may bind to five different receptors, namely D_1 - D_5. Activation of the metabotropic receptors D_1 or D_5 stimulates adenylate cyclase via a G_s protein. Subsequently, adenylate cyclase catalyses the conversion of ATP to the second messenger cAMP and pyrophosphate. Activation of the G_i protein coupled to D_2, D_3 or D_4 receptors causes either inhibition of adenylate cyclase and a decrease in cAMP or the influx of K^+ and subsequent hyperpolarization of the cell.

Re-uptake into the presynaptic terminal via selective DA transporters is the main mechanism to inactivate dopaminergic transmission. In the axon terminal, the transmitter is either transported back into release vesicles (“recycled”) or metabolised to DOPAC by mitochondrial monoamine oxidase (MAO). DA and DOPAC can also be carried into other cells, where they are metabolized to methoxytyramine (MT) and homovanillic acid (HVA) by catechol-o-methyltransferase (COMT) (Figure 5).

1.2.4. The hippocampal formation

The hippocampus, a prominent structure of the rat nervous system, has given rise to the interest of numerous researchers, since it was discovered at the beginning of the century, that all vertebrates, even the most primitive ones (cyclostomes) have a structure homologous to the hippocampus. The first data on possible hippocampal functions were collected during the observation of patients with lesions in the hippocampal cortex. The most famous patient, H.M. was intensively studied around 1950, and neuropsychological investigations continued until today. Suffering of serious pharmacoresistant epilepsy, he was, at 27 years old, subjected to a bilateral ablation of the temporal lobes. The consequences of this surgery were dramatic because he was then suffering of severe anterograde amnesia. It was concluded from this case that, even if the hippocampus does not store the memory, it plays a critical role in its formation, being especially concerned in explicit memory.

In the rat, the hippocampus is inserted in a more spread region, called the hippocampal region. It includes two sets of cortical structures namely the hippocampal formation and the parahippocampal region. Without entering into details, the hippocampal formation comprises the dentate gyrus, the hippocampus “proper” and the subiculum. As to the parahippocampal region, it consists of the entorhinal, the perirhinal and postrhinal cortices as well as the presubiculum and parasubiculum.

The hippocampal formation occupies part of the temporal lobe of the brain and extends in a C-shaped form from the septal nuclei of the basal forebrain rostrocaudally, over and behind the diencephalon, to the incipient temporal lobe caudoventrally, as shown on Figure 6A. The longitudinal axis of the hippocampal formation extends from its septal to its temporal poles.

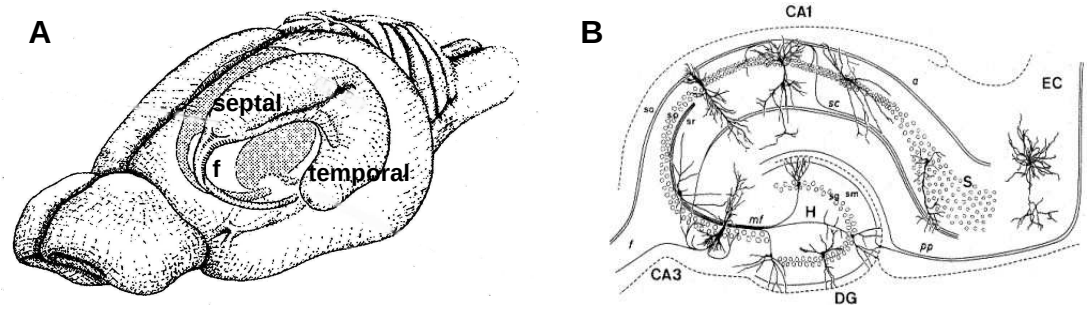

Figure 6. **(A)** Three-dimensional position of the hippocampal formation in the rat brain. The septo-temporal axis is represented as well as one afferent bundle, the fornix (f, see text for details). From (Amaral and Witter, 1995). **(B)** Internal structure of the hippocampus. CA1-3: Ammonic fields 1-3; DG: dentate gyrus; EC: entorhinal cortex; f: fornix; H: hile; mf: mossy fibers; pp: perforant path; s: subiculum; sc: Schaffer

collaterals; sg: stratum granulosum; sm: stratum moleculare; so: stratum oriens; sp: stratum pyramidal; sr: stratum radiatum. The Hammon's horns are made of the following layers: the Alveus, the stratum oriens, stratum pyramidal containing the cell bodies of the pyramidal cells, the stratum radiatum and the stratum moleculare. The dentate gyrus is made of the stratum granulosum containing the cell bodies of the granule cells, the molecular layer and finally, the polymorphic layer.

If transversal sections are made through the hippocampus (exactly as in the present thesis in order to obtain "hippocampal slices" for transmitter release experiments), two intermingled U-shaped structures can be seen. These are the dentate gyrus (DG) and the Ammon's horn, the latter being further divided in three parts namely, CA1, CA2 and CA3 (CA being the abbreviation for *Cornu ammonis*).
As shown in Figure 6B, the hippocampus and the DG contain several layers, each of them consisting of different cell types. Indeed, the hippocampus is composed of five layers (when the neocortex contains six of them), whereas, in the DG, three layers are distinguishable. These two parts of the hippocampal formation contain two main types of neurons, i.e., the pyramidal neurons, present in the hippocampus, and the granular cells, in the DG. These principal cells, that use glutamate as a transmitter, represent 90% of hippocampal neurons. The remaining 10% are GABAergic interneurons (Freund and Buzsaki, 1996) that, organized in a neural network, control and regulate the function of principal cells. Moreover, the hippocampal neuropil is enriched by noradrenergic (from the locus coeruleus), serotonergic (from the raphé nuclei) and cholinergic (from the septal nuclei) axon terminals (Vizi and Kiss, 1998), the corresponding fibers of which run perpendicular to the plane of the slice shown in Figure 6B.

The glutamatergic neurons mentioned above form a trisynaptic neuronal loop in the hippocampal formation, which is a cortico-hippocampo-cortical loop. The first synapse of this loop is made between glutamatergic afferents from the entorhinal cortex and granule cells of the DG. The latter cells send their axons, the so-called "mossy fibers" (see Figure 6B), to the proximal dendrites of CA3 pyramidal cells. These cells, in turn, project to the dendritic region of CA1 pyramidal cells via the "Schaffer collaterals". Finally, the main efferent projections arise from the CA1 pyramidal cells and terminate in the subiculum and entorhinal cortex.

Afferents to the hippocampal formation originate in four main regions. As already seen in the former section, one afferent projection is mainly cholinergic and arises from the MSDB complex to innervate every layer of the hippocampus with varicosities that exhibit a low frequency at synaptic junctions (Umbriaco et al., 1995). The major (90-

95%) postsynaptic elements of this projection are pyramidal neurons (Freund and Buzsaki, 1996), but there is also evidence for synaptic contacts onto GABAergic interneurons (Leranth and Frotscher, 1987). Moreover, it was shown that this septohippocampal projection also contains GABAergic neurons, the axons of which end on GABAergic interneurons. It was further shown that these GABAergic cells reciprocally innervate the septal region, the predominant target of these projections, being PARV-positive GABAergic neurons of the MSDB complex. In addition to the septum, hippocampal interneurons send so-called “commissural projections” to the contralateral hippocampus.

The hippocampus is also innervated by noradrenergic fibers originating exclusively in the locus coeruleus. These fibers travel largely ipsilaterally in the dorsal noradrenergic bundle to reach every layer of the hippocampus (Oleskevich et al., 1989).

Finally, a third afferent hippocampal innervation is made of serotonergic fibers originating in both the dorsal and the median raphé nuclei (Conrad et al., 1974). Axons from the dorsal raphé have small varicosities (Jacobs and Azmitia, 1992) that do not make synaptic contacts. Conversely, fibers from the median raphé are studded with large boutons that always form synapses (Freund and Buzsaki, 1996). Thus, 5-HT is released through synapses that are mostly established with dendrites and somata of GABAergic interneurons (Freund et al., 1990; Freund, 1992) as well as, at nonsynaptic sites for long distance diffusion.

1.3. NEUROTRANSMISSION

1.3.1. General aspects

As this work focuses on neurotransmission and its modulation via presynaptic receptors, some general comments on these two phenomena will be given.

The neuron as the primary functional unit of the central nervous system (CNS) was first recognized in the early 20th century with the work of the Spanish anatomist Ramón y Cajal. As functional units, neurons transmit and process informations. Neuronal informations primarily consist of action potentials, i.e. electrical impulses that are propagated in the neuronal circuitry. However, even if experiments by Luigi Galvani in the 18th century, who studied the nerve/muscle contact, led to development of the bioelectricity concept, the discussion whether the communication between nerve and

muscles was electrical or chemical by nature was open until 1921, when the Austrian physiologist Otto Loewi (1873-1961) discovered a substance, that he named “vagusstoff”, because its release subsequent to stimulation of the vagus nerve caused reduction in the beating of the frog heart (Loewi, 1921). This substance was the first demonstration of chemical synaptic transmission and was later confirmed to be acetylcholine (ACh). The synapse, or contact point between neurons, is either chemical or electrical. As regards “electrical synapses”, they interconnect neurons with channels through which ions can be exchanged and the electrical impulses propagated directly from neuron to neuron. However, these synapses are rather rare in adult mammals and the majority of neuronal communications uses “chemical synapses”. In this case, an action potential, initiated in the neuronal cell body travels to all of its nerve terminals to be transformed into synaptic secretory signals. When reaching the nerve ending, the action potential activates voltage-gated ion channels which cause calcium (Ca^{2+}) ions to flow into the cells. These ions allow synaptic vesicles filled with neurotransmitters to fuse with the presynaptic membrane and to release their content by exocytosis (Rettig and Neher, 2002). The newly released neurotransmitters diffuse across the synaptic cleft and bind to specific receptors on the postsynaptic neuron. Depending on the type of receptor, this binding elicits either EPCS (excitatory postsynaptic currents) or IPSC (inhibitory postsynaptic currents), the summation of which allows (or not) to reach the potential threshold and to generate a new action potential in the postsynaptic neuron. The signal in the postsynaptic neuron is thus modulated by the interaction of different transmitters and receptors, i.e. also by the amounts of the presynaptically released transmitter(s). To stop the synaptic signal, neurotransmitters are either taken up by the presynaptic neuron (“re-uptake”) or metabolised by specific enzymes in the synaptic cleft. They can also be taken up by neighbouring cells such as glial cells or diffuse out of the synaptic cleft and thus reach more distant postsynaptic receptors. Finally, the newly released transmitters may also activate the so-called “presynaptic” receptors, which modulate the amount of the transmitter released either from the axon terminal itself (“presynaptic autoreceptors”), or from axon terminals belonging to other neurons (“presynaptic heteroreceptors”; see below).

1.3.2. Molecular aspects of neurotransmission

In as much as this work deals with neurotransmitter release, it is inconceivable not to describe the molecular aspects of this mechanism. Nevertheless, this very rich

research field cannot be described in full detail and thus the interested reader is referred to additional references.

In the presynaptic nerve terminal, neurotransmitters are actively transported into synaptic vesicles through specific transporters (Roghani et al., 1994), whereby they become integrated into the vesicle cluster representing a reserve pool of releasable vesicles. Filled vesicles dock at a specialized active zone on the presynaptic membrane where they undergo a priming reaction making them competent for Ca^{2+} triggered fusion-pore opening. This priming process involves the formation of a multiprotein complex that anchors the vesicles to the plasma membrane in close juxtaposition to other signaling elements. This multiprotein complex comprises proteins of the plasma membrane as well as some of the vesicle membrane (Jahn et al., 2003). Initially, a core complex is formed between syntaxin 1A and SNAP-25 (25 kd synaptosome associated protein) from the plasma membrane and VAMP/synaptobrevin (vesicle associated membrane protein) with a stoichiometry of 1:1:1. These three proteins provide a high-affinity receptor scaffold for the protein α-SNAP, and its arrival allows the recruitment of NSF (N-ethylmaleimide-sensitive ATPase). ATP hydrolysis, together with dissociation of NSF/α-SNAP, may cause partial fusion of the vesicle with the plasma membrane. Ca^{2+} channels (Bennett, 1997), mostly of the N- (predominantly α_{1B} subunits) and P/Q- (predominantly α_{1A} subunits) types, also present in this specialized zone, provide the final Ca^{2+}-trigger for exocytosis (Martin-Moutot et al., 1996; Yokoyama et al., 1997). Upon depolarisation of the nerve terminal, the Ca^{2+} channels that have been appropriately targeted to release sites open, thereby rapidly elevating the local Ca^{2+} concentration at the pore to more than 200 µM. It appears that internal stores of Ca^{2+}, such as the endoplasmic reticulum, also play a crucial role in the intracellular Ca^{2+} concentration (Berridge, 1998). Ca^{2+} then interacts with Ca^{2+}-sensing molecules of the multiprotein complex most likely with synaptotagmin (Bommert et al., 1993; Geppert et al., 1994) - allowing the ultimate fusion of the vesicle and the release of its content into the synaptic cleft (Sudhof, 2004). Subsequent to fusion and opening (exocytosis), the vesicles undergo endocytosis and recycle via several routes: local re-use (vesicles are re-acidified and re-filled with neurotransmitters without undocking, thus remaining in the readily releasable pool [“kiss-and-stay”]), fast recycling without an endosomal intermediate (vesicles undock and recycle locally [“kiss-and-run”]) or clathrin-mediated endocytosis with slower recycling via endosomes (Gandhi and Stevens, 2003; Rizzoli and Betz, 2003).

1.3.3. Presynaptic receptors

It is known today that the efficiency of the transmitter release process can be influenced by several factors that continuously modulate the strength of synaptic communication. Presynaptic nerve terminals possess receptors for the same neurotransmitter that they release, known as presynaptic **autoreceptors** (Göthert, 1986; Starke et al., 1989b). They constitute a possibility of self-regulation of the amplitude of the neuron's chemical signal (release and biosynthesis of transmitter). But neurons additionally possess receptors for other transmitters released in the vicinity of the synapse, known as **heteroreceptors**. Both types of receptors are of considerable interest for neuronal communication, but also as potential targets for therapeutic agents (Göthert, 1990; Göthert and Schlicker, 1993). For instance, in the hippocampus, it is known that the major transmitter systems modulate "each other" via synaptic and non-synaptic interactions and via, of course, action on auto- and heteroreceptors. All these interactions were shown to be indispensable in the fine tuning communication between neurons within a neuronal circuit (Vizi and Kiss, 1998).

Presynaptic receptors include members of both the G-protein-coupled receptors (GPCRs or metabotropic) (Miller, 1990; Wu and Saggau, 1997) and the multisubunit ligand-gated ion channel (ionotropic) (McGehee and Role, 1996) families. For reviews on presynaptic receptors, see (Starke et al., 1989a; Miller, 1998). G-protein-coupled presynaptic receptors can act in different ways to modulate neurotransmitter release. Indeed, these receptors may either inhibit presynaptic Ca^{2+} channels (De Waard et al., 1997; Zamponi et al., 1997) [but see (Qin et al., 1997)], or activate presynaptic hyperpolarizing K^+ channels, via the $\beta\gamma$-subunit of the G-protein, or inhibit adenylate cyclase via the $\alpha_{i/o}$-unit of the G-protein (Boehm and Kubista, 2002; Krejci et al., 2004; Sari, 2004; Kubista and Boehm, 2006). Finally, it has been suggested that presynaptic receptors might also directly influence some component(s) of the vesicle-releasing complex. Although the precise mechanisms involved in these processes are still unclear, there is increasing evidence that effects downstream to Ca^{2+} entry may be implicated in the modulation of neurotransmitter release (Scanziani et al., 1995). As regards ionotropic receptors mentioned above, they may also participate in the regulation of neurotransmitter release: via their opening, that lead to modifications in ion balance in the nerve terminal (McGehee and Role, 1996).

How to assess the activity of presynaptic receptors?

Various techniques are available. For instance transmitter release can be measured indirectly *in vivo* and *in vitro* by electrophysiological assessment of the postsynaptic response to the transmitter outflow. Another *in-vivo* technique largely used in this field, is the measurement of transmitter concentrations in distinct brain areas using *in vivo* microdialysis coupled to sensitive HPLC-detection. However, such *in vivo* techniques rarely allow conclusions about the *site* of the modulation of the transmitter release (i.e. about the exact location of the receptors involved) since interneuronal loops may be implicated in the effects. Therefore, *in vitro* methods on synaptosomes and on brain slices have also been used to measure the outflow of neurotransmitters. The latter technique is closest to, and probably the best indicator, of transmitter release and its modulation. In order to appraise activity of presynaptic receptors, methods to measure transmitter overflow were developed (Gaddum, 1953; Cambridge and Holgate, 1955). *In vitro* experiments essentially investigated the effects of drug applications to synaptosomes (Maura and Raiteri, 1986), cell cultures (Ehret et al., 2001; Birthelmer et al., 2007; Ehret et al., 2007b) or slices of various brain regions [e.g. from rats (Cassel et al., 1995b; Jackisch et al., 1999b; Suhr et al., 1999a; Birthelmer et al., 2003f; Birthelmer et al., 2003c; Birthelmer et al., 2003a) and humans (Feuerstein et al., 1992; Feuerstein et al., 1996d; Albrecht et al., 1999)], that were previously loaded with a tritiated ([^{3}H]) precursor or transmitter and subsequently exposed to high potassium concentrations or electrical stimulation (experiments with brain slices are considered as *ex vivo*). Electrically-evoked transmitter release in such brain slices allows to measure the release and its modulation of numerous neurotransmitters in a variety of situations [e.g. effects of pharmacological agents, normal or pathological aging, diseases models, modifications of the neuronal environment…(Cassel et al., 1995a; Jackisch et al., 1999a; Jackisch et al., 1999c; Gazyakan et al., 2000)]. For these reasons this technique was also used in the present work to evaluate the effects of increased expression of the 5-HT$_{1B}$ receptor on the modulation of the release of acetylcholine, both *in vitro* and *in vivo.* The exact methodology is described below in Materials & Methods.

1.4. THE 5-HT_{1B} RECEPTOR

Since the 5-HT_{1B} receptor represents one of the most interesting subjects of the present thesis it will be described here in much more detail.

Initially, the 5-HT_{1B} receptor has been claimed to exist only in rodents (Pedigo et al., 1981), but it was later shown that it is, in fact, the species variant of the human 5-$HT_{1D\beta}$ receptor (Adham et al., 1992; Boess and Martin, 1994), with which it shares 93% homology in the amino acid sequence. Indeed, they have distinct pharmacological profiles due to a single amino acid difference at position 355 (asparagine for the rat vs. threonine for the human) (Oksenberg et al., 1992). In the present thesis, when not further specified, the term "5-HT_{1B} receptor" will always refer to the rat variant.

The 5-HT_{1B} receptor has been shown to be involved in several physiological functions, behaviours and psychiatric diseases including locomotor activity, learning and memory, drug abuse reinforcement, migraine, anxiety states and aggressive behaviour (Clark and Neumaier, 2001; Sari, 2004).

As regards the distribution of the 5-HT_{1B} receptor in the CNS, autoradiographic studies using [^{3}H]5-HT (in the presence of 8-OH-DPAT), [^{125}I]-cyanopindolol (CYP, in the presence of isoprenaline) or [^{125}I]-GTI (serotonin-5-O-carboxymethyl-glycyl-[^{125}I]-tyrosinamide) have shown high densities of 5-HT_{1B} sites in the rat basal ganglia (particularly the substantia nigra, globus pallidus, ventral pallidum and entopedoncular nucleus) but also in the dorsal subiculum. Moderate densities of these binding sites were found in the superficial gray layer of the superior colliculus, periaqueductal grey, cerebral cortex, amygdala, hypothalamus and the superior layer of dorsal horn of the spinal cord. This distribution pattern has been confirmed by immunocytochemical studies (Sari et al., 1997; Sari et al., 1999).

1.4.1. Coupling of the 5-HT_{1B} receptor

As already mentioned, the 5-HT_{1B} receptor belongs to the metabotropic receptor family or G-protein coupled receptors. This seven transmembrane domains receptor has been shown to couple to $G_{i/o}$ proteins (Seuwen et al., 1988; Maroteaux et al., 1992; Lin et al., 2002), thus inhibiting adenylate cyclase (Bouhelal et al., 1988). Furthermore, experimental evidence exists that 5-HT_{1B} receptors could also be directly coupled to Ca^{2+}-dependent K^{+} channels, which regulate cellular and neuronal excitability (Le Grand et al., 1998).

1.4.2. Subcellular localization of the 5-HT_{1B} receptor

Several studies using the cloning results of the 5-HT_{1B} receptor as well as specific radioligands were conducted to exactly localize 5-HT_{1B} mRNA and the subsequently produced receptor protein. For instance, it was shown in the mouse caudate-putamen, that medium spiny neurons, that project to the globus pallidus and substantia nigra, contain a high level of 5-HT_{1B} mRNA. Conversely, in the projection zones cited above, only high levels of the 5-HT_{1B} proteins but no 5-HT_{1B} mRNA were detected. The same distribution was found concerning pyramidal cells of the CA1 region of the hippocampus, which contain 5-HT_{1B} mRNA, whereas the corresponding receptor protein was found predominantly in the subiculum, the projection zone of CA1 pyramidal neurons (Boschert et al., 1994). A similar observation, made in the cerebellum, led the researchers to conclude that the 5-HT_{1B} receptor might be localized on axon terminals while its functional expression is low or absent at the somatodendritic level. Further studies were conducted to define the mechanism responsible for this specific subcellular location of the 5-HT_{1B} receptor. These studies used hippocampal neurons but also different lines of epithelial cells (suggested to share common protein targeting mechanisms with neurons; (Dotti and Simons, 1990). Ghavami and co-workers, using MDCK II epithelial cells and hippocampal cells in culture, as well as *in vivo* mouse models, showed that the 5-HT_{1B} receptor is transported to the axon terminals whereas the 5-HT_{1A} is localized at the somatodendritic level of the same neurons (Ghavami et al., 1999). It was further suggested that the third intracellular loop and/or the C-terminal portion (comprising the two last transmembrane domains) of the 5-HT_{1B} receptor might act as axonal targeting signals (Jolimay et al., 2000).

1.4.3. Functional role of 5-HT_{1B} autoreceptors

Due to the lack of available specific compounds, particularly antagonists, the 5-HT_{1A} receptor was, for long time, thought to be the only modulatory receptor of 5-HT release, especially in the DRN (Verge et al., 1986). Of course, numerous studies confirmed that in this nucleus, serotonergic cell firing is under the control of the 5-HT_{1A} receptor (Sprouse and Aghajanian, 1987) as well as, is the intra-raphé release of 5-HT (Blier et al., 1998). Moreover, these findings were confirmed by immunocytochemical studies localizing 5-HT_{1A} receptors on 5-HT neurons (Sotelo et al., 1990).

The development of specific agonists (Macor et al., 1990) and antagonists (Walsh et al., 1995), especially for the 5-HT_{1B} receptor, made it possible to further characterize the receptor subtypes involved in the modulation of cell firing and 5-HT release in the DRN but also in the MRN.

As regards the serotonergic regulation of *cell firing* of serotonergic neurons, some discrepancies still remain between different works. Sprouse and colleagues, in their study on the electrophysiological responses (both *in vitro* and *in vivo*) of 5-HT neurons, concluded that, in the rat, the 5-HT_{1B} receptor has no effect on this variable (Sprouse and Aghajanian, 1987). However, more recent studies in the mouse showed that the 5-HT_{1B} agonists RU-24,969 and CP-94,253 both increased DRN cell firing (Evrard et al., 1999). These effects were attenuated by the 5-$HT_{1B/1D}$ antagonist, GR-127,935 and were absent in the 5-HT_{1B} knock-out (KO) mouse. The authors concluded that the effect of 5-HT_{1B} receptors was mediated indirectly via 5-HT_{1A} receptor. Indeed, the 5-HT_{1B} receptor agonists inhibit 5-HT release, thereby reducing the endogenous 5-HT tone which in turn diminishes the 5-HT_{1A} receptor-induced decrease of cell firing. A similar indirect effect was also reported in the guinea pig frontal cortex both *in vitro* and *in vivo* (Roberts et al., 1996). Finally, in a study from 2001, it was shown in the rat, that the firing of serotonergic neurons is under the control of the 5-HT_{1B} receptor but in the MRN only (Adell et al., 2001). These different works seem to indicate that the control of cell firing differs in the two raphé nuclei as well as between species (Roberts et al., 2001).

Regarding the effects of the 5-HT_{1B} receptor on 5-HT *release*, however, more clear-cut results were obtained. Firstly, a modulation of electrically-evoked 5-HT release through activation of the 5-HT_{1B} receptor was directly shown by our group in cultured raphé neurons (Birthelmer et al., 2007). Moreover, CP-93,129 (a selective 5-HT_{1B} agonist) decreased 5-HT release, evoked by short train stimulation of the DRN and measured by fast cyclic voltametry (Hopwood and Stamford, 2001). This effect was not blocked by WAY-100,635 (a specific 5-HT_{1A} antagonist) but by SB216,641, the selective 5-HT_{1B} antagonist. Thus, the modulation of 5-HT release in the DRN seems to be under the control of 5-HT_{1B} receptors. Moreover, the same results were obtained in the MRN (Roberts et al., 2001). Several other *in vitro* studies demonstrated that there is a strong correlation between the potency with which 5-HT receptor agonists inhibit 5-HT release, and their affinity for the rat 5-HT_{1B} binding sites. A similar correlation holds for the potency with which antagonists block the receptor (Engel et al., 1986). Furthermore, studies using 5-HT_{1B} KO mice and electro-physiological recordings of the postsynaptic potentials concluded that the 5-HT_{1B} receptor has an inhibitory action on

5-HT release in the dorsal raphé (Morikawa et al., 2000), or on hippocampal and cortical serotonergic axon terminals (Rutz et al., 2006b).

In addition to its role on the regulation of serotonergic cell body activity in the DRN and MRN, and because of its terminal position on nerve fibers, the 5-HT_{1B} receptor was also shown to modulate 5-HT release in other brain regions such as the frontal cortex (Göthert and Weinheimer, 1979; Brazell et al., 1985; Göthert et al., 1987), the hippocampus (Maura et al., 1986), the septum (Ehret et al., 2007a), the hypothalamus (Friedman and Wang, 1988), the striatum, the cerebellum (Raiteri et al., 1986) and the spinal cord (Brown et al., 1988) in the rat. All these brain regions contain serotonergic nerve terminals but are devoid of the corresponding cell bodies, thus excluding the involvement of somatodendritic modulation of 5-HT release. For instance, *in vitro* [^{3}H]-5-HT release in brain cortical slices allowed Limberger and co-workers to suggest the existence of the 5-HT_{1B} autoreceptor in the rat brain (Limberger et al., 1991). Using *in vivo* microdialysis, some authors concluded that both in the frontal cortex and dentate gyrus, 5-HT_{1B} receptors had a modulatory role on 5-HT release (Roberts et al., 1997).

1.4.4. Functional role of 5-HT_{1B} heteroreceptors

In addition to its autoreceptor function, the 5-HT_{1B} receptor has been suggested to modulate transmitter release at nerve terminals of other neuronal types. In this case, the receptor has been defined as a heteroreceptor. The first indication that led researchers to speculate about a heteroreceptor role for the 5-HT_{1B} receptor was the mismatch in the distribution of 5-HT_{1B} binding sites and the 5-HT_{1B} mRNA in some brain regions (Boschert et al., 1994; Bruinvels et al., 1994). Moreover, binding and autoradiographic studies of 5-HT_{1B} receptor sites after specific neuronal lesions in the brain, or several pathological states provided evidence that they are also located on non-serotonergic terminals (Fillion et al., 1979), especially in areas densely innervated by cholinergic and dopaminergic fibers such as the substantia nigra, striatum, cortex or hippocampus (Quirion and Richard, 1987). Several *in vitro* (neurotransmitter release from synaptosomes or slices) and *in vivo* microdialysis studies, as well as electrophysiological measurements of synaptic potentials have been conducted to identify which neurotransmitters are influenced by 5-HT_{1B} heteroreceptors. For instance, 5-HT_{1B} receptors have been shown to inhibit the release of GABA (Tanaka and North, 1993; Morikawa et al., 2000; Yan and Yan, 2001a) or noradrenaline (Göthert et al., 1986). Glutamate release in the locus coeruleus (Bobker and Williams, 1989), subiculum (Boeijinga and Boddeke, 1993), cingulated cortex (Tanaka and North,

1993), nucleus accumbens (Muramatsu et al., 1998) or hippocampus (Mlinar and Corradetti, 2003) was also shown to be modulated by the 5-HT_{1B} receptor. Other studies have observed that in the striatum or nucleus accumbens, the release of dopamine (DA) is under the control of the 5-HT_{1B} receptor (Sarhan et al., 1999). It seems that the 5-HT_{1B} receptor has a facilitatory role in the nigrostriatal pathway even if this result remains controversal (Alex and Pehek, 2007). Conversely, in the mesolimbic pathway, the 5-HT_{1B} receptor in the VTA has been shown to facilitate DA release by inhibiting the release of GABA (Yan and Yan, 2001a, 2001b; O'Dell and Parsons, 2004; Yan et al., 2004b). Also in the frontal cortex, the 5-HT_{1B} receptor appears to facilitate DA release (Iyer and Bradberry, 1996) and again, it seems likely that this effect is mediated indirectly via possible (GABAergic) interneurons. Conversely, when assessing simultaneous quantification of 5-HT, DA and NA levels in single frontal cortex dialysates of freely-moving rats, Gobert and co-workers failed to find any modulatory influence of the 5-HT_{1B} receptor neither on DA, nor on NA release (Gobert et al., 1998).

Serotonergic modulation of ACh release via 5-HT_{1B} heteroreceptors (or additional 5-HT receptors) plays an important role in the present work. Already early *in vitro* studies have demonstrated a presynaptic 5-HT_{1B} receptor-mediated effect on cholinergic transmission in the rat brain. For instance, Raiteri's group investigated the evoked (15 mM K^+) release of [^{3}H]-ACh from hippocampal synaptosomes. 5-HT inhibited this ACh release, an effect which was not antagonized by 5-HT_{1A}, 5-HT_{1C} and 5-HT_2 antagonists, but instead, was mimicked by a 5-HT_1 agonist and blocked by the 5-$HT_{1A/1B}$ antagonist propanolol (Maura and Raiteri, 1986). More recently, it was shown in primary septal cell cultures that, at DIV14, CP-93,129, the selective 5-HT_{1B} receptor agonist had an inhibitory effect on the electrically-evoked overflow of [^{3}H]-ACh. This effect was diminished in the presence of the selective 5-HT_{1B} antagonist, GR-55,562 (Ehret et al., 2007a). This finding was also confirmed by numerous studies on synaptosomal preparations (Bolanos and Fillion, 1989; Bolanos-Jimenez et al., 1993; Bolanos-Jimenez et al., 1994).

These effects of 5-HT_{1B} receptor stimulation on ACh release were subsequently also demonstrated on hippocampal slices. When such slices were electrically stimulated, the evoked [^{3}H]-ACh was prevented by exogenous 5-HT, an effect mimicked by 5-HT_1 but not 5-HT_{1A} agonists. Moreover, the 5-HT_1 antagonist methiotepin potentiated the evoked [^{3}H]-ACh release. All together, these results indicate that the release of ACh may be tonically inhibited by 5-HT in the rat hippocampus through the activation of

receptors that seem to belong to the 5-HT_{1B} subtype (Maura et al., 1989). More recently, it was shown that the selective 5-HT_{1B} agonist, CP-93,129 had an inhibitory effect on the electrically-evoked overflow of [^{3}H]ACh in hippocampal slices, and the potency of this inhibitory effect was increased with the concentration of the drug (Cassel et al., 1995a; Birthelmer et al., 2002; Birthelmer et al., 2003e). Finally, studies of our group on 5-HT_{1B} receptor KO mice revealed, that CP-23,129 acted no longer inhibitory on hippocampal ACh release (Rutz et al., 2006b).

No effects of serotonin have been described on the baseline release of acetylcholine from synaptosomes or slices so that it can be considered that the serotonin-induced inhibition is operating when the cholinergic neurons are active. One study also showed, that the 5-HT_{1B} receptor-mediated inhibitory effect of exogenous 5-HT in hippocampal slices could be enhanced if the facilitatory influence of substance P (SP) containing interneurons is eliminated by blocking 5-HT_{2A} receptors. These receptors mediate a stimulatory effect of 5-HT on SP release, which in turn enhances hippocampal ACh release through stimulation of NK1 receptors present on cholinergic terminals. Thus, this enhancement may counterbalance the 5-HT_{1B}-mediated inhibition of ACh release (Feuerstein et al., 1996a). Taken together, all these *in vitro* studies clearly demonstrated that serotonergic mechanisms mainly mediated via 5-HT_{1B} receptors modulate cholinergic function at the level of the presynaptic cholinergic terminal.

Several studies also investigated the effects of 5-HT on hippocampal ACh release using *in vivo* methods consisting in local or systemic delivery of drugs. For instance, following local application of the 5-HT_{1B} agonist CGS-120,66B to the dorsal hippocampus of freely moving rats (using a microdialysis probe), the spontaneous ACh release was decreased, an effect which was not affected by pre-treatment with NAN-190 (a selective 5-HT_{1A} antagonist) (Izumi et al., 1994).

In vitro and *in vivo* studies have also suggested a modulatory role of the 5-HT_{1B} receptor on cholinergic transmission in other brain regions. For instance, in the rat frontal cortex, endogenous 5-HT was shown to facilitate ACh release, an effect that seemed to be mediated by 5-HT_{1B} receptors (Consolo et al., 1996). However, given the fact that the 5-HT_{1B} receptor acts in an inhibitory manner, this finding was suggested to be mediated indirectly, probably via inhibitory cortical inputs onto cholinergic neurons. In the striatum, *in vitro* experiments also showed an inhibitory action of serotonin on ACh release (Jackson et al., 1988). The same conclusion was drawn from *in vivo* experiments, even if it seems that this effect is mediated via the 5-HT_{1A} receptor subtype (Rada et al., 1993).

There is a considerable amount of experiments, both *in vitro* and *in vivo,* that investigated the modulation of ACh release by 5-HT. To have a closer look on them, the reader is referred to (Cassel and Jeltsch, 1995).

Finally, as already briefly mentioned above [see: (Feuerstein et al., 1996a)], it is noteworthy that ACh release is also under the direct or indirect control of additional serotonergic receptors such as, for instance, 5-HT_{1A} receptors that seem to have a stimulatory effect. Recent microdialysis studies confirmed the stimulatory role of 5-HT_{1A} receptors on cholinergic neurotransmission since local or systemic administration of 8-OH-DPAT increased the hippocampal level in normal (Fujii et al., 1997) and fimbria-fornix lesioned animals with intra-hippocampal grafts of fetal septal cell suspensions (Erb et al., 1997).
Facilitation of hippocampal ACh release has also been suggested to be mediated by 5-HT_3 receptors, at least in the rat (Consolo et al., 1994b). Moreover, 5-HT_4 receptor activation has been proposed to positively affect ACh release in the frontal cortex but not in the dorsal hippocampus (Consolo et al., 1994a).

It is of special interest also for the present thesis, that the phenomenon of serotonergic modulation of cholinergic function in the CNS has several functional implications, in particular in cognitive processes. As discussed in the previous paragraphs, histological, electrophysiological as well as *in vitro* and *in vivo* pharmacological data support the hypothesis, that there are neuroanatomical substrates in different brain regions (e.g. hippocampus, cortex or striatum) for serotonergic/cholinergic interactions. Thus, it seems to be generally accepted at present, that such interactions have a real functional significance (Cassel and Jeltsch, 1995; Steckler and Sahgal, 1995; Buhot, 1997; Ruotsalainen et al., 1998; Buhot et al., 2000). For instance, from a number of studies using 5-HT_{1B} KO mice, it was concluded that 5-HT_{1B} receptors might be implicated in at least some specific memory processes, as for example spatial memory (Malleret et al., 1999; Buhot et al., 2003b; Wolff et al., 2003); for reviews on this topic, see (Meneses, 1999; Buhot et al., 2000; Meneses, 2001). Besides a possible role in cognition, 5-HT_{1B} receptors also seem to be involved in the regulation of locomotor activity, reinforcing effects of drugs of abuse (alcohol, cocaine, ecstasy), migraine, stress sensitivity, mood, aggressive behaviour, depression and anxietry states (Clark and Neumaier, 2001; Groenink et al., 2003; Sari, 2004).

1.5. STRATEGIES TO STUDY 5-HT_{1B} RECEPTOR FUNCTION

As discussed in the previous sections, investigations on the cellular functions and physiological and behavioural implications of 5-HT_{1B} receptors were done using several techniques. The most widely applied of them were pharmacological experiments using 5-HT agonists and antagonists, or molecular genetic tools using, for instance, knock-out (KO) mice. Nevertheless, these techniques also have well-known disadvantages. For instance, the lack of selectivity of pharmacological compounds was, for long time, an obstacle to understand specific processes. Moreover, the tremendous complexity of 5-HT receptor subtypes made it difficult to produce compounds with a selective specifity for a given subtype. Additionally, depending on their way of administration, such compounds, most of the time, do not allow to distinguish in which brain area or on which neuronal population they were producing their effects.

These remarks are especially true when studying the specific involvement of serotonergic receptors. Indeed, the serotonergic system is the most widespread of the CNS as its fibers connect numerous populations of neurons in all brain regions. Thus, it is extremely difficult to link observed serotonergic effects to a special group of 5-HT_{1B} receptors located on a particular population of neurons. Moreover, it is not possible to manipulate 5-HT_{1B} heteroreceptors in physiological and behavioural models without also impinging on 5-HT_{1B} autoreceptors, a fact that may complicate interpretation of the data. For example, stimulating presynaptic 5-HT_{1B} autoreceptors will inhibit 5-HT release, thereby reducing the activation of postsynaptic 5-HT_{1B} heteroreceptors. Therefore, even the infusion of selective 5-HT_{1B} agonists may cause alterations in the spatial and temporal pattern of the release of 5-HT and further transmitters. Similarly, 5-HT_{1B} antagonists may increase endogenous 5-HT release and simultaneously block the effects of this increased 5-HT transmission at 5-HT_{1B} heteroreceptors in other neurons.

As regards transgenic mice, they were extensively used in order to understand the role of several types of receptors. In particular, the use of null mutant, or KO mice, was applied to the study of the 5-HT_{1B} receptor. Mice lacking the 5-HT_{1B} receptor were first studied by (Saudou et al., 1994). These authors generated homozygous mutant mice lacking both copies of the gene encoding the 5-HT_{1B} by homologous recombination in embryonic stem cells. A major concern with interpreting these effects is inherent in most KO strategies. Because the receptor has been absent during the development of the animal, it is possible that behavioural and physiological alterations may be the consequences of compensatory changes in a variety of neural systems rather than a

direct effect of the missing receptor. Indeed, an impaired 5-HT_{1B} activity early in brain development may lead to developmental adaptations. It is known that serotonergic neurons appear early during embryogenesis, suggesting that they could play a role in brain development and that the 5-HT_{1B} receptor could be one of the serotonergic receptors involved in these ontogenic mechanisms (Gaspar et al., 2003; Luo et al., 2003) Moreover, the complete deletion of 5-HT_{1B} receptors throughout the whole animal makes it difficult, if not impossible, to distinguish between effects mediated by 5-HT_{1B} autoreceptors and those mediated by 5-HT_{1B} postsynaptic heteroreceptors.

For instance, (Shippenberg et al., 2000) proposed that alterations in presynaptic neuronal activity are a compensatory response to deletion of the 5-HT_{1B} receptor gene and thus might contribute to enhanced behavioural effects of psychostimulants observed in these KO mice. In another study on 5-HT_{1B} receptor KO mice, (Gardier et al., 2001) observed compensatory changes in the functional activity of somatodendritic 5-HT_{1A} receptors. Also several further studies analysing the effects of 5-HT_{1B} receptor gene-deletion in the mouse brain (Saudou et al., 1994; Malleret et al., 1999; Buhot et al., 2003a; Wolff et al., 2003; Rutz et al., 2006a) suggested developmental compensations as a consequence of 5-HT_{1B} receptor gene deletion. Finally, conflicting results were obtained using traditional pharmacological approaches or gene deletion strategies, respectively. For example, administration of GR-127,935, a 5-$HT_{1B/1D}$ antagonist, decreased the locomotor effect of cocaine and had no effect on cocaine self-administration in wild-type mice (Harrison et al., 1999; Scearce-Levie et al., 1999b; Scearce-Levie et al., 1999a), but enhanced both locomotor and rewarding effects of cocaine in 5-HT_{1B} receptor KO mice (Rocha et al., 1998). Such discrepancies are likely to result not only from compensatory changes that took place during the development of the KO mice due to the lack of the 5-HT_{1B} receptor [for review, see (Gingrich and Hen, 2001)], but might also be due to differences in the genetic background of strains used to generate KO mice using homologous recombination.

For these reasons, in the present thesis we investigated the role of 5-HT_{1B} receptors not by a general deletion of this receptor but by a selective and neuron-specific overexpression of 5-HT_{1B} receptors via “targeted gene transfer”. To that end, we used a stereotaxic (i.e. brain region-specific) application of a viral gene vector, namely a replication-deficient Herpes simplex virus type 1 (HSV-1) containing the genomic information to (over)express the 5-HT_{1B} receptor. The next section will develop the aim and properties of viral-mediated gene transfer as well as the specific characteristics of HSV.

1.6. THE TRANSFER OF GENES

In **Part 1** of the present thesis the functional consequences of an increased expression of 5-HT_{1B} receptors in cholinergic cells were studied both *in vitro* and *in vivo*, following a viral vector-mediated gene transfer. Therefore the subsequent sections of the Introduction are designed to provide an overview of modern gene transfer techniques with special emphasis on the use of replication deficient HSV-1 amplicon vectors for the current project.

1.6.1. Non-viral gene transfer techniques

The transfer of external genes into cells can be achieved by several non-viral and viral techniques. As regards non-viral gene transfer techniques, they comprise an eclectic mix of chemical, physical and electrical methods for gene transfer. In general, these techniques are advantageous for gene transfer into postmitotic neurons because they are easy to use, relatively untoxic and not constrained to deliver plasmids below a relatively small size. However, the efficiency of these non-viral transfection methods is generally rather low.

Chemical transfection methods include calcium phosphate coprecipitation, liposomes, and high molecular weight cationic polymers, several “structures” that are thought to enter cells by endocytosis (Washbourne and McAllister, 2002).
Physical gene transfer methods include the techniques of “microinjection” and “biolistics”. Microinjection consists in direct injection of plasmid DNA into the nucleus of a neuron (Martinou et al., 1995) or of cRNA into the cytoplasm (Ikeda et al., 1995). Biolistics (short for biological ballistics), consists in bombarding neurons at high velocity with DNA-coated gold particles (McAllister et al., 1997).
As regards *electrical transfection* methods, electroporation is thought to be one of the most promising non-viral methods for gene transfer into postmitotic neurons. It is believed that electrical shocks transiently open pores in the cell membrane, allowing charged molecules to enter cells by electrophoresis. This method results in a high number of healthy, highly expressing transfected neurons (Inoue and Krumlauf, 2001).
Although they are non pathogenic, the non-viral vectors discussed above still suffer from a low transfection rate as well as from a, sometimes important, toxicity (in the case, for instance, of liposomal aggregation in the blood).

1.6.2. Viral-mediated gene transfer

More than ten viral vector types are currently in use today for gene transfer in basic research as well as for therapeutic applications. Most of them derive from common human viral pathogens. Due to their ability to insert and express DNA or RNA into host cells, viruses had a natural predisposition to be used as vectors. Not surprisingly, the infection efficiencies (up to 95% for neurons) are extremely high as compared to non-viral methods. Recombinant viral vectors can be locally applied or focally injected into a group of neurons, either in culture or in tissue, in order to produce a highly localized expression of a gene of interest. However, these advantages are counterbalanced by some serious limitations: their potential toxicity to neurons, the effort and time to construct recombinant viral vectors, limitations on size of the DNA expression cassette and potential safety hazards to laboratory personnel (Washbourne and McAllister, 2002).

Two principal types of viral vectors exist: the simple capsid virions (comprising adenovirus and adeno-associated virus) and the enveloped virions (comprising retrovirus/lentivirus, alphavirus and herpes virus).

As the goal of this section is not to detail all characteristics of the different available viral vectors, Table 2 summarizes their principal features and Table 3 describes in a few words their main advantages and disadvantages [see also (Kay et al., 2001)]. Moreover, the interested reader is referred to several pertinent articles or reviews (see Table 3) dealing with the therapeutic applications of these vectors. The next paragraphs will give more details about the vector of interest in the present thesis, the Herpes simplex virus type 1.

	HSV recombinant	HSV Amplicon	Adenovirus	AAV	Retrovirus	Lentivirus
Virion Type	Herpes virus (dsDNA)	Herpes virus (dsDNA)	Adenovirus (dsDNA)	Parvovirus (ssDNA)	Retrovirus (RNA)	Retrovirus (RNA)
Particle size	120-300 nm	120-300 nm	80-120 nm	20-30 nm	100 nm	100 nm
Transgene capacity	30-50 kb	150 kb	20 kb	3.5-4 kb	7-8 kb	7-8 kb
Genomic Integration	Episomal 100%	Episomal 100%	Episomal 100%	Episomal 90%	Integrated	Integrated
Tropism	Broad; neurotropic	Broad; neurotropic	Strong for most tissues	Broad	Dividing cells only	Broad, including neurons
Duration of expression *in vivo*	Months	Days	Days	Months	Days to months	> 12 months

Table 2. Main technical features of the most widely viral vectors used in basic research and therapeutic applications. AAV, Adeno-associated virus; dsDNA, double stranded DNA; HSV, Herpes simplex virus; ssDNA, single stranded DNA. Adapted from (Davidson and Breakefield, 2003) and (Neve et al., 2005).

	ADVANTAGES	DISADVANTAGES
HSV recombinant	Neurotropic Transient transgene expression Episomal Transduces dividing and non-dividing cells Large transgene capacity Concentrates to high titers (10^8iu/ml) Ease of molecular manipulations	Immunogenic Some possible toxicity Instability of transgene expression
HSV amplicon	Neurotropic Transient transgene expression Episomal Transduces dividing and non-dividing cells Very large transgene capacity Low toxicity Low immunogenecity Concentrates to high titers (~10^8iu/ml) Ease of molecular manipulations	Requires co-propagation with HSV-1 helper virus
Adenovirus *Ref: A*	Broad host and cell type range Episomal Concentrates to very high titers (~10^{10}iu/ml) High levels of transgene expression Persistent transgene expression	Broad cell type range Elicits host immune response Small transgene capacity Difficult molecular manipulation Persistent transgene expression
AAV *Ref: B*	Broad host and cell type range Persistent transgene expression Not pathogenic or immunogenic Growth to high titers (>10^{12}iu/ml)	Broad host and cell type range Small transgene capacity
Retrovirus *Ref: C*	Persistent gene transfer Useful for cell marking / lineage analysis	Integrates into host DNA (insertional mutagenesis)
Lentivirus *Ref: D*	Integrates into host DNA Permanent transgene expression Stable expression Transduction of non-dividing cells	Integrates into host DNA (insertional mutagenesis) Permanent transgene expression Small transgene capacity Dangerous human pathogen

Table 3. Advantages and disadvantages of the currently used viral vectors. AAV, Adeno-associated virus; HSV, Herpes simplex virus, iu, infective units. Adapted from (Carlezon et al., 2000; Sena-Esteves et al., 2000; Neve et al., 2005). Concerning, HSV vectors, references will be given in the next paragraphs. For the other vectors, references are as follows: **A,** (Conner et al., 2001; Lotze and Kost, 2002; Turunen et al., 2002; Sapolsky, 2003; Graat et al., 2007); **B,** (Klein et al., 1998; Elliger et al., 1999; Ghodsi et al., 1999; Bankiewicz et al., 2000; Passini and Wolfe, 2001; Hemminki et al., 2002; Jin et al., 2002; Kang et al., 2007); **C,** (Rosenberg et al., 1988; Mohajeri et al., 1999; Blesch et al., 2002; Devroe and Silver, 2002; Strauss and Costanzi-Strauss, 2007) and **D,** (Kordower et al., 2000; Brooks et al., 2002; Georgievska et al., 2002; Palfi et al., 2002; Breckpot et al., 2007).

1.7. HERPES SIMPLEX VIRUS TYPE 1

1.7.1. The viral infection

Herpes simplex virus type 1 (HSV-1) belongs to the Group I of dsDNA viruses (ds: double stranded). In the virus classification, it also belongs to the *Herpesviridae* Family, *Alphaherpesviridae* Subfamily and *Simplexvirus* Genus. In humans HSV manifests itself in two common viral infections, each marked by painful, cold sores (*herpes labialis*) on the skin or mucous membranes such as the mouth or lips (HSV-1, oro-facial infections) or the genitals (HSV-2). The disease is contagious and incurable with present therapeutic possibilities. Nevertheless, some antiviral medications are used for controlling herpes outbreaks including acyclovir, pencyclovir, valacyclovir or famcyclovir (Arduino and Porter, 2006; Greco et al., 2007). Most primary infections are silent. In clinically apparent cases, vesicles usually develop between 1-3 days post exposure and remain localized to the site of inoculation. HSV-1 and HSV-2 can enter a lytic life cycle or establish a latent infection in the ganglia of the nerves supplying the epithelial site of the primary infection. The viral genome persists in the neuronal nuclei in an episomal (extrachromosomal) form; the only transcribed RNA appears to be that of the latency-associated transcripts (LATs). Latently infected neurons function normally and are not rejected by the immune system. Moreover, this state of latency may persist for many years. Reactivation may be provoked by several stimuli including sunlight, physiological stress, febrile illnesses, menstruation or immunosuppression. In this case, a cycle of viral replication occurs in the neuron (see Appendix 2) and viral particles are anterogradely transported to nerve terminals and reinfect the skin or mucous membranes in the area supplied by the nerve, initiating a recurrent disease (Divito et al., 2006).

In some very rare but serious situations, an infection can result in Herpes simplex encephalitis, leading (without treatment) to rapid death in 70% of the cases. Even with effective treatment, it is fatal in around 20% of cases, and causes serious long-term neurological damage in over half the survivors.

The herpes virus family comprises eight members known to cause human disease, including HSV-1 and HSV-2, but also the varicella-zoster virus (VZV or HSV-3), Epstein-Barr virus (EBV or HSV-4), cytomegalovirus (CMV of HSV-5), human B cell lymphatic virus (HSV-6), roseola poorly characterized virus (HSV-7) and the Kaposi's sarcoma-associated herpesvirus (KSHV or HSV-8).

1.7.2. Structure of HSV-1

The HSV-1 virion consists of an icosahedral nucleocapsid of about 100 nm in diameter, which is surrounded by a lipid bilayer envelope into which at least eight virus-encoded glycoproteins are incorporated. Between the capsid and the envelope is a layer of proteins, termed the tegument (Homa and Brown, 1997).

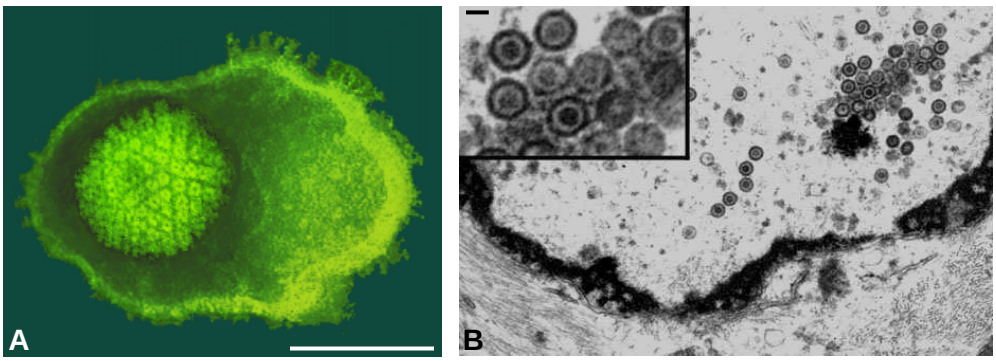

Figure 7. Electron micrograph pictures showing Herpes simplex viruses. **(A)** When the envelope breaks and collapses away from the capsid, negatively stained virions have a typical "fried-egg" appearance. **(B)** Picture showing HSV viral particles in neuronal nucleus. Both scale bars in A and B (insert) represent 100 nm.

1.7.3. Virus entry into the host cell

Binding of the viral particles at the cell membrane occurs due to interaction of viral glycoproteins (gB, gD, gH and gL are essential, while gC, gE, gG, gI, gJ, gK and gM seem to be dispensable *in vitro*) with host cell surface proteoglycans of the heparan sulfate (HS) class (Shieh et al., 1992). Initial binding of HSV-1 to cell surface HS is followed by gD-mediated attachment to a second receptor, the first of which has been shown to be a member of the TNFα/NGF receptor family. A number of other “mediators” have been identified, such as nectin-2, 3-O-sulfated HS or nectin-1, the latter being considered as the main HSV-1 entry receptor (Geraghty et al., 1998; Mata et al., 2001). This close binding results in host cell membrane/viral envelope fusion followed by penetration and release of the capsid into the cytoplasm of the host cell (Spear, 2004). Anchored on the host microtubule, the capsid is transported, thanks to cytoplasmic dynein associated to its co-factor dynactin, to nuclear pores, through which the viral DNA is transported into the nucleus (Dohner et al., 2006). The viral DNA is then associated to the α-TIF protein, which enhances the expression of immediate-early viral genes via cellular transcription factors (Frampton et al., 2005); [for a review, see (Burton et al., 2001a)].

1.7.4. Genome of HSV-1

HSV-1 contains a double-stranded DNA with a large genome of 152 kb encoding nearly 84 genes (Roizman, 1996) and more than 70 open translational reading frames (ORFs), so that the genetic map is rather complex [see Appendix 1 and (Frampton et al., 2005)].

The genome is arranged as unique long (U_L) and unique short (U_S) segments, each of which are flanked by inverted repeated sequences so that six important regions can be described:

- The "*a-sequences*", are present at the ends of the linear molecule and implicated in its circularization and in packaging the DNA into the virion;
- The "*long-repeat (L_R)*" segment is composed of 9 kb that encodes both an important immediate early regulatory protein (α0) and most of the genes for the latency associated transcript (LAT), as well as its promoter;
- The "*short-repeat (R_S)*" segment of 6.6 kb encodes the α immediate early protein. As a transcriptional activator, it acts along with α0 and α27 (in the U_L, see below) to stimulate the infected cell for all viral gene expression that leads to viral DNA replication;
- The "*Unique long (U_L)*" region, 108 kb, expresses at least 56 proteins some of which are DNA replication enzymes or capsid proteins;
- The "*Unique short (U_S)*" region encodes 12 ORFs, a number of which are glycoproteins important notably in response to host defense;
- The "*origins of replication (Ori_L)*", are situated in the middle of the U_L region and Ori_S in the R_S region. Both operate during infection to give a replication complex.

Viral gene expression occurs in a temporal cascade (Honess and Roizman, 1974), with immediate early (α) genes expressed first, followed by early (β) and then late (γ) gene expression. The products of α genes are infected cell proteins 0 (ICP0), ICP4, ICP22, ICP27 and ICP47, and are primarily involved in activation of the host transcriptional machinery as well as transcriptional regulation. β gene products are involved in viral DNA replication, and γ gene products primarily encode structural proteins. Details about the replication steps of HSV are given in Appendix 2.

HSV-1 is today widely used as a vector for gene transfer in basic research in an attempt to better understand physiological, behavioural or pharmacological mechanisms. In addition, however, it is also used in connection with possible

therapeutic applications. This latter use is especially due to its natural neurotropism and its ability to transfer large transgenes. Moreover, as it is able to initiate a long-term latent state as intranuclear episomes, it also avoids insertional mutagenesis (Glorioso et al., 1995; Glorioso and Fink, 2004). Thus, gene therapy utilizing genetically engineered HSV-1 is under active investigation for the treatment of both cancer and somatic diseases (Burton et al., 2001b; Burton et al., 2002, , 2005).

1.8. HSV-1 MEDIATED 5-HT_{1B} RECEPTOR GENE TRANSFER

1.8.1. HSV-1 Amplicon vectors

As already mentioned above, two types of replication-deficient HSV vectors are currently used. These include *genomic vectors* and *amplicon vectors*. Genomic vectors are those in which the foreign DNA is cloned into the viral genome itself.

Conversely, amplicon vectors are developed from a plasmid (amplicon) carrying the transgene, to which minimal HSV sequences are added that allow it to be packaged into virus particles with the aid of a helper virus (see also Methods). The idea of the amplicon vector originated with the discovery of defective HSV-1 particles that appeared in, and interfered with, HSV-1 stocks that were passaged at high multiplicities of infection. Examination of the genomes of these defective HSV-1 particles revealed that they carried only a minimal subset of DNA sequences from the wild-type genome (Spaete and Frenkel, 1982). It was found that incorporation of these sequences (“a” cleavage/packaging site and HSV origin of replication, ori_S) into a plasmid is sufficient to give it the ability to be replicated and packaged into viral particles when it is introduced into cells that are superinfected with wild-type virus (helper virus). For each recombinant viral particle, the plasmid is repeatedly replicated until a length of 150 kb is reached, resulting in particles that contain multiple concatemers of the original plasmid (Vlazny et al., 1982). One main advantage of the HSV amplicon vector is that cloning manipulations are relatively easy, due to the small size (5-10 kb) of the plasmid. Moreover, amplicon vectors accept very large transgenes (Table 3). The limitation of the vector is, that it has to be co-propagated with a HSV-1 helper virus resulting in stocks that are a mixture of helper and amplicon viruses. However, cytotoxic effects of these stocks limited the amount of vector used to infect cells. Moreover, wild-type HSV-1 revertants sometimes appeared during the amplicon

packaging process, exacerbating the cytotoxicity of the viral preparation. Fortunately, improvement of the packaging procedures has minimized cytopathic effects and immune responses of present-day defective HSV-1 amplicon vectors. In addition, helper virus-free packaging systems are available today (Fraefel et al., 1996; Carlezon et al., 2000; Sena-Esteves et al., 2000; Neve et al., 2005).

1.8.2. Transfer of the 5-HT_{1B} receptor gene

This paragraph will give some examples of successful 5-HT_{1B} receptor gene transfer using HSV-1 amplicon. This technique was used by Clark and co-workers (2002) to overexpress the 5-HT_{1B} receptor in serotonergic neurons from the dorsal raphé nucleus (DRN) while avoiding direct effects on the 5-HT_{1B} heteroreceptors expressed in non-serotonergic neurons (Clark et al., 2002). First of all, they confirmed the expression and biological activity of both transgenic proteins (GFP and 5-HT_{1B} receptor) *in vitro*. Indeed, after transfection of COS7 cells with the plasmid expressing both GFP and the epitope-tagged 5-HT_{1B} receptor, they showed expression of both proteins. Moreover, transfection into JEG-3 cells showed that the epitope-tagged 5-HT_{1B} receptor was able to inhibit adenylate cyclase thus being functionally active. Finally, they produced an HSV amplicon from the plasmids cited above and packaged it using replication-deficient HSV. These viral particles were transfected into PC12 cells and levels of 5-HT_{1B} mRNA were measured using RT-PCR. As regards viral particles stereotaxically injected in the DRN, these authors showed that the overexpressed 5-HT_{1B} receptors were translocated from the raphé nucleus to the forebrain; moreover they showed that overexpression of the 5-HT_{1B} receptor in these rats led to changes of their behaviour after inescapable stress, suggesting a role of this receptor in depression and anxiety (Clark et al., 2002). In order to better understand these effects of “stress context”, the same authors also used fear potentiation of startle in rats previously subjected to the intra-DRN injection of viral vectors expressing the 5-HT_{1B} receptor gene (Clark et al., 2004). In this case, the increased expression of 5-HT_{1B} receptor decreased the fear-potentiated startle ratio whereas previous stress-exposure normalized this ratio instead of increasing it, as expected by the authors. The authors were able to extend and to precise their previous results, as the fear potentiation of startle was shown to model a specific type of anxiety and to be dependent on the basolateral and central nuclei of the amygdala. Moreover, they concluded that the experimental situations used in the former series of tests involved more generalized anxiety while the latter depended more on specific situational fear (Clark et al., 2004).

The same group also reported that viral mediated increased expression of the 5-HT_{1B} receptor in nucleus accumbens shell neurons (NAcc) that project to the ventral tegmental area (VTA) induced behavioural sensitisation to cocaine. Indeed, the injection of 10 mg/kg of cocaine directly into the NAcc had more potent effects on locomotor stimulating effect of cocaine in rats injected with HA1B/GFP vector than in those injected with the GFP-only vector. Moreover, in a place conditioning paradigm, HA1B/GFP rats showed place preference for the cocaine-associated compartment at lower doses of cocaine (5 or 10 mg/kg) than GFP-only rats did (place preference at 10 and 20 mg/kg, 5 mg/kg were ineffective). By using such a gene transfer technique, these authors were able to conclude that mesolimbic 5-HT_{1B} receptors play an important role in the regulation of the motivational effects of cocaine. The authors assumed that the 5-HT_{1B} transgene receptor was expressed in the GABAergic medium spiny neurons that are the bulk of projecting neurons from the NAcc to the VTA (Neumaier et al., 2002; Barot et al., 2007). Finally, it was also shown that after injection of the viral vector expressing the 5-HT_{1B} receptor into the NAcc, rats increased their voluntary alcohol consumption without modification of their overall fluid intake or of their metabolism, thus supporting the notion that 5-HT_{1B} receptors in Nacc shell neurons axons mediate the increased ethanol consumption (Hoplight et al., 2006). Finally, (Tabbaa et al., 2005) have shown that HSV-1 is an effective vector to deliver genes in different regions of the mature mammalian brain. Indeed, they found, after *in vivo* injection of the vector into the medial septum/diagonal band of Broca, an expression of their reporter gene (ß-galactosidase) in the projection region of these structures, i.e., the neocortex.

As obvious from the aforementioned publications, HSV-1 mediated transfer of the 5-HT_{1B} receptor gene has been used to study the importance of autoreceptors, i.e., of the 5-HT_{1B} receptor on serotonergic neurons. In addition, however, the vector system has also been used to study the involvement of 5-HT_{1B} heteroreceptors following its injection into non-serotonergic regions of the brain: e.g. the nucleus accumbens. Thus, it has been shown that this technique of HSV-1 amplicon-mediated gene transfer is a useful tool to study the implication of the serotonergic system in the effects of drugs or in different behavioural paradigms.

Nevertheless, the *functional* consequences of an increased expression of the 5-HT_{1B} receptor on a more cellular level, especially its relevance for transmitter release modulation, have never been studied before. Moreover, to our knowledge, gene transfer-mediated overexpression of 5-HT_{1B} heteroreceptors in septohippocampal cholinergic neurons, which – as discussed above – are important in

serotonergic/cholinergic interactions in cognitive processes has never been investigated so far.

Thus, the first aim of the present thesis was to characterize the possibility to transfer the 5-HT_{1B} receptor gene in non-serotonergic neurons and to study the effects of the increased expression of the 5-HT_{1B} receptor protein in the target region of the injection site. To our knowledge, this work is the first to study both in vitro and in vivo effects of increased expression of the 5-HT_{1B} receptor in cholinergic neurons of the septal region.

1.9. 3,4-METHYLENEDIOXYMETHAMPHETAMINE (MDMA)

Effects of 3,4-methylenedioxymethamphetamine (MDMA) both *in vivo* and *in vitro* were studied in **Parts 2, 3 and 4** of the present thesis. Therefore the following sections are designed to summarize the present knowledge about the acute and chronic deleterious effects (and their mechanisms) of this drug of abuse.

1.9.1. Acute effects of MDMA in Humans

The amphetamine derivative 3,4-methylenedioxymethamphetamine (MDMA), commonly known as “ecstasy”, has become a popular recreational drug among young people, especially in the club culture. The drug was first patented in 1914 in Germany but its toxicology was only examined in the 1950s by the U.S. military. In 1978, Shulgin and Nichols reported that MDMA was psychoactive in humans and in the 1980s, MDMA started to be used in psychotherapy, in order to increase the self-esteem of patients and to facilitate therapeutic communication. In 1986, the drug became illegal. As with any illicit compound, both doses and purity of ecstasy tablets vary greatly (Ziporyn, 1986), but they have regularly been found to contain between 80 and 150 mg of MDMA. Current statistics (2005) show that in France, 2.8% of young girls and 4.2% of young boys aged of 17 consumed ecstasy in their lifetime at least once (OFDT, Observatoire français des drogues et des toxicomanies). Several studies on the use patterns of MDMA users were conducted or are still ongoing in different countries, and tend to show a very widespread use of this drug as well as an increase of its consumption (Solowij et al., 1992; Webb et al., 1996; Williamson et al., 1997; Winstock et al., 2001; Strote et al., 2002). Notably, it was reported that the majority of MDMA

users are poly-drug users (Gouzoulis-Mayfrank and Daumann, 2006), who frequently combine MDMA with substances such as alcohol, cannabis or other stimulants (amphetamine, cocaine).

The amphetamine derivative MDMA is structurally similar to the hallucinogenic compound mescaline and mediates feelings of euphoria, emotional openness, empathy, reduction of negative thoughts and decrease in inhibitions as well as an heightened perception of sound, colour and touch. Occurring 20 to 60 min after ingestion, the effects can last for 3 to 5 hours (Peroutka et al., 1988; Parrott and Lasky, 1998; Liechti and Vollenweider, 2000b). Besides such "positive" effects, which are the reasons for taking ecstasy pills, MDMA can cause diverse acute "negative" side effects during the peak period after MDMA ingestion: elevated blood pressure, increased heart rate (tachycardia) and temperature (hyperthermia), nausea, chills, sweating, tremor, muscles tension, insomnia, hepatotoxicity, cardiotoxicity, hypertension, hyponatremia (Peroutka et al., 1988; McCann et al., 1996; Mas et al., 1999; Parrott, 2001; Harris et al., 2002; Schifano et al., 2003; Freedman et al., 2005). Some reports stated that symptoms, such as increased systolic and diastolic blood pressure were attenuated by citalopram (a 5-HT reuptake inhibitor) pre-treatment, arguing for an implication of a carrier-mediated release of presynaptic 5-HT in these effects. A similar study concluded that haloperidol, a DA D_2 receptor antagonist, did not alter any of the physiological effects listed above (Liechti et al., 2000a; Liechti et al., 2000b; Liechti and Vollenweider, 2000b, 2000a). It should be emphasized, that hyperthermia was reported to be one of the main symptoms of acute MDMA-induced toxicity and that body temperatures of more than 43℃ were noted (Green et al., 1995; Green et al., 2004). Modifications of cerebral blood flow and brain activity were also observed and were mostly characterized by regional changes that could explain some of the psychological effects of MDMA (Gamma et al., 2000; Frei et al., 2001). In addition to the "positive" feelings mentioned above, adverse psychological effects were also observed after MDMA ingestion, including depression, irritability, panic attacks, visual hallucinations and paranoid delusions (Parrott and Lasky, 1998; Vollenweider et al., 2002; Parrott, 2004). Again, pre-treatment with a single high dose of citalopram inhibited most of the psychological effects of MDMA except for the MDMA-induced increases in emotional excitability and sensitivity, indicating that these effects of MDMA might *not* involve 5-HT uptake sites but could rather rely on the dopaminergic transmission (Liechti et al., 2000a; Tancer and Johanson, 2007).

1.9.2. Long-term effects of MDMA in Humans

Several studies showed severe depletion of striatal 5-HT and 5-HIAA in the brain of chronic users of MDMA (Kish et al., 2000). Moreover, examination of 5-HT binding sites with PET and 5-HT transporter ligands [^{11}C]McN-5652 showed a lower density of brain 5-HT transporter sites in MDMA users, which positively correlated with the extent of previous MDMA use (McCann et al., 1998; Ricaurte et al., 2000). Central 5-HT function has also been assessed by neuroendocrine challenge tests: intravenous infusion of D-fenfluramine (a specific 5-HT releasing agent) leads to an increase in serum prolactin and cortisol concentrations which is likely to occur via enhanced synthesis and release of 5-HT. The concentration of these two compounds were significantly lower in a MDMA user group as compared to control subjects (Gerra et al., 1998). After one year of abstinence, the prolactin concentration was still significantly lower in MDMA users and similar to that recorded previously (after three weeks of abstinence). These observations suggest the presence of a long-lasting impairment of brain serotonergic function in recreational users of MDMA (Gerra et al., 2000). It was also reported that chronic MDMA users have significantly lower levels of 5-HIAA in the cerebrospinal fluid (CSF) than control subjects, the reduction being greater in females than in males. Moreover, another group found than the 5-HIAA levels in the CSF decreased with increasing doses of MDMA (Bolla et al., 1998).

As regards long-term *physiological* effects of chronic use of MDMA, they include temporomandibular joint syndrome (affecting the joint of the lower jaw), dental erosion and myofacial pain (McCann et al., 1996). Long-term *psychologica*l effects of chronic use of MDMA have been shown to persist long after cessation of drug use. Thus, visual hallucinations and paranoid delusions can persist together with anxiety, depression, panic disorders and cognitive impairments (McCann et al., 1999; Parrott et al., 2000). It was also reported that problems in neuropsychological performances that occur in MDMA users, including impaired working memory and verbal recall, are not reversed by prolonged abstinence, suggesting a possible irreversible and selective neurotoxic lesion (Morgan et al., 2002). For a review on possible cognitive deficits, see (Green et al., 2003).

1.9.3. Relating animal to human data

Human clinical data on the effects of MDMA are more complicated to obtain due to ethical considerations, but also due to the fact that subjective effects have to be taken into account. Moreover, many subjects are poly-drug users so that it cannot be stated unequivocally that any effect identified results from MDMA solely. Finally, a significant percentage of ecstasy tablets also contain additional psychoactive compounds (e.g. ketamine).

In view of these considerations and although results obtained in animal models cannot be directly translated to humans (de la Torre and Farre, 2004; Easton and Marsden, 2006), they can give valuable informations on potential mechanisms, substrates or risks of drug interactions and rats seem to be a reliable subject for further analysis of the acute and long-term effects of drugs.

1.9.4. Acute effects of MDMA in rats

Locomotor activity

Today, it is well accepted that MDMA induces an increase in locomotor activity together with other symptoms related to the so-called “serotonin syndrome” (such as head-weaving, piloerection, forepaw treading, proptosis, penile erection, ejaculation, salivation and defecation). It was reported that MDMA-induced dose-related increase in locomotor activity was prevented by pre-treatment with fluoxetine (a selective 5-HT reuptake inhibitor) or with PCPA (p-chlorophenylalanine) the 5-HT synthesis inhibitor, indicating that 5-HT release plays a key role in this behavioural effects of the drug (Callaway et al., 1990; Daws et al., 2000; Bankson and Cunningham, 2002). Several reports aimed at identifying the receptor involved in the locomotor effect of MDMA. Thus, the MDMA-induced locomotor response was reduced following pre-treatment with the 5-HT_{2A} receptor antagonist MDL-100,907 implicating this 5-HT receptor in this phenomenon (Kehne et al., 1996). Moreover, blockade of the 5-HT_{2C} receptor by SB-242,084 enhanced the stimulant effect of MDMA (Fletcher et al., 2006), whereas blockade of 5-$HT_{2B/2C}$ receptors greatly enhanced MDMA-induced locomotion, indicating that this receptor normally has an inhibitory influence. In addition, it was demonstrated that 5-HT_{2C} receptors have a modulatory role on the locomotor response to MDMA and that activation of 5-HT_{2C} and 5-HT_{2A} receptors brings opposite effects (Bankson and Cunningham, 2002). Moreover, while the 5-HT_{1A} receptor was not found

to be implicated in the locomotor effects of MDMA, the 5-HT_{1B} seemed to be involved. Indeed, 5-$HT_{1A/1B}$ receptor agonists such as RU-24,969 and CGS-120,66B increased locomotor activity in rodents (Cheetham and Heal, 1993; Rempel et al., 1993) and MDMA-induced hyperactivity was blocked by the selective 5-$HT_{1B/1D}$ antagonist, GR-127,935 (McCreary et al., 1999; Bankson and Cunningham, 2002; Fletcher et al., 2002).

Even if these results seem reliable, the hyperactivity induced by MDMA is a very complex phenomenon and seems to implicate both 5-HT, DA and probably other components. For instance, Bubar et al., (2004) suggested that MDMA administration increased DA release via stimulation of D_1 and D_2 receptors and showed that both D_1 and D_2 antagonists partially reversed the hyperactivity produced by MDMA in rats (Bubar et al., 2004). In addition, it was found that 6-hydroxydopamine lesions of the DA terminals in the nucleus accumbens attenuated the MDMA-induced hyperactivity (Gold et al., 1989). Furthermore, it was demonstrated that the 5-$HT_{2A/2C}$ antagonist, ritanserin, significantly attenuated MDMA-induced DA release in the nigrostriatal pathway thus involving, at least in part, these receptors in the regulation of striatal DA efflux by MDMA (Yamamoto et al., 1995). Some perturbations of motor control were also shown to occur after MDMA treatment of rats (Marston et al., 1999).

Anxiety

With regard to anxiety-related behaviours, results are still controversial. For instance, using the elevated plus-maze, some authors reported an *anxiogenic* effect of MDMA (at doses of 1.25 - 5 mg/kg) whereas in other situations such as the social interaction test, MDMA produced an apparent *anxiolytic* response (Morley and McGregor, 2000; Ho et al., 2004; Ando et al., 2006).

Thermoregulation

A predominant physiological consequence of MDMA application to animals remains a modification in thermoregulation depending on the ambient temperature (Dafters and Lynch, 1998; Green et al., 2004; Green et al., 2005). After a single MDMA injection in rats, a hyperthermic response occurred at ambient room temperature (24℃), whereas a hypothermic response was seen at ambient temperature of 11℃ (Dafters, 1994). In more detailed studies, it was shown that following single MDMA injections hyperthermia occurred at 22℃ but hypothermia at 17 ℃: thus the switching point, which decides in between MDMA-induced hyper- or hypothermia, seems to be near the normal ambient room temperature (20℃) (Dafters and Lynch, 1998).

In order to understand the mechanisms by which MDMA raises body temperature, it was shown that a dose which induced an increase in rectal temperature did not modify the temperature of the rat tail (Mechan et al., 2002b). Since vasodilatation of the rat tail vessels is a major mechanisms by which rats lose temperature (Grant, 1963), these results suggest that MDMA interferes with heat loss mechanisms and consequently, the higher the ambient temperature, the more impaired the ability to lose heat to the environment. There is today major evidence that MDMA induces the release of 5-HT and DA from their respective terminals and assumptions were made that hyperthermia was associated with increased 5-HT release (Shankaran and Gudelsky, 1999). Administration of L-tryptophan and a monoamine oxidase inhibitor, hence an increase in 5-HT release and synthesis, resulted in hyperthermia (Nisijima et al., 2004). Moreover, p-chloroamphetamine, another 5-HT releasing drug, also produces hyperthermia (Colado et al., 1993).

Multiple 5-HT receptor subtypes appear to contribute to the pyretic effects of MDMA, within which, the role of the 5-HT_2 subtype has been confirmed. Indeed, activation of 5-HT_{2A} receptors increases both body temperature and cutaneous sympathetic nerve activity in rabbit (Blessing and Seaman, 2003). Other data showed attenuation of MDMA-elicited hyperthermia by 5-HT_{2A} antagonists (Nash et al., 1988; Schmidt et al., 1990). Nevertheless, more recent studies favour the implication of the dopaminergic system in the hyperthermic response to MDMA. Thus, although administration of the 5-HT reuptake inhibitor fluoxetine produced a major inhibition of MDMA-induced 5-HT release, it had no effect on its hyperthermic response (Sugimoto et al., 2001; Mechan et al., 2002b). Moreover, the same authors found that most 5-HT receptor antagonists but also the dopamine D_2 receptor antagonist remoxipride failed to antagonise the MDMA-induced hyperthermia. In contrast, the dopamine D_1 receptor antagonist SCH-23,390 proved to be an effective blocker of the hyperthermic response of MDMA. Therefore, it was suggested that MDMA-induced hyperthermia results from an increased release of DA that in turn acts at D_1 receptors to increase the core temperature [for a review, see (Green et al., 2004)].

It should be noted that behavioural and physiological effects of MDMA observed in rats are associated with changes of monoamine concentrations in the brain [for review, see (Green et al., 2003)]. Indeed, systemic administration of MDMA to rats affects the function of different monoamine transporters, such as that for 5-HT reuptake (SERT), with the highest potency, but also that for DA (DAT) and NA transport (Battaglia et al., 1987).

Acute effects of MDMA on serotonergic function

In vivo microdialysis showed that administration of MDMA to rats induces an acute and rapid release of 5-HT (Yamamoto et al., 1995; Gudelsky and Nash, 1996; Sabol and Seiden, 1998; Mechan et al., 2002b) as well as a marked decrease of brain 5-HT concentrations although with some delay (Colado and Green, 1994; Aguirre et al., 1995; Connor et al., 1998). The dose-related increase in extracellular concentration of 5-HT in the striatum and medial prefrontal cortex (Gudelsky and Nash, 1996) or the hippocampus (Mechan et al., 2002a) was shown to be attenuated by pre-treatment with 5-HT reuptake inhibitors, indicating that MDMA-induced 5-HT release involves a carrier-mediated mechanism. The 5-HT-releasing properties of MDMA were also demonstrated *in vitro* using different preparations, such as synaptosomes from the frontal cortex or hippocampus (Berger et al., 1992; O'Loinsigh et al., 2001) and striatal slices (Schmidt, 1987b). Also *in vitro*, this MDMA-induced 5-HT release was shown to rely on a carrier-mediated mechanism. Moreover, MDMA was shown to bind the 5-HT transporter with a high affinity (Steele et al., 1987; Battaglia et al., 1988b). In addition, MDMA inhibits tryptophan hydroxylase (TPH), the rate limiting enzyme required for 5-HT synthesis (Stone et al., 1987a; Stone et al., 1987b; Schmidt and Taylor, 1988; Johnson et al., 1992a; Che et al., 1995).

Several hypotheses were proposed to understand the mechanism of the inhibitory action of MDMA on TPH. For instance, it has been shown that depletion of DA in the CNS by administration of AMPT (α-methyl-*p*-tyrosine), or reserpine, or by selective lesion of the nigrostriatal DA projections with 6-hydroxydopamine (6-OHDA), partially blocked the MDMA-induced reduction of TPH activity (Stone et al., 1988). Although a single, direct, central injection of MDMA did not alter cortical or striatal TPH activity, a continuous i.c.v. infusion of the drug for 1h resulted in a significant reduction in TPH activity, suggesting a peripheral generation of an active metabolite responsible for the effects of MDMA (Schmidt and Taylor, 1988). The possible involvement of Ca^{2+} influx has also been suggested (Johnson et al., 1992a). Finally, it was also proposed that the hyperthermia caused by MDMA (see above) can influence the activity of TPH. In fact, a significant reduction of TPH activity was observed in hippocampus, striatum and frontal cortex of hyperthermic animals after MDMA administration at an ambient temperature of 25°C, whereas no modification of the enzyme activity was noticed in hypothermic animals (MDMA administration at 6°C) (Che et al., 1995). These findings support the hypothesis of a participation of free radicals in these effects, as free radical formation is enhanced by hyperthermia (Colado et al., 1999a). Finally, similarly to other amphetamine analogs, MDMA also inhibits the catabolic enzymes monoamine oxidase

A and B (MAO-A, MAO-B), thus reducing the metabolism of both 5-HT and DA in nerve terminals, thereby also contributing to the increased release of these transmitters (Leonardi and Azmitia, 1994).

Acute effects of MDMA on dopaminergic function

In vivo microdialysis experiments and *in vitro* studies showed that MDMA administration also increased the release of DA from cerebral tissue (Nash and Brodkin, 1991; Nash and Yamamoto, 1992; Gudelsky et al., 1994; Yamamoto et al., 1995; Koch and Galloway, 1997; Sabol and Seiden, 1998). In contrast to the carrier-mediated mechanism involved in MDMA-induced release of 5-HT, however, the implication of DA reuptake sites in the releasing effect of MDMA on DA remains controversial. Even if MDMA is able to bind to the DA transporter (DAT) (Steele et al., 1987; Battaglia et al., 1988b), the drug was suggested to enter dopaminergic nerve endings by diffusion rather than via DAT (O'Shea et al., 2001). On the other hand, when MDMA was directly injected into the brain or added on brain slices preparations, GBR12,909, a highly selective DA uptake inhibitor prevented the DA release induced by MDMA (Nash and Brodkin, 1991; Koch and Galloway, 1997). On the contrary, using *in vivo* microdialysis, it was shown that after peripheral MDMA administration, the same antagonist produced a further increase in the release of DA (Mechan et al., 2002b).
In addition, increased 5-HT release induced by MDMA was suggested to be involved in the effect of MDMA on DA release, at least in the striatum. Indeed, pre-treatment with fluoxetine significantly attenuated the MDMA-induced DA release in this structure (Gudelsky and Nash, 1996; Koch and Galloway, 1997). Moreover, the 5-HT_2 receptor was implicated in this effect, as the presence of the selective 5-HT_2-agonist 2,5-dimethoxy-4-iodoamphetamine (DOI) potentiated the MDMA-induced DA release in striatal slices (Gudelsky et al., 1994). Finally, following central infusion of ritanserin (a 5-$HT_{2A/2C}$ receptor antagonist), a significant attenuation of MDMA-induced DA release was observed in both substantia nigra and striatum, indicating a modulation of MDMA-induced DA release via 5-$HT_{2A/2C}$ receptors, but probably also via modulation of the GABAergic innervation of the substantia nigra (Yamamoto et al., 1995).

Acute effects of MDMA on noradrenergic function

In vitro, MDMA has been found to induce an increase of both basal and stimulated [^{3}H]-NA from brain tissue, an effect that was blocked by desipramine (Fitzgerald and Reid, 1990). The same effect was observed on synaptosomal preparations (Rothman et al., 2001). Short-term changes were also noticed in the firing rate of noradrenergic neurons

of the locus coeruleus (Arrue et al., 2003). Nevertheless, the effects of MDMA on noradrenergic transmission *in vivo* are unclear due to lack of experimental datas.

Further acute effects of MDMA

Direct evidence for the formation of free radicals in the brain followed by neurotoxic damage was provided by Colado et al. (1997), using *in vivo* microdialysis in the hippocampus. The activation of 5-HT transporters and serotonergic nerve endings seems to be responsible for this effect (Colado et al., 1997; Shankaran et al., 1999, , 2001). Finally, MDMA was shown to induce the expression of immediate early genes such as Fos, egr-1 and Arc in several brain structures such as the cortex, striatum and thalamus (Green et al., 2003).

1.9.5. Long-term effects of MDMA in rats

Neurotoxic effects

Much evidence has been provided, suggesting a long-term depletion of 5-HT and its metabolite 5-HIAA in the brain following administration of MDMA (Green et al., 2003). Despite the fact that the dose required to induce neurotoxicity is strain-dependent, some general observations were made. Subsequent to an initial decrease in 5-HT content, resulting from acute MDMA-induced 5-HT release, concentrations return toward pre-treatment levels within 24h. Thereafter, a second phase of depletion is visible one week post-treatment (Schmidt, 1987a). Other studies indicated that high or frequent doses of MDMA are necessary to produce neurotoxic signs in the rat brain, such as reduction of 5-HT and 5-HIAA levels or of binding of [^{3}H]-paroxetine to 5-HT transporters (O'Shea et al., 1998). Long-term effects of MDMA administration were also shown to include a reduction in the activity of TPH (Stone et al., 1987b). In addition to these biochemical datas, also histological studies confirmed the loss or at least weakening of serotonergic functions after MDMA administration. Thus, it has been shown that the density of serotonergic axons in brain regions such as the cortex, striatum and thalamus was reduced (O'Hearn et al., 1988). Moreover it has been observed, that neuronal axons and terminals rather than cell bodies were predominantly affected by MDMA (Battaglia et al., 1991; Schmued, 2003), even if other reports questions this issue (Wang et al., 2004). A comprehensive study attributed neurotoxicity to metabolites of MDMA (Esteban et al., 2001). For a recent review on MDMA-induced neurotoxicity, see (Baumann et al., 2007).

Regarding the spontaneous recovery of such neuronal damage, contradictory results were obtained; while a complete recovery of 5-HT and 5-HIAA contents was seen in all brain regions after one year (Battaglia et al., 1988a; Scanzello et al., 1993), other studies indicated a region-dependent recovery of 5-HT depletion (Lew et al., 1996; Sabol et al., 1996). Experiments using centrally applied MDMA clearly argue in favour of the involvement of metabolite(s) in neurotoxicity. Indeed, while a centrally administered high concentration of MDMA caused a release of 5-HT, it failed to induce neurodegeneration of 5-HT terminals. Such findings suggest that MDMA must be metabolised peripherally and that the resulting compounds will then induce free radical formation and neurotoxicity in the brain (Esteban et al., 2001). As mentioned above, it also appeared that MDMA-induced neurotoxicity is dependent on body temperature, with hypothermia having a protective effect. Moreover, it was shown that free radical formation in the brain following MDMA administration is greatly enhanced in hyperthermic animals thus supporting the hypothesis that free radicals formed especially under hyperthermic conditions are responsible for the neurotoxic effect of MDMA (Colado et al., 1998).

Concerning the DA content in the brain following treatment with MDMA, several studies suggested no toxicity of MDMA to dopaminergic nerve terminals (Lew et al., 1996; Sabol et al., 1996; Colado et al., 1997; Colado et al., 1999b).

Behavioural and physiological effects

Repeated administrations of MDMA were also shown to produce long-term physiological and behavioural changes. As regards *body temperature*, conflicting data were obtained and sensitisation to a second dose of MDMA (Dafters and Lynch, 1998) as well as attenuation (Shankaran and Gudelsky, 1999) or no change were observed. Nevertheless, evidence was given that prior administration of several doses of MDMA altered the ability of rats to regulate their body temperature when exposed to a high-temperature environment (Mechan et al., 2001).

Concerning *locomotor activity*, controversial observations were made. For instance, after a regimen of MDMA (at 5, 10 or 20 mg/kg twice daily for 4 days), locomotor activity returned to baseline/control values within 48h after cessation of the drug administration, although it was higher in MDMA-treated rats during the period of drug treatment (McNamara et al., 1995). In contrast, other authors reported a reduction in locomotor activity of the rats one week after multiple doses of MDMA given within one day a few hours apart from each other (Wallace et al., 2001).

Behavioural data also showed *cognitive impairments* of MDMA-treated rats in the performance of the DNMTP test (Marston et al., 1999), suggesting that these deficits were attributable to serotonergic dysfunction. Moreover, MDMA exposure during brain development led to dose-related impairments of sequential learning and spatial learning and memory (Broening et al., 2001).

Finally, studies on prior MDMA exposure on *anxiety* in various models provided conflicting results. For instance, Morley and co-workers (2001) found in the elevated plus maze and social interaction tests that rats treated 3 months earlier with MDMA showed more anxiety than control rats (Morley et al., 2001). On the contrary, both an increased time in the “open-field” and an apparent anxiolytic response in the elevated plus maze were seen when rats were tested 73 to 80 days after a neurotoxic dose of MDMA (Mechan et al., 2002a). On the other hand, none of these authors measured 5-HT content in the CNS following the neurotoxic regimen of MDMA given to rats, and strain differences in the rats used may also explain the conflicting datas obtained. However, the study of Morley (2001) has been repeated and clear evidence also for a loss of 5-HT was given (Gurtman et al., 2002), confirming previous findings that 5-HT depletion can result in either anxiolytic or anxiogenic effects.

1.10. EFFECTS OF ETHANOL

As mentioned above, ecstasy users frequently consume MDMA together with other drugs of abuse. Certainly, one of the most frequent combinations of MDMA abuse is that with ethanol (EtOH). Since in **Parts 2, 3 and 4** of the present thesis especially the effects of the *combination* of MDMA with EtOH will be studied both *in vivo* and *in vitro*, the following chapters will summarize the current knowledge about the effects of EtOH *alone* or *in combination with MDMA* on the *in vitro* and *in vivo* parameters of special interest to the present work.

1.10.1. General effects and involvement of the 5-HT_{1B} receptor

General effects

Especially due to its easy availability, alcohol has become a plague in human beings in terms of excessive consumption and the physiological, behavioural and social consequences linked to this consumption. In rats, it has been shown that peripheral

administration of increasing doses of EtOH induced sedation, ataxia and bradykinesia. It was underlined that lower doses of EtOH were needed to show reduced locomotion and slowing of operant responding (respectively 0.25 and 1 g/kg) as compared to ataxia or sedation. The latter effects were measured by the rotarod technique and appeared after i.p. injection of 2.0 g/kg EtOH (Chuck et al., 2006). Other behavioural effects of EtOH were also observed, such as memory disruption (Givens, 1995), alterations in motor coordination [e.g. (Gallate et al., 2003) but see (Metz et al., 2003)] or anxiety-related behaviours (Ryabinin, 1998; Langen et al., 2002; Gallate et al., 2003).

Involvement of 5-HT$_{1B}$ receptors

Interestingly, the 5-HT$_{1B}$ receptor, one of the main topics of the present thesis, has been associated with alcohol abuse in both human and animal models. Thus, it has been suggested that the serotonin 5-HT$_{1B}$ receptor plays a role in modifying the reinforcing (McBride et al., 1993; Crabbe et al., 1996; Risinger et al., 1996), intoxicating (Crabbe et al., 1996) and discriminative stimulus effects of EtOH (Grant and Colombo, 1993; Grant et al., 1997; Porcu and Grant, 2004), as well as in regulating its voluntary intake (McBride et al., 1993; Crabbe et al., 1996; McBride et al., 1997). Evidence supporting a role of the 5-HT$_{1B}$ receptor in mediating the effects of EtOH came from various studies. Polymorphisms in the 5-HT$_{1B}$ receptor gene have been linked to antisocial personality and alcoholism in humans (Lappalainen et al., 1998). For instance, lower densities of the 5-HT$_{1B}$ receptor were found in the cortex, septum and amygdala of alcohol-preferring P lines of rats (McBride et al., 1997). Furthermore, the involvement of 5-HT$_{1B}$ receptors in alcohol drinking behaviour is further supported by observations showing decreased alcohol consumption after treatment with 5-HT$_{1B}$ agonists (Higgins et al., 1992; Tomkins and O'Neill, 2000; Wilson et al., 2000). In addition, 5-HT$_{1B}$ receptor KO mice showed an increased voluntary alcohol consumption and higher sensitivity to some ataxic effects of alcohol as compared to their wild-type littermates [(Crabbe et al., 1996; Boehm et al., 2000) but see (Bouwknecht et al., 2000)]. Nevertheless, the results of experiments involving 5-HT$_{1B}$ receptor KO mice are still controversal as some experiments did not support these effects (Crabbe et al., 1999; Gorwood et al., 2002).

From a neurochemical point of view, several lines of evidence suggest that DA neurons in the ventral tegmental area (VTA) are important for the reinforcing effects of EtOH and for its self-administration (Brodie et al., 1999; Yan, 1999). Interestingly, activation of 5-HT$_{1B}$ receptors in the VTA has been reported to increase DA release in the

ipsilateral nucleus acumbens (NAcc) (Yan and Yan, 2001b; Yan et al., 2004a). Therefore, the reported suppression of alcohol intake by 5-HT_{1B} receptor agonists (see above) may be due to the 5-HT_{1B} receptor activation-induced potentiation of the effect of EtOH on mesolimbic DA neurons, which leads to reduced amounts of alcohol consumption to produce similar CNS effects (Yan et al., 2005). Recently, using virally-mediated gene transfer of the 5-HT_{1B} receptor, the group of John Neumaier showed an increased voluntary alcohol consumption after increased expression of the 5-HT_{1B} receptors in the NAcc (Hoplight et al., 2006).

1.10.2. Effects of ethanol on neurotransmitter release

When given systemically, EtOH increases both the release of DA and 5-HT in the NAcc (Di Chiara and Imperato, 1988; Yoshimoto et al., 1992). Although the mechanisms underlying this increase remain unclear, there is some evidence showing that a local action of EtOH may contribute to (but certainly not exclusively account for) the stimulation of DA release. For instance, retrodialysis of EtOH into the NAcc and VTA results in increased release of DA, which is lasting for slightly more than 2 hours, and which then returns to baseline levels *even before* EtOH has been eliminated from blood (Yim et al., 1998; Lof et al., 2007). *In vitro*, it was shown that application of EtOH to brain slices which include the VTA resulted in a concentration-dependent increase of the firing of dopaminergic neurons (Gessa et al., 1985; Brodie et al., 1990). Interestingly, the excitation of VTA dopaminergic neurons elicited by cocaine was also enhanced by EtOH (Bunney et al., 2000). Moreover, local application of EtOH increased the release of DA also in the striatum (Wozniak et al., 1991). In this context it should be mentioned, that EtOH-sensitive sites were found on the DA transporter when expressed in xenopus oocytes or HeLa cells (Maiya et al., 2002).

The release of 5-HT is also enhanced by local application of EtOH (Yan et al., 1996), although this effect was sensitive neither to the absence of calcium, nor to the presence of tetrodotoxine. Such observations suggest that, at least in this study, the EtOH-induced 5-HT release was non-exocytotic and independent of action potential propagation. It is noteworthy, however, that given systemically, EtOH decreases the firing rate of 5-HT neurons in the dorsal raphé, but increases 5-HT release in caudate-putamen, suggesting that this release of 5-HT could in fact depend on a mainly local action of EtOH (Thielen et al., 2001). Other studies, based on local application of EtOH, support this issue at least for the VTA, as they show a facilitation of 5-HT release by EtOH [e.g.(Yoshimoto et al., 1992)]. Interestingly, based on electrophysiological

recordings in VTA-containg slices, 5-HT was described to potentiate the EtOH-induced activation of VTA neurons (Brodie et al., 1995).

Taken together all these data suggest, that under certain conditions, the effects of EtOH on the release of DA and/or 5-HT may partly rely upon local mechanisms, which, of course, does not mean that *only* local mechanisms account for all effects observed after systemic administration of EtOH. For instance, according to a recent study by (Lof et al., 2007), it has been suggested that indirect, secondary mechanisms involving ACh in the VTA, and more particularly the activation of nicotinic receptors in this region, could also take part in the increased DA release within the NAcc; in that context, it is notworthy that DA release, as shown *in vitro* (Grady et al., 1992; Grady et al., 1994; Grady et al., 2002; Quik et al., 2003; Cao et al., 2005), can be elicited by activation of presynaptic nicotinic heteroreceptors on dopaminergic terminals in various brain regions (Wonnacott, 1997; Wonnacott et al., 2000). Finally, it was also argued that NMDA receptor-evoked release of ACh was reduced in the presence of EtOH (2-6‰) (Darstein et al., 1998).

1.11. EFFECTS OF MDMA IN COMBINATION WITH ETOH

As noted above, MDMA is one of the most popular recreational drugs among young people and it appears that, presumably to boost its effects, the combination of MDMA with other drugs of abuse (Scholey et al., 2004) like amphetamine, cocaine, cannabis, and EtOH, is a frequent pattern of MDMA consumption in human beings. Due to both its social role and easy availability, EtOH seems to be that drug, which is most frequently combined with MDMA (Pedersen and Skrondal, 1999; Hernandez-Lopez et al., 2002; Lora-Tamayo et al., 2004; Schifano, 2004). For instance, investigations in Australia (Topp et al., 1999) or Spain showed that 40-60% of MDMA users consume alcohol before or simultaneously. To give another example, a study of MDMA users admitted in a hospital in Zürich found that 51.9% of them had consumed EtOH in combination with MDMA (Liechti et al., 2005). In view of these facts, it is surprising that informations about the effects (and their mechanisms) of this combined abuse are rather sparse.

For instance in humans, it was shown that the combination of MDMA and EtOH induced a longer lasting euphoria and prolonged feelings of well-being than when MDMA is consumed alone. Moreover, the subjective sensation of sedation caused by alcohol was reduced in the presence of MDMA, whereas feelings of alcohol-induced

drunkenness and the impairment of psychomotor performances (objective measure of intellectual efficiency and sedation) were unchanged (Hernandez-Lopez et al., 2002). Experiments investigating acute effects of the combination of EtOH with MDMA suggested that potentiating effects could be perceived subjectively, presumably by pharmacodynamic and/or pharmacokinetic interactions (Oesterheld et al., 2004). Data concerning impulsivity during and after intoxication with MDMA in combination with EtOH are controversial, possibly due to differences in the subjective tests used, which indicate both decreases and increases in impulsivity (McCann et al., 1994; Butler and Montgomery, 2004). Using behavioural measures of impulsivity (defined by the inability to anticipate and reflect on the consequences of decision making, or by the failure to inhibit a response in a rapid response task), MDMA acutely decreases motor impulsivity due to improvement in impulse control. Alcohol increased the proportion of commission errors, which reflects, according to the authors, an impairment of perceptual or attentive processing rather than an increase of motor impulsivity *per se*. Interestingly, none of the behavioural measures of impulsivity showed a MDMA x EtOH interaction effect. This lack of interaction appears to indicate that the CNS stimulant effects of MDMA were never sufficient to overcome alcohol-induced impairment of impulse control or risk-taking behaviour (Ramaekers and Kuypers, 2006).

Another study showed that the combination of MDMA with EtOH also affects the immune system; T cells of the CD4 type were suppressed, the reduction of B lymphocytes was weaker than that observed when EtOH was given alone. Moreover, the equilibrium between pro-inflammatory (Interleukin-1β, TNFα, IL-6) and anti-inflammatory (IL-4, IL-10 and TGFβ) cytokines was shifted towards immunosuppression (Pacifici et al., 2001).

As regards pharmacokinetic aspects, it is noteworthy that MDMA or EtOH seem to influence the plasma concentration of the other drug when given in combination. Indeed, plasma levels of MDMA are increased by 13% in the presence of EtOH whereas the plasma concentration of EtOH is decreased by 9 to 15% after MDMA administration (Hernandez-Lopez et al., 2002).

Recently, also our own group became interested in the psychomotor and pyretic effects of the combination of MDMA with EtOH. We observed, that EtOH (1.5 g/kg, i.p.) potentiated the psychomotor effects of MDMA (10 mg/kg, i.p.), while it attenuated its pyretic effects (6.6 mg/kg, i.p.) (Cassel et al., 2004). It was one of the aims of the present thesis to explore the mechanism(s) of this pharmacological interaction on a more neuropharmacological level.

1.12. AIMS OF THE PRESENT THESIS

As outlined in more details in the previous sections of the Introduction, it was the aim of the present work to explore the following questions:

Part 1:

In view of the importance of 5-HT_{1B} receptors for serotonergic-cholinergic interactions both in cognition and in the presynaptic modulation of ACh release, this part of the thesis explores the model of an enhanced expression of this 5-HT_{1B} receptor in cholinergic neurons, both *in vitro* (primary cholinergic cell cultures) and *in vivo* (septohippocampal cholinergic neurons). The main question to be answered in this part was: can the overexpression of the 5-HT_{1B} heteroreceptor in cholinergic neurons following HSV-1-mediated gene transfer be demonstrated both immunocyto-chemically and functionally, and more particularly in transmitter release experiments.

Part 2:

Herein, we further investigated the behavioural and functional consequences of a treatment of rats with MDMA, either alone or in combination with EtOH. A special question to be answered was whether the combined pretreatment with these drugs of abuse will lead to functional changes in the presynaptic 5-HT_{1B} autoreceptor-mediated modulation of 5-HT release in the cortex or hippocampus of rats several weeks after suspension of drug administrations. Thus, again the 5-HT_{1B} receptor will be in the focus of interest.

Part 3:

This part aimed at exploring the pharmacological interaction of MDMA with EtOH. However, the focus is now on direct presynaptic effects in transmitter release models *in vitro*. We have tried to answer the following questions: does the direct combination of MDMA with EtOH *in vitro* affects the release of 5-HT in tissue slices of the rat hippocampus, cortex and striatum? Is the striatal release of DA or ACh affected by this combination?

Part 4:

In view of the possibility, which was studied in the first part of the thesis, to use a targeted gene transfer technique to explore the functional role of 5-HT_{1B} receptors in selected behavioural paradigms, this part now integrates (at least part) the knowledge

obtained from the previous sections, although the technique does not focus on the same population of neurons. There the question was: does an increased expression of the 5-HT_{1B} autoreceptor in serotonergic axon terminals (following stereotaxic injection of the HSV-1 vector into the dorsal raphé nucleus) affect the locomotor response of MDMA injected either alone or in combination with EtOH.

2. MATERIALS & METHODS

2.1. EXPERIMENTAL ANIMALS

All procedures involving animals and their care were conducted in conformity with the institutional guidelines that are in compliance with national (France: council directive 87848, October 19, 1987, Ministère de l'Agriculture et de la Forêt, Service Vétérinaire de la Santé et de la Protection Animale; permission 67-215 to J-C.C.; Germany: DtTSchG, 25.5.1998, last modification: 21.6.2005 and the European Communities Council Directive of 24 November 1986 (86/609/EEC) and international (NIH publication 5586-23, revised 1985) laws and policies. All efforts were made to minimize animal suffering and to reduce the number of animals used with respect, however, of the statistical constraints.

Pregnant female rats

Donors for the preparation of primary septal cell cultures were female Wistar rats (**Part 1**). They were kept in an animal house (University of Freiburg, Zentrale Tierhaltung, Stefan-Meier-Straße 8) in Macrolon® cages in a room with controlled temperature and 12:12h light/dark cycle. All female rats had a regular cycle and showed clear signs of impending ovulation. Male and female rats were mated overnight and separated the next morning (= day 1 of pregnancy). Pregnant females were kept in separated cages until the 17^{th} day of pregnancy, the day on which they were used for the preparation of septal cell cultures (see 2.4.).

Virus-injected male rats

Male rats of the Long-Evans breed were used for these *in vivo* experiments (**Part 1**). When arriving from France (Centre d'Elevage R. Janvier, Le Genest St-Isle), they were brought and kept in an animal house (University of Freiburg, Zentrale Tierhaltung, Stefan-Meier-Straße 8) in individual transparent Macrolon® cages (42 × 26 × 15 cm) in temperature-controlled rooms that were maintained on a 12:12h light/dark cycle (light on at 7:00) under controlled temperature (19° ± 1℃). The rats were housed with *ad libitum* access to food and water throughout the experiment. All rats were aged of 3 months at the time of surgery.

Rats used to study long-term effects of MDMA +/- EtOH administration

Thirty-one adult male Long-Evans rats (Centre d'Elevage R. Janvier, Le Genest St-Isle) were used for this experiment (**Part 2**). They were all aged of 3 months at the time of

injections. Rats were housed individually in transparent Makrolon® cages (42 × 26 × 15 cm) under controlled temperature (23°C) and a 12:12 h light/dark cycle (lights on at 7:00). Food and water were provided *ad libitum*. After arrival in the laboratory, animals were allowed to acclimate for one week before the experiments were started.

Drugs and treatments procedures: EtOH (20% [w/v]) was prepared from absolute EtOH diluted in 0.9% NaCl and injected intraperitoneally (i.p.) at a dose of 1.5 g/kg. At this dose, EtOH typically results in a blood concentration of about 175 mg/dl (i.e., 1.75‰). MDMA (3,4-methylenedioxymethamphetamine) was diluted in 0.9% NaCl and injected i.p. at a dose of 10 mg/kg. The drugs, whether administered alone or in combination, were injected at a volume of 7.5 ml/kg. For the combined administration, MDMA was dissolved in the 20% EtOH solution. On four subsequent days, 24h apart, rats were treated with one of the drugs or their combination. These rats were tested for body temperature changes during the first hours after treatment administration and – at other defined delays following treatment – in behavioural paradigms [T-maze alternation, beam-walking, elevated-plus-maze]. Some rats were also killed by microwave irradiation to measure (by HPLC with electrochemical detection) catecholamine levels (NA, DA, DOPAC) in defined brain structures. Finally, in between 3 and 6 weeks following pre-treatment with the MDMA ± EtOH, the animals were killed by decapitation, their brains removed and dorsal parts of both hippocampi and of the frontoparietal cortex were cut in slices to assess the evoked [^{3}H]-5-HT release.

Rats used to study in vitro effects of MDMA +/- EtOH

Male rats of the Long-Evans strain were used for these experiments (**Part 3**). When arriving from France (3-4 months; Centre d'Elevage R. Janvier, Le Genest St-Isle), they were brought and kept in an animal house in individual transparent Macrolon® cages (42 × 26 × 15 cm) in rooms that were maintained on a 12:12h light/dark cycle (light on at 7:00) under controlled temperature (23°C). The rats were housed with *ad libitum* access to food and water until the experiment. In these experiments, they were killed by decapitation, their brains quickly removed and dissected. Subsequently we studied the effects of MDMA ± EtOH on the spontaneous outflow and electrically-evoked overflow of [^{3}H]-5-HT in striatal, hippocampal and frontoparietal cortex slices as well as that of [^{3}H]-DA in striatal slices.

Rats used to study effects of MDMA +/- EtOH following targeted gene transfer

Adult male Long-Evans rats (3 months; Centre d'Elevage R. Janvier, Le Genest St-Isle) were used for this experiment (**Part 4**). When arriving at the laboratory, they were kept in individual transparent Makrolon cages (42 × 26 × 15 cm) under controlled temperature (23°C) and a 12:12h light/dark cycle (lights on at 7:00). Food and water were provided *ad libitum*. After their arrival, rats were allowed to acclimate for one week before being daily handled by an experimenter for 3 days. These rats were first subjected to unilateral implantation of a cannula in the dorsal raphé before being injected (about 11 days later) with the viral vectors. Afterwards, rats were i.p. injected with EtOH (1.5 g/kg), MDMA (6.6 mg/kg) or their combination and their locomotor activity was measured over 5 hours.

2.2. CHEMICALS AND DRUGS

Table 4 summarizes the substances used in the experiments as well as the suppliers from which they were purchased. Substances employed for stereotaxic microinjections into the rat brain, cell culture preparation and immunocytochemistry are listed in the corresponding paragraphs.

Re-uptake inhibitors	**Molecular weight (g/mol)**	**Transmitter**	**Firm**
Hemicholinium-3	574.4	Cholin	ChemCon, Germany
Fluvoxamine maleate	435.3	5-HT	Gift from Duphar, The Netherlands
6-Nitroquipazine	574.4	5-HT	BioTrend/Tocris, Germany
Nomifensine Hydrogen maleate	354.2	DA	Gift from Hoechst, Germany

Receptor ligands	**Molecular weight (g/mol)**	**Effect**	**Firm**
Bicuculline	509.3	$GABA_A$ antagonist	Sigma, Germany
CGP-56999A [3[[1-(**R**)-(3-carboxyphenyl)ethyl]amino] 2-(S)-hydroxy-propyl]-cyclohexyl-methyl-phosphinic acid	389.4	$GABA_B$ antagonist	Novartis

CP-93,129 3-(1,2,5,6-tetrahydropyrid-4-yl)pyrrollo[3,2-b]pyrid-5-one	215.0	5-HT_{1B} agonist (selective)	Pfizer, USA
Ethanol	46.1	Solvent, Drug of abuse	Carl Roth, Germany
GR 55,562 dihydrochlorid 3-[3-(Dimethylamino)propyl]-4-hydroxy-N-[4-(4-pyridinyl)phenyl]benzamid dihydro¬chlorid	466.0	5-HT_{1B} antagonist (selective)	Biotrend/Tocris, Germany
MDMA 3,4-methylenedioxymethamphetamine hydrocholrid	229.7	Drug of abuse	Sigma, Germany
Methiotepine mesylate	452.6	Mixed 5-$HT_{1A/1B}$ antagonist	Sigma, Germany

Radioactive compound	**Specific activity (Ci/mmol)**	**Firm**
[*methyl*-^{3}H]choline chloride	81, 82, 83 or 84	Amersham-Bioscience, Germany
[^{3}H]5-HT 5-[1,2-^{3}H(*N*)]hydroxytryptamin Kreatinin Sulfat	27 or 30	Perkin Elmer, Germany
[^{3}H]Dopamine dihydroxyphenylethylamine 3,4-[ring-2,5,6-^{3}H]-(DA)	60	Perkin Elmer, Germany

Table 4. Summary of chemicals, receptor ligands and radioactive compounds used during the superfusion experiments.

2.3. HERPES SIMPLEX VIRUS

In this section, only a brief description of the production procedure of the viral vectors will be given. For more detail, the reader is referred to comprehensive publications (Clark et al., 2002; Neve et al., 2005). It should be noted, that the viral vector was prepared by Timothy Sexton in the laboratory of John F. Neumaier (University of Washington, Harborview Medical Center, Seattle, Washington, USA). Basically, two types of replication-defective HSV vectors were used, the genomic vectors in which the foreign DNA of interest is cloned into the viral genome itself (Fink et al., 1996; Mata et al., 2002; Goins et al., 2004) and the amplicon vectors, the latter being the one used in this study to express the 5-HT_{1B} receptor. The viral vector consists of a plasmid (amplicon) to which minimal HSV-1 sequences are added, allowing it to be packaged into viral particles with the aid of a helper virus. The basic amplicon, called pHSV-PrpUC consists of a ColiE1 backbone together with the HSV sequences, namely, the

HSV-1 “a” cleavage/packaging site and the HSV origin of replication (ori_S). The HSV IE 4/5 promoter drives the expression of the inserted cDNA. Figure 8 depicts the different steps of the construction process of HSV-based amplicon vectors. In this example, the vector is designated to increase the expression of the transcription factor cyclic AMP response element binding protein, CREB. Moreover, for easier readability, only three HSV ori_S are shown for the recombinant virus. Usually, as each recombinant viral particle contains multiple origins of replication, in the case of HSV-CREB, repeated 5 kb plasmids up to 150 kb of total length would give 30 ori_S. Figure 8 is adapted from (Carlezon et al., 2000).

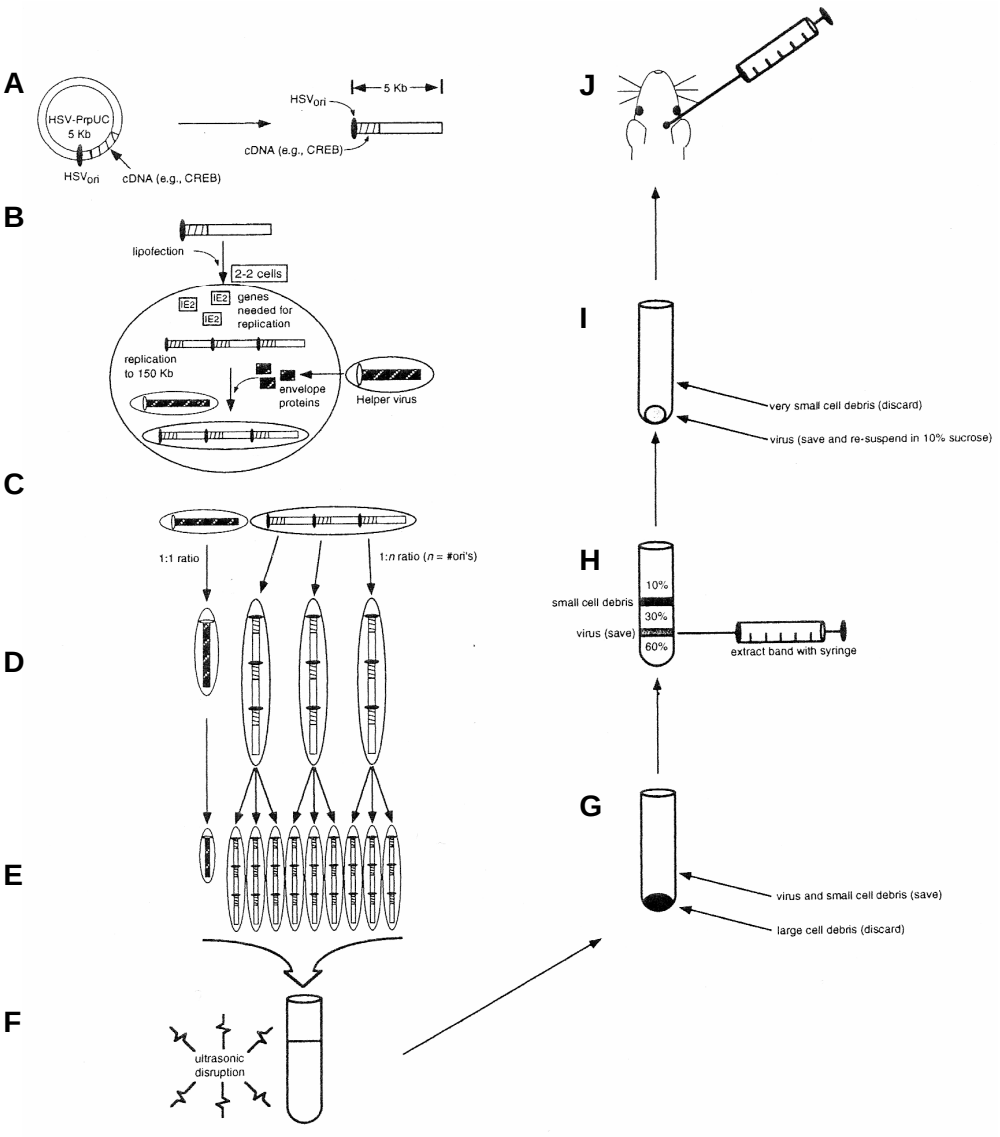

Figure 8. Schematic illustration of the construction process of an HSV-based amplicon vector. As an example, this diagram shows the processing of a virus able to express the transcription factor “cyclic AMP response element binding” (CREB). This procedure is identical to that used to obtain the viral particles expressing the 5-HT_{1B} receptor. The different steps are as follows:

A. The starting point is the cloning of the transgene (here CREB) cDNA into the HSV viral backbone (pHSV-PrpUC, see above).

B. The resulting amplicon is transfected (using lipofection) into 2-2 (African green monkey kidney epithelium) cells that provide immediate early genes (IE2) critical for replication and package. The co-transfection of the helper virus allows replicating and packing the plasmid of interest into viral particles.

C to E. Amplification of the viral particles stocks. In order to achieve a favourable ratio of recombinant vector to helper virus, the stocks derived from transfection of the packaging cells followed by superinfection with helper virus are repeatedly passaged (infected, grown and harvested) on the host, i.e., 2-2 cells. Experiments have shown that a total of 3 passages allows to yield a vector/helper virus ratio greater that 100:1.

F. Following these 3 passages, cells are disrupted by ultrasonic treatment.

G. A low speed centrifugation allows to separate the virus from large cell debris that are discarded but small cell debris persist in the preparation.

H. To further purify the viral solution, the virus is banded on a sucrose gradient followed by high speed centrifugation to pellet the virus. This additional step further reduced the toxicity of the viral preparation. Moreover, this step enables concentration of the vector to titers exceeding 10^8/ml.

I. The preparation undergoes a last centrifugation before re-suspension of the virus in 10% sucrose.

J. The viral solution can be used for microinjections in the rat brain (see below).

In the present experiment, both viral gene transfer vectors (see below) were carrying the cDNA for Green Fluorescent Protein (GFP) for fluorescence microscopic identification of transfected cells. The vector designed to transfer information for 5-HT_{1B} receptor expression also included the 5-HT_{1B} receptor cDNA. In addition, to allow immunocytochemical detection of 5-HT_{1B} receptor expression, its cDNA was tagged with the cDNA for hemagglutinin (HA, for which antibodies are commercially available). Thus, a reconstructed amplicon containing two transcriptional units terminated by SV40 (simian virus 40) polyadenylation sites, the first expressing HA-5-HT_{1B} from a HSV promoter/enhancer and the second expressing GFP from a CMV promoter/enhancer was created (HA1B/GFP vector). As a control, a second amplicon expressing only GFP was also prepared (GFP vector). Both amplicons were then packaged as described above in Figure 8 [see also (Clark et al., 2002; Neve et al., 2005)]. As soon as the viral suspensions arrived from Seattle (Washington, USA) in our laboratory, 5 µl-aliquots were prepared and kept at –80°C until use. Figure 9 shows the amplicon maps used for HA-5-HT_{1B} and GFP expression.

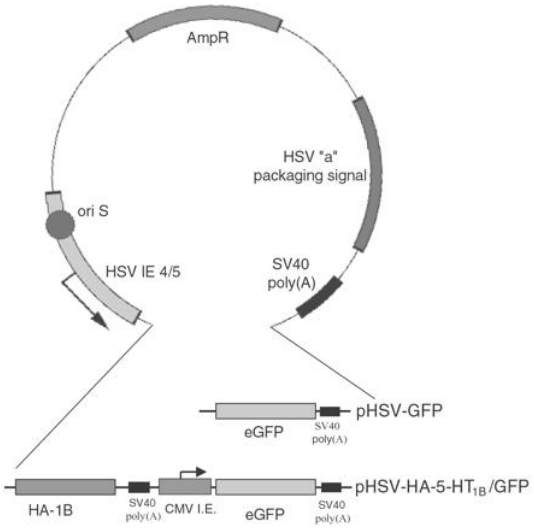

Figure 9. Amplicon maps used for HA-5-HT_{1B} and GFP expression. The plasmids pHSV-HA1B/GFP and pHSV-GFP were constructed as described above and confirmed by sequence analysis. For both plasmids, the original amplicon was pHSV-PrpUC backbone. In the case of the pHSV-HA1B/GFP plasmid, the HA-5-HT_{1B} and GFP gene sequences were interrupted by an SV40 polyadenylation site. Moreover, the two genes have different promoter/enhancers controlling expression to reduce competition effect, namely, HSV IE 4/5 for the HA-5-HT_{1B} gene and CMV IE for the GFP gene. The original sequences belonging to the basic amplicon (pHSV-PrpUC) are ori S; the HSV origin of replication and the HSV "a" packaging signal. AmpR: ampicillin resistance gene; SV40 poly(A): SV40 polyadenylation site. From (Clark et al., 2002).

2.4. PRIMARY SEPTAL CELL CULTURES

2.4.1. Age of the embryos

It is known that the developmental age of the embryos is critical for the preparation of viable cell cultures containing one relevant population of neurons. If the embryos are too young, the relevant population of neurons have not yet differentiated. But if they are too old, the neurons have developed already extensive processes and the dissection will produce axotomy and important cell death. A large number of studies have demonstrated that there is an optimal developmental time window for the collection of each particular CNS region. For instance, it has been shown that cholinergic cells of the ventral forebrain, containing the developing septum and diagonal band nuclei, are born predominantly between embryonic days 12 and 16 (Semba and Fibiger, 1988). Previous experiments in our laboratory showed that embryos taken at the 17^{th} day of pregnancy were appropriate to generate viable cell cultures with a high number of cholinergic cells (Ehret et al., 2001; Ehret et al., 2007b). For these reasons, pregnant

Wistar rats at embryonic day 17 (ED17) were taken every Monday and Wednesday to prepare the cholinergic cell cultures.

2.4.2. Dissection of the pregnant rat

All steps were performed under sterile conditions with sterilized materials, 70%-alcohol cleaning and under a laminar flow. After being deeply anaesthetized with sodium pentobarbital (1 to 1.3 ml of a 6% stock solution, corresponding to about 200 mg/kg sodium pentobarbital), pregnant rats were placed on their back in a cleaned (but not sterile) plastic box, the bottom of which being previously covered with a paper towel, near the laminar flow. After cleaning of the skin with 70%-alcohol, it was held with forceps and a first incision in the peritoneal cavity was made just above the genitalia. The incision was then enlarged on both sides until the ends of the uterine horns. The uterine horns were then removed by a cut at each extremity before being placed (under the laminar flow) in a Petri dish filled with ice-cold, sterile, phosphate-buffered saline (PBS, Biochrom KG, Berlin, Germany). The rat was then sacrificed by a cut in the heart.

2.4.3. Dissection of the embryos

Under sterile conditions, each embryo was taken out of its individual amniotic sac and placenta and placed in a Petri dish filled with ice-cold, sterile PBS. Figure 10 shows the shape and aspect of an E17-embryo, of which the Crown-Rump Length (CRL) is 14 mm.

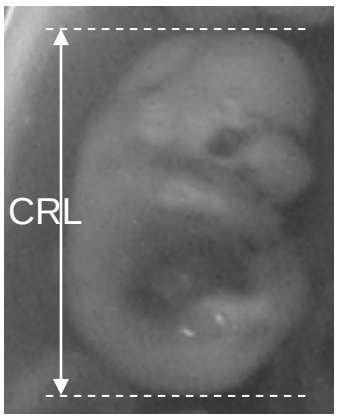

Figure 10. Picture of an E17-embryo. The CRL (Crown-Rump Length) is defined as the greatest length of the embryo as measured in a straight line without any attempt to straighten the natural curvature of the specimen.

In agreement with the Animals (Scientific Procedure) Act 1986, HMSO, London, embryos - since they were older than E11 - were first killed by decapitation (red dotted line in Figure 11A). All further brain dissection steps were done in ice-cold, sterile PBS

under a stereomicroscope according to (Dunnett and Björklund, 1992). Briefly, as shown in Figure 11A, a first cut was made above the eyes to separate the brain from the rest of the head. As the cranial bone has not yet formed in E17 embryos, brains were easily removable from the head and cleaned from skin and meninges (Figure 11C). The brain was then placed on its ventral surface and the two hemispheres removed from each other. Figure 11D shows a sagittal section in the frontal part of the embryonic brain, where the septal pieces that are located along the midline on the ventro-medial part of each hemisphere are designated by the letter S. Each hemisphere was opened on its dorsal surface (as shown on Figure 11D by the two red lines) and the septal pieces that appear lighter than the other structures were separated from the rest of the tissue. All septal pieces obtained from the embryos of a pregnant rat were collected in a 2.5 cm-ice cold Petri dish filled with ice-cold and sterile PBS.

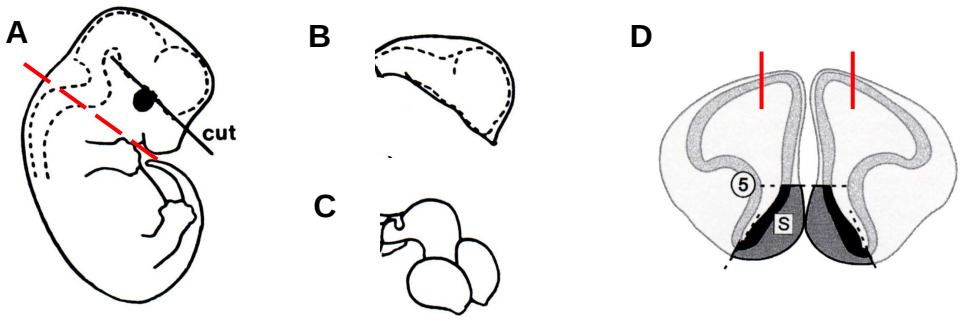

Figure 11. Steps of the dissection of an E17-rat embryo. **(A)** After being taken out of its amniotic sac and placenta, each embryo is first decapitated (red hatched line) before the brain is separated from the rest of the head. **(B)** The skin, bones and meninges are then removed from the brain to get only the two hemispheres shown in **(C). (D)** Sagittal section of the hemispheres. The septal tissue (S) is located along the midline on the ventro-medial part of each hemisphere. The red lines represent the cuts made to open the hemispheres before separating the septal pieces from the rest of the tissue. Adapted from (Dunnett and Björklund, 1992).

2.4.4. Preparation of cell suspension from septal pieces

Tissue pieces containing the septal region of the embryos from one pregnant rat were transferred in a 10 ml-Falcon tube and incubated for 20 min at 37℃ in 1 ml of trypsin-EDTA solution (0.5 %, Sigma, Taufkirchen, Germany) to dissociate the tissues. Trypsinization was stopped by the addition of 500 µl of NU-serum (NU-serum IV culture supplement, Becton Dickinson, Franklin Lakes, NJ, USA). Subsequently the cells were dissociated by gentle trituration using a fire-polished Pasteur pipette. The suspension was then centrifuged at 1000 rpm (rotations per minute) for 5 min and the pellet was

resuspended in 1 ml of growth medium (see Table 5). After a second trituration, the suspension was recentrifuged (1000 rpm, 5 min) and the pellet resuspended in the final volume of 125 µl growth medium per septum. After a third trituration to correctly homogenize the cell suspension, cells were plated onto 96-well plates (100 µl of the final suspension per well; for "seeding densities" of the suspended cells, see below). Each well contained 1 circular glass coverslip (5 mm diameter; "cell culture discs") previously coated with poly D-lysine (poly-D-lysine hydrobromide, Sigma Aldrich, Taufkirchen, Germany).

Cells were cultured at 37℃ in a humidified 95% air /5% CO_2 atmosphere for 14 days *in vitro* (DIV) in the growth medium (Table 5). After approximately 7 DIV, 12 glass coverslips (with their attached cells) were transferred into small Petri dishes filled with prewarmed growth medium. During the whole culture growth period the medium was changed every 3-4 days.

Cell cultures growth medium

	Amount in 100 ml growth medium	Firm
Dulbecco's modified Eagle's medium (DMEM medium Nut. Mix. F-12 with Glutamax-1)	90 ml	GibcoBRL Life Technologies, Eggenstein, Germany
NU-serum IV culture supplement	10 ml	Becton Dickinson,
insulin / transferrin / Na-selenit	0.5/0.5/0.0005 mg	Sigma
penicillin / streptomycin	5 mg	GibcoBRL Life Technologies
hNT-3 (human neurotrophin-3)	5 µg	Alomone/ICS, Munich, Germany
mNGF (mouse nerve growth factor)	1 µg	Alomone/ICS

Table 5. Composition of the growth medium, used for preparation and maintenance of cell cultures from the fetal septal region. All amounts are given for a final volume of 100 ml of growth medium. When necessary (usually, every 6 to 8 weeks), fresh medium was prepared with all original substances. Each time, 10 falcon tubes of 10 ml were prepared and freezed at –80℃ until use. Between the replacements of growth medium in the cell cultures, the tubes were kept at 4℃.

2.4.5. Density of cells

Not routinely, but for several cell cultures prepared during this thesis, 10 µl of the final cell suspension for seeding were used for counting of the cell density using a "Thoma

counting chamber". In agreement with a previous study of our laboratory, septal cells were then seeded at a final density of about 1.5×10^5 cells per 100 µl suspension.

2.4.6. Infection of cell cultures with viral vectors

At DIV 9, twelve cell culture discs were transferred to each of a 3.5 cm-Petri dishes filled with 1.5 ml prewarmed growth medium and then further grown for 3 days. At DIV 11 the viral vectors were added together with fresh growth medium at a concentration of 1 µl viral suspension (~100.000 infective units) per ml of growth medium. Finally, ACh release experiments using these cultures or fixation of the cells for immunocytochemical staining, respectively, were performed another three days later (i.e. at DIV 14). This time schedule was used, as the viral vectors were shown to induce a maximal expression of the 5-HT_{1B} receptor 3 to 4 days after viral infection (Clark et al., 2002).

2.5. STEREOTAXIC MICROINJECTIONS IN THE RAT BRAIN

2.5.1. The stereotaxic apparatus and implantation coordinates

A Stoelting® stereotaxic frame was used in this study. This apparatus allows fine and precise coordinate measurements in the rat brain in three dimensions. Each single structure of the brain can be reached by using its coordinates with respect to one of the reference point of the skull, namely "Bregma" or "Lambda". Figure 12 shows the reference points commonly used on the rat skull to perform surgery on the rat brain. In the present work, the following coordinates were chosen according to the Rat Brain Atlas (Paxinos and Watson, 1998) for intraseptal injections (**Part 1**):

AP (anterior-posterior): + 0.8 mm
ML (medio-lateral): ± 0.5 mm
DV (dorso-ventral): – 5.6 mm.

All coordinates were taken from Bregma and the head of the rat was positioned in order to have a "flat skull" (meaning Bregma and Lambda points at the same dorso-ventral position).

For stereotaxic injections into the dorsal raphé nucleus, the following coordinates were chosen from the same atlas:

AP: – 7.4 mm

ML: + 2.8 mm

DV: – 5 mm, from Bregma.

This structure was approached with an angle of 25° in order to avoid penetration and thus disruption of the third ventricle.

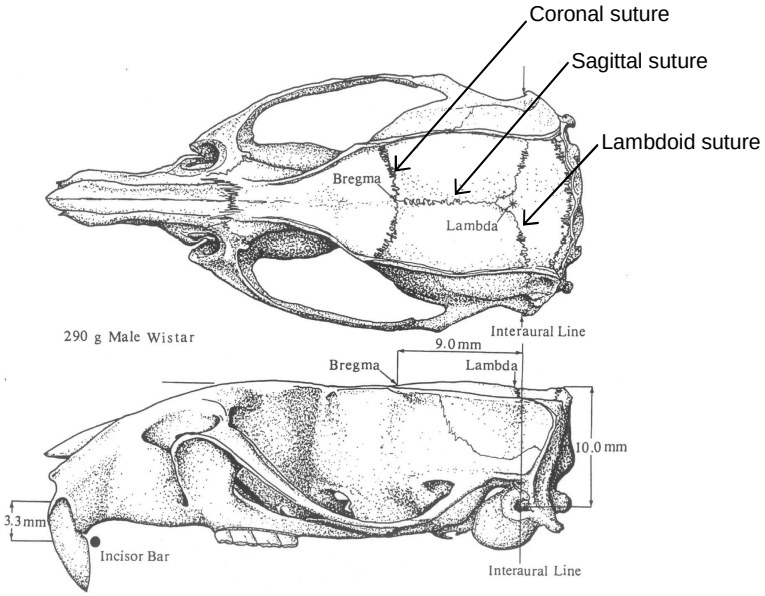

Figure 12. Dorsal and lateral view of the skull of a 290 g Wistar rat. The positions of Bregma, Lambda and the plane of the interaural line are shown above the lateral view. The distance between the horizontal plane passing through the interaural line is shown on the right of the lateral view. The distance between the incisor bar and the horizontal plane passing through the interaural line is shown on the left of the lateral view. Lambda (midpoint of the curve of best fit along the lambdoid suture) is 0.3 mm anterior to the coronal plane passing through the interaural line. From: (Paxinos and Watson, 1998)

2.5.2. Implantation of guide cannulae into the rat brain

Bilateral implantation of guide cannulae into the medial septum (MS) was used in the experiments of **Part 1**, whereas in **Part 4**, the same procedure was used to implant a unique cannula into the dorsal raphe nucleus (DRN). All surgical procedures were performed under aseptic conditions using 70%-alcohol and sterilized material. The male Long-Evans rats were anaesthetized with isoflurane (2-3 %, 1-chloro-2,2,2-trifluoroethyl-difluoromethylether; Forene®, Abbott GmbH, Wiesbaden, Germany) and the scalp fur was shaved before the animal was placed in the stereotaxic frame. The animals were kept under anaesthesia during the surgery using a gas mask fixed to the incisor bar of the stereotaxic frame. Due to technical problems related to set up failures, some of the rats were anaesthetized by a mixture of xylasine hydrochloride (20 mg/ml; Rompun® 2%, BAYER, Leverkusen, Germany) and ketamine (25 mg/ml;

Ketanest®, Parke-DAVIS GmbH, Karlsruhe, Germany) using an injection volume of 0.4375 or 0.22 ml per 100 g body weight. After scalp incision, the coordinates of Bregma were taken and two small holes were drilled at the place for cannula(e) implantation. The stainless steel guide cannula(e) (length 12 mm, outer diameter 0.40 mm, inner diameter 0.3 mm; Cortat S.A., Courrendlin, Switzerland) targeting the MS or the DRN were implanted at the coordinates given in the former paragraph. Guide cannula(e) were kept in place by acrylic dental cement (PALADUR®; Kulzer & Co. GmBH) tightly fixed to the skull by anchor screws (1 mm in diameter). This dental cement ”cap” was rounded to avoid injury of the rat subsequent to disinfection of the surrounding skin (see Figure 13). At the end of surgery, a stainless steel dummy (Cortat S.A., Courrendlin, Switzerland) was placed in each of the guide cannulae in order to avoid any obstruction. Finally, each rat received an intramuscular injection of an antibiotic, i.e. benzylpenicilline-benzathine (Pendysin® 1.2 Mio, Jenapharm GmbH, Jena, Germany) or benzylpenicilline (Extencilline®, 0.3 ml/rat). After surgery, animals were allowed to recover from anaesthesia in the surgery room before being returned to their home cage and brought back to the animal house.

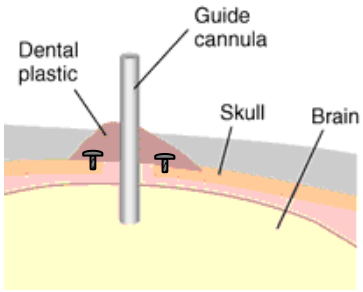

Figure 13. Scheme of one implanted guide cannula. The cannula is kept in place with dental cement tightly fixed to the skull by anchor screws.

2.5.3. Microinjection of the viral vector

Injections of the GFP and HA1B/GFP viral vectors were performed under aseptic conditions and isoflurane (2-3 %) or xylasine/ketamine anaesthesia between 3 and 13 days after guide cannulae implantation. The microinjection needles (length 25 mm, outer diameter 0.28 mm, inner diameter 0.18 mm; Cortat S.A., Courrendlin, Switzerland) were connected to a Hamilton syringe (10 µl, Hamilton Bonduz, Bonduz, Switzerland) by means of a catheter and the syringe was fixed in a microinjection pump (World Precision Instruments, Sarasota, FL, USA). Because the microinjection needles were 2 mm longer than the guide cannulae, we were able to inject the viral vectors at

two different sites in depth: –7.6 and –6.6 mm (from the skull) in order to infect the whole MS area (**Part 1**). In **Part 4** of this thesis, the dorsal raphé nucleus was transfected at –7 mm (from the skull).

For each site, the injection of 1 µl of virus suspension (~100.000 infective units) was performed at a rate of 200 nl/min, the injection time lasting for a total of 5 minutes. In order to allow diffusion of the viral particles from the injection site and to avoid any suction back into the needle during its removal, the microinjection needle was left in place for 5 additional minutes before being slowly retracted. This procedure was repeated for each site of injection (one in the DRN and four in the MS). At the end of the microinjection, the stainless steel dummy was replaced into each guide cannulae in order to avoid any obstruction. Following injections, animals were allowed to recover from anaesthesia before being replaced in their home cages and returned to the animal colony.

2.6. ELECTRICALLY-EVOKED RELEASE OF TRITIATED TRANSMITTER

2.6.1. General comments

The technique of superfusion of tissue slices was first described in 1953 (Gaddum, 1953) and was further explored two years later as a useful tool for the study of the effects of various drugs (Cambridge and Holgate, 1955). This method allows a quantitative measuring of the electrically-evoked release of neurotransmitters either in rat brain slices or in primary cell cultures. Moreover, it provides a possibility to finely assess the presynaptic mechanisms modulating the release of neurotransmitters. In the next paragraphs, each step of the method will be described in detail. The same apparatus was used for both kinds of “tissue” (brain slices or primary septal cell cultures) with some differences specified hereafter.

Experimental principle: In short, the investigated tissue is preloaded with a radioactively labelled compound that is either a precursor of a neurotransmitter (e.g. [^{3}H]-choline) or the neurotransmitter itself (e.g. [^{3}H]-5-HT). During superfusion of this tissue, electrical field stimulations leads to exocytotic release of the radioactive neurotransmitter. To assess the effects of presynaptically active drugs on the release, they are added before the stimulation. Thus, measurement of the released radioactivity, collected in fractions,

allows to quantify the release as well as its possible modulation via presynaptic auto- or heteroreceptors. This *ex vivo* technique also gives the possibility to investigate effects of changes in the neuronal environment, such as following brain lesions or neuronal grafts, on the release of neurotransmitters and its presynaptic modulation.

2.6.2. Modified Krebs-Henseleit buffer

A modified Krebs-Henseleit buffer (KH-buffer) was prepared freshly for each superfusion experiment according to Farnebo and Hamberger (Farnebo and Hamberger, 1971). This buffer was used for the preparation of the brain slices, their incubation with radioactice compounds as well as the preperfusion and superfusion *per se*. It was prepared by mixing given amounts of Farnebo A and B stock solutions. Both components were first diluted 1:10 in bidistilled water (from a Milli-Q® Biocel; Filter: Millipak 40, 0.22 µm, Millipore, Great Britain) and then mixed together (final dilution, 1:20). This buffer, which in its composition is comparable to the extracellular fluid, is the only one in contact with the neuronal tissue during the experiment. To support the viability of the tissue, it is continuously oxygenated and temperated at 37℃. Table 6 shows the composition of Farnebo A and B solutions.

FARNEBO A			**FARNEBO B**		
Substance	Molecular weight (g/mol)	g/2000 ml	Substance	Molecular weight (g/mol)	g/2000 ml
NaCl	58.45	275.88	$NaHCO_3$	84.01	84.01
KCl	74.56	14.32	KH_2PO_4	136.09	6.53
$CaCl_2 \times H_2O$	147.02	7.65			
$MgSO_4 \times 7H_2O$	246.5	11.83			

Table 6. Composition of FARNEBO A and B solutions. All substances were ordered from Carl Roth GmbH + Co (Karlsruhe, Germany).

After 30 min of gassing (with carbogen; 95% O_2/5% CO_2), three additional substances were added to the buffer (Table 7). The resulting mixture was further gassed (for a total of 45 min minimum), afterwards the pH was adjusted to 7.4 with 1N NaOH.

Substance	Molecular weight (g/mol)	g/4000 ml
L(+) Ascorbic Acid	176.12	0.02
Na_2-EDTA	372.24	0.004
α-D(+) Glucose	198.07	8

Table 7. Additional substances of the KH-buffer added after 30 min of gazing with their molecular weight and final concentration in g/4000 ml.

The final KH-buffer contains the substances in the concentrations shown in Table 8. All substances were purchased from Merck, Germany.

FINAL COMPOSITION OF KH-BUFFER	
Substance	Concentration [mM]
NaCl	118
KCl	4.8
$CaCl_2 \times H_2O$	1.3
$MgSO_4 \times 7H_2O$	1.2
$NaHCO_3$	25
KH_2PO_4	1.2
L(+) Ascorbic acid	0.57
Na_2-EDTA	0.03
α-D(+) Glucose	10

Table 8. Composition of the Krebs-Henseleit (KH) buffer. After mixing of all the compounds in distilled water, the buffer is gazed with carbogen and the pH adjusted to 7.4.

After preparation of the KH buffer, an aliquot (usually 200 ml) was cooled on ice for the dissection of tissue and the preparation of brain slices, whereas the remaining part was prewarmed in the 37℃-water bath (25℃ for the cell cultures) for the preperfusion and superfusion steps. Moreover, during the whole experiment the KH-buffer was continuously saturated with carbogen (95% O_2/5% CO_2). Routinely, for an experiment with 24 brain slices or cell cultures, 4 L of buffer were necessary. In the next paragraphs, the composition of incubation or superfusion buffer as well as the corresponding added drugs will be specified.

2.6.3. Tissue preparation for the superfusion experiments

Preparation of tissue slices

Rats were deeply anaesthesized with CO_2 in a Plexiglas box (22 x 33 x 33 cm) before being quickly killed by decapitation. Curved dissection scissors were used to incise the skin and to open the skull. The meninges (dura matter) were then cut with fine scissors to avoid destruction of the brain during its removal from the skull. The brain was immediately immersed in a small beaker filled with ice-cold KH-buffer. To minimize enzymatic degradation the brain tissue was cooled during dissection and, all steps took place on a circular paper filter kept on a aluminium-block (10 x 10 x 5 cm) cooled down to 4°C. Both hippocampi were dissected out success ively as depicted in Figure 14.

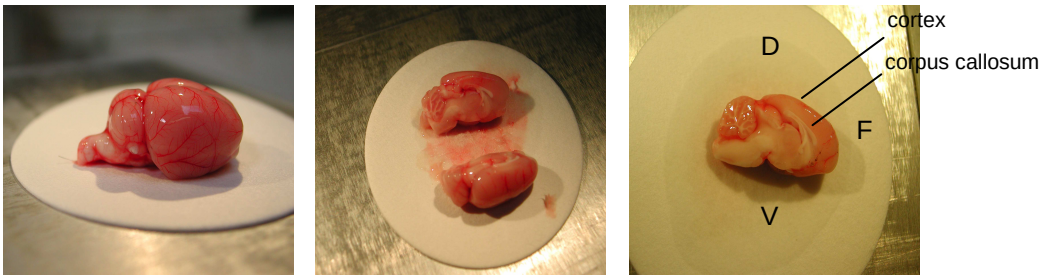

Figure 14. The two hemispheres were first separated along the fissura longitudinalis cerebralis. Each half brain was placed on its lateral surface and a sharp spatula was introduced below the corpus callosum to separate the cortical part (cortex) – in which the hippocampus is located – from the rest of the subjacent structures. The hippocampus was then extracted from the surrounding cortex with a scalpel and placed on another paper filter. With D: dorsal; F: frontal and V: ventral.

As soon as both hippocampi were collected on the filter, they were cut in 350 µm thick coronal slices in the septo-temporal axis with a McIlwain tissue chopper (Bachofer, Germany) as shown in Figure 15.

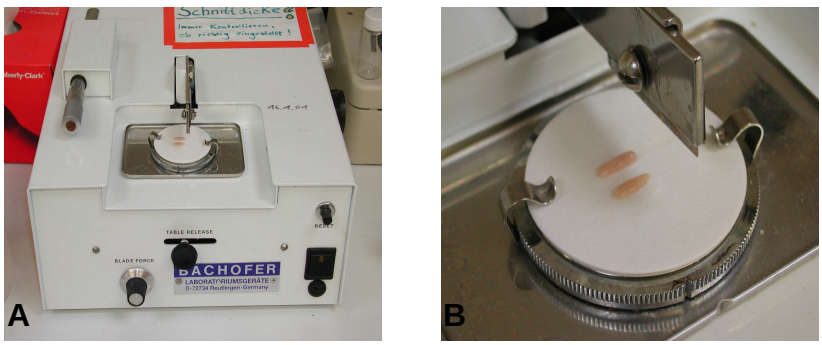

Figure 15. **(A)** Picture of the tissue chopper used in our experiment set with the filter paper with both hippocampi to be cut. **(B)** Focus on the razor blade.

In experiments using rats injected with MDMA alone or in combination with EtOH (**Part 2**), 350 µm thick slices from the dorsal hippocampus and the dorsal part of the frontoparietal cortex were prepared. Furthermore, the ventral parts of both tissues were kept for HPLC measurements of the monoamines contents. For experiments in which the presynaptic effects of MDMA and/or EtOH were investigated *in vitro* (**Part 3**), 300 µm thick slices of the striatum, hippocampus and frontoparietal cortex were prepared as described previously (Birthelmer et al., 2003d; Cassel et al., 2005) using the same tissue chopper as depicted in Figure 15.

Incubation of the slices

The slices were first separated in a glass tube and washed three times with KH-buffer before being transferred into a small Petri dish (Falcon®, 3.5 x 1 cm, Becton Dickinson, USA) into which the tritiated precursor was added. The tritiated precursor, [^{3}H]-choline (for the release of ACh) was used at a concentration of 0.1 µmol/L. In a similar manner [^{3}H]-5-HT or [^{3}H]-DA (both at concentrations of 0.1 µmol/L) were used to study the release of 5-HT or DA, respectively. The slices were then incubated under slight agitation for 30 or 45 min at 37°C and under a carbogen atmosphere (Incubator Type B5050E, Heraeus, Germany) to allow specific uptake of the radioactive transmitter (or precursor). Following incubation and before their transfer into the superfusion chambers, the slices were washed 3-4 times with about 2 to 3 ml prewarmed KH-buffer to remove excess of radioactivity.

Incubation of septal cell cultures

Concerning the septal cell cultures, the procedure was slightly different. The transmitter release experiments always took place on the 14th day *in vitro* (DIV14) as it was shown in previous experiments that two weeks in culture was optimal to obtain a significant number of differentiated “release-able” cholinergic neurons (Ehret et al., 2001). The KH-buffer prepared for the superfusion experiment with cell cultures was exactly the same as that described above. Since the growth medium of the cultures contains (among further compounds possibly also interfering with the release experiments) relatively high amounts of *unlabelled* choline (which might dilute the *tritiated* choline), it had to be carefully washed away using about 3×2 ml of prewarmed and gassed KH buffer. The final incubation medium was the same as that for the brain slices, namely 2 ml of KH-buffer in which the radioactive precursor ([^{3}H]-choline) was diluted at a final concentration of 0.1 µM. The incubation of the cell cultures took place during 30 min in the same incubator and under the same conditions as described above.

2.6.4. The superfusion apparatus

To ease legibility, hippocampal, neocortical or striatal slices and septal cell cultures are grouped in the next paragraphs under the name “tissue”. At the end of the description of a classical superfusion experiment, two tables (Table 10 and Table 11) will list the specific parameters related to each experimental design.
Superfusion of neuronal tissue took place in so called “superfusion chambers” that were especially conceived for the superfusion experiments (produced in the workshop of the Institute for Clinical and Experimental Pharmacology, Freiburg-im-Breisgau, Germany). Directly loading with the tritiated precursor, the tissue was washed with KH-buffer before being transferred to the superfusion chambers.

Structure and functioning of the superfusion chambers

Each superfusion chamber consisted of two Plexiglas plates of 7 x 7 x 1 cm. There are 12 superfusion chambers per superfusion apparatus. Figure 16 shows a detailed diagram of the chambers used in these experiments. The top plate consisted of one of the two platinum electrodes, namely the *cathode* (8 mm in diameter; [a]) and a rubber joint [b] to isolate the tissue from the surrounding water bath (see below).
The middle diagram of Figure 16 shows a lateral view of both parts of the superfusion chamber. In the centre of the bottom plate was a hole of 4 mm-depth and 10 mm in diameter containing the second platinum electrode namely the *anode* [g]. A Plexiglas disc (outside diameter: 10 mm, inside diameter: 5 mm and thickness 3 mm for the brain slices and outside diameter: 10 mm, inside diameter: 8 mm and thickness: 3 mm for the cell culture discs [d]) was inserted in the hole above the electrode. This so-called “inlet” was closed before the experiment on each side with two polypropylene nets [f] in between which the tissue is kept [e] during the whole superfusion experiment. Each superfusion chamber was fixed to an arm with a metal tray [h], which allows to submerge twelve chambers simultaneously into the water-bath.
The small space containing the tissue is connected to two “tunnels”, one for the influx of KH-buffer (IN) and the other one for its efflux (OUT; see right-hand side diagram). During the experiment, the tissue was continuously superfused with KH-buffer using a pump (see below). Since air bubbles would modify or even prevent electrical conductivity, each superfusion chamber is also equipped with an air trap [i].

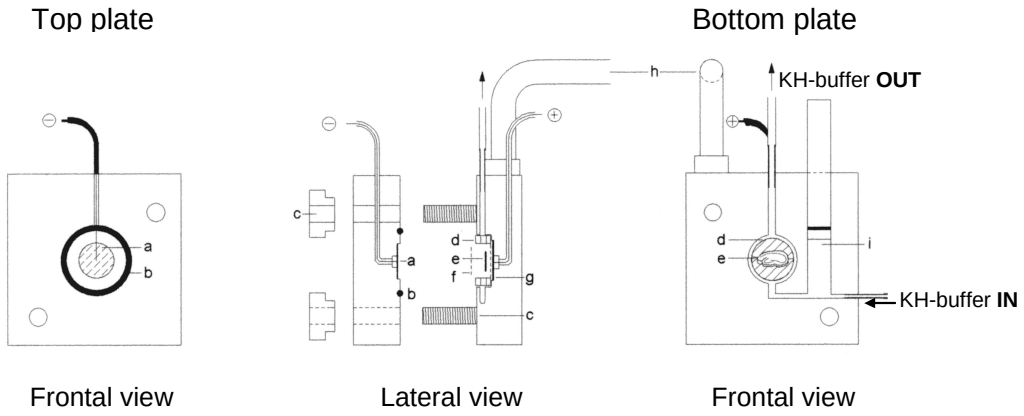

Figure 16. Schematic drawing of the superfusion chambers. Frontal view, top plate: [a] platinum electrode (cathode); [b] rubber joint. Lateral view: [a] platinum electrode (cathode); [b] rubber joint; [c] screws; [d] Plexiglas-chamber inlet; [e] brain slice or cell culture disc; [f] polypropylene net; [g] platinum electrode (anode); [h] metal tray. Frontal view, bottom plate: [d] Plexiglas-chamber inlet; [e] brain slice or cell culture disc; [h] metal tray; [i] air-trap. See text for detailed explanations.

Structure and functioning of the superfusion apparatus

The next paragraphs will describe a typical superfusion experiment.

Our laboratory was equipped with two identical superfusion apparatus thus allowing superfusion and electrical stimulation of tissues in 24 superfusion chambers simultaneously. Figure 17 shows the components of the superfusion apparatus. For the release experiments on cell cultures, another apparatus was employed. Both were, however, identical except for the position of the peristaltic pump. Indeed, in the former case, the pump was placed in between the superfusion chambers and the fraction collector (Figure 17), whereas in the latter, it was placed in between the buffer reservoir and the superfusion chambers (not illustrated).

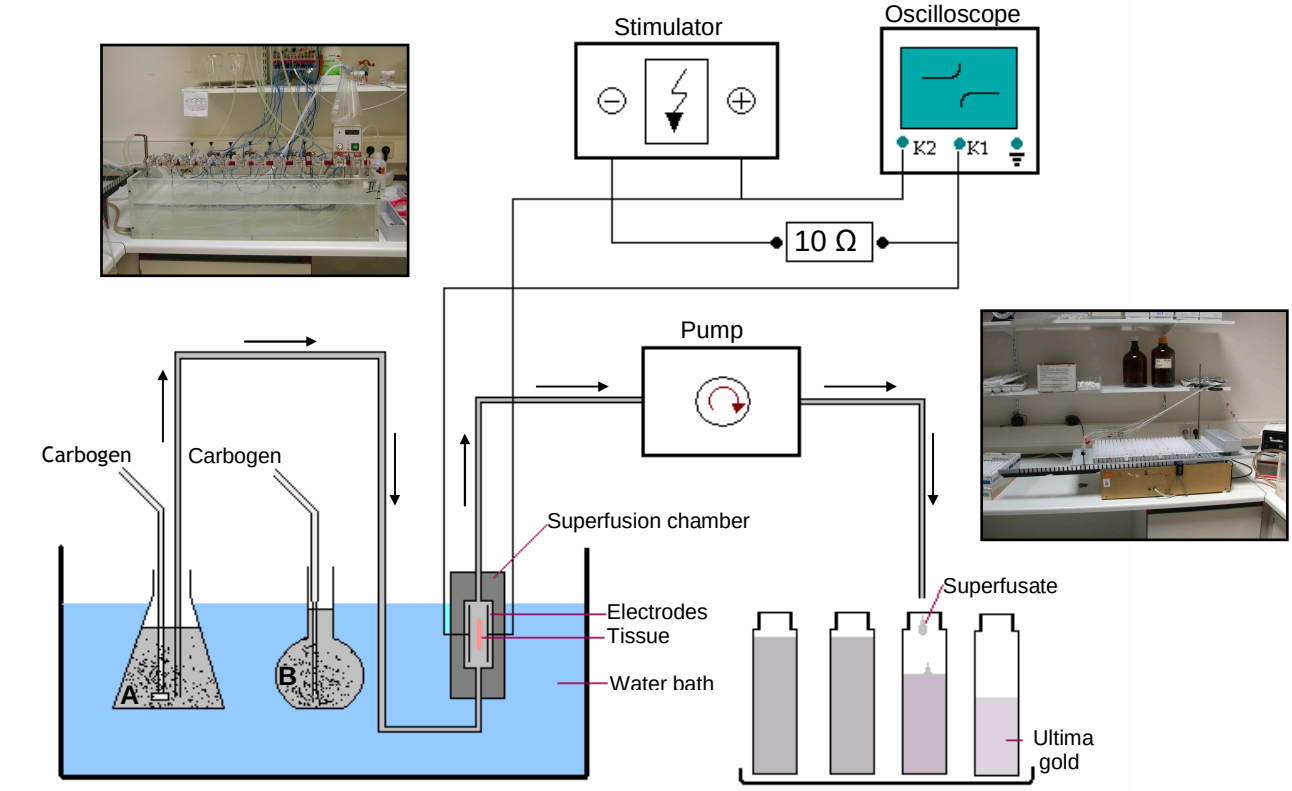

Figure 17. Schematic representation of the superfusion apparatus for electrically-evoked release. Black arrows indicate the flow direction of the KH-buffer during the experiment. **(A)** reservoir for KH-buffer; **(B)** KH-buffer containing additional drugs. During the experiment, all solutions were gassed with carbogen and immersed in the water bath (kept at 37℃ for brain slices, and at 25℃ for cell cultures). Thanks to the peristaltic pump, the KH-buffer (± drugs) is flowing though the chambers, in continuous contact with the tissue. During the experiment, the tissue was electrically stimulated – two or three times – using a stimulator (Type 251/I, Hugo Sachs Electronik, Germany) connected to two platinum electrodes delivering electrical fields at a preselected voltage gradient and frequency (see Tables 9, 10 & 11). The resulting current through the tissue was measured using an the oscilloscope (HM 205-3, Hameg, Germany). The superfusate fractions containing the radioactive outflow were collected every 2 or 4 min (depending on the experimental protocol) and the fraction collector was programmed to automatically determine the duration of the collection time. The scintillation cocktail Ultima Gold (3 ml) was already pipetted into the scintillation vials before the experiment.

Preperfusion

Subsequently to the transfer of the tissue into the superfusion chambers, the chambers were closed after removal of air bubbles and vertically positioned in a water bath (Plexiglass aquarium, 80 x 37 x 21 cm) maintained at 37℃ with a heating regulatory apparatus (Lauda A-100, Dr. R. Wolser, Germany) for the experiments with brain slices and at 25℃ for the experiments with cell cultures. The start of the pump marks the beginning of the superfusion experiment.

The preperfusion allows the removal of (1) radioactively-labelled transmitters that were not stored into the intraneuronal vesicles during tissue loading, or (2) their metabolic degradation products that may be present in the extracellular zones of the slices. For this purpose, the tissue was continuously superfused with KH-buffer at a rate of 0.6 or

1.2 ml/min using a peristaltic pump (IPC High Precision Multichannel Dispenser, Ismatec, Zürich, Swiss). The preperfusion lasted 30 or 45 min depending on the experimental set up. Moreover, after 15 or 25 min of preperfusion, the tissue was prestimulated (18 rectangular pulses, 3 Hz, 2 ms, 4 V, 25 - 28 mA) to remove labelled transmitter from the so-called (but still hypothetical) “readily-releaseable pools” in the nerve endings. No prestimulation period was given, however, in experiments on cell cultures.

Time scale of a typical superfusion experiment:

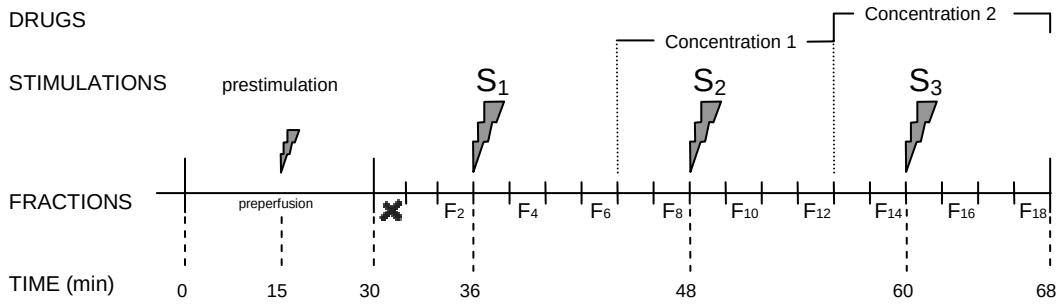

Figure 18. Example of the time scale of a typical superfusion experiment. In this example, the preperfusion of the tissue lasted for 30 min and a prestimulation was given after 15 min. The fraction collector was started after 30 min of superfusion but the first fraction served as a “checkpoint” for the functioning of the pump and was always discarded (red cross). During the fraction collection period the tissue was stimulated for the first time after 36 min (S_1), for the second time, after 48 min (S_2) and for the third time, after 60 min (S_3). At the beginning of the 7^{th} fraction, a receptor ligand was given to the tissue and at the beginning of the 13^{th} fraction, the same ligand was given at a higher concentration. At the end of the experiment (after 68 min of superfusion), the tissue was taken out of the chambers and dissolved. Both the amount of radioactivity in the superfusate samples and in the tissue samples were measured in an liquid scintillation counter.

Collection of superfusate fractions and electrical stimulations

After preperfusion, the superfusion and collecting of the fractions started. The fraction collector (ISCO® Retriever, Lincoln, USA), previously pre-programmed, started to collect 2 or 4 min-fractions in polyethylene scintillation vials (Packard, Germany) filled with 3 ml of the scintillation cocktail (Ultima Gold®; Perkin Elmer, Groningen, The Netherlands). At specific times during the superfusion, the tissues were electrically stimulated (see Table 9 for stimulation parameters and respective currents obtained). All 12 chambers of each of two superfusion setups were electrically connected in series; consequently the strength of electrical currents between the platinum electrodes (in mA) was identical in all 12 chambers. Electrical fields stimulated the tissues, which were positioned in parallel to the platinum electrodes. The electrical currents obtained during application of electrical rectangular pulses were measured using an oscilloscope

(see Figure 17). Drugs to be tested were added to the superfusion buffer before the second or third stimulation onwards.

At the end of the superfusion experiment, the chambers were opened and the tissues collected to measure their remaining tritium content. For this purpose tissues were transferred into glass vials (one slice or the two cell cultures discs per glass vial) containing 0.25 ml Solvable® (Perkin Elmer, Groningen, The Netherlands) to completely dissolve the tissue. Finally, 4 ml of Ultima Gold® were added to these samples. All scintillation vials (those with superfusate and tissue samples) were closed carefully, shaken vigorously and put into a Liquid Scintillation Counter (Liquid Scintillation Analyzer, Packard Tricarb 2900TR) in order to measure their radioactivity during 4 minutes.

2.6.5. Specific conditions of various superfusion experiments

Stimulations conditions

Table 9 summarizes the parameters of the electrical stimulations applied to the brain slices or cell cultures, respectively. The cell cultures were not prestimulated.

	Septal cell cultures	**Hippocampal slices (1)**	**Hippocampal, Frontoparietal or Striatal slices (2)**
Number of rectangular pulses	360	90	360
Frequency (Hz)	3	3	3
Duration (ms)	0.5	2	2
Voltage per chamber (V)	9.4	8	4
Current (mA)	90 –100	50 – 56	25 – 28
Prestimulation	none	After 15 min : 18 pulses, 3 Hz, 2 ms, 4 V, 25-28 mA	18 pulses,3 Hz, 2 ms, 4 V, 25-28 mA or no prestimulation

Table 9. Stimulation parameters for superfusion experiments on brain slices or septal cell cultures, respectively. **(1)** Hippocampal slices from virus-injected rats (**Part 1**): **(2)** Slices from rats pretreated with MDMA +/- EtOH (prestimulation after 15 min) (**Part 2**) or from experiments studying MDMA +/- EtOH *in vitro* (prestimulation after 25 min) (**Part 3**). The latter slices were the only not subjected to a prestimulation period (**Part 3**).

Superfusion conditions

Table 10 and Table 11 summarize the specific conditions applied to the brain slices and septal cell cultures during the superfusion phase.

	Hippocampal slices (1)	**Septal cell cultures**
Released transmitter	[^{3}H]-ACh	[^{3}H]-ACh
Water bath T°C	37 °C	25 °C
Tissue per chamber	1 slice	2 discs, back to back
Tissue size	350 µm	–
Pump rate (ml/min)	1.2	0.6
Superfusion chambers	Identical except for the inlets that were larger for the cell cultures	
Substances throughout	Hemicholinium-3 (10 µM)	
Preperfusion (min)	30	45
Fraction duration (min)	2	4
Stimulation (after x min)		
S_1	36	57
S_2	52	85
S_3	68	–
Drug addition (after x min)	44 60	73
Drugs	CP-93,129 at 0.01, 0.1, 1 & 10 µM	CP-93,129 at 0.1, 1 & 3 µM
Superfusion time (min)	76	129

Table 10. Superfusion conditions used for the hippocampal slices in the case of virus-injected rats **(1)** and virus-infected septal cell cultures experiments. All parameters that are identical are not specified.

Originally, the septal cell cultures were subjected to 3 electrical stimulations. However, the results of the "control cultures" (i.e., without any drug addition before S_2 or S_3) indicated that the release was substantially decreased at S_3 vs. S_2. We therefore thought that the chosen experimental design was too long for cultures, which are more fragile than slices. Thus, we decided not to take into account the results of the third stimulation. Nevertheless, all cell cultures were subjected to the same protocol (Table 10) and all the results were analysed in an identical way.

	Hippocampal or Frontoparietal slices (2)	**Hippocampal, Frontoparietal or Striatal, slices (3)**
Released transmitter	[^{3}H]-5-HT	[^{3}H]-5-HT and/or [^{3}H]-DA
Water bath T°C	37 °C	37 °C
Tissue per chamber	1 slice	1 slice
Tissue size	350 µm	300 µm
Pump rate (ml/min)	1.2	0.6
Substances throughout	6-Nitroquipazine (1 µM)	Fluvoxamine (1 µM) for DA and Nomifensine (1 µM) for 5-HT release
Superfusion chambers	Identical	
Preperfusion (min)	30	45
Fractions duration (min)	2	4
Stimulation (after x min)		
S_1	36	57
S_2	52	101
S_3	68	–
Drug addition (after x min)	44 60	77
Drugs	CP-93,129 at 0.001, 0.01, 0.1 & 1 µM or Methiotepine at 0.1 and 1 µM	EtOH 2‰ / MDMA 0.3 or 3 µM / EtOH 2‰ + MDMA 0.3 or 3 µM
Superfusion time (min)	76	125

Table 11. Superfusion conditions used for the experiments **(2)** on slices from rats pretreated with MDMA +/- EtOH (**Part 2**) or **(3)** on slices from experiments studying MDMA +/- EtOH *in-vitro* (**Part 3**). Only the release of [^{3}H]-5-HT was assessed in hippocampal and frontoparietal slices.

2.6.6. Calculations

Tritium accumulation in the tissue

The experimental parameter “accumulation of tritium” provides informations on the content of radioactivity in the tissue at the beginning of the fraction collection period, i.e. following preincubation *and* preperfusion periods. The accumulation of tritium in one slice or one cell culture (sum of 2 discs), is calculated as the sum of the tritium contents of all the fractions of the corresponding chamber (in dpm) and of the tritium content of the tissue (also in dpm) at the end of the superfusion. Considering the specific radioactivity of the transmitter (in Ci/mmol) and considering that 1 Ci = 2.22×10^{12} dpm, it becomes then possible to calculate the tritium content of the slice at

the onset of the superfusion in pmoles. In the “Results” part, these values will be specified in pmoles/slice or pmoles/cell culture disc.

Relative tritium outflow in one fraction (FR; Fractional Rate)

When considering the results obtained from the superfusion experiments, we have the possibility to analyse different parameters. The tritium outflow subsequent the n^{th} stimulation constitutes the “electrically-evoked overflow (S_n)” of tritium from the tissue. Moreover, the tissue also spontaneously releases tritium in the absence of electrical stimulation, which constitutes the “basal outflow of tritium (b_n)”. In the following chapter, these two variables will be given either in absolute values (in nCi) or as a percentage of the tritium content at the onset of the respective stimulation period (or fraction), i.e. in relative values. This relative value represents a “normalization” of the absolute values and reduces the variability of the data, which is especially due to differences in the size of the slices.

This normalization of the tritium outflow in a specific fraction “n” is designed as the fractional rate (FR). It represents the outflow of tritium in fraction “n” during a given time, expressed as a percentage of the tritium content of the tissue at the onset of the corresponding fraction. The FR is obtained by the following formula:

$$FR_n\ (\%) = \frac{[^3H]\text{-content in the fraction} \times 100}{[^3H]\text{-content in the slice} \times t}$$

With t = duration of the corresponding fraction.

Basal outflow of tritium (b_n)

Since drugs present throughout superfusion or pretreatments of the animals may affect the spontaneous outflow of radioactivity from the tissue, the “basal outflow of tritium” was always calculated from the data. The basal outflow of tritium (b_n) is defined as the tritium outflow in a defined fraction. For instance, in the present experiments the basal efflux “b_1” corresponds to that in the fraction preceding the first stimulation (S_1) and “b_2” to that in the fraction preceding the second stimulation (S_2). The basal tritium outflow is given either in absolute (nCi [^{3}H]-outflow per duration of the fraction) or in relative terms (in percent of the [^{3}H] content of the tissue per duration of the fraction). In the later case, b_n corresponds to the fractional rate of the fraction preceding the stimulation.

To assess whether drugs added before the n^{th} stimulation have an effect on the spontaneous release of tritium, we also routinely calculated the “basal efflux quotient” as shown below. Therefore, when this quotient is smaller (or greater) in the presence of

a drug than the corresponding control values (no drug addition before S_n), it may be concluded that the added drug had an inhibitory (or facilitatory) effect on the spontaneous release of tritium.

$$\text{Basal efflux quotient} = \frac{b_n}{b_1}$$

b_n = FR of basal tritium outflow in the fraction preceding S_n

b_1 = FR of basal tritium outflow in the fraction preceding S_1

Electrically-evoked overflow of tritium

To calculate the stimulation-evoked overflow of tritium (S_n), in percent of the tritium content of the tissue before the onset of the corresponding stimulation, the fractional rate of the fraction corresponding to the start of the stimulation and the three subsequent FR are summed up. From this sum, the basal tritium is subtracted, assuming a linear decrease of the basal outflow of [^{3}H] from the fraction before S_n to the fraction S_{n+4}.

S_n/S_1 quotient: the effects of drugs on the electrically-evoked overflow of tritium

To quantify the effects of receptor ligands ("drugs") on the evoked release of neurotransmitters, the evoked overflow of tritium at S_2 or S_3, i.e. after drug addition, is compared to S_1, i.e. the evoked overflow of tritium at the first stimulation, without any drug. This S_n/S_1 ratio of the overflow evoked by the corresponding stimulation period (n = 2 or 3) can be given as an absolute value or as a relative value, i.e. as a percentage of the appropriate control ratio (no drug addition before S_2 or S_3, respectively). When no drug is added, the control ratio is considered to represent a tritium overflow of 100%. Thus, when a drug decreases this ratio to 60% for instance, it has an inhibitory effect of 40% on the release and when it increases this ratio to 120%, it has a facilitatory potency of 20% on the release.

In addition, in some experiments (i.e., release of [^{3}H]-DA and [^{3}H]-5-HT from striatal slices) the effects of EtOH, MDMA or their combination added 24 min before S_2 onwards were on the spontaneous outflow of [^{3}H] were also calculated. In this case we analysed the "drug-evoked overflow of [^{3}H]" (in % of tissue-[^{3}H]) by calculating the "area under the curves" (see Figure 53 in Results) from 77 to 97 min of superfusion, using the corresponding fractional rate values and then substracting the basal tritium outflow in a similar manner as for the calculation of the evoked overflow at S_n.

2.6.7. Statistics

As regards [^{3}H]-ACh release from hippocampal slices of stereotaxically transfected animals (**Part 1**) or assessment of the locomotor activity of transfected rats (**Part 4**), GFP fluorescence served as an indicator of viral transfection. Thus, before any statistics were performed, 40 µm vibratome slices were observed under a fluorescence microscope in order to check for the site of the cannula tracks as well as for GFP-positive cells in the MS or DRN. Consequently, data of rats, in which the cannulae were not implanted into the proper region or for which no GFP-positive cells could be detected were discarded from all statistical analyses.

All data were analysed using analysis of variance (ANOVA) followed, when appropriate, by pair-wise comparisons using the Newman-Keuls test (Winer, 1971). All analyses were performed with STATISTICA, Statsoft, version 5.1.

All values shown in the figures and tables are Means ± SEM of n slices subjected to the corresponding experimental setting. The level of corresponding significance was noted with * when $p < 0.05$ (significant), ** when $p < 0.01$ (very significant) and *** when $p < 0.001$ (extremely significant).

The type of ANOVA (number of factors, numbers of levels of each factor…) performed for each experiment is detailed in the corresponding section in Results.

2.7. IMMUNOCYTOCHEMISTRY

2.7.1. General principle

The first step in any staining procedure described hereafter, consisting in fixing of cell cultures or brain slices. It allows to preserve the structure of the tissue and to immobilize the molecules of interest, in particular the antigens. The fixative used was paraformaldehyde (PFA) at 4% in 0.1 M phosphate buffer (PB; pH 7.4, Biochrom KG, Berlin, Germany). All immunoreactions (except one, see 0) were indirect, i.e. a primary antibody fixes to the target antigen and a secondary antibody, linked to a tracer, recognizes and fixes to the primary antibody.

As previously described, both hippocampi were dissected from brains of the virus-injected rats to measure [^{3}H]-ACh-release. From the same rats, the frontal part of the brain containing the septal region, was fixed in PFA 4% in 0.1M PB for 24 h and rinsed

in 0.1 M PB for 24 h. Using a vibratome (Leica VT 1000S, Wetzlar, Germany), coronal 40 µm-sections were prepared from these brain pieces. All sections were collected in 0.1 M PB. Some of them were directly mounted on microscopic glass slides and inspected for GFP-stained cells under a fluorescent microscope (see Results). Some other were immunostained for ChAT and HA.

Immunostaining for GFAP (glial fibrillary acidic protein)

GFAP staining is used for specific visualization of glial cells. After fixing and washing, cells were directly incubated with a Cy3-conjugated mouse anti-GFAP antibody (1:2000, Sigma, Taufkirchen, Germany) in 0.1 M PB for 1 hour. After 3 washings of 10 min each, cells were mounted on glass slides with fluorescence-specific medium (Vectashield® Hard Set Mounting medium, Vector Laboratories, Burlingame, CA, USA). Immunostaining of GFAP was only performed on primary septal cell cultures.

Immunostaining for ChAT (choline acetyltransferase)

The immunostaining for ChAT (choline acetyltransferase) is used to stain cholinergic neurons in cultures or tissues as this synthezising enzyme is highly specific of this neuronal type (Levey et al., 1983).

Non-fluorescent ChAT-immunostaining

In order to saturate all antigenic sites, cells/sections were incubated for 30 min/1 h in normal donkey serum (NDS, Dutscher, Brumath, France) at 10% in a PBS Triton solution. The PBS Triton solution was prepared as follows: Triton X-100 at 0.005% and 0.2 mg/ml sodium merthiolate (antiseptic) diluted in PBS 0.1 M at the desired final volume. Thereafter, cells/sections were washed once in PBS 0.1 M before being incubated overnight at 4°C with goat anti-ChAT mono clonal antibody (AP144P Chemicon International, Temucula, USA) at a concentration of 1/500 or 1/1000 in PBS triton. The following day, cells/sections were washed 3 times (5/10 min each) in PBS 0.1 M and then incubated for 45 min/1h30 with a biotinylated donkey anti-goat secondary antibody (1/500 in PBS triton, AB1778 Chemicon International, Temucula, USA). Cells/sections were subsequently washed and incubated for 1 h with the avidin-biotin complex prepared with the Kit “Elite” Vectastain® ABC (Vector Laboratories, USA). Both reactants were diluted at 1/500 in PBS triton in the dark. Cells/sections were then washed 2 times (5/10 min each) with PBS 0.1 M and once with Tris buffer for 10 min at 0.06 g/ml diluted in bidistilled water, pH adjusted to 7.6). The last step consisted of revealing the DAB using again a kit (Vector Laboratories International,

Burlingame, USA). Cells/sections were incubated for approximately 30 min but the evolution of the coloration was followed under a binocular magnifying glass and stopped when appropriate. Finally, cells/sections were again washed 2 times (5/10 min each) in PBS 0.1 M before being mounted using Vectashield® mounting medium.

Fluorescent ChAT-immunostaining

Cells/brain sections were treated with 5/10% NDS and 0.5 % Triton x-100 (in 0.1 M PB) for 30 min/1 h before being incubated with goat anti-ChAT primary antibody (1:500, affinity purified polyclonal antibody, Chemicon International, Hampshire, United Kingdom) in 0.1 M PB (supplemented with 1 % NDS and 0.5 % Triton x-100) for 12 hours at 4℃. After washing with 0.1 M PB (3 ×10 min), cells/sections were subsequently stained by the addition of Cy3-conjugated donkey anti-goat antibody (1:500, Rockland, Gilbertsville, PA, USA) in 0.1 M PB (supplemented with 1 % NDS and 0.5 % Triton x-100) for 1/2 hour(s) at room temperature. Following a last washing period (4×30 min in 0.1 M PB), cultures/sections were placed on microscope glass slides and mounted with Vectashield® mounting medium.

Immunostaining for HA (Hemagglutinin)

After fixing, cells/brain sections were treated with 5/10% NGS and 0.5 % Triton x-100 (in 0.1 M PB) for 30 min/1 h before being incubated with mouse anti-HA antibody (1:1000, HA.11 monoclonal antibody, purified, Covance, San Diego, CA, USA) in 0.1 M PB (supplemented with 1 % NGS and 0.5 % Triton x-100) for 12 hours at 4℃. After washing in 0.1 M PB (3×10 min), they were subsequently stained by the addition of Cy3-conjugated goat anti-mouse antibody (1:500, Dianova, Hambourg, Germany) in 0.1 M PB for 2 hours at room temperature. Following a last washing period (4×30 min in 0.1 M PB), cultures/sections were placed on microscope glass slides and mounted with Vectashield® mounting medium.

Immunostaining for GAD_{67} (Glutamate Decarboxylase)

This staining was only performed on primary septal cell cultures. Cells were treated with 10% normal goat serum (NGS, Vector Laboratories) and 0.5 % Triton x-100 (in 0.1 M PB) for 30 min before being incubated with mouse anti-GAD_{67} primary Antibody (1:5000, affinity purified monoclonal antibody, Chemicon International, Hampshire, United Kingdom) in 0.1 M PB (supplemented with 1 % NGS and 0.5 % Triton x-100) for 12 hours at 4℃. After washing with 0.1 M PB (3 ×10 min), they were subsequently stained by the addition of Alexa 568-conjugated goat anti-mouse antibody (1:500,

InVitrogen GmbH, Karlsruhe, Germany) in 0.1 M PB for 1 hour at room temperature. Following a final washing period (4×30 min in 0.1 M PB), cultures were placed on microscope glass slides and mounted with Vectashield® mounting medium.

Immunostaining for GAD_{67} (Glutamate Decarboxylase) / NF-200 (Neurofilament) / DAPI

This staining was only performed on primary septal cell cultures. Cells were treated with 5% NGS and 0.2 % Triton x-100 (in 0.1 M PB) for 30 min before being incubated with rabbit anti-NF-200 primary Antibody (1:5000, gently provided by Shanting Zhao) in 0.1 M PB (supplemented with 1 % NGS and 0.5 % Triton x-100) for 12 hours at 4℃. After washing with 0.1 M PB (3×10 min), they were subsequently incubated with mouse anti-GAD_{67} (1/5000) in 0.1 M PB (supplemented with 1% NGS, 0.2% Triton x-100) for 12 hours at 4℃. Thereafter, cells were wa shed with 0.1M PB (3×10 min) and stained by the addition of Alexa 568-conjugated goat anti-mouse antibody (1:500) and Alexa 488-conjugated goat anti-rabbit in 0.1 M PB for 3 hours at room temperature (this solution also contained DAPI for coloration of the cells nuclei). Following a last washing period (4×30 min in 0.1 M PB), cultures were placed on microscope glass slides and mounted with Vectashield® mounting medium.

Immunostaining for PARV (Parvalbumine)

This non-fluorescent staining was only performed on brain sections of the septal region. All steps were strictly identical to those described for the non-fluorescent ChAT staining of brain sections. The only differences were as follows: the primary antibody was mouse anti PARV antibody (1/2000; AB 1572, Chemicon International, Temecula, USA) and the secondary antibody was biotinylated horse anti mouse antibody (1/200; BA 2001, Vector Laboratories Burlingame, USA)

2.7.2. Microscopy

Brain slices and cell cultures, once stained, were first screened under a fluorescence microscope for overview pictures (AxioPhot with AxioCam, using AxioVision software, Zeiss, Oberkochen, Germany). Subsequently, some of them were further analysed using a confocal laser microscope [AxioVert 135 (Zeiss, Oberkochen, Germany) equipped with the confocal emission unit MRC 1024 (BioRad, Hercules, CA, USA) and the MetaMorph 7.0 software (Universal Imaging, Downingtown, PA, USA)].
All pictures taken under the fluorescence microscope were obtained in black & white before being coloured using Corel draw® Graphics Suite – Version 12.

2.8. HIGH-PERFORMANCE LIQUID CHROMATOGRAPHY (HPLC)

Tissue preparation: Rats were killed by microwave irradiation (1.5 s; 6.3 kW; Sairem, Villeurbanne France) in order to rapidly inactivate brain enzymes. After decapitation, the brain was extracted and dissected on a cold plate in order to extract the prefrontal, frontal, temporal and occipital cortices, the striatum, the septum and both hippocampi which were separated into a dorsal (septal pole) and a ventral (temporal pole) portions. The left and right structures from each rat were pooled, weighed and kept at – 80°C until neurochemical determination. Concentrations of DA and its main metabolite, DOPAC, NE, 5-HT and its main metabolite 5-HIAA were measured using high-performance liquid chromatography (HPLC) with electrochemical determination. The tissue samples were prepared by homogenization in 1N formic acid/acetone (18/8.5, vol/vol), and the formic extract was used for monoamine determinations.
Determination of monoamines concentrations: The monoamine concentrations were measured without further purification. The HPLC system consisted of an ESA liquid chromatography pump (ESA Inc., Bedford) coupled to an ESA Coulochem II detector (Eurosep Instruments) equipped with a 5014 high-performance analytic cell (ESA Inc., Bedford). The detector potential at the analytic cell was set at + 0.4V. High-performance liquid chromatography analysis was performed on a C18 Spherisorb ODS2 reverse-phase column (5 µm pore size, 4.6 mm in diameter, 25 cm long). The mobile phase consisted of 0.1 M NaH_2PO_4, pH = 3, containing 0.1 mM/l of EDTA, 1.7 mM/l L-octane sufonic acid sodium salt and 10% acetonitrile. The flow rate was 1 ml/min.

2.9. BODY TEMPERATURE MEASUREMENTS

Rectal temperature was measured with a Pic indolor Vedo Flex (Artsana-Grandate, Italy) digital thermometer with a 0.1 ℃ precision, and lubricated with Vaseline. Determination of the temperature took a maximum of 30 s. The first measurement was taken 1 h before drug treatment (between 11:00 and 11:20 am). The other measurements were made 30, 60, 120, 180 and 300 min after drug administration. The ambient temperature during measurements was of 23 ± 0.1℃. Group sizes were: SALINE n = 5; EtOH n = 6; MDMA n = 5 and EtOH+MDMA n = 7.

2.10. BEHAVIOURAL ASSESSMENTS

2.10.1. Alternation in the T-maze test

Rats were tested for spontaneous alternation in the T-maze test, i.e. without any food reward. All testings were performed between 12:00 and 18:00. The apparatus was a gray Perspex T maze (10 cm high × 10 cm wide) with a transparent Perspex roof and a 40-W white lamp located 105 cm above the choice point. The 45-cm-long stem and 21-cm-long side arms ended in 20-cm-long interchangeable start/goal boxes. Guillotine doors were located at the entrance to the stem and on each side arm, thus allowing for the rat to be confined in the start box or in the chosen arm. For each trial, the rat was first subjected to a forced run for which it was placed in the start box for 10 s before the guillotine door was opened. Once the rat had reached the end of the forced arm (the other arm being closed), it remained in this arm for 30 s before another run was allowed (with both arms open). Start and goal boxes were interchanged with the rat inside. One trial (consisting in a forced run followed by a test run) was given each day during four days, and two additional trials were given on the 5^{th} day (4 h apart) so that six possible alternations were tested for each rat over the 5-day period. The experimenter was not aware of the rat's previous treatment. The variable considered was the percent alternation on the six trials ([number of alternations/6] x 100).

2.10.2. Sensory-motor coordination in the beam-walking test

This test was also conducted between 12:00 and 18:00. Assessment of motor coordination was performed by placing each rat on a 2 x 200 cm^2 wooden beam elevated 80 cm above the floor level, which was divided into four 50-cm segments, and in contact with the home cage on one extremity. All rats were trained according to the following protocol: in the first session, the rats were placed on the beam at 50 cm from the goal box (i.e., their home cage) on five consecutive occasions. In the next session, the rats were placed at 50, 100, 150 and 200 cm from the goal box, successively, with only one run allowed for each distance. In the third session, the rats were placed twice at 100 cm and twice at 200 cm from the goal box. In the fourth session, the rats were placed at 200 cm for three consecutive runs. On the next day, all rats were tested for three consecutive trials as in the fourth session and their performance was rated. For each virtual 50-cm segment of the beam, the experimenter rated the locomotor behaviour, by giving a score of 1 per segment when the rat traversed the segment with all paws on the upper surface of the beam. Conversely, a score of 0 was given for each segment on which the rat slipped or placed its toes on the side surface of the beam. The overall score was calculated by adding the scores of the three runs (maximal score = 12). The observer was not aware of the rat's previous treatment.

2.10.3. Anxiety in the elevated plus-maze test

We used conditions under which rats do not normally avoid entering the open arm. Forty five min before the test was started each rat was brought individually to the testing room and kept in the home cage. The elevated plus-maze apparatus was made of black Plexiglas and consisted of four arms (50 cm long x 10 cm wide) fixed to a central platform (10 x 10 cm): two of them had 40-cm high walls (closed arms), and two had 1.5-cm high borders instead of the walls (open arms). The arms crossed at a right angle and the apparatus was elevated 73 cm above the floor. The testing room was equipped with four halogen lamps, positioned on the diagonals of the plus maze (45° from each arm), at an identical distance from the central platform. For both open arms, the intensity of the light was 10 Lux. For testing, rats were placed individually in the centre of the maze with their head facing a closed arm (the same for all rats). Between each test, the apparatus was wiped clean with a solution of 2.0 % cider vinegar. Each test lasted for 5 min. The measures were recorded by an experimenter, blind to the

treatments, who observed the rats via a monitor connected to a camera (fixed on the desk, 300 cm above the floor level). An entry in a given arm was counted when the rat had completely entered the arm (4 paws + tail in the arm). The primary measures were the number of entries and the time spent in each arm. Entries and time in the centre were also recorded. These measures enabled us to compute the number of entries and time spent on open and in closed arms, respectively. To balance for potential locomotion biases, the absolute number of entries and time on the open arms was expressed as a percentage of the total number of entries in all arms or of the time spent in these arms, respectively (open/[closed + open]x100).

2.10.4. Locomotor activity

Spontaneous activity of the rats was measured in their home cage, and all rats were tested at once. No experimenter entered into the room in which activity was measured during recording. The cages were taken from the colony room and placed on shelves (eight cages per shelf) in a separate room (light conditions as in the colony room). Rats had free access to food and water during activity recording. Each cage was positioned in between two crossing infrared light beams, targeted on two photocells, 4.5 cm above floor level and 28 cm apart. The number of crossings in the cage (successive interruptions of the beams, and thus only two-dimensional movements) was monitored continuously by a microcomputer. After each drug administration, the activity was recorded continuously for 5 h. The drugs were injected at 12:00 noon. The ambient temperature during measurements of locomotor activity was 25℃ ± 0.1℃, thus about two degrees higher than in the colony room. This difference was due to a fortuitous disturbance of temperature control on the first day, and we decided to keep that value for the three other days to ensure as stable as possible experimental conditions for all activity recording.

3. RESULTS

3.1. INCREASED EXPRESSION OF THE 5-HT_{1B} RECEPTOR *IN VITRO* AND *IN VIVO* (PART 1)

Overview

This part of the thesis explored the possibility to enhance the expression of the 5-HT_{1B} heteroreceptor in cholinergic neurons using virally mediated gene transfer.

In the first section, the goal was (1) to identify infected cells, (2) to show that the 5-HT_{1B} receptor was expressed in infected cells and finally, (3) to provide evidence that some of these transfected cells containing the 5-HT_{1B} receptors were cholinergic neurons.

In the second section, the possible functional consequences of the transfection of the 5-HT_{1B} receptor on the presynaptic modulation of electrically-evoked ACh release were assessed with a superfusion technique. It is noteworthy that immunocytochemical stainings and neurotransmitter release experiments were performed on *different* septal cell cultures, which were, however, always prepared and cultured according to the same protocol.

3.1.1. Microscopic aspects of the original and transfected cells in culture

3.1.1.1. Non-infected septal cell cultures

Dissociated septal cells grew well in medium supplemented with mNGF and hNT-3 on circular poly D-lysine-coated glass coverslips. The pictures of Figure 19 show primary septal cell cultures at DIV 14, in which cholinergic neurons were stained using an antibody against ChAT. As evident from Figure 19, at DIV 14 cultured cholinergic cells were mainly organized in aggregates and extended their neurites so that all aggregates were extensively linked to each other in a network covering the whole glass plate. Light microscopic observation (not shown) revealed that this network was composed of multiple layers.

This staining procedure was performed in order to have an impression of cholinergic cells and their organization in untreated septal cell cultures. As this type of staining procedure may, however, impair the possibility to observe GFP-positive cells (following transfection with viral vectors), it was not further used in this study. Thus, all subsequent stainings on septal cell cultures used a fluorescent secondary antibody.

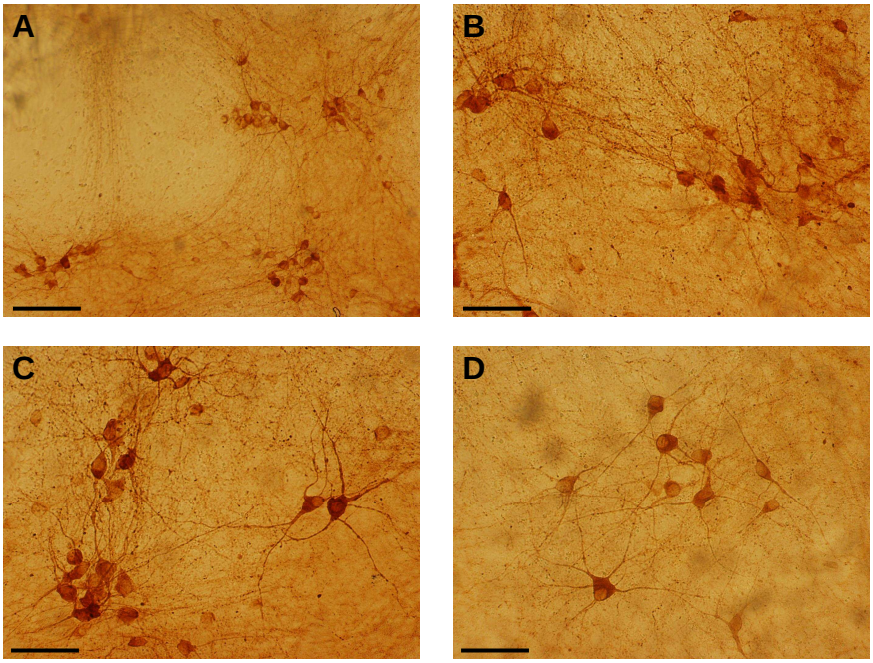

Figure 19. Microscopic aspect of ChAT-immunostaining of not transfected primary septal cell cultures (at DIV 14). As evident from pictures **(A) to (D)**, cholinergic cells in the primary septal cultures were organized in aggregates linked to each other by extensive neurites. Scale bar in A: 100 µm; scale bar in B-D: 60 µm.

Neurofilament-200, DAPI and Glial Fibrillary Acidic Protein stainings

The presence of neuronal and glial cells in primary septal cell cultures was checked using the corresponding antibodies. Thus, a primary antibody labeling the axonal marker protein neurofilament-200 (NF-200) was combined with a staining for cell nuclei [labeling of DNA A and T bases using DAPI (4,6-DiAmino-2-PhenylIndole)]. DAPI-staining results in a blue coloration of all (non-neuronal and neuronal) nuclei. Moreover, another antibody against Glial Fibrillary Acidic Protein (GFAP) was used to reveal glial cells.

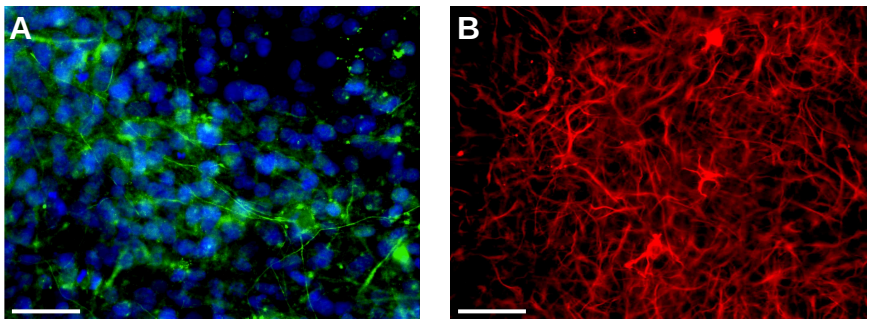

Figure 20. Microscopic aspect of non-transfected primary septal cell cultures stained for **(A)** the neuronal axonal marker protein Neurofilament-200 (or NF-200; green staining) and DAPI (blue staining) and **(B)** the Glial Fibrillary Acidic Protein (or GFAP; red staining) as described in Methods. Scale bar: 20 µm.

As shown in Figure 20, primary septal cells cultured from the fetal rat brain at ED17 contained neuronal as well as non-neuronal cells. The non-neuronal cells, labeled with GFAP were most probably of the glial type. These glial cells were organized in a layer covering the entire glass coverslips. Figure 20**A** shows a combination of the labeling of the axonal extensions stained using a marker of the axonal protein neurofilament-200 and a labeling of all nuclei present in the cell culture. The result shows a high number of nuclei as well as a high number of neuronal projections.

Choline acetyltransferase labeling

In order to check which cells in the septal cultures were cholinergic, in addition to the DAB-staining shown in Figure 19, a immunofluorescent labelling was performed to visualize the highly specific cholinergic marker ChAT. This technique was also used to address the question whether ChAT-positive cells in the cultures were transfected following incubation in the presence of the viral vectors (see below).

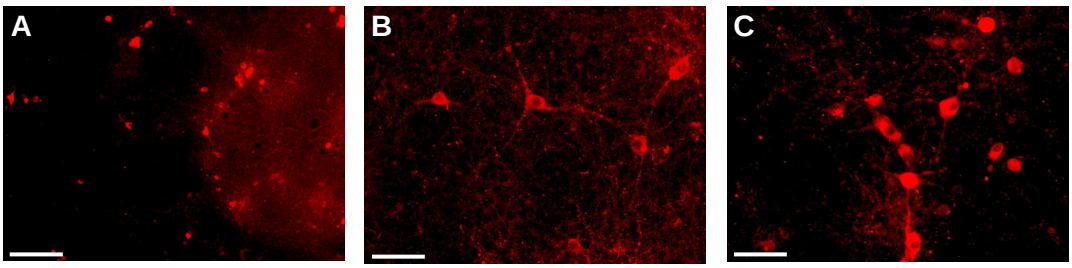

Figure 21. Microscopic aspect of non-transfected primary septal cell cultures labeled for ChAT at DIV 14. Scale bar in A: 100 µm and in B-C: 60 µm.

Figure 21 depicts this staining on non-infected cells. It is confirmed that the primary septal cell cultures are composed of multiple cell layers containing a high proportion of cholinergic neurons organized in aggregates. Even if a fluorescent staining does not allow a as fine and accurate observation of the cells as does the DAB staining, the microscopic aspect of the cells was comparable in both cases.

Glutamic Acid Decarboxylase 67 labeling

GAD_{67} is an isoform of the Glutamic Acid Decarboxylase, the enzyme synthesizing GABA. In contrast to the other isoform of this enzyme (GAD_{65}), which has an axonal localization, GAD_{67} seems to be located in the somata and the dendrites of GABAergic neurons. Nevertheless, these two enzymes have a very similar amino acid sequence in their primary structure so that they are thought to have similar active sites. Both GAD isoforms are considered specific markers for GABAergic neurons.

As for the ChAT labeling, prior to observation of the possible colocalization of GAD_{67} and GFP markers in infected cells, some non-infected cells were subjected to a staining against GAD_{67}.

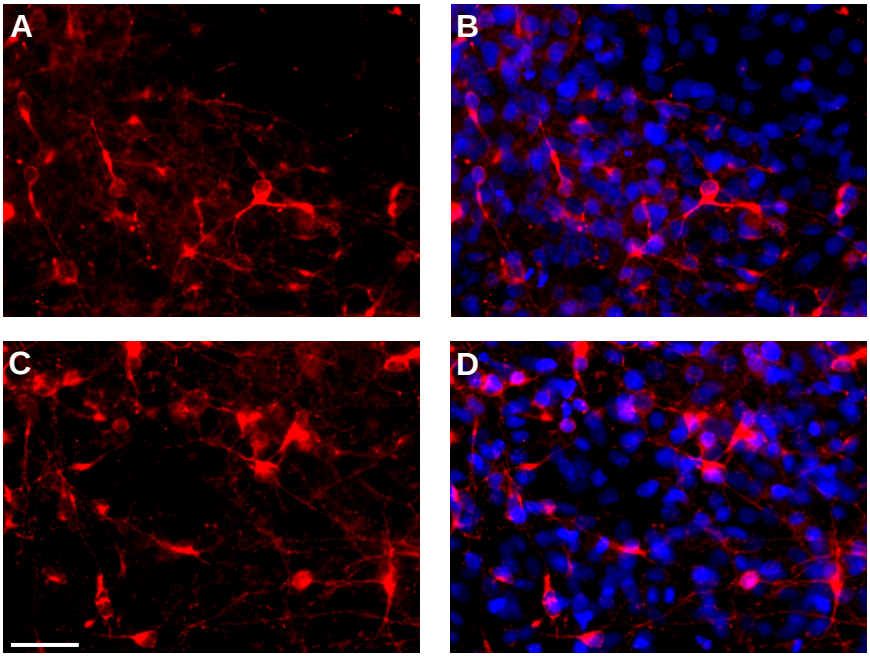

Figure 22. Microscopic aspect of non-transfected primary septal cell cultures labeled for **(A) & (C)** Glutamic Acid Decarboxylase 67 (GAD_{67}), the enzyme synthesizing GABA and **(B) & (D)** the same labeling combined to DAPI-staining. Scale bar (60 µm) is valid for all pictures.

As shown in Figure 22A, an important number of GAD_{67}-positive cells was detected in the primary septal cultures.

In order to better identify the neurochemical type of septal cells after their infection with the viral vectors, we also performed stainings against the 5-HT_{1B} receptor, Somatostatin, Neurotensin and Substance P (SP). As regards the 5-HT_{1B} receptor, the aim was to directly label the receptor in order to check their presence after transfection with the HA1B/GFP vector. Concerning the three neuropeptides, they were shown to be present in septal neurons. Firstly, stainings were performed on non-infected cells but unfortunately, the results did not allow us to properly observe labelled cells. Indeed, the fluorescent signals were very weak making the visualization of neurons impossible. For these reasons, these stainings were not further used on viral vectors-infected cells.

3.1.1.2. Characterization of GFP-positive cells in septal cell cultures infected with viral vectors

Primary cell cultures from the rat fetal septal region were transfected either with the viral construct expressing only GFP (GFP group) or with the viral construct expressing both GFP and the 5-HT_{1B} receptor (tagged with hemagglutinin [HA]; HA1B/GFP group). Both viral vectors were carrying the cDNA for the *Green Fluorescent Protein* (GFP). Thus, visualization of GFP-positive cells in primary septal cell cultures allows the identification of cells infected with the viral particles. Figure 23 shows GFP-positive cells in primary septal cell cultures at different magnifications. As the viral vectors potentially infect all neuronal types, the proportion of infected cells in the culture was always relatively high. Moreover, due to the different washings during immunostaining and also due to the fact that viral particles enter the cells, no background staining was present during observation of GFP-positive cells. Consequently, as shown on Figure 23B, C or D, even some GFP-positive neurites were detectable.

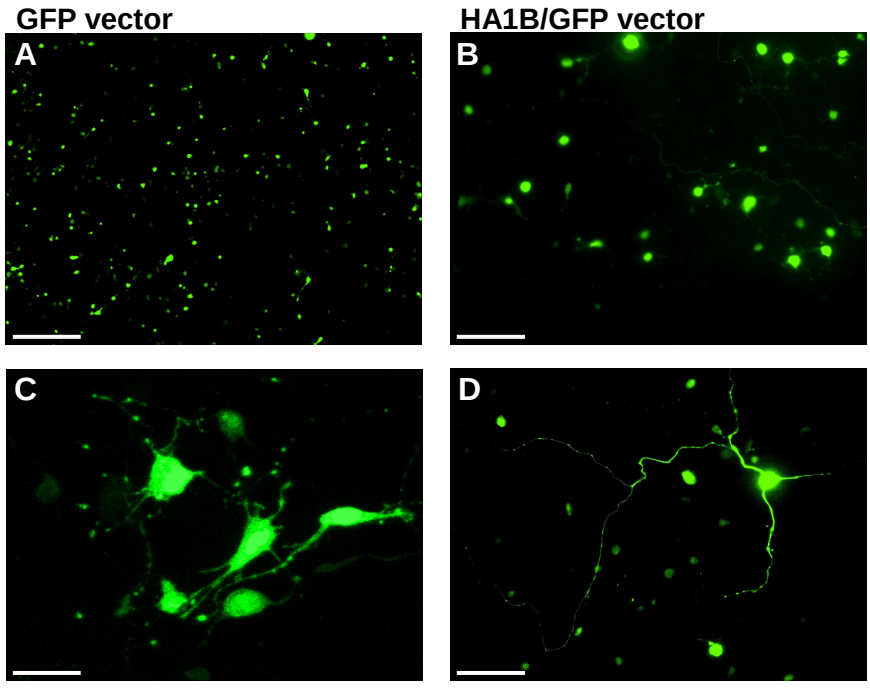

Figure 23. Microscopic aspect of GFP-positive cells in primary septal cell cultures. At DIV 11, cells were transfected with either the GFP or the HA1B/GFP vector (by mixing the viral solution directly with the growth medium at a concentration of 1 µl viral solution / 1 ml growth medium). Following fixation (at DIV 14) and rinsing, cells were either directly observed under a fluorescent or confocal microscope. **(A) & (C)** Cells infected with GFP vector. **(B) & (D)** Cells infected with HA1B/GFP vector. **A, B & D.** Cells observed under a fluorescence microscope. **C.** Cells observed under a confocal microscope. Scale bars; A: 200 µm; B: 150 µm; C: 50 µm and D: 60 µm.

Neurotropism of HSV vectors

Again the glial marker GFAP allowed us to show the presence of a large number of glial cells in the cultures. However, in cultures transfected with the GFP vector or HA1B/GFP vector (not shown), no colocalization between GFP and GFAP was found, confirming that the HSV vectors used in this study are neurotropic vectors (Figure 24).

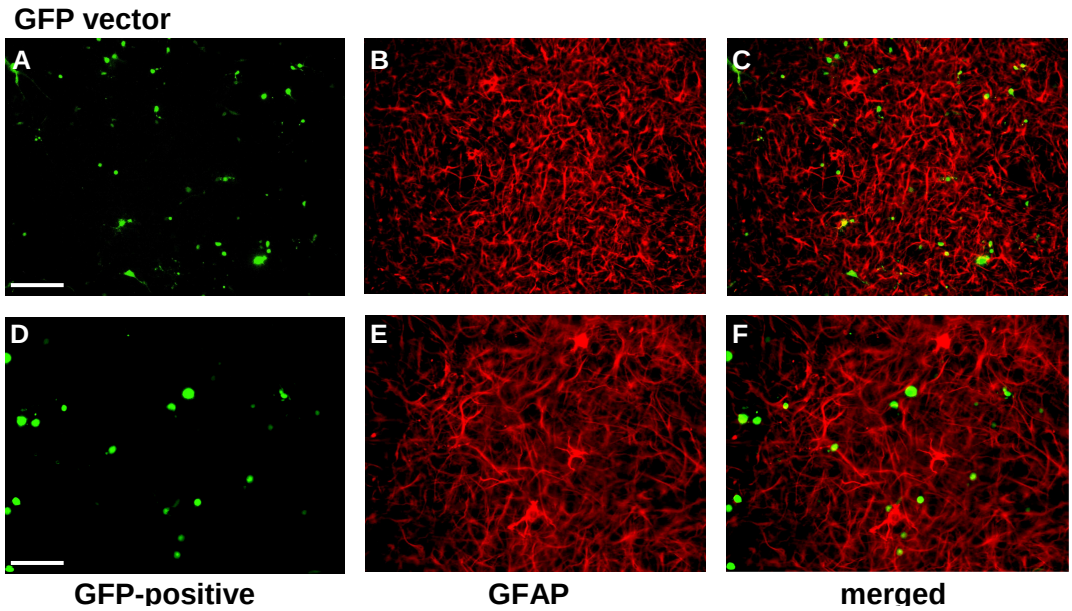

Figure 24. Microscopic aspect of GFAP-immunostained septal cell cultures. **(A) & (D)** GFP-positive cells in the septal cell cultures. **(B) & (E)** GFAP labeling at the same position as in pictures A & D, respectively. **(C) & (F)** Merged pictures of A & B and D & E, respectively. Scale bar in A, B & C: 100 µm. Scale bar in D, E & F: 80 µm.

Hemagglutinin labeling

As described in Methods, a hemagglutinin (HA) epitope tag was introduced into the N-terminus of the 5-HT_{1B} gene to allow easier detection of 5-HT_{1B} receptor expression. As shown in Figure 25, neuronal cells transfected with GFP only exhibited the classical green fluorescence of GFP, whereas a labeling of cells with an antibody against hemagglutinin could not be shown (Figure 25A to C). In contrast, cell cultures transfected with the HA1B/GFP construct exhibited both GFP as well as hemagglutinin labeling and these two labels were colocalized in an important proportion of cells (see arrow heads in Figure 25D to F).

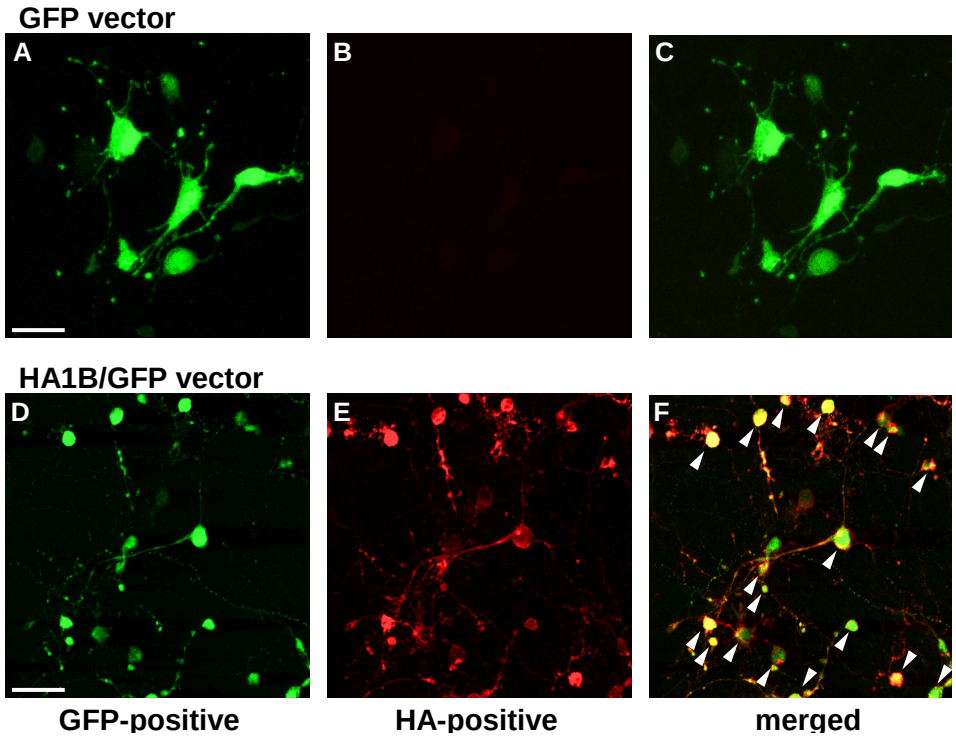

Figure 25. Microscopic aspect of HA immunostained septal cell cultures. **(A) & (D)** GFP-positive cells. **(B) & (E)** HA labeling at the same position as in pictures A & D, respectively. **(C) & (F)** Merged pictures of A & B and D & E, respectively. The yellow color in F indicates colocalization of the expression of HA and GFP within the same cells (see white arrows). Scale bars in A (40 µm) and D (60 µm) are respectively valid for B & C and E & F. All pictures were taken under the confocal microscope.

Choline acetyltransferase labeling

In order to check whether some of the GFP-positive cells in transfected septal cell cultures were cholinergic, a labeling of ChAT was performed. As evident from Figure 26, cell cultures of the rat fetal septal area transfected with the GFP or the HA1B/GFP vectors showed (at different levels of magnification) many GFP-positive cells (Figure 26A, D, G & J). Moreover, some of the cells were also ChAT-positive (Figure 26B, E, H & K). Finally, as evident from the merged pictures, in some of the neurons expressing GFP a colocalization with the presence of ChAT can be shown (Figure 26C, F, I & L). In addition to these observations it should also be noted, that some ChAT-positive neurons were negative for GFP (not visible in Figure 26) and that some GFP-positive cells were not stained for ChAT (see Figure 26B & C). According to these remarks, we were also able to confirm that the ChAT-positive cells observed are due to a real labeling rather than presenting false positive results. However, because of the high density of the cellular network, it was not possible to quantify the number of cholinergic cells and their proportion with respect to all neuronal cells. Moreover, despite its good quality, the ChAT staining did not always allow us to detect neurites.

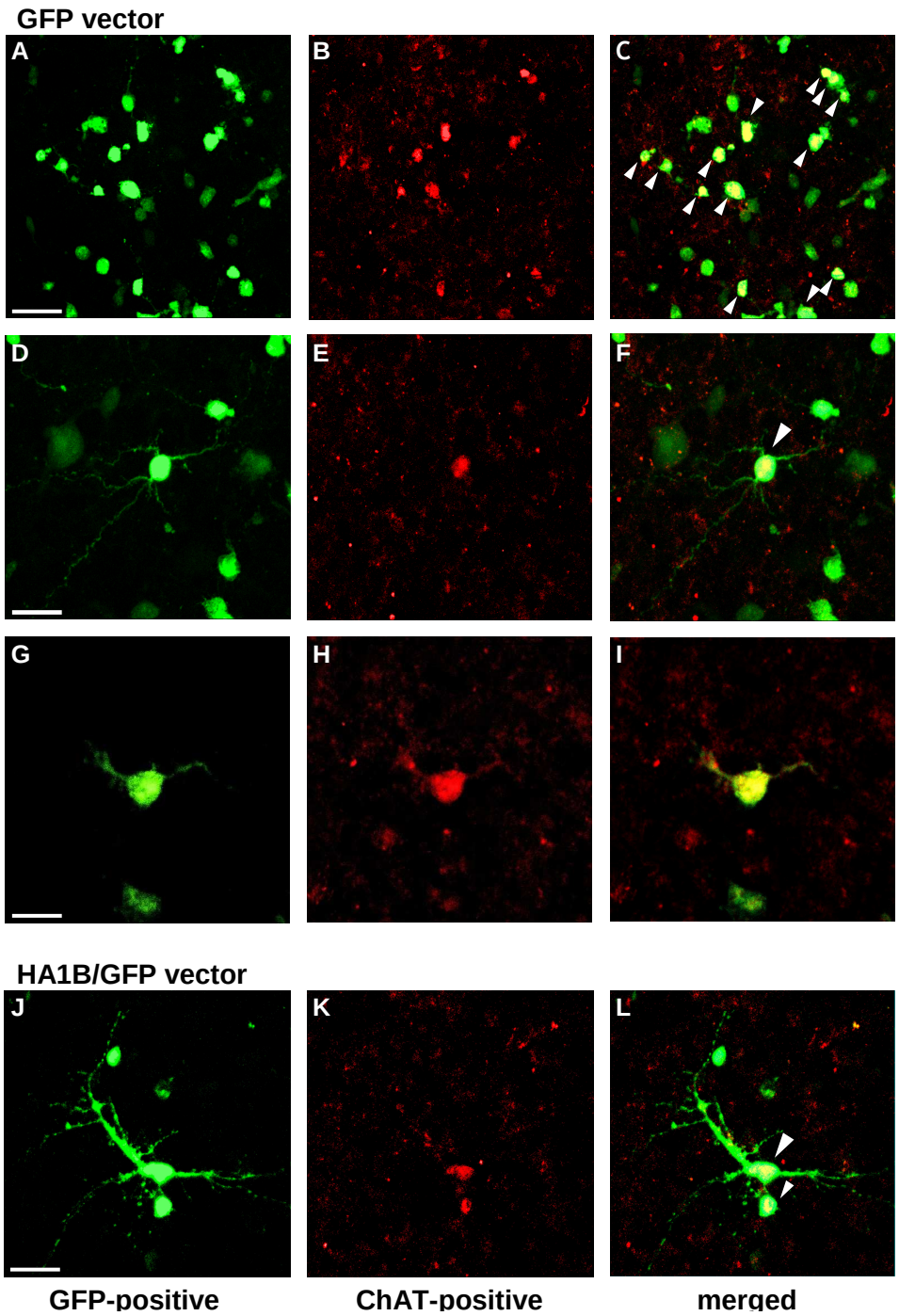

Figure 26. Microscopic aspect of ChAT immunostained septal cell cultures transfected with either the GFP **(A to I)** or the HA1B/GFP vector **(J to L)**. **(A), (D), (G) & (J)** GFP-positive cells. **(B), (E), (H) & (K)** ChAT labeling at the same position as in pictures A, D, G & J, respectively. **(C), (F), (I) & (L)** Merged pictures of A & B; D & E; G & H and J & K, respectively. The yellow color in C, F, I & L indicates colocalization of the expression of ChAT and GFP within the same cells (see white arrow heads). Scale bars in A (50 µm), D (20 µm), G (10 µm) & J (20 µm) are respectively valid for B & C; E & F; H & I and K & L. All pictures were taken under the confocal microscope.

GAD_{67} labeling

As the embryonic septal region of the rat brain at ED17 contains some GABAergic cells, the purpose of this staining was to check whether some GFP-positive cells could be identified as GABAergic neurons. As shown in Figure 27, it is possible to detect cells co-expressing both GFP and GAD_{67}, confirming that the viral particles were potentially entering all types of neurons present in the cultures. Pictures of Figure 27 were taken from cell cultures infected with the GFP vector but the same results were obtained with cell cultures transfected with the HA1B/GFP vector.

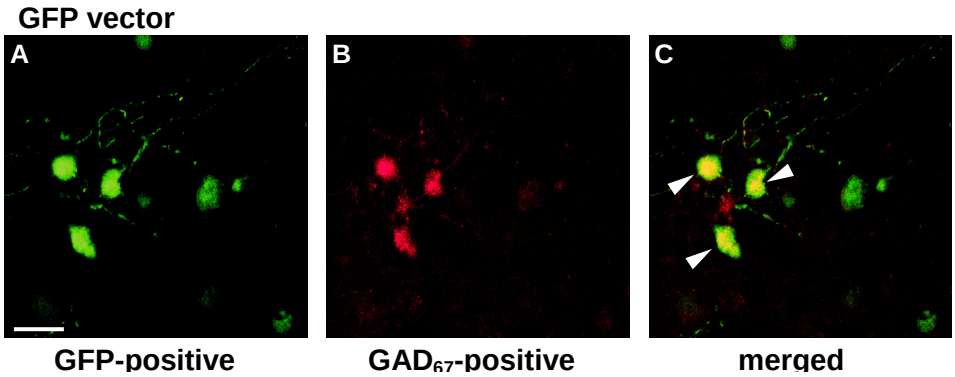

Figure 27. Microscopic aspect of GAD_{67} immunostained septal cell cultures. **(A)** GFP-positive cells. **(B)** GAD_{67} labeling at the same position as in picture A. **(C)** Merged picture of A & B. The yellow color in C indicates colocalization of the expression of GAD_{67} and GFP within the same cells (see white arrows). Scale bar in A (20 µm) is also valid for B & C. All pictures were taken under the confocal microscope.

3.1.2. Microscopic aspects of septal sections from non-injected rats or from rats stereotaxically transfected with viral vectors

3.1.2.1. Septal sections from non-injected rats

The pictures shown in Figure 28 were taken from septal sections of the brains of rats that were not subjected to viral vectors injections. Nevertheless, also in these rats a "sham operation" was performed, namely a bilateral stereotaxic implantation of guide cannulae into the septal region. Such septal sections were thus taken to verify the correctness of the implantation coordinates. Moreover, microscopic inspection of the injection sites showed that a destruction of the tissue as well as a reactive gliosis appeared following implantation, at the level of the guide cannulae. Nevertheless, inasmuch as the guide cannulae were implanted 2 mm above the injection site, only a minor damage of the target zone was observed (data not shown).

Figure 28 represents a staining of such septal sections of non-injected "sham" rats using antibodies against ChAT, or the GABergic marker parvalbumin (PARV),

respectively. As described in the Introduction, GABAergic neurons in the medial septum are located along the midline whereas the cholinergic ones have a more lateral position. That is confirmed on Figure 28 A & C onto which the midline is visible.

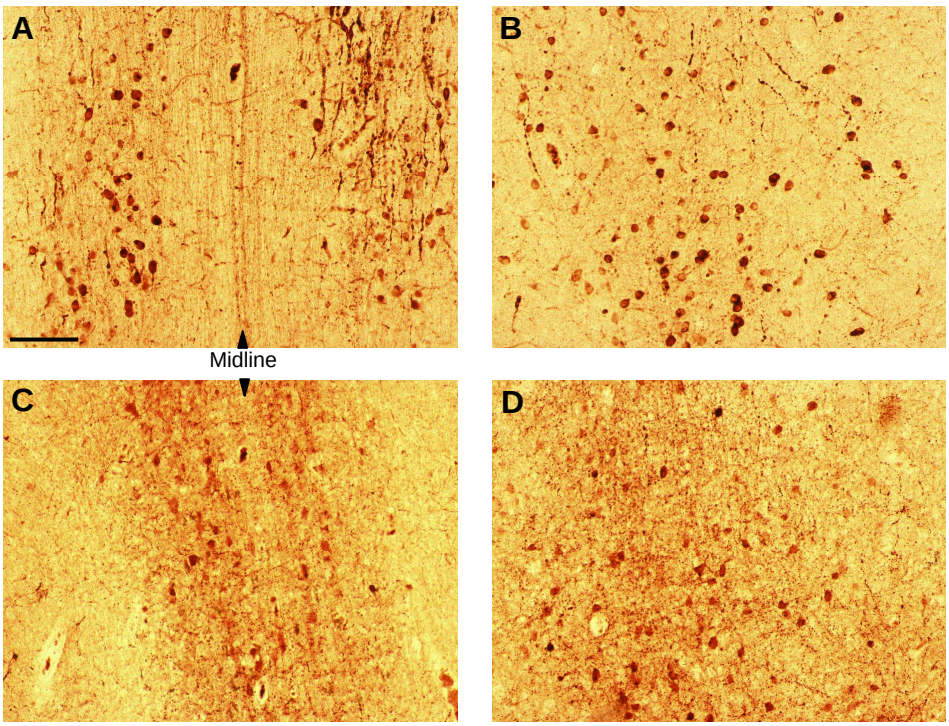

Figure 28. ChAT- (A & B) and PARV-immunostainings (C & D) of septal slices from non-injected "sham" rats. **(A) & (B)** show dark brown-cholinergic neurons using a staining against ChAT. **(C) & (D)** show brown-GABAergic neurons using a staining against PARV. Pictures A & C are both taken at the midline level. Scale bar: 200 µm.

3.1.2.2. Septal sections from virus-injected rats

GFP positive cells

Figure 29 shows an example of sections from a brain of a rat injected with the HA1B/GFP vector. On the right-hand side of picture A, the track of one cannula is visible (reactive gliosis or inflammatory response showing up as autofluoresence). GFP-positive cells were clearly detected in the vicinity of the extremity of the cannula track. All rats in which the guide cannulae were not implanted properly or in which no GFP-positive cells could be detected in the septal region were discarded from further statistical analyses.

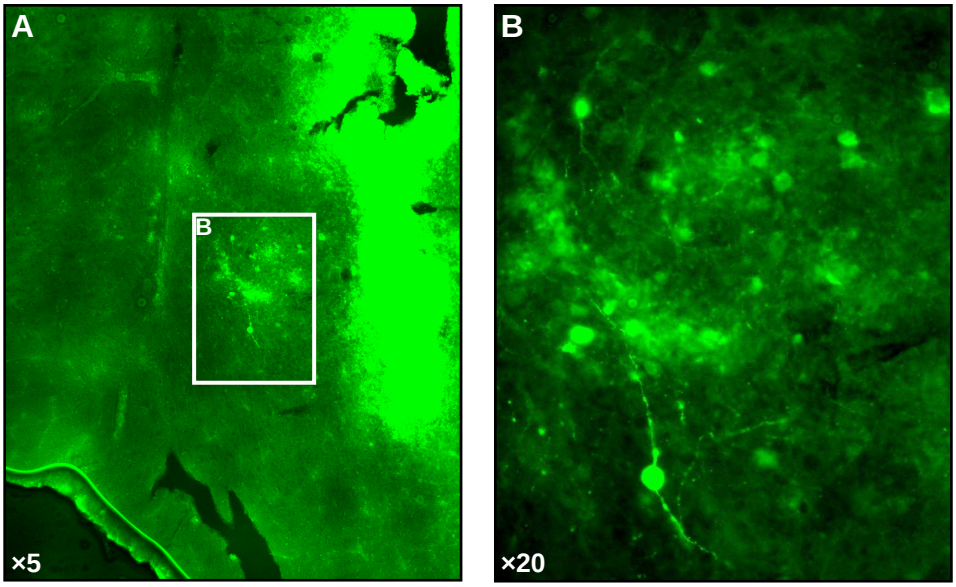

Figure 29. Microscopic aspect of septal slices from brain of rats injected with HA1B/GFP vector. **(A)** shows an overview of the septal region in which the cannula track is visible (right-hand side of the picture). **(B)** is a magnification of the frame in the A picture showing GFP-positive cells.

Hemagglutinin immunostaining

As mentioned in Methods, a hemagglutinin (HA) epitope tag was introduced into the N-terminus of the 5-HT_{1B} gene to allow detection of the transfected 5-HT_{1B} receptor. As shown in Figure 30A, many neuronal cells of the septal region of rats stereotaxically transfected with the GFP vector showed a green fluorescence but in none of these cells a staining for HA could be detected (Figure 30B and C). In contrast, septal cells of rats transfected with the HA1B/GFP vector exhibited both a staining for GFP (Figure 30D), as well as for the HA (Figure 30E and F).

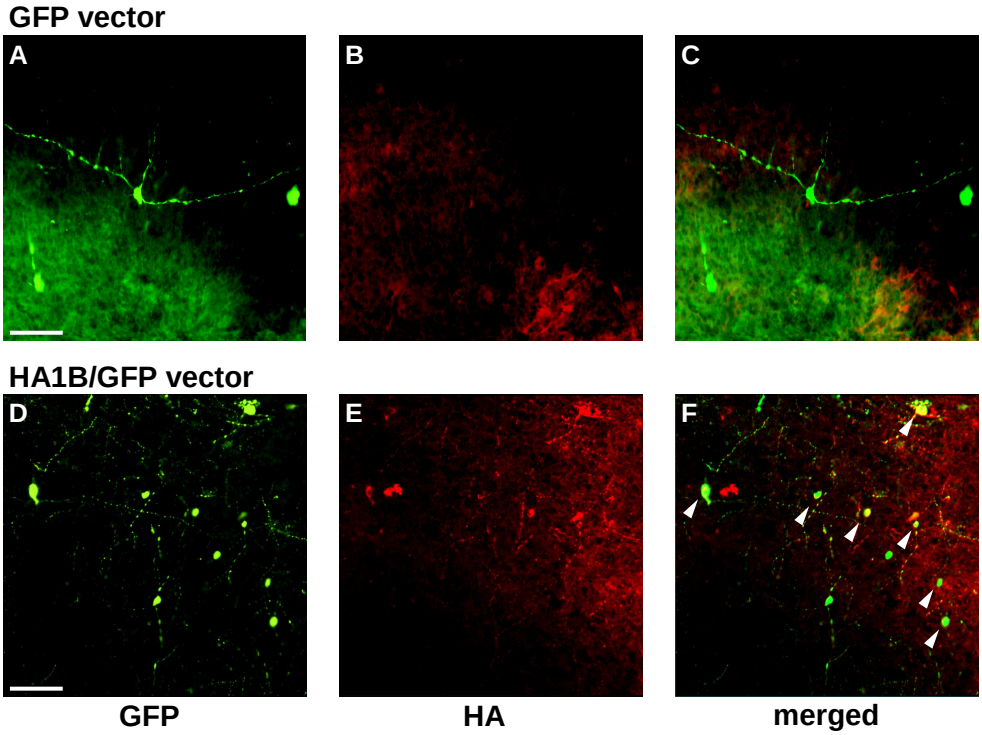

Figure 30. Microscopic aspect of the septal region of rats transfected with the GFP or the HA1B/GFP vector, respectively, using hemagglutinin (HA) immunostaining. **(A), (B), (C)** pictures from a brain infected with the GFP vector; **(D), (E),** and **(F)** pictures from a brain infected with the HA1B/GFP vector. **(A)** and **(D)** show cells expressing GFP**, (B)** and **(E)** show stainings using the HA antibody. In **C** and **F** the corresponding pictures are merged (**A** + **B** and **D** + **F**, respectively). The yellow color in F (not visible in C) indicates the colocalization of GFP and HA expression within the same cells (see arrows). Scale bar in A: 20 µm (valid for B and C); scale bar in D: 50 µm, valid for E and F.

Choline acetyltransferase immunostaining

In order to check whether some of the cells transfected with the HA1B/GFP vector were cholinergic, we also performed ChAT immunocytochemistry in slices of the septal region of stereotaxically transfected rats. As shown above (Figure 29) many cells in the septal region were GFP-positive and thus indicative for a virally-mediated expression of this protein. In addition, however, it can be demonstrated that some of these cells (Figure 31 depicts only one example) are both GFP-positive as well as stained with an antibody against ChAT. Microscopic observation of a large number of cells also revealed GFP-positive cells that were negative for ChAT as well as cholinergic neurons that had no GFP fluorescence. In this context it should be noted, however, that the colocalization of ChAT and GFP might be underestimated, because ChAT antibodies do not penetrate well into the tissue sections whereas GFP expression is easily detectable also in deeper regions of the tissue.

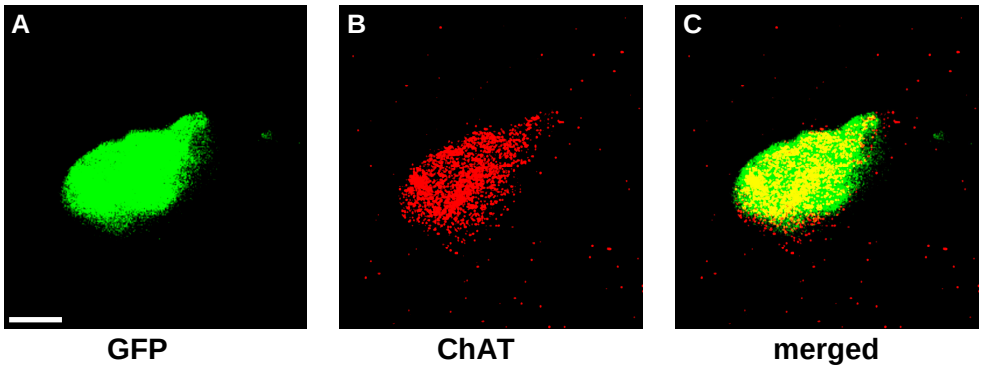

Figure 31. Microscopic aspect of the septal region of the rat transfected with the HA1B/GFP vector using immunostaining against ChAT. **(A) C**ell expressing GFP at a high level of magnification and **(B)** the same cell but stained for ChAT. **(C)** represents the corresponding merged picture (**A** + **B**). The yellow color in C indicates a colocalization of GFP and ChAT expression within the same cell. Pictures were taken under the confocal microscope. Scale bar: 20 µm.

3.1.3. Increased expression of 5-HT_{1B} receptors in septal cell cultures in vitro: Effects on electrically-evoked [^{3}H]-ACh overflow

3.1.3.1. Electrically-evoked [^{3}H]-ACh overflow in non-infected cell cultures

Before starting experimentation on septal cell cultures with the viral vectors, preliminary experiments were conducted on non-infected cells. For this purpose, primary cell cultures were prepared according to the protocol described in Methods. At DIV 14, cell cultures were carefully washed with KH-buffer and then incubated with [^{3}H]-choline. Following incubation, cells were washed again, superfused and electrically stimulated twice (S_1, S_2).

The results showed that the non-infected primary septal cell cultures (n = 35) accumulated 1.509 ± 0.031 pmol/cell culture discs of the tritiated precursor. The basal outflow of tritium amounted to 0.911 ± 0.065 nCi, which corresponds to 0.726 ± 0.043 % of the accumulated [^{3}H]. The first electrical stimulation (S_1) elicited an evoked overflow of [^{3}H] from these cells of 0.776 ± 0.106 nCi, which corresponds to 0.644 ± 0.09 % of the [^{3}H]-content of the cell cultures in the time period just before electrical stimulation.

Eight minutes before the second electrical stimulation, the selective 5-HT_{1B} agonist CP-93,129 was added to the superfusion buffer at three different concentrations: 0.1, 1 and 3 µM. One-way ANOVA of the S_2/S_1 ratios, taking into account the drug concentration as a factor was performed in order to compare all values to the control value (data are shown in Figure 32). ANOVA showed that there was an overall significant effect of the Concentration ($F[3,31] = 15.73$; $p < 0.001$). This effect was due to a significant inhibitory effect of CP-93,129 on the electrically-evoked overflow of tritium, whatever concentration was considered. Indeed, 0.1 µM of CP-93,129 decreased the electrically evoked [^{3}H]-overflow by about 22% ($p < 0.01$), 1 µM by about 29% ($p < 0.001$) and 3 µM by about 38% ($p < 0.001$) as compared to untreated controls.

In order to check whether CP-93,129 also affected the spontaneous outflow of tritium from such cell cultures, we considered the basal efflux quotient (b_2/b_1 in nCi or in % of the accumulated [^{3}H]). One-way ANOVA taking into account the Concentration was performed in order to compare all values to the control value (data not shown). ANOVA showed that there was no significant effect of the Concentration ($F[3,30] = 1.04$; n.s.), suggesting that CP-93,129, had no effect on the spontaneous outflow of tritium.

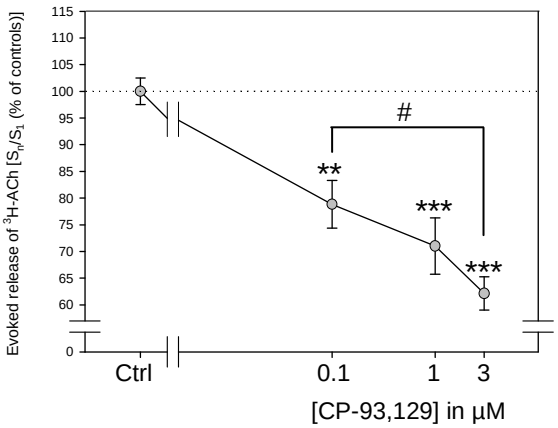

Figure 32. Effects of increasing concentrations of CP-93,129 on the electrically-evoked release of [^{3}H]-ACh in non-infected primary septal cell cultures. At DIV 14, cells were washed, incubated with [^{3}H]-choline, superfused continuously and electrically stimulated twice. CP-93,129 at three concentrations (0.1, 1 and 3 µM) was added 8 min before the second stimulation onwards. Values are shown as Mean ± SEM of the S_2/S_1 ratios in % of the corresponding untreated controls (no drug before S_2). n = 10 (Controls); n = 12 (0.1 µM of CP-93,129); n = 6 (1 µM) and n = 7 (3 µM). ** $p < 0.01$ and ***$p < 0.001$ as compared to Controls (Ctrl) values. $^{\#}$ $p < 0.05$.

In another set of experiments on non-infected septal cell cultures, half of them were superfused continuously and electrically stimulated twice as described above, whereas the other half was superfused in the presence of the selective 5-HT_{1B} antagonist GR-55,562 (1 µM) throughout the whole superfusion time. Using both superfusion conditions, the selective 5-HT_{1B} receptor agonist CP-93,129 (0.1 or 1 µM) was added to the superfusion medium before the second electrical stimulation (S_2). Using the cells superfused with no substance throughout, CP-93,129 at 0.1 µM decreased the [^{3}H]-overflow to 67.97 ± 7.53 % of the controls and at 1 µM to 74.72 ± 8.23 % of the controls (n = 8). However, when GR-55,562 was present in the superfusion medium throughout superfusion, CP-93,129 at 0.1 µM had no inhibitory influence on the [^{3}H]-overflow (101.07 ± 11.64 % of the controls), whereas CP-93,129 at 1 µM decreased it to 83.68 ± 11.10 % of the controls (n = 8). Student's t-test showed that the inhibitory influence of 0.1 µM of CP-93,129 on [^{3}H]-ACh release was abolished by the presence of GR-55,562 in the superfusion medium ($p < 0.05$). The analysis also showed that the presence of the 5-HT_{1B} recetor antagonist had no effect on the basal outflow of [^{3}H] from the cells.

3.1.3.2. Electrically-evoked [^{3}H]-ACh release in GFP and HA1B/GFP-infected cells

Since one cannot exclude a priori that the viral transfection *per se* may affect functional aspects in the cultured cells, the GFP group always served as controls for the HA1B/GFP group.

Accumulation of [^{3}H]-choline in primary septal cell cultures

Data (in pmoles [^{3}H]-choline accumulation/cell culture disc) are shown in Figure 33 (light gray bars). Statistical comparison of the two groups of virally transfected cell cultures (GFP, or HA1B/GFP, respectively) using ANOVA did not reveal any significant differences in the amounts of accumulated [^{3}H]-choline (F[1,203] = 0.018; n.s.).

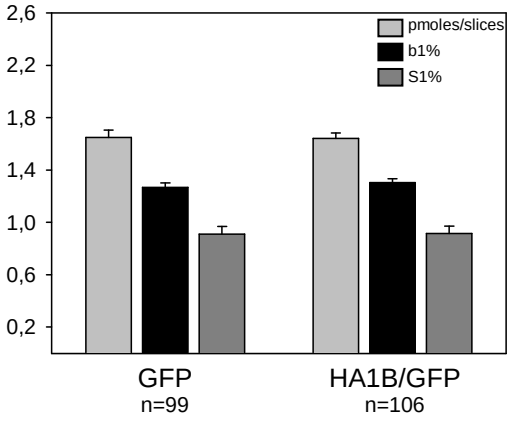

Figure 33. Accumulation of [^{3}H]-choline in primary septal cell cultures (in pmoles/slice; light gray bars), basal [^{3}H]-outflow in % of the accumulated [^{3}H] in the cultures (black bars) and electrically-evoked [^{3}H]-overflow in % of the accumulated [^{3}H] (dark gray bars) from GFP- and HA1B/GFP-infected cells. Following incubation with [^{3}H]-choline, cells were carefully washed, superfused and electrically stimulated twice. During superfusion, the KH-buffer was supplemented with the inhibitor of the high affinity choline uptake transporter, hemicholinium-3 at 10 µM. Each bar represents the mean of 99 or 106 cell cultures values, respectively, + SEM.

Basal outflow of tritium in primary septal cell cultures

Data (b_1-values in % of accumulated [^{3}H]) are shown in Figure 33 (black bars). Statistical analysis (ANOVA) of the basal outflow rates was performed on both absolute (in nCi) and relative (in % on the accumulated [^{3}H]) values, showing that there were no significant differences between values of cell cultures transfected with the GFP or HA1B/GFP vector. [absolute values: F[1,203] = 0.062; n.s.; relative values: F[1,203] = 0.733; n.s.].

Electrically-evoked overflow of tritium in primary septal cell cultures

Data (S_1-values in % of accumulated [^{3}H]) are shown in Figure 33 (dark gray bars). Statistical analysis (ANOVA) of the electrically-evoked [^{3}H]-overflow was performed on both absolute (in nCi) and relative (in % of the accumulated [^{3}H]) values. ANOVA showed no significant difference between the GFP and HA1B/GFP groups whatever variable was considered ($F[1,203] = 0.071$; n.s. when considering absolute values or $F[1,203] = 0.0031$; n.s. when considering relative values).

Effects of CP-93,129 on the evoked overflow of tritium in primary septal cell cultures

These experiments were performed to assess whether the function, i.e. the efficacy of the 5-HT$_{1B}$ receptor, was changed following transfection of septal cell cultures with the viral vectors. Therefore, following incubation of the cultures for 3 days with the GFP vector (= controls) of with the HA1B/GFP vector, the inhibitory effects of the selective 5-HT$_{1B}$-agonists CP-93,129 on the evoked release of [^{3}H]-ACh was evaluated.

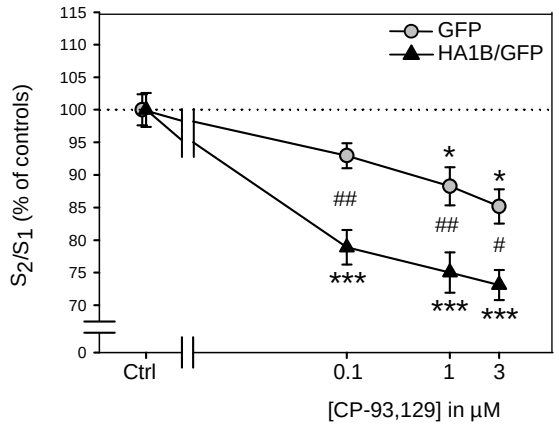

Figure 34. Electrically-evoked [^{3}H]-ACh overflow and its 5-HT$_{1B}$ receptor mediated modulation in GFP- and HA1B/GFP-infected primary septal cell cultures. Three days after infection of the cultures with the viral vectors, cells were washed, preincubated with [^{3}H]-choline, superfused continuously in the presence of hemicholinium-3 (10 µM) and electrically stimulated twice (S_1, S_2: see Methods). The curves represent the effects of various concentrations of the 5-HT$_{1B}$ receptor agonist CP-93,129 added before S_2 on the evoked overflow of [^{3}H]. Effects of CP-93,129 are shown as the ratio S_2/S_1 (in % of the corresponding drug free controls) of the evoked [^{3}H]-overflows elicited at the corresponding stimulation period. Means ± SEM. n = 25-9-24 (GFP group) or n = 31-14-24 (HA1B/GFP group), respectively per increasing CP-93,129 concentration. * $p < 0.05$ and *** $p < 0.001$ as compared to the respective drug-free controls (Ctrl). $^{\#}$ $p < 0.05$ and $^{\#\#}$ $p < 0.01$ when comparing the GFP and HA1B/GFP groups.

During superfusion, various concentrations of CP-93,129 were added to the medium before S_2. The inhibitory effects of this drug are shown in Figure 34. Data were analyzed using a two-way ANOVA combining the viral “Vector” as a first factor (GFP or

HA1B/GFP vector) and the “Drug concentration” as a second factor (slices where either controls [drug-free] or superfused with CP-93,129, at 0.1, 1 or 3 µM). ANOVA showed that there was an overall significant effect of Vector ($F[1,197] = 21.53$; $p < 0.001$) and of Drug concentration ($F[3,197] = 28.50$; $p < 0.001$), as well as a significant interaction between these factors ($F[3,197] = 3.79$; $p < 0.05$). The Drug concentration effect was due to a significant effect of CP-93,129 in both groups as compared to control slices (no drug addition before S_2). Indeed for the GFP group, 1 µM of CP-93,129 decreased the [^{3}H]-ACh release by about 12% ($p < 0.05$) and 3 µM by 15% ($p < 0.05$), as compared to respective controls. For the HA1B/GFP group, 0.1 µM of CP-93,129 decreased the [^{3}H]-ACh release by 22% ($p < 0.001$), 1 µM by 25% ($p < 0.001$) and 3 µM by 27% ($p < 0.001$), as compared to the respective controls. Moreover, the Vector effect as well as the interaction between both factors was due to an effect of CP-93,129 that was significantly more potent in septal cultures treated with the HA1B/GFP vector as compared to those treated with GFP virus for all concentrations tested ($p < 0.01$ for 0.1 and 1 µM of CP-93,129 and $p < 0.05$ for 3 µM of CP-93,129).

In order to assess whether the CP-93,129 had also an effect on the spontaneous release of tritium, we considered the basal efflux quotient (b2/b1 in nCi or in % of the accumulated [^{3}H]). Two-way ANOVA taking into account the factor Vector (GFP or HA1B/GFP) and the factor Drug concentration (Controls [drug-free] or CP-93,129 at 0.1, 1 or 3 µM) was performed in order to compare all values to the control value (data not shown). ANOVA showed that there was no significant effect of the Vector ($F[1,197] = 0.14$; n.s.). Conversely, there was an overall effect of the Drug condition ($F[3,197] = 3.35$; $p < 0.05$), but no interaction between these two factors ($F[3,197] = 1.02$; n.s.). Thus, CP-93,129 had no effect on the spontaneous outflow of tritium when comparing the GFP and the HA1B/GFP groups.

3.1.3.3. Role of GABA on [^{3}H]-ACh overflow in GFP and HA1B/GFP-infected cells

In these experiments both the $GABA_A$ antagonist Bicuculline (20 µM) and the $GABA_B$ antagonist CGP-56,999A (1 µM) were present throughout the experiment in the superfusion medium in addition to hemicholinium-3 (10 µM). In the following sections, these two experimental groups will be named GFP_{GABA} and $HA1B/GFP_{GABA}$, respectively.

Accumulation of [^{3}H]-choline in primary septal cell cultures

Data (in pmoles/cell culture disc) are shown in (light gray bars). ANOVA of the [^{3}H]-choline accumulation did not show any significant difference between the two groups (F[1,34] = 0.16; n.s.).

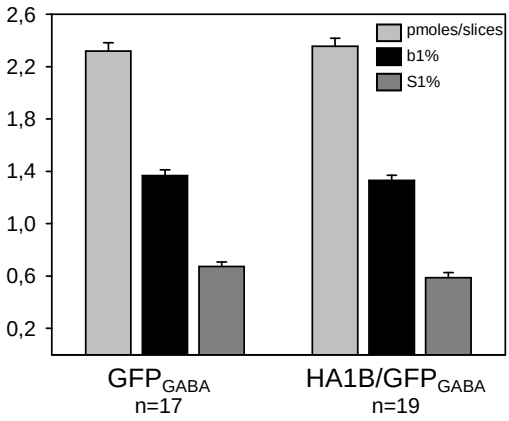

Figure 35. Accumulation of [^{3}H]-choline in primary septal cell cultures (in pmoles/slice; light gray bars), basal [^{3}H]-outflow (in % of the accumulated [^{3}H]) in the cultures (black bars) and electrically-evoked [^{3}H]-overflow (in % of the accumulated [^{3}H]; dark gray bars) from GFP- and HA1B/GFP-infected cells. Three days after infection of the cultures with the viral vectors, cells were washed, preincubated with [^{3}H]-choline, superfused and electrically stimulated twice. During superfusion the KH-buffer was supplemented with the inhibitor of the high affinity choline uptake transporter, hemicholinium-3 at 10 µM as well as with the antagonists for $GABA_A$ (bicuculline 20 µM) and $GABA_B$ (CGP-56,999A at 1 µM) receptors. Each bar represents the mean of 17 or 19 cell cultures values, respectively, + SEM.

Basal outflow of tritium in primary septal cell cultures

Data (b_1-values in % of accumulated [^{3}H]) are shown in Figure 35 (black bars). The statistical analysis of the basal [^{3}H]-outflow was performed on both absolute (in nCi) and relative values (in % of accumulated [^{3}H] per cell culture disc), but only relative values are shown in Figure 35. ANOVA of the baseline [^{3}H]-outflow from cell cultures showed no significant difference between the cultures infected with the GFP or the HA1B/GFP vector, whether on absolute (F[1,34= 0.13; n.s.) or relative values (F[1,34] = 0.39; n.s.).

Electrically-evoked overflow of tritium in primary septal cell cultures

Data (S_1%-values) are shown in Figure 35 (dark gray bars). Statistical analysis of the electrically-evoked overflow of tritium was performed on both absolute (in nCi) and relative values (in % of the accumulated [^{3}H] per cell culture disc) but only relative values are shown in Figure 35. ANOVA of the electrically-evoked overflow of tritium (in % of the accumulated tritium) showed no significant difference between the GFP_{GABA} and HA1B/GFP_{GABA} groups, whether on absolute (F[1,34] = 2.28; n.s.) or relative values (F[1,34] = 2.54; n.s.).

Statistical comparison of superfusion conditions (± $GABA_{A/B}$ antagonists)

In order to check whether the addition of $GABA_{A/B}$ antagonists to the superfusion medium throughout superfusion had an effect on the accumulation of [^{3}H]-choline or on the basal or the evoked outflow of [^{3}H], the data shown in Figure 33 and Figure 35 were compared statistically as follows:

- GFP vs. GFP_{GABA}
- HA1B/GFP vs HA1B/GFP_{GABA}

where GFP_{GABA} and HA1B/GFP_{GABA} represent the cell cultures transfected with the GFP and HA1B/GFP vectors, respectively, that were subsequently superfused with a buffer containing both $GABA_A$ and $GABA_B$ antagonists in addition to hemicholinium-3 (10 µM).

ANOVA of the *[^{3}H]-choline accumulation* values shown in Figure 33 and Figure 35 showed a significant difference between the GFP and GFP_{GABA} groups ($F[1,113] = 24.53$; $p < 0.001$) as well as between the HA1B/GFP and HA1B/GFP_{GABA} groups ($F[1,119] = 40.42$; $p < 0.001$). For both groups, these differences were due to a significant increase of the [^{3}H]-choline accumulation in GFP_{GABA} and HA1B/GFP_{GABA} as compared to GFP and HA1B/GFP, respectively.

Statistical analysis of the *basal [^{3}H]-outflow* values shown in Figure 33 and Figure 35 was performed on both absolute (in nCi) and relative values (in % of the accumulated [^{3}H]). ANOVA revealed a significant difference between the GFP and GFP_{GABA} groups ($F[1,113] = 17.47$; $p < 0.001$) as well as between the HA1B/GFP and HA1B/GFP_{GABA} groups ($F[1,119] = 25.03$; $p < 0.001$) when considering absolute b_1 values. Conversely, when analyzing relative values, no statistical difference was detected between these groups (GFP vs GFP_{GABA}: $F[1,113] = 0.91$; n.s. and HA1B/GFP vs HA1B/GFP_{GABA}: $F[1,119] = 0.069$; n.s.).

Statistical analysis of the *electrically-evoked [^{3}H]-overflow* values shown in Figure 33 and Figure 35 was performed on both absolute (in nCi) and relative (in % of the accumulated [^{3}H]) values. ANOVA of the electrically-evoked overflow of [^{3}H] showed no significant difference between the GFP and GFP_{GABA} ($F[1,113] = 0.31$; n.s.) or between HA1B/GFP and HA1B/GFP_{GABA} ($F[1,119] = 0.097$; n.s.) groups when considering absolute values. Moreover, when analyzing relative values, ANOVA also showed no significant difference between the GFP and GFP_{GABA} groups ($F[1,113] = 2.72$; n.s.), whereas a significant difference between the HA1B/GFP and HA1B/GFP_{GABA} groups ($F[1,119] = 5.16$; $p < 0.05$) was detected. This difference was due to an electrically-evoked [^{3}H]-overflow (in % of accumulated [^{3}H]) that was significantly lower in the HA1B/GFP_{GABA} group as compared to the HA1B/GFP group.

Effects of CP-93,129 on the evoked overflow of tritium in primary septal cell cultures when $GABA_{A/B}$ antagonists are present throughout superfusion

These experiments were performed to assess wether the function of the 5-HT_{1B} receptor was changed following transfection of septal cell cultures with the viral vectors even if $GABA_A$ and $GABA_B$ receptors were blocked during the release experiment.

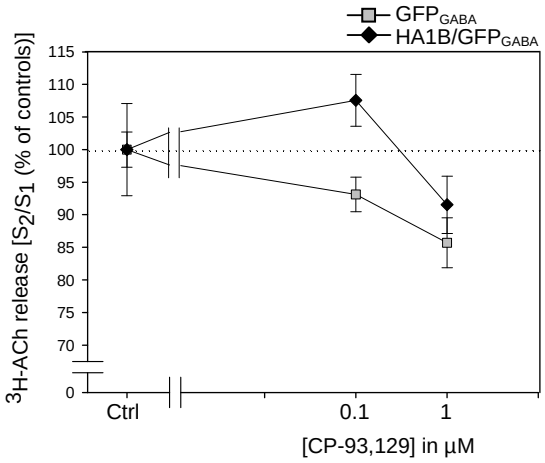

Figure 36. Electrically-evoked [^{3}H]-ACh release and its 5-HT_{1B} receptor mediated modulation in GFP- and HA1B/GFP-infected primary septal cell cultures. Three days after infection of the cultures with the viral vectors, cells were washed, preincubated with [^{3}H]-choline, superfused continuously and electrically stimulated twice (S_1, S_2: see Methods). During superfusion the KH-buffer was supplemented with hemicholinium-3 (10 µM) as well as with the antagonists for $GABA_A$ (bicuculline 20 µM) and $GABA_B$ (CGP-56,999A 1 µM) receptors The curves represent the effects of two concentrations of the 5-HT_{1B} receptor agonist CP-93,129 added before S_2 on the evoked overflow of [^{3}H]. Effects of CP-93,129 are shown as the ratio S_2/S_1 (in % of the corresponding drug free controls) of the evoked [^{3}H]-overflows elicited at the corresponding stimulation period. Means ± SEM. n = 6-5 (GFP group) or n = 5 (HA1B/GFP group), respectively per increasing CP-93,129 concentration.

The inhibitory effects of CP-93,129 under these superfusion conditions are shown in Figure 36. Data were analyzed using a two-way ANOVA combining the “Vector” as a first factor (GFP or HA1B/GFP vector) and the “Drug concentration” as a second factor (slices where either controls [drug-free] or superfused with CP-93,129, at 0.1 or 1 µM). ANOVA showed that there was an overall significant effect of Vector ($F[1,25] = 5.20$; $p < 0.05$) and of Drug concentration ($F[2,25] = 5.04$; $p < 0.05$), but no interaction between these factors ($F[2,25] = 2.13$; n.s.). The Drug Concentration effect was due to a significant difference in the HA1B/GFP group, between the two concentrations of CP-93,129 tested ($p < 0.05$). The difference between the two groups for the concentration of 0.1 µM of CP-93,129 tended to be significant ($p = 0.058$).

3.1.4. Increased expression of 5-HT_{1B} receptors in septohippocampal neurons: Effects on electrically-evoked [^{3}H]-ACh overflow

As for the septal cell cultures, preliminary experiments were performed using hippocampal slices on non-injected rats.

3.1.4.1. Electrically-evoked [^{3}H]-ACh overflow in hippocampal slices from non-injected rats

In this section various parameters of the [^{3}H]-ACh release model were determined in hippocampal slices of non-injected rats of the same strain (Long-Evans), in order to investigate by comparison with the corresponding data of virus injected rats (see below), whether the surgical procedure and injection into the septal region *per se* had an influence on transmitter release. In addition, these experiments were designed to provide further evidence for the presence of 5-HT_{1B} receptors on the axon terminals of septohippocampal cholinergic nerves.

The protocols of the [^{3}H]-ACh release experiments on hippocampal slices of these naïve rats, were strictly identical to those used with virus-injected rats. Four concentrations of the selective 5-HT_{1B} agonist, CP-93,129 (0.01, 0.1, 1 and 10 µM) were tested. Moreover, for half of the slices, the selective 5-HT_{1B} antagonist, GR-55,562 was added to the superfusion buffer throughout the whole experiment. Please note that whatever protocol is considered, the expression “throughout the experiment” always means that the substance was present during the incubation of the slices as well as during the whole superfusion period (see Methods).

Accumulation of [^{3}H]-choline in hippocampal slices of non-injected rats

Data (in pmoles/slice) are shown in Figure 37 (light gray bars). ANOVA of the [^{3}H]-choline accumulation in the absence or presence, respectively, of GR-55,562 throughout the experiment showed a significant difference between the two groups ($F[1,90] = 29.23$; $p < 0.001$). This difference was due to an accumulation of [^{3}H] that was significantly higher in slices that were superfused with a buffer containing GR-55,562.

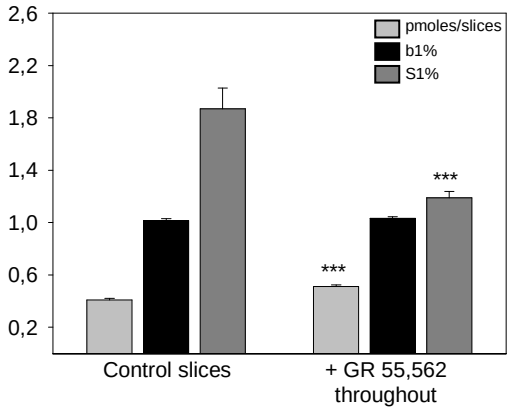

Figure 37. Accumulation of [^{3}H]-choline in hippocampal slices (in pmoles/slice; light gray bars), basal [^{3}H]-outflow (in % of the accumulated [^{3}H] per slice; black bars) and electrically-evoked [^{3}H]-overflow (in % of the accumulated [^{3}H] per slice; dark gray bars) from non-injected rats. The left part represents slices that were, superfused with a KH-buffer containing hemicholinium-3 (10 µM) only, whereas the right part represents slices superfused in the additional presence of the selective 5-HT$_{1B}$ antagonist, GR-55,562. Each bar represents the mean of 47 or 45 slice values, respectively, + SEM. ***$p < 0.001$ as compared to slices superfused with a control buffer, i.e. without GR 55,562.

Basal outflow of tritium in hippocampal slices of non-injected rats

Data (b_1-values in % of accumulated [^{3}H]) are shown in Figure 37 (black bars). Statistical analysis was performed on both absolute (in nCi) and relative (in % of the accumulated [^{3}H] in each slice) values but only relative ones are shown. ANOVA of the basal [^{3}H]-outflow from hippocampal slices showed a significant difference between slices treated throughout the experiment in the presence of GR-55,562 or not when considering absolute values ($F[1,90] = 39.06$; $p < 0.001$). In contrast, no difference was detected between these two groups when analyzing relative values ($F[1,90] = 39.06$; n.s.).

Electrically-evoked overflow of tritium in hippocampal slices of non-injected rats

Data (S_1-values in % of accumulated [^{3}H]) are shown in Figure 37 (dark gray bars). Again, statistical analysis was performed on both absolute (in nCi) and relative (in % of the accumulated [^{3}H]) values, but only relative ones are shown. ANOVA of the electrically-evoked [^{3}H]-overflow from hippocampal slices treated throughout the experiment in the presence or absence of GR-55,562 showed no significant differences between the two groups when considering absolute values ($F[1,90] = 2.52$; n.s.). Conversely, when analyzing relative values, ANOVA showed a significant difference between the two experimental conditions ($F[1,90] = 16.14$; $p < 0.001$). This difference was due to an overflow of tritium that was significantly decreased in the slices superfused with buffer containing the selective 5-HT$_{1B}$ antagonist, GR-55,562.

Effects of CP-93,129 on the evoked overflow of tritium in hippocampal slices of non-injected rats

These experiments had the following two aims: (1) to check if there was a concentration-dependency of the inhibitory effects of CP-93,129 and (2) to verify that the effects of CP-93,129 could be antagonized by the selective 5-HT_{1B} receptor blocker GR-55,562.

Four concentrations of the selective 5-HT_{1B} receptor agonist, CP-93,129, were tested in these experiments. The slices were successively subjected to this drug from the second (0.01 or 0.1 µM) or the third (1 or 10 µM) stimulations onwards with the concentration increasing from S_2 to S_3. Moreover, as mentioned above, one half of the slices were superfused with "Control buffer" whereas for the other half, the buffer contained the selective 5-HT_{1B} receptor antagonist, GR-55,562 (1 µM) in addition to hemicholinium-3 (10 µM).

Data (Figure 38) were analyzed using two-way ANOVA with repeated measures (the same slices were subjected to two concentrations of the same drug), comprising the following factors: "Throughout substance" (two levels: +/- GR-55,562 at 1 µM), "Drug concentration" (three levels: control [no drug] or "CP_1" [0.01 or 1 µM of CP-93,129] or "CP_2" [0.1 or 10 µM of CP-93,129]). The repeated measures factor was considered as Stimulation rank and corresponded to S_2/S_1 or S_3/S_1 values in % of the corresponding drug-free controls. ANOVA showed that there was an overall significant effect of the Throughout substance ($F[1,86] = 9.04$; $p < 0.01$), of the Drug concentration ($F[2,86] = 30.64$; $p < 0.001$) as well as of the Stimulation rank ($F[1,86] = 181.31$; $p < 0.001$). Moreover, there was a significant interaction between the Throughout substance and the Drug concentration ($F[2,86] = 3.34$; $p < 0.05$), as well as between the Drug concentration and Stimulation rank ($F[2,86] = 48.84$; $p < 0.001$). Finally there was also a significant interaction between the three aforementioned factors ($F[2,86] = 4.59$; $p< 0.05$). The Drug concentration effect was due to a significant inhibitory effect of CP-93,129 in both groups as compared to the corresponding control slices. The interaction between the Drug concentration and the Stimulation rank was due to a significant decrease of the [^{3}H]-ACh release when the concentration of CP-93,129 was increased, which was found in both groups. Indeed, in the group where the superfusion buffer contained no throughout substance and except for the lowest concentration (0.01 µM), 0.1 µM of CP-93,129 decreased [^{3}H]-ACh release by almost 14% ($p < 0.001$), 1 µM by 20% ($p < 0.001$) and 10 µM by 28% ($p < 0.001$) as compared to control slices.

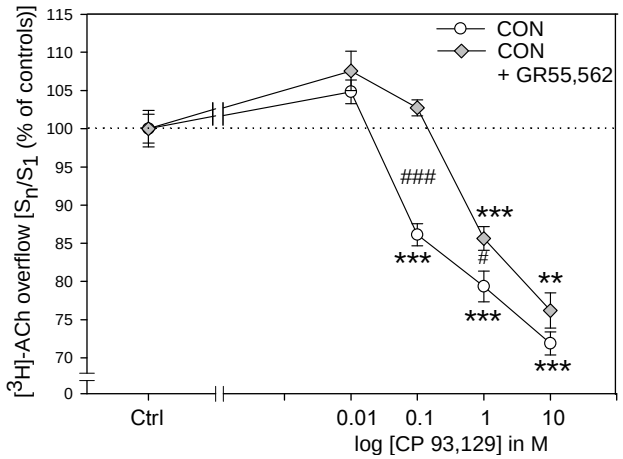

Figure 38. Effect of various concentrations of the 5-HT_{1B} receptor agonist, CP-93,129 added before S_n on the evoked overflow of [^{3}H] on hippocampal slices superfused (gray diamonds) or not (open dots) with a buffer containing 1 µM of the specific 5-HT_{1B} antagonist GR-55,562. Following incubation of the slices with [^{3}H]-choline, they were washed, superfused continuously and electrically stimulated three times (S_1, S_2, S_3). Effects of the different concentrations of CP-93,129 are shown as the ratio S_n/S_1 (in % of drug free controls) of the evoked [^{3}H]-overflows elicited at the corresponding stimulation period. Values are shown as Means ± SEM. n = 13 - 18 per CP-93,129 concentration. ** $p < 0.01$ and ***$p < 0.001$ as compared to the corresponding drug-free controls (Ctrl). $^{\#}$ $p < 0.05$ and $^{\#\#\#}$ $p < 0.001$ as compared to slices superfused with the control buffer (no addition of GR-55,562).

In the group, where the superfusion buffer contained 1 µM of GR-55,562, the concentration-effect curve of CP-93,129 was shifted to the right in a parallel manner. In fact, 1 µM of CP-93,129 decreased [^{3}H]-ACh release by 14% ($p < 0.001$) and 10 µM by almost 24% ($p < 0.001$) as compared to control slices. The interaction between all factors was due to an antagonization of the inhibitory effect of CP-93,129 in the presence of GR-55,562 in the superfusion buffer. Indeed, for the concentration of 0.1 and 1 µM of CP-93,129, the addition of GR 55,562 (1 µM) to the superfusion buffer, significantly antagonized the inhibitory effect of CP-93,129 ($p < 0.001$ and $p < 0.05$, respectively). When 0.1 µM of CP-93,129 was tested in the presence of GR 55,562, the S_2/S_1 ratio even approached the control value (102.7% vs. 86.1% when no GR 55,562 was present in the superfusion buffer, $p < 0.001$).

In order to see whether CP-93,129 had an effect on the spontaneous ACh release, we also analyzed the basal efflux quotient b_n/b_1. Data (not shown) were analyzed using two-way ANOVA with repeated measures (the same slices were subjected to two concentrations of the same drug), comprising the following factors: “Throughout substance” (two levels: +/- GR 55,562 at 1 µM), “Drug concentration” (three levels: control [no drug] or “CP_1” [0.01 or 1 µM of CP-93,129] or “CP_2” [0.1 or 10 µM of CP-93,129]). The repeated measures factor was considered as Stimulation rank and corresponded to b_2/b_1 or b_3/b_1 values in % of the corresponding drug-free controls.

ANOVA showed no overall significant effect of any of the considered factors (Throughout substance factor: ($F[1,86] = 0.26$; n.s.), Drug concentration factor ($F[2,86] = 0.53$; n.s.) or Stimulation rank ($F[1,86] = 2.74$; n.s.). Moreover, there was no interaction between any of these factors.

3.1.4.2. Comparison of GFP virus-injected to non-injected rats

In this section, [^{3}H]-ACh release data from non-injected rats (CON group) will be compared to those of GFP rats in order to answer the question, whether the surgical procedure and virus injection *per se* somehow could affect hippocampal transmitter release. The purpose was also to check whether the GFP group represents an appropriate control for the HA1B/GFP group.

Data of this comparison are shown in Table 12. ANOVA of the [^{3}H]-choline accumulation in hippocampal slices showed no significant difference between GFP and CON rats ($F[1,150] = 0.532$; n.s.). ANOVA of the values of baseline of [^{3}H]-outflow showed a significant difference between GFP and CON rats when considering absolute (in nCi; $F[1,105] = 27.23$; $p < 0.001$) or relative values (in % of accumulated [^{3}H]; $F[1,150] = 52.76$; $p < 0.001$). The latter difference was due to a basal outflow that was significantly lower (by 19%) in the GFP group as compared to the CON group. Concerning the electrically-evoked [^{3}H]-overflow, ANOVA showed no significant difference between the two groups when considering absolute values (in nCi; $F[1,105] = 3.79$; n.s.), but a weak and significant difference between these groups when analyzing relative values (in % of the accumulated [^{3}H]; $F[1,150] = 4.14$; $p = 0.04 < 0.05$). This effect was due to a lower evoked overflow (by 17%) in the GFP group as compared to the CON group.

Table 12 also compares the presynaptic inhibitory effects of CP-93,129 on the evoked release of [^{3}H]-ACh in these two groups. In order to do so, we performed a two-way ANOVA with a repeated measures factor. Indeed, some slices were successively subjected to 0.01 (S_2) and 1 µM of CP-93,129 (S_3) whereas another subset was subjected to 0.1 (S_2) and 10 µM (S_3) of the same drug. The ANOVA comprised the following factors: “Vector” (two levels: CON or GFP vector), “Drug concentration” (three levels: control [no drug] or “CP_1” [0.01 or 1 µM of CP-93,129] or “CP_2” [0.1 or 10 µM of CP-93,129]). The repeated measures factor was considered as Stimulation rank and corresponded to S_2/S_1 or S_3/S_1 values in % of the corresponding control. ANOVA showed that there was an overall effect of the Drug concentration ($F[2,101] = 52.77$; $p < 0.001$) as well as of the Stimulation rank ($F[1,101] = 328.1$; $p < 0.001$). Moreover,

there was a significant interaction between these two factors (F[2,101] = 100.81; p< <0.001). This significant interaction was due to an inhibitory effect of CP-93,129 in both groups as compared to the control (drug-free) slices. Moreover, this inhibition was stronger when the concentration of CP-93,129 was increased (this inhibition corresponds to the concentration-response curve of CP-93,129 in the hippocampal slices of these rats. Moreover, the analysis also showed that the inhibitory effect of CP-93,129 was stronger in the GFP group as compared to the CON group for the concentrations 0.01 ($p < 0.01$) and 1 µM ($p < 0.05$).

In addition, in order to see whether CP-93,129 had effects on the spontaneous outflow of tritium, we analyzed the basal efflux quotient b_n/b_1 in % of the corresponding drug-free control. Two-way ANOVA with reapeted measures comprised the following factors: "Vector" (two levels: CON or GFP vector), "Drug concentration" (three levels: control [no drug] or "CP_1" [0.01 or 1 µM of CP-93,129] or "CP_2" [0.1 or 10 µM of CP-93,129]). The repeated measures factor was considered as Stimulation rank and corresponded to b_2/b_1 or b_3/b_1 values in % of the corresponding control. ANOVA showed no significant difference between CON and GFP rats for any of the factors. Thus, CP-93,129 at the four concentrations tested had no effect on the spontaneous release of ACh.

Parameter	**CON**	**GFP**
pmoles/slice	0.41 ± 0.01	0.40 ± 0.01
b_1 (% of tissue-^{3}H)	1.02 ± 0.02	0.82 ± 0.02***
S_1 (% of tissue-^{3}H)	1.87 ± 0.16	1.55 ± 0.06*
CP-93,129 concentration	**Effects of CP-93,192 (in % of controls)**	
0.01 µM	104.83 ± 1.54	98.44 ± 1.81**
0.1 µM	86.13 ± 1.44	87.96 ± 2.25
1 µM	79.34 ± 2.03	75.59 ± 1.29*
10 µM	71.89 ± 1.51	73.95 ± 2.17

Table 12. Comparison of hippocampal ACh release models in CON rats (no surgery) with GFP virus-injected rats (GFP group): tissue accumulation of [^{3}H] (pmoles/slice), basal (b_1-values) and evoked overflow of [^{3}H] (S_1-values), and effects of CP-93,129 on the evoked overflow. Hippocampal slices of CON (47 slices) and GFP rats (60 slices) were incubated with [^{3}H]-choline, superfused and electrically stimulated as described in Methods. The effects of the 5-HT_{1B} receptor agonist CP-93,129 added before S_n are shown as the ratios (S_n/S_1) of the evoked overflows of [^{3}H] elicited at the corresponding stimulations (in % of the respective drug-free control values); means (± S.E.M); statistics: *p < 0.05; **p < 0.01; ***p < 0.001 vs. group CON.

3.1.4.3. Electrically-evoked [^{3}H]-ACh overflow in GFP and HA1B/GFP-injected rats

In this section, transmitter release data from rats of the GFP group were compared to that of rats of the HA1B/GFP group in order to assess the question, whether enhanced expression of the 5-HT_{1B} receptor (in addition to that of GFP) affects the extent and modulation of hippocampal [^{3}H]-ACh release. The time course of such [^{3}H]-ACh release experiments is shown in Figure 39, in which the "fractional rate of tritium outflow" was plotted against time (see Methods). Each value of all the slices subjected to identical experimental conditions was taken into account. These plots shown in Figure 39 give an overview of the progress of each experiment.

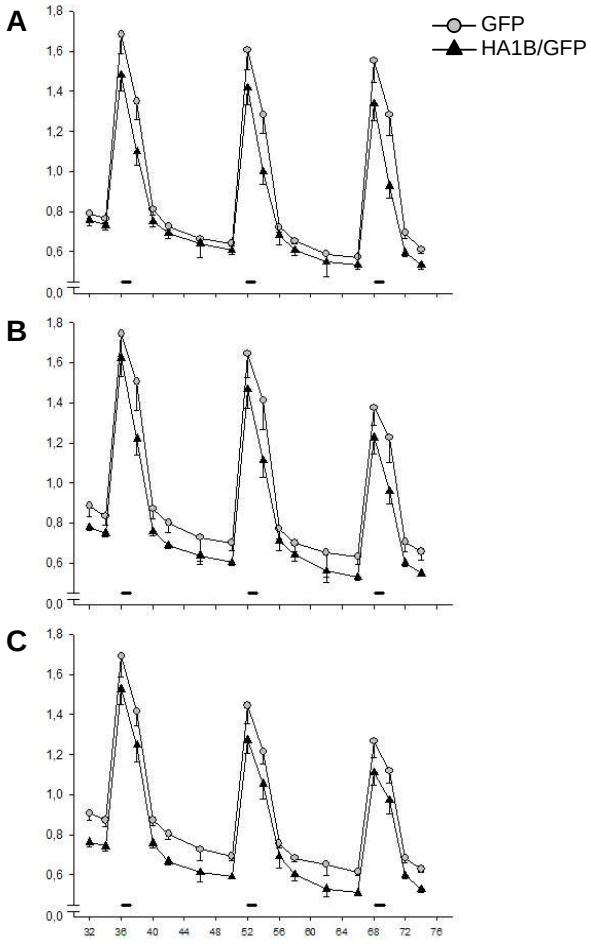

Figure 39. Time course of [^{3}H]-outflow in rat hippocampal slices incubated with [^{3}H]-choline. Following incubation, slices were washed, superfused continuously and electrically stimulated three times (S_1, S_2, S_3, small horizontal lines. Each electrical stimulation lasted for 30 s (slices were given 90 pulses at 3 Hz, see Methods). Fractions were collected every 2 min and electrical stimulations were applied after 36, 52 and 68 min, respectively. **(A)** Control slices, i.e., slices that were not subjected to any drug during the experiment. **(B)** CP-93,129 was added to the superfusion buffer before S_2 (0.01 µM) and S_3 (1 µM)

onwards. **(C)** CP-93,129 was added to the superfusion buffer before S_2 (0.1 µM) and S_3 (10 µM) onwards. Each value represents the mean of 20 or 19 slices – SEM for the GFP and HA1B/GFP groups, respectively.

Accumulation of [^{3}H]-choline in hippocampal slices of virus-injected rats

Data (in pmoles/slices) are shown in Figure 40 (light gray bars). ANOVA of the [^{3}H]-choline accumulation showed no significant difference between the GFP and HA1B/GFP groups (F[1,115] = 0.491, n.s.).

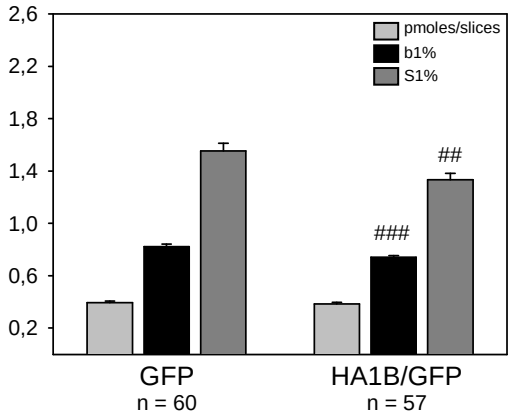

Figure 40. Accumulation of [^{3}H]-choline in hippocampal slices (in pmoles/slice; light gray bars), basal [^{3}H]-outflow (in % of the accumulated [^{3}H] per slice; black bars) and electrically-evoked [^{3}H]-overflow (in % of the accumulated [^{3}H] per slice; dark gray bars) from rats injected with GFP and HA1B/GFP virus. Three days after stereotaxic injection of either GFP or HA1B/GFP viral vectors into the rat septal region, hippocampal slices were prepared from the brains. Following incubation of the slices with [^{3}H]-choline, they were washed, superfused continuously (in the presence of hemicholinium-3 at 10 µM) and electrically stimulated three times (S_1, S_2, S_3). Each bar represents the mean of 60 (GFP group) or 57 (HA1B/GFP group) slice values + SEM. $^{##}p < 0.01$ and $^{###}p < 0.001$ as compared to slices of the GFP group.

Basal outflow of tritium in hippocampal slices of virus-injected rats

Data (b_1-values in % of accumulated [^{3}H]) are presented in Figure 40 (black bars). Statistical analyses were performed on both absolute (b_1-value in nCi) and relative (b_1 in % of accumulated [^{3}H] in each slices) values, but only relative values are illustrated in the graph. ANOVA of the basal [^{3}H]-outflow from hippocampal slices showed a significant difference between the GFP and the HA1B/GFP groups on both absolute (F[1,115] = 5.57; $p < 0.05$) and relative values (F[1,115] = 11.92; $p < 0.01$). This difference was due to a basal [^{3}H]-outflow that was significantly lower (by about 10%) in rats of the HA1B/GFP group as compared to rats of the GFP group.

Electrically-evoked overflow of tritium in hippocampal slices of virus-injected rats

Data (S_1-values in % of accumulated [^{3}H]) are shown in Figure 40 (dark gray bars). As for the baseline, statistical analyses were performed on both absolute (S_1 in nCi) and

relative (S_1 in % of the accumulated [^{3}H] in each slice) values but only relative values are illustrated in the figure. ANOVA of the electrically-evoked [^{3}H]-overflow from hippocampal slices showed a significant difference between the two groups on both absolute ($F[1,115] = 8.98$; $p < 0.01$) and relative values ($F[1,115] = 8.43$; $p < 0.01$). This difference was due to an electrically-evoked [^{3}H]-overflow that was significantly lower (by 15%) in slices from rats of the HA1B/GFP group as compared to those of the GFP group.

Effects of CP-93,129 on the evoked overflow of tritium in hippocampal slices of virus-injected rats

These experiments aimed at analyzing whether, in hippocampal slices of rats with enhanced expression of the 5-HT$_{1B}$ receptor (HA1B/GFP group), the concentration dependent inhibitory effect of CP-93,129 was more pronounced than in hippocampal slices of rats expressing GFP only (GFP group).

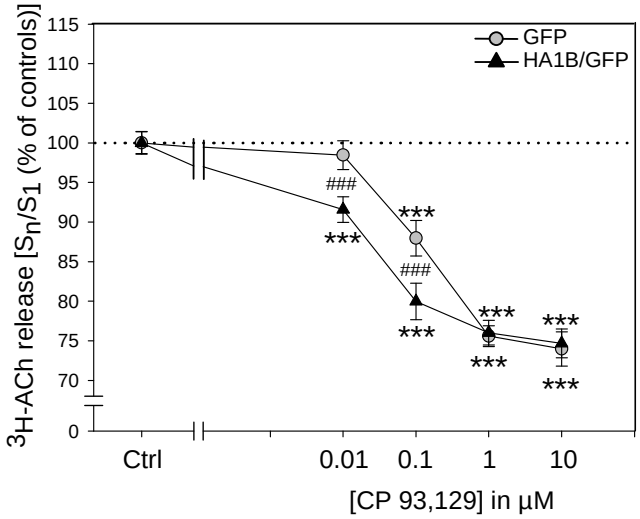

Figure 41. Electrically-evoked [^{3}H]-ACh release and its 5-HT$_{1B}$ receptor mediated modulation in hippocampal slices of virus-injected rats. Three days after stereotaxic injection of either GFP or HA1B/GFP viral vectors into the rat septal region, hippocampal slices were prepared from the brains and incubated with [^{3}H]-choline. Subsequently, they were washed, superfused continuously in the presence of hemicholinium-3 (10 µM) and electrically stimulated three times (S_1, S_2, S_3: see Methods). The curves represent the effects of various concentrations of the 5-HT$_{1B}$ receptor agonist CP-93,129 added before S_n on the evoked overflow of [^{3}H]. Effects of CP-93,129 are shown as the ratio S_n/S_1 (in % of the corresponding drug free controls) of the evoked [^{3}H]-overflows elicited at the corresponding stimulation period. Means ± SEM. n = 19-20 per CP-93,129 concentration. ***$p < 0.001$ as compared to the corresponding drug-free control (Ctrl) and $^{###}p < 0.001$ as compared to the GFP group.

Data are presented in Figure 41. CP-93,129 was added to the superfusion buffer from 8 min before S_2 and S_3 onwards, with concentrations increasing from S_2 to S_3. Indeed, some slices were successively subjected to 0.01 (S_2) and 1 µM of CP-93,129 (S_3) whereas another subset was subjected to 0.1 (S_2) and 10 µM (S_3) of the same drug.

Therefore, to compare the effect of CP-93,129 in GFP and HA1B/GFP groups on ACh release, a two-way ANOVA, considering a repeated-measure factor was performed. The factors were: “Vector” (two levels: GFP or HA1B/GFP vector), “Drug concentration” (three levels: control [no drug] or “CP_1” [0.01 or 1 µM of CP-93,129] or “CP_2” [0.1 or 10 µM of CP-93,129]). The repeated measures factor was considered as Stimulation rank and corresponded to S_2/S_1 or S_3/S_1 values in % of the corresponding control. ANOVA showed that there was an overall significant effect of Drug concentration ($F[2,111] = 66.99$; $p < 0.001$) and of the Stimulation rank ($F[1,111] = 153.44$; $p < 0.001$), as well as a significant interaction between Vector and Stimulation rank ($F[1,111] = 11.86$; $p < 0.001$) and a significant interaction between Drug concentration and Stimulation rank ($F[2,111] = 50.99$; $p < 0.001$). The interaction between all factors was close to reach significance ($F[2,111] = 3.03$; $p = 0.052$). The Drug concentration effect was due to a significant inhibitory effect of CP-93,129 in both groups as compared to control slices. The interaction between the different factors was due to a significant decrease of the [^{3}H]-ACh overflow when the concentration of CP-93,129 was increased, which was found in both groups. Indeed, for the GFP group, 0.1 µM of CP-93,129 decreased the [^{3}H]-ACh overflow by 12% ($p < 0.001$), 1 µM by 24% ($p < 0.001$) and 10 µM by 26% ($p < 0.001$) as compared to controls. The lowest concentration of CP-93,129 (0.01 µM) failed to significantly inhibit [^{3}H]-ACh overflow in this group ($p = 0.41$). For the HA1B/GFP group, 0.01 µM of CP-93,129 decreased the [^{3}H]-ACh overflow by 9% ($p < 0.001$), 0.1 µM by 20% ($p < 0.001$), 1 µM by 24% ($p < 0.001$) and 10 µM by 25% ($p < 0.001$) as compared to controls, indicating a shift to the left of the concentration-response curve in the HA1B/GFP group as compared to the GFP group. This was confirmed by the post-hoc comparisons, which showed that for the concentrations 0.01 and 0.1 µM, CP-93,129 decreased the overflow of [^{3}H]-ACh with a significantly higher potency in the HA1B/GFP group as compared to the GFP group ($p < 0.001$ for both concentrations).

In order to see whether CP-93,129 had an effect on the spontaneous release of ACh, a similar analysis was performed on the basal efflux quotient b_n/b_1 in % of the corresponding drug-free control. Therefore, to compare the effect of CP-93,129 in GFP and HA1B/GFP groups on spontaneous ACh release, a two-way ANOVA with repeated measures was performed, comprising the following factors: “Vector” (two levels: GFP or HA1B/GFP vector), “Drug concentration” (three levels: control [no drug] or “CP_1” [0.01 or 1 µM of CP-93,129] or “CP_2” [0.1 or 10 µM of CP-93,129]). The repeated measures factor was considered as Stimulation rank and corresponded to b_2/b_1 or b_3/b_1 values in % of the corresponding control. ANOVA showed no significant overall effect

of the factor Vector ($F[1,111] = 0.062$; n.s.) as well as no effect of the Stimulation rank ($F[1,111] = 0.07$; n.s.). However, it showed a slight but significant effect of the Drug Concentration ($F[2,111] = 3.53$; $p < 0.05$). Finally, no significant interaction between these factors was detected. The Drug concentration effect was due to a slight decrease of the spontaneous outflow of ACh following the application of 10 µM of CP-93,129 in the GFP group. No differences between the GFP and the HA1B/GFP groups were noticeable.

Effects of GR-55,562 on the evoked overflow of tritium in hippocampal slices of virus-injected rats

In order to check whether the effects observed in the former section were specific for the 5-HT_{1B} receptor, some complementary experiments were performed with addition of the 5-HT_{1B} specific antagonist, GR-55,562. As the concentrations 0.01 and 0.1 µM of CP-93,129 exhibited inhibitory effects on the electrically-evoked release of [^{3}H]-ACh, only these two concentrations were used and the slices were stimulated only twice. Two sets of experiments were performed: **(1)** the selective 5-HT_{1B} agonist, CP-93,129 (0.01 and 0.1 µM) was added to the superfusion medium 8 min before S_2 onwards, whereas the selective antagonist GR-55,562 (1 µM) was present in the superfusion buffer (in addition to hemicholinium-3 at 10 µM) throughout superfusion; **(2)** only hemicholinium-3 (10 µM) was present in the superfusion buffer throughout the experiment and GR-55,562 (1 µM) was added to the superfusion buffer from 8 min before S_2 onwards.

(1) Effects of CP-93,129 in presence of GR-55,562 throughout superfusion

Accumulation of [^{3}H]-choline in hippocampal slices of virus-injected rats

Data (in pmoles/slice) are shown in Figure 42 (light gray bars). ANOVA of the [^{3}H]-choline accumulation in hippocampal slices showed a significant difference between the GFP and HA1B/GFP groups ($F[1,42] = 31.82$; $p < 0.001$). This difference was due to an accumulation of [^{3}H] that was significantly higher in slices from rats of the HA1B/GFP group as compared to those of the GFP group.

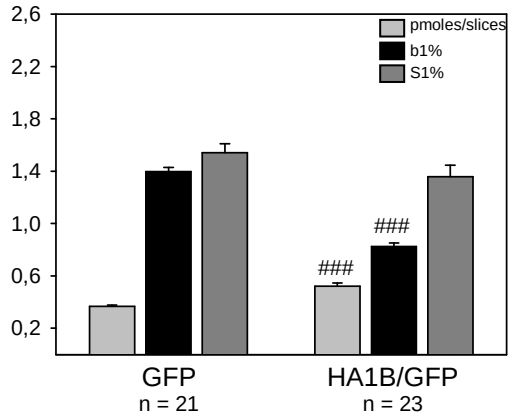

Figure 42. Accumulation of [^{3}H]-choline in hippocampal slices (in pmoles/slice; light gray bars), basal [^{3}H]-outflow (in % of the accumulated [^{3}H] per slice; black bars) and electrically-evoked [^{3}H]-overflow (in % of the accumulated [^{3}H] per slice; dark gray bars) from GFP and HA1B/GFP virus-injected rats. Three days after stereotaxic injection of either GFP or HA1B/GFP viral vectors into the rat septal region, hippocampal slices were prepared from the brains. Following incubation of the slices with [^{3}H]-choline, they were washed, superfused continuously in the presence of GR-55,562 (1 µM) in addition to hemicholinium-3 (10 µM) and and electrically stimulated twice (S_1, S_2). Each bar represents the mean of 21 (GFP group) or 23 (HA1B/GFP group) slice values + SEM. $^{###}p < 0.001$ as compared to slices of the GFP group.

Basal outflow of tritium in hippocampal slices of virus-injected rats

Data (b_1-values in % of accumulated [^{3}H]) are presented in Figure 42 (black bars). Statistical analyses were performed on both absolute (in nCi) and relative (in % of accumulated [^{3}H] in each slices) values, but only relative values are illustrated in the graph. ANOVA of the basal [^{3}H]-outflow from hippocampal slices showed a significant difference between the GFP and the HA1B/GFP groups on both absolute ($F[1,42] = 4.64$; $p < 0.05$) and relative values ($F[1,42] = 198.13$; $p < 0.001$). This difference was due to a basal [^{3}H]-outflow that was significantly lower (by about 59%) in rats of the HA1B/GFP group as compared to those of the GFP group.

Electrically-evoked overflow of tritium in hippocampal slices of virus-injected rats

Data (S_1-values in % of accumulated [^{3}H]) are shown in Figure 42 (dark gray bars). As for the baseline, statistical analyses were performed on both absolute (in nCi) and relative (in % of the accumulated [^{3}H] in each slice) values but only relative values are illustrated in the figure. ANOVA of the electrically-evoked [^{3}H]-overflow from hippocampal slices showed a significant difference between the two groups on absolute values ($F[1,42] = 5.19$; $p < 0.05$) but not on relative ones ($F[1,42] = 2.72$; n.s.).

Effects of CP-93,129 on the evoked overflow of tritium in hippocampal slices of virus-injected rats when GR 55,562 is present in the buffer throughout superfusion

A two-way ANOVA was performed, combining the following factors: "Vector" (two levels, GFP and HA1B/GFP) and "Drug" (three levels, Control [no drug at S_2], CP-93,129 at 0.01 µM and CP-93,129 at 0.1 µM). The ANOVA showed that there was neither an overall significant effect of the factor Vector ($F[1,38] = 1.066$; n.s.) nor of the factor Drug ($F[2,38] = 0.445$; n.s.), as well as no interaction between these two factors ($F[2,38] = 0.38$; n.s.). Thus blocking the 5-HT_{1B} receptor on cholinergic terminals by GR-55,562 prevented the inhibition of [^{3}H]-ACh overflow by CP-93,129. Indeed, when considering the previous result (see Figure 41), CP-93,129 at 0.01 and 0.1 µM decreased the electrically-evoked ACh release by 9 ($p < 0.001$) and 20% ($p < 0.001$) in the group HA1B/GFP group, respectively (as compared to the corresponding drug-free controls). When GR-55,562 is present in the superfusion buffer throughout the experiment, CP-23,129 no longer decreased ACh release in this group whatever its concentration.

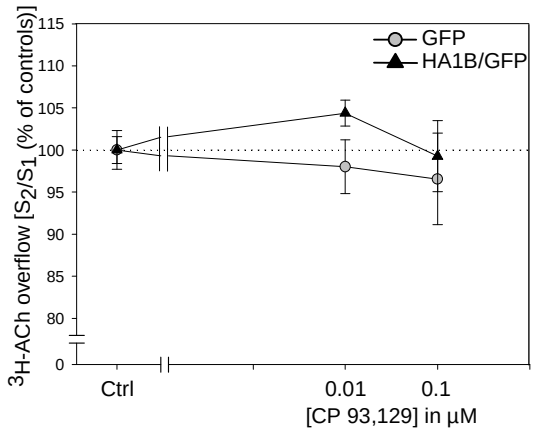

Figure 43. Electrically-evoked [^{3}H]-ACh overflow in the presence of of the 5-HT_{1B} receptor antagonist GR-55-562 and its modulation by CP-23,129 in hippocampal slices of virus-injected rats. Three days after stereotaxic injection of either GFP or HA1B/GFP viral vectors into the rat septal region, hippocampal slices were prepared from the brains and incubated with [^{3}H]-choline. Subsequently, they were washed, superfused continuously in the presence of both hemicholinium-3 (10 µM) and GR-55,562 (1 µM) and electrically stimulated twice (S_1, S_2). Effects of CP-93,129 are shown as the ratio S_2/S_1 (in % of the corresponding drug-free controls) of the evoked [^{3}H]-overflow elicited at the corresponding stimulation period. Means ± SEM. n = 7 - 8 per group.

In fact, using 0.01 µM of CP-93,129, the S_2/S_1 ratio amounted to 104.4% and with 0.1 µM to 99.3% of controls, and thus values which did not differ from the corresponding controls. Moreover, these values were shown to be statistically different from those obtained using the same concentrations of CP-93,129 but in the absence of GR-55,562 in the superfusion buffer. As already shown, 0.01 µM of CP-93,129 decreased the

release of ACh by 9% and at 0.1 µM by 20% as compared to the corresponding drug-free controls. ANOVA between these values and those obtained when GR-55,562 was present in the superfusion buffer showed that there was a significant effect of the "Drug throughout" (± GR 55,562; $F[1,49] = 35.77$; $p < 0.001$), as well as of the "Drug" (controls or 0.01 or 0.1 µM of CP-93,129; $F[1,49] = 9.68$; $p < 0.01$) but no interaction between both factors. These effects were due to a significant prevention of the inhibitory effects of CP-93,129 by GR-55,562 for both concentrations used (0.01 µM: $p < 0.01$ and 0.1 µM: $p < 0.001$).

In order to check whether CP-93,129 had an effect on spontaneous outflow of [^{3}H] in the presence of GR-55,562 throughout, a two-way ANOVA was performed on the basal efflux quotient b_2/b_1 in % of the corresponding drug-free control. ANOVA took into account the factors "Vector" (GFP or HA1B/GFP) and "Drug" (Control [no drug at S_2], CP-93,129 at 0.01 µM and CP-93,129 at 0.1 µM). The ANOVA showed that there was no overall significant effect of the factor Vector ($F[1,38] = 3.66$; n.s.) or of the second, Drug ($F[2,38] = 2.32$; n.s.) as well as no interaction between these two factors ($F[2,38] = 1.04$; n.s.).

(2) Effects of GR-55,562 on the evoked overflow of tritium in hippocampal slices of virus-injected rats

Accumulation of [^{3}H]-choline in hippocampal slices of virus-injected rats

Data (in pmoles/slice) are shown in Figure 44 (light gray bars). ANOVA of the [^{3}H]-choline accumulation in hippocampal slices showed no significant difference between the GFP and HA1B/GFP groups ($F[1,41] = 3.55$; n.s.).

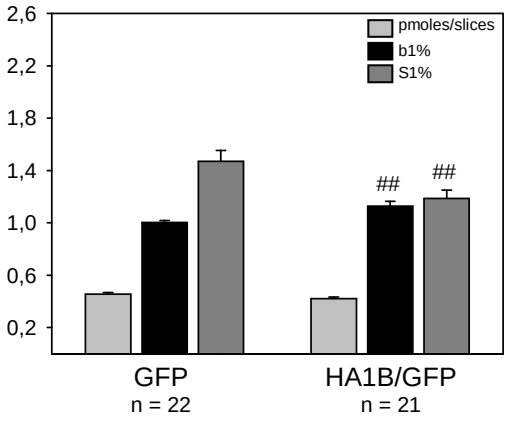

Figure 44. Accumulation of [^{3}H]-choline in hippocampal slices (in pmoles/slice; light gray bars), basal [^{3}H]-outflow (in % of the accumulated [^{3}H] per slice; black bars) and electrically-evoked [^{3}H]-overflow (in % of the accumulated [^{3}H] per slice; dark gray bars) from GFP and HA1B/GFP virus-injected rats. Three days after stereotaxic injection of either GFP or HA1B/GFP viral vectors into the rat septal region, hippocampal slices were prepared from the brains. Following incubation of the slices with [^{3}H]-choline, they were

washed, superfused continuously (in the presence of hemicholinium-3 at 10 µM) and electrically stimulated twice (S_1, S_2). Each bar represents the mean of 22 (GFP group) or 21 (HA1B/GFP group) slice values + SEM. $^{\#\#}p < 0.01$ as compared to slices of the GFP group.

Basal outflow of tritium in hippocampal slices of virus-injected rats

Data (b_1-values in % of accumulated [^{3}H]) are presented in Figure 44 (black bars). Statistical analyses were performed on both absolute (in nCi) and relative (in % of accumulated [^{3}H] in each slices) values, but only relative values are illustrated in the graph. ANOVA of the basal [^{3}H]-outflow from hippocampal slices showed a significant difference between the GFP and the HA1B/GFP groups on relative values ($F[1,40] = 9.18$; $p < 0.01$) but not on absolute ones ($F[1,40] = 0.46$; n.s.). This difference was due to a basal [^{3}H]-outflow that was significantly higher (by about 11%) in rats of the HA1B/GFP group as compared to rats of the GFP group.

Electrically-evoked overflow of tritium in hippocampal slices of virus-injected rats

Data (S_1-values in % of accumulated [^{3}H]) are shown in Figure 44 (dark gray bars). As for the baseline, statistical analyses were performed on both absolute (in nCi) and relative (in % of the accumulated [^{3}H] in each slice) values, but only relative values are illustrated in the figure. ANOVA of the electrically-evoked [^{3}H]-overflow from hippocampal slices showed a significant difference between the two groups on both absolute ($F[1,40] = 14.73$; $p < 0.001$) and relative values ($F[1,40] = 7.68$; $p < 0.01$). This difference was due to an electrically-evoked [^{3}H]-overflow that was significantly lower (by 20%) in slices from rats of the HA1B/GFP group as compared to those of the GFP group.

Effects of GR-55,562 on the evoked overflow of tritium in hippocampal slices of virus-injected rats

Data are presented in Figure 45. The selective 5-HT_{1B} receptor antagonist GR-55,562 was added to the superfusion buffer from 8 min before S_2 onwards at a concentration of 1 µM. To compare the effect of GR-55,562 on electrically-evoked release of [^{3}H]-ACh in hippocampal slices prepared from rats of the GFP and HA1B/GFP groups, a one-way ANOVA was performed taking into account the factor “Vector” (GFP or HA1B/GFP). ANOVA showed no significant effect of this factor ($F[1,19] = 1.58$; n.s.). Moreover, in none of the groups, the values in presence of GR-55,562 were different from the drug-free control values.

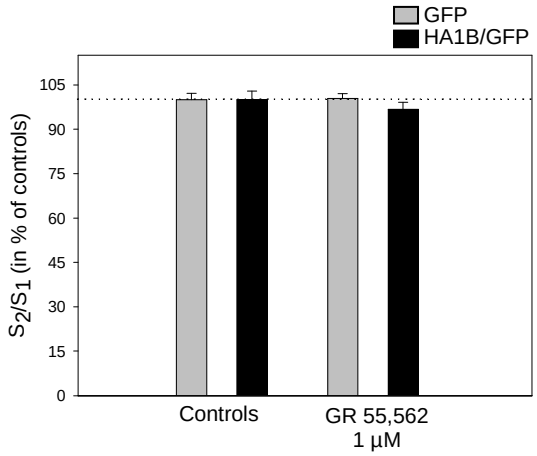

Figure 45. Electrically-evoked [^{3}H]-ACh release hippocampal slices of virus-injected rats: effects of the 5-HT_{1B} receptor antagonist GR-55,562. Three days after stereotaxic injection of either GFP or HA1B/GFP viral vectors into the rat septal region, hippocampal slices were prepared from the brains and incubated with [^{3}H]-choline. Subsequently, they were washed, superfused continuously in the presence of hemicholinium-3 (10 µM) and electrically stimulated twice (S_1, S_2). The effects of 1 µM of the 5-HT_{1B} receptor antagonist GR-55,562 added before S_2 on the evoked overflow of [^{3}H] are shown ("Controls": no drug addition before S_2). All effects are shown as the ratio S_2/S_1 (in % of the corresponding drug-free controls) of the evoked [^{3}H]-overflow elicited at the corresponding stimulation period. Means ± SEM. n = 10-11 per group.

To summarize, we shown in **Part 1** that following infection of primary septal cell cultures with the GFP or HA1B/GFP vectors or following intraseptal injection of these vectors, some cholinergic neurons were GFP-positive, indicative of a transfection of these cells. Moreover, infection with the HA1B/GFP vector led to expression of the HA tag showing that the concerned cells were transfected with the 5-HT_{1B} receptor. In septal cell cultures, expression of this receptor did not modify the basal and electrically-evoked overflow of [^{3}H]-ACh, whereas the 5-HT_{1B} receptor agonist, CP-93,129 had a higher inhibitory potency on the evoked overflow of [^{3}H]-ACh in cultures infected with the HA1B/GFP vector as compared to those infected with the GFP vector. As regards hippocampal slices from rats injected with the viral vectors, we showed that in slices of the HA1B/GFP group, the electrically-evoked overflow of [^{3}H]-ACh was decreased as compared to that measured in slices of the GFP group. Moreover, as in the cell cultures, the selective 5-HT_{1B} receptor agonist had a higher inhibitory potency in slices of the HA1B/GFP group. Therefore, it can be concluded from this part that it is possible to increase the expression of the 5-HT_{1B} heteroreceptor in cholinergic neurons using a virally-mediated gene transfer technique and that this expression has functional consequences on the release of ACh.

3.2. LONG-TERM EFFECTS OF MDMA +/- ETOH ADMINISTRATION IN RATS (PART 2)

This part of the thesis investigates - several days or weeks after rats have been treated with MDMA alone or in combination with EtOH – whether effects of these drugs of abuse can be detected on behavioural, neurochemical and neuropharmacological parameters. Over four consecutive days, Long-Evans rats received 1.5 g/kg EtOH and/or 10 mg/kg MDMA, or saline (7.5 ml/kg). Thus the following 4 treatment groups will be considered throughout this part of the thesis: SALINE, EtOH, MDMA and EtOH+MDMA. Starting 30 min after the last injections, acute effects of this combination were measured on body temperature.

3.2.1. Acute effects of MDMA on body temperature

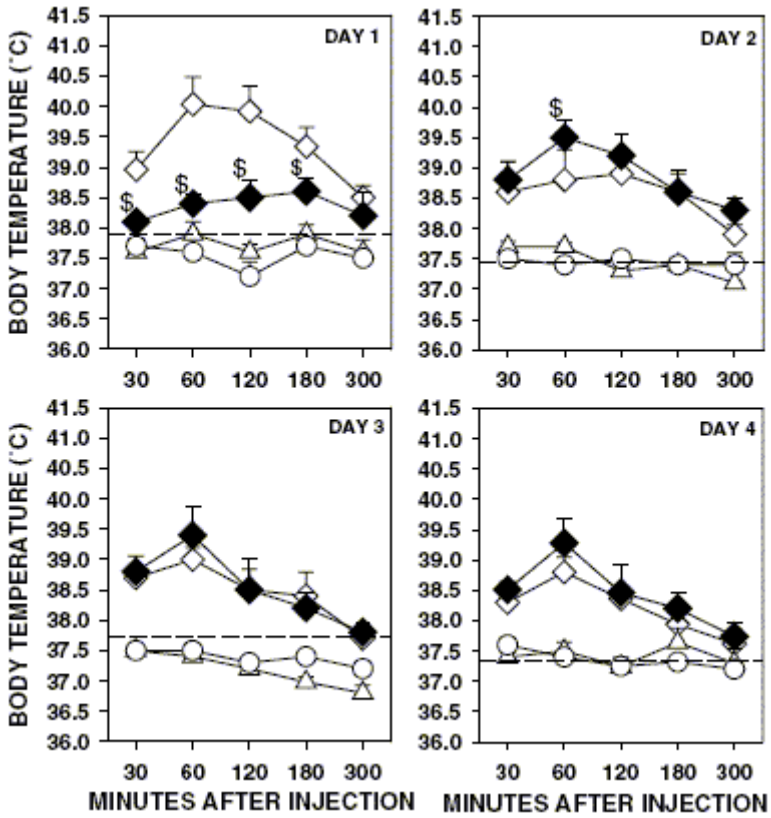

Figure 46. Mean body temperature (+ SEM) at five delays (30, 60, 120, 180 and 300 min) after injection of saline, EtOH, MDMA or EtOH+MDMA. In each panel the dashed line indicates the average body temperature of all rats measured 60 min before treatment administration (SEM approximately 0.1°C). To prevent an overload of statistical symbols in the figure only the significant differences between MDMA and EtOH+MDMA rats are indicated: $^{\$}p < 0.05$. On all 4 days, the temperature in MDMA and EtOH+MDMA rats was significantly higher than that measured in SALINE or EtOH rats. The difference between overall temperatures in SALINE and EtOH rats was not significant.

Whatever day was considered, 1 h before drugs/combination administration, the average body temperature did not significantly vary among groups (Day 1: 37.9 ± 0.1; Day 2: 37.5 ± 0.1; Day 3: 37.7 ± 0.1; Day 4: 37.4 ± 0.1°C). The other data are shown in Figure 46. Treatment (SALINE, EtOH, MDMA and EtOH+MDMA) × Time (30, 60, 120, 180 and 300 min after injection) × Day (days 1, 2, 3 and 4) ANOVA showed all factors and interactions to be significant. The Treatment effect ($F[3,19] = 15.7$; $p < 0.001$) was due to a temperature increase in MDMA and EtOH+MDMA rats ($p < 0.001$). The Time effect ($F[4,76] = 15.2$; $p < 0.001$) was due to temperatures that were significantly higher, mainly 60, 120 and 180 min after treatment with the highest level achieved at 60 min ($p < 0.05$ at least). The Day effect was due to body temperatures that were significantly higher on day 1 or 2 as compared to the subsequent ones ($p < 0.05$). Treatment × Time interaction can be explained by the peak that was observed at the post-injection delay of 60 min in MDMA and EtOH+MDMA rats. The Treatment × Day interaction is due to the temperature fluctuations in MDMA and EtOH+MDMA rats. The Time × Day interaction can be explained by the fact that, on the longest post-injection delays, the overall temperature reached weaker values on the last two days as compared to the first two ones. Part of the Treatment × Time × Day interaction is due to a temperature that, on day 1, was significantly higher in MDMA rats as compared to EtOH+MDMA ones on time points 1 ($p < 0.05$), 2 ($p < 0.001$), 3 ($p < 0.05$) and 4 ($p < 0.05$), not 5. This difference was not observed on the subsequent days. Also, on time point 2 of day 2, the temperature was significantly higher in EtOH+MDMA rats as compared to MDMA rats ($p < 0.05$).

In summary, MDMA-induced hyperthermia was partly prevented by EtOH co-administration, but only after the first treatment.

3.2.2. Behavioural data

3.2.2.1. T-maze alternation test

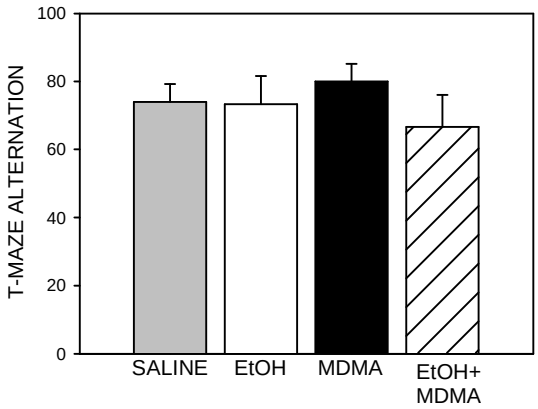

Figure 47. Alternation rates in the four groups of rats tested, i.e., SALINE (grey bar), EtOH (white bar), MDMA (black bar) and EtOH+MDMA (striped bar).

This test started 4 days after the last injection. As shown in Figure 47, there was no effect of Treatment on this behavioural measure. The average alternation rates were 74.0 ± 5.2 (SALINE), 73.3 ± 8.3 (EtOH), 80.0 ± 5.2 (MDMA) and 66.7 ± 9.4 (EtOH+MDMA).

3.2.2.2. Beam-walking test

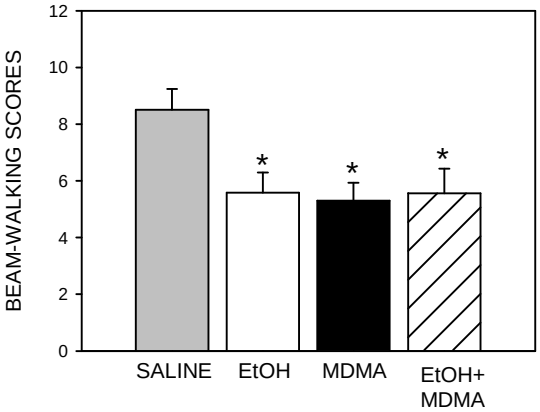

Figure 48. Beam-walking scores (mean + SEM; maximal score 12) in the four groups of rats, i.e., SALINE (grey bar), EtOH (white bar), MDMA (black bar) and EtOH+MDMA (striped bar). * $p < 0.05$ significantly different from SALINE.

This test started 10 days after the last injection. As shown in Figure 48, there was a significant effect of the treatment, the beam-walking scores being weaker in rats given one or both drugs (maximum score 12). Indeed, ANOVA showed an overall Treatment

effect (F[3,37] = 4.1; p < 0.05). Multiple comparisons showed that the beam-walking scores were significantly lower in EtOH, MDMA and EtOH+MDMA rats as compared to controls (p < 0.05). The means among the three drug treatment groups were not significantly different from each other.

3.2.2.3. Elevated plus maze test

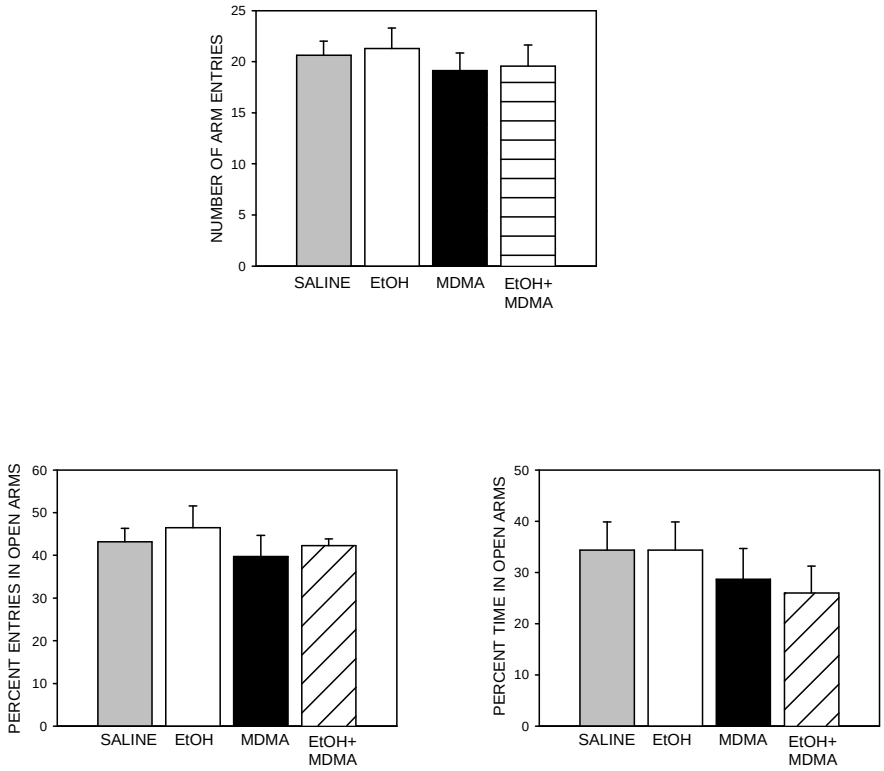

Figure 49. Total number of arm entries, percent entries in open arms as well as percent time in open arms in the elevated plus maze. There was no statistical difference detected among the four treatment groups, i.e., SALINE (grey bar), EtOH (white bar), MDMA (black bar) and EtOH+MDMA (striped bar).

This test started 19 days after the last injection. As shown in Figure 49, ANOVA of the total number of arm entries failed to show a significant Treatment effect (F[3,27] < 1.0; n.s.; score in SALINE was 20.6 ± 1.4). ANOVA also failed to show a significant Treatment effect on other variables (percent entries in open arms, F[3,27] < 1.0; n.s.; score in SALINE was 43.2 ± 3.2 or percent time on open arms, F[3,27] < 1.0; n.s.; score in SALINE was 34.4 ± 5.5).

3.2.3. Neurochemical data

Twenty days after the last injection, some of the rats from each group of rats tested for spontaneous alternation and beam walking were killed and their brain taken for

neurochemical determination of catecholamines concentrations in various cortical and other brain regions. The remaining ones were kept for superfusion experiments.

Noradrenaline concentration

Data are presented in Table 13. In none of the brain regions we observed a significant effect of Treatment on the concentration of noradrenaline. There was a trend however, seen in the frontoparietal cortex ($F[3,29] = 2.37$; $p < 0.1$).

Dopamine (DA) concentration

Mean concentrations are presented in Table 13. ANOVA showed a significant Treatment effect in the striatum ($F[3,29] = 3.1$; $p < 0.05$) and the temporal cortex ($F[3,29] = 3.8$; $p < 0.01$). In the striatum, DA concentration was significantly lower in EtOH+MDMA as compared to MDMA rats ($p < 0.05$). In EtOH+MDMA rats, the DA concentration also tended to be less than in saline-treated rats ($p = 0.08$). In the temporal cortex, the DA concentration was significantly greater in EtOH+MDMA rats as compared to the EtOH rats ($p < 0.05$) and tended to be greater than in MDMA rats ($p = 0.08$). In the other regions, there was no significant Treatment effect.

DOPAC concentration

Data are shown in Table 13. ANOVA showed a significant Treatment effect in the temporal cortex ($F[3,29] = 3.4$; $p < 0.05$) and in the ventral hippocampus ($F[3,29] = 4.2$; $p < 0.05$). In the temporal cortex, the concentration of DOPAC was significantly higher in EtOH+MDMA rats as compared to EtOH or MDMA rats ($p < 0.05$ for both cases). In the ventral hippocampus, DOPAC concentration was significantly reduced in EtOH and MDMA rats as compared to their saline-treated counterparts ($p < 0.05$ in both cases). In the other regions, there was no significant Treatment effect.

Catecholamine/brain region	Group			
	SALINE, n=8	**EtOH, n=10**	**MDMA, n=8**	**EtOH+MDMA, n=7**
Noradrenaline				
Prefrontal Cx	102 ± 8	109 ± 4	99 ± 3	109 ± 7
Frontoparietal Cx	91 ± 7	75 ± 4	92 ± 6	82 ± 5
Temporal Cx	95 ± 8	76 ± 7	82 ± 6	87 ± 6
Occipital Cx	59 ± 4	51 ± 2	57 ± 5	54 ± 3
Striatum	77 ± 10	49 ± 7	66 ± 2	52 ± 5
Septum	498 ± 49	395 ± 39	397 ± 20	408 ± 46
Dorsal Hippo	119 ± 8	94 ± 7	109 ± 5	107 ± 6
Ventral Hippo	209 ± 6	189 ± 26	192 ± 7	176 ± 9
Dopamine				
Prefrontal Cx	575 ± 118	577 ± 171	482 ± 147	572 ± 123
Frontoparietal Cx	140 ± 25	110 ± 13	146 ± 21	172 ± 23
Temporal Cx	95 ± 17	49 ± 13	62 ± 9	**108 ± 18**$^{\#}$
Occipital Cx	15 ± 1	21 ± 2	25 ± 7	22 ± 2
Striatum	2354 ± 220	2107 ± 138	2568 ± 121	**1738 ± 286**$^{\$}$
Septum	858 ± 80	687 ± 79	994 ± 175	684 ± 128
Dorsal Hippo	29 ± 4	27 ± 4	39 ± 7	22 ± 3
Ventral Hippo	24 ± 2	33 ± 10	23 ± 3	19 ± 3
DOPAC				
Prefrontal Cx	76 ± 17	73 ± 17	67 ± 18	73 ± 15
Frontoparietal Cx	33 ± 7	29 ± 3	42 ± 8	45 ± 8
Temporal Cx	16 ± 2	12 ± 2	13 ± 2	**21 ± 4**$^{\#,\$}$
Occipital Cx	4 ± 1	6 ± 1	6 ± 1	6 ± 1
Striatum	364 ± 51	330 ± 16	385 ± 25	327 ± 32
Septum	183 ± 19	150 ± 13	224 ± 37	141 ± 20
Dorsal Hippo	16 ± 1	17 ± 1	20 ± 1	15 ± 1
Ventral Hippo	35 ± 1	21 ± 4	20 ± 4	28 ± 4

Table 13. Concentration of catecholamines in the different brain structures of SALINE, EtOH, MDMA and EtOH+MDMA rats (all values correspond to Mean ± SEM and are given in pg/mg of irradiated tissue. Cx: Cortex and Hippo: Hippocampus. $^{\#}$significantly different from EtOH, $p < 0.05$ and $^{\$}$significantly different from MDMA, $p < 0.05$.

Serotonin (5-HT) and 5-HIAA concentrations

The concentration of 5-HT was significantly affected in all regions ($F[3,29] = 4.5$; $p < 0.01$ or less, Figure 50). In the prefrontal cortex, the concentration of 5-HT was significantly reduced in EtOH+MDMA as compared to EtOH rats ($p < 0.01$); in the latter, the 5-HT concentration was also significantly higher than in SALINE rats ($p < 0.05$). In the three other cortical regions (frontoparietal, temporal, occipital), the 5-HT concentration was significantly lower in MDMA and EtOH+MDMA rats as compared to

SALINE rats ($p < 0.05$), and in EtOH+MDMA rats as compared to EtOH ones ($p < 0.05$). In the striatum, a significant reduction of the 5-HT concentration was found in the MDMA and EtOH+MDMA rats as compared to SALINE rats ($p < 0.001$ in both cases). In the septal region, the concentration of 5-HT was significantly lower in EtOH+MDMA rats as compared to EtOH or SALINE rats ($p < 0.01$); in MDMA rats, the reduction was also significant as compared to SALINE ($p < 0.05$). Finally, in the dorsal hippocampus, the 5-HT concentration was significantly less in EtOH+MDMA and MDMA rats as compared to SALINE-treated animals ($p < 0.01$ at least) as well as in MDMA vs. EtOH rats ($p < 0.05$). The picture was similar in the ventral hippocampus.

As regards the concentration of 5-hydroxyindoleacetic acid (5-HIAA), data are also shown in Figure 50. The 5-HIAA levels were comparable to those of 5-HT. Indeed, in the prefrontal cortex, 5-HIAA concentration was significantly lower in the MDMA and EtOH+MDMA groups as compared to the SALINE group ($p < 0.05$); also, the 5-HIAA concentration was significantly decreased in the EtOH+MDMA rats as compared to the EtOH rats ($p < 0.05$). In addition, the concentration of 5-HIAA was significantly higher in this region of EtOH-treated rats as compared to their SALINE-treated counterparts ($p < 0.05$). No differences among the four groups were detected in the frontoparietal cortex. In the temporal and occipital cortices, in both MDMA and EtOH+MDMA rats, the 5-HIAA concentration was decreased as compared to the SALINE rats ($p < 0.05$). Furthermore, in the temporal cortex, this concentration was also lower in EtOH+MDMA rats as compared to EtOH ones ($p < 0.05$). In the striatum and the spetum, the 5-HIAA concentration was, in EtOH+MDMA rats, lower to that of the SALINE and EtOH rats ($p < 0.05$ in each case). Finally, in the dorsal and the ventral hippocampus, the concentration of 5-HIAA was decreased in the MDMA and EtOH+MDMA rats as compared to the SALINE rats ($p < 0.05$ for both). Furthermore, in both subdivisions, the 5-HIAA concentration was also lower in EtOH+MDMA rats as compared to their EtOH-treated counterparts ($p < 0.05$).

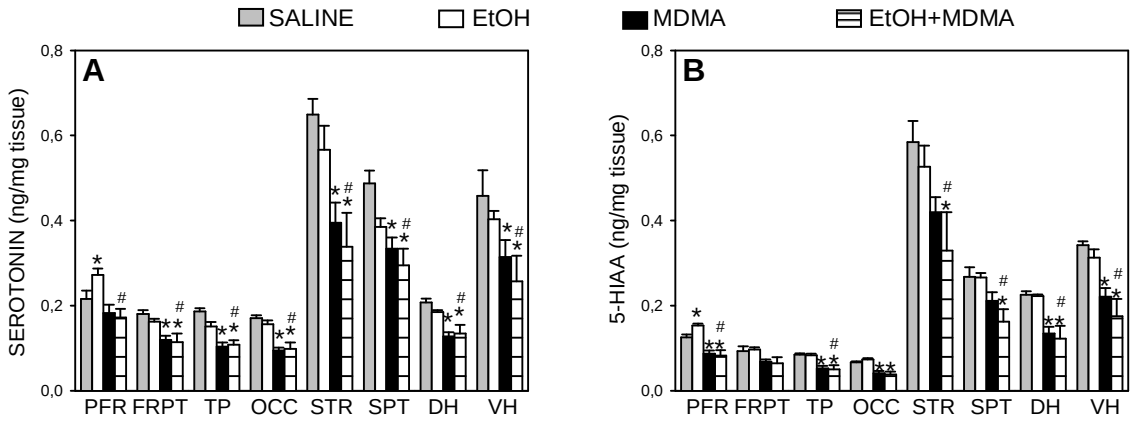

Figure 50. Concentration (Mean + SEM) of 5-HT (A) and 5-HIAA (B) in various regions of the cortex (PFR: prefrontal; FRPT: frontoparietal; TP: temporal; OCC: occipital) and other brain regions (STR: striatum; SPT: septum; DH: dorsal hippocampus: VH: ventral hippocampus) in the four groups of rats, i.e., SALINE (grey bars), EtOH (white bars), MDMA (black bars) and EtOH+MDMA (striped bars). *p < 0.05 significantly different from SALINE and $^{\#}$p < 0.05 significantly different from EtOH.

5-HIAA / 5-HT ratio

These data are not illustrated. ANOVA showed a significant Treatment effect on the 5-HIAA/5-HT ratio only in the septal region and in the dorsal hippocampus ($F[3,29] = 3.0$ and 8.8, respectively; $p < 0.05$). In the septal region, multiple comparisons failed to show any significant difference between treatment conditions: the ratio tended to be smaller in EtOH+MDMA rats as compared to EtOH rats and larger in EtOH rats as compared to SALINE ones ($p < 0.10$). In the dorsal hippocampus, the ratio was significantly smaller in EtOH+MDMA rats as compared to each of the three other groups ($p < 0.05$ at least). In MDMA rats, this ratio was also significantly smaller than in EtOH rats ($p < 0.05$).

3.2.4. Electrically-evoked [^{3}H]-5-HT overflow

The rats tested in the elevated plus maze were further used to assess the *in vitro* release of 5-HT and its presynaptic modulation in two brain regions, i.e., the dorsal hippocampus and the frontoparietal cortex. These experiments started about 3 weeks after the last treatment and lasted for a 3-week period.

Accumulation of [^{3}H]-5-HT by cortical and hippocampal slices

Data are shown in Table 14. ANOVA of the [^{3}H]-5-HT accumulation showed no significant Treatment effect, neither in the cortex ($F[2,27] < 1.0$; n.s.), nor in the hippocampus ($F[3,27] < 0.1$; n.s.).

	Group			
	SALINE, n=7	**EtOH, n=8**	**MDMA, n=7**	**EtOH+MDMA, n=9**
Cortex				
[^{3}H]5-HT accumulation (pmol/slice)	0.634 ± 0.03	0.646 ± 0.04	0.690 ± 0.03	0.697 ± 0.03
Baseline [^{3}H]-5-HT outflow (nCi)	0.429 ± 0.03	0.482 ± 0.06	0.430 ± 0.03	0.441 ± 0.02
Baseline [^{3}H]-5-HT outflow in % of [^{3}H] accumulation	2.360 ± 0.16	2.220 ± 0.11	2.146 ± 0.06	2.192 ± 0.08
Electrically-evoked [^{3}H]-5-HT overflow (nCi)	0.756 ± 0.03	0.899 ± 0.06	**0.982 ± 0.09***	**1.043 ± 0.07***
Electrically-evoked [^{3}H]-5-HT overflow in % of [^{3}H] accumulation	4.186 ± 0.28	4.863 ± 0.27	4.950 ± 0.32	5.23 ± 0.33
Hippocampus				
[^{3}H]5-HT accumulation (pmol/slice)	0.779 ± 0.06	0.813 ± 0.06	0.761 ± 0.02	0.730 ± 0.05
Baseline [^{3}H]-5-HT outflow (nCi)	0.456 ± 0.03	0.509 ± 0.04	0.421 ± 0.02	0.420 ± 0.02
Baseline [^{3}H]-5-HT outflow in % of [^{3}H] accumulation	2.022 ± 0.06	2.139 ± 0.06	1.902 ± 0.05	2.055 ± 0.07
Electrically-evoked [^{3}H]-5-HT overflow (nCi)	1.033 ± 0.09	1.002 ± 0.07	1.043 ± 0.03	1.124 ± 0.06
Electrically-evoked [^{3}H]-5-HT overflow in % of [^{3}H] accumulation	4.564 ± 0.12	4.330 ± 0.08	4.756 ± 0.15	**5.316 ± 0.20*$^{,\#,\$}$**

Table 14. Accumulation of [^{3}H]-5-HT, basal outflow of [^{3}H] and electrically-evoked overflow of [^{3}H]-5-HT in cortical and hippocampal slices from SALINE, EtOH, MDMA and EtOH+MDMA rats. All values are Mean ± SEM. Outflow and overflow are indicated in absolute values or as a percentage of the tritium accumulated in each slice. *significantly different from SALINE, $^{\#}$significantly different from EtOH and $^{\$}$significantly different from MDMA, $p < 0.05$ for all.

Baseline outflow of tritium in cortical and hippocampal slices

Data are presented in Table 14. ANOVA of baseline outflow of tritium from cortical or hippocampal slices showed no significant Treatment effect on absolute (nCi) or relative (in percent of the accumulated [^{3}H]) outflow ($F[3,27]$ always lower than 2.2; $p > 0.10$; n.s.).

Electrically-evoked overflow of tritium in cortical and hippocampal slices

The data are shown in Table 14. ANOVA of the electrically-evoked overflow from cortical slices showed a significant Treatment effect on absolute values (nCi; $F[3,27] = 3.69$; $p < 0.05$), but not on relative ones (in percent of the accumulated [^{3}H]; $F[3,27] = 2.1$; n.s.). This Treatment effect was due to significantly larger evoked [^{3}H]-overflow in MDMA and EtOH+MDMA rats as compared to SALINE rats ($p < 0.05$). In the hippocampus, there was a significant Treatment effects on the relative ($F[3,27] = 8.2$; $p < 0.001$), but not on absolute release ($F[3,27] < 0.1$; n.s.). This effect was due to a significantly larger relative release in EtOH+MDMA rats as compared to SALINE ($p < 0.01$), EtOH ($p < 0.001$) and MDMA ($p < 0.05$) rats.

Effects of CP-93,129 and methiotepin in cortical and hippocampal slices

Drugs to be tested were added to the superfusion medium from 8 min before S_2 and S_3 onwards, with concentrations increasing from S_2 to S_3. These drugs were the selective 5-HT_{1B} receptor agonist, CP-93,129 (at four concentrations, i.e., 0.001, 0.01, 0.1 and 1 µM) and the mixed 5-$HT_{1A/1B}$ antagonist, methiotepin (at two concentrations, 0.1 and 1 µM).

In cortical slices

As regards the effects of CP-93,129 (Figure 51), ANOVA showed no significant overall Treatment effect ($F[3,27] = 1.9$; n.s.). There was a significant Concentration effect ($F[3,81] = 1105.2$; $p < 0.001$). The interaction between both factors tended to be significant ($F[9,81] = 1.9$; $p = 0.06$). The Concentration effect can be explained by a concentration-dependent decrease of the release. The release was significantly larger in MDMA and EtOH+MDMA rats than in SALINE rats ($p < 0.05$ in both cases) at the concentration of 0.001 µM CP-93,129, and in EtOH+MDMA rats, at the concentration of 0.01 µM ($p < 0.01$).

Concerning the effects of methiotepin in cortical slices (Figure 51), ANOVA showed no significant overall Treatment effect ($F[3,27] = 1.6$; n.s.). There was a significant Concentration effect ($F[1,27] = 388.7$; $p < 0.001$), but no interaction between both factors ($F[3,27] < 1.0$; n.s.). At the lowest concentration of methiotepin, the overall release was increased by about 30% as compared to drug-free controls, whereas, at the highest, it was increased by 83%.

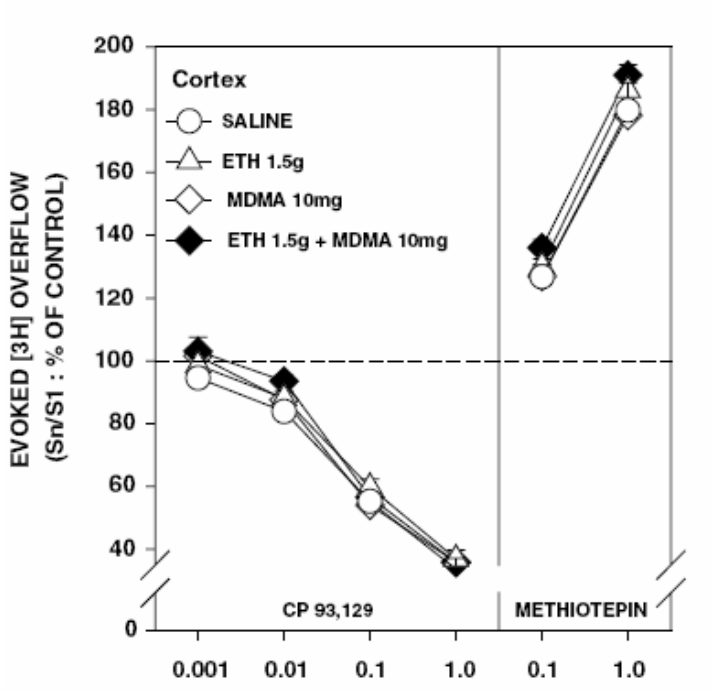

Figure 51. Effect of the autoreceptor selective agonist CP-93,129 (left panel) or the non-selective 5-$HT_{1A/1B}$ receptor antagonist methiotepin (right panel) on the electrically-evoked release of [^{3}H]-5-HT in cortical slices from rats of the four groups (SALINE, EtOH, MDMA and EtOH+MDMA). Data are the Mean + SEM evoked overflow expressed as a ratio (S_n/S_1), and subsequently normalized for each concentration (0.001-1 µM) by computing the percent of control values (no drug added to the superfusate). The dashed line indicates the drug-free control level (no change of the release). The inhibition of the evoked release was significant for concentrations 0.01 to 1 µM in the cortex, as compared to the corresponding drug-free control (not illustrated).

In hippocampal slices

As regards the effects of CP-93,129 (Figure 52), ANOVA showed significant effects of Treatment ($F[3,27] = 7.6$; $p < 0.001$) and Concentration ($F[3,81] = 999.5$; $p < 0.001$), but not of the interaction between both factors ($F[9,81] < 1.0$; n.s.). The Treatment effect was due to inhibitory effects of CP-93,129 on 5-HT release that were significantly more pronounced in EtOH+MDMA rats than in the other ones ($p < 0.05$). The Concentration effect can be explained by a concentration-dependent decrease of the release. Multiple comparisons showed that the release in EtOH+MDMA rats was significantly lower than in each of the three other groups ($p < 0.05$ at least), regardless of the concentration.

Concerning the effects of methiotepin in hippocampal slices (Figure 52), ANOVA showed significant Treatment effect ($F[3,27] = 5.7$; $p < 0.01$), Concentration effect ($F[1,27] = 580.2$; $p < 0.001$) and of the interaction between these two factors ($F[3,27] = 4.2$; $p < 0.05$). The Treatment effect was due to the facilitatory effect of methiotepin, which was smaller in EtOH+MDMA rats than in rats from the other groups ($p < 0.05$). The Concentration effect was due to a larger increase at the highest concentration

(+78%) of the drug. Multiple comparisons showed that for each concentration, the release in EtOH+MDMA rats was significantly lower than in the other groups ($p < 0.05$).

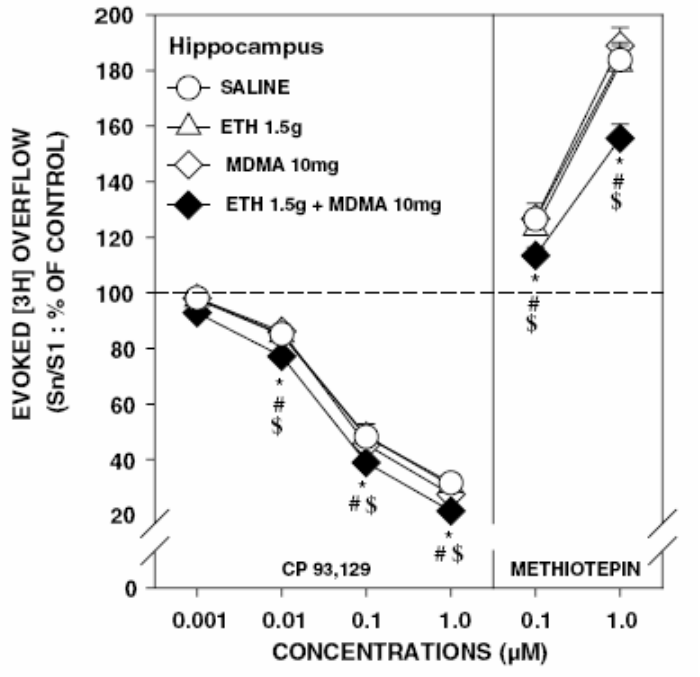

Figure 52. Effect of the autoreceptor selective agonist CP-93,129 (left panel) or the non-selective 5-$HT_{1A/1B}$ receptor antagonist methiotepin (right panel) on the electrically-evoked release of [^{3}H]-5-HT in hippocampal slices from rats of the four groups (SALINE, EtOH, MDMA and EtOH+MDMA). Data are the Mean + SEM evoked overflow expressed as a ratio (S_n/S_1), and subsequently normalized for each concentration (0.001-1 µM) by computing the percent of control values (no drug added to the superfusate). The dashed line indicates the drug-free control level (no change of the release). The inhibition of the evoked release was significant for concentrations 0.01 to 1 µM in the hippocampus, as compared to the corresponding drug-free control (not illustrated). *$p < 0.05$ significantly different from SALINE, $^{\#}p < 0.05$ significantly different from EtOH and $^{\$}p < 0.05$ significantly different from MDMA.

3.3. ACUTE EFFECTS OF MDMA +/- ETOH ON NEUROTRANSMITTER RELEASE *IN VITRO* (PART 3)

It was the aim of this part of the thesis to investigate the effects of MDMA, EtOH and their combination on the spontaneous and electrically-evoked release of 5-HT and DA in striatal slices of rats, a brain region particularly involved in hyperlocomotion. As shown in previous studies (see Introduction), EtOH potentiated the hyperlocomotor effect of MDMA in rats. Thus it seemed reasonable to hypothesize that the nigrostriatal dopaminergic system might be part of the putative substrate where EtOH and MDMA may interact. Moreover, for comparison, the effects of MDMA, EtOH and their combination were also investigated on 5-HT release in hippocampal and neocortical slices of the same rats.

3.3.1. [^{3}H]-5-HT overflow in striatal slices

Incubation of striatal slices with [^{3}H]-5-HT (0.1 µM; in the presence of nomifensine 1 µM), led to the accumulation of 1.10 ± 0.03 pmoles/slice of [^{3}H]-5-HT (n = 103). Subsequently the slices were superfused in the presence of the DA reuptake blocker nomifensine (1 µM). The basal outflow of [^{3}H] (b_1) in the fraction preceding the first electrical field stimulation period amounted to 3.98 ± 0.04 % of tissue-[^{3}H] (n = 106), whereas the electrically-evoked [^{3}H]-overflow at S_1 amounted to 3.10 ± 0.08 % of tissue-[^{3}H] (n = 103). Figure 53 illustrates the time course of the tritium outflow from striatal slices incubated with [^{3}H]-5-HT (given as fractional rates of [^{3}H]-outflow [mean ± SEM, n = 15 – 16]) under the influence of drugs added 24 min before the second stimulation period (S_2).

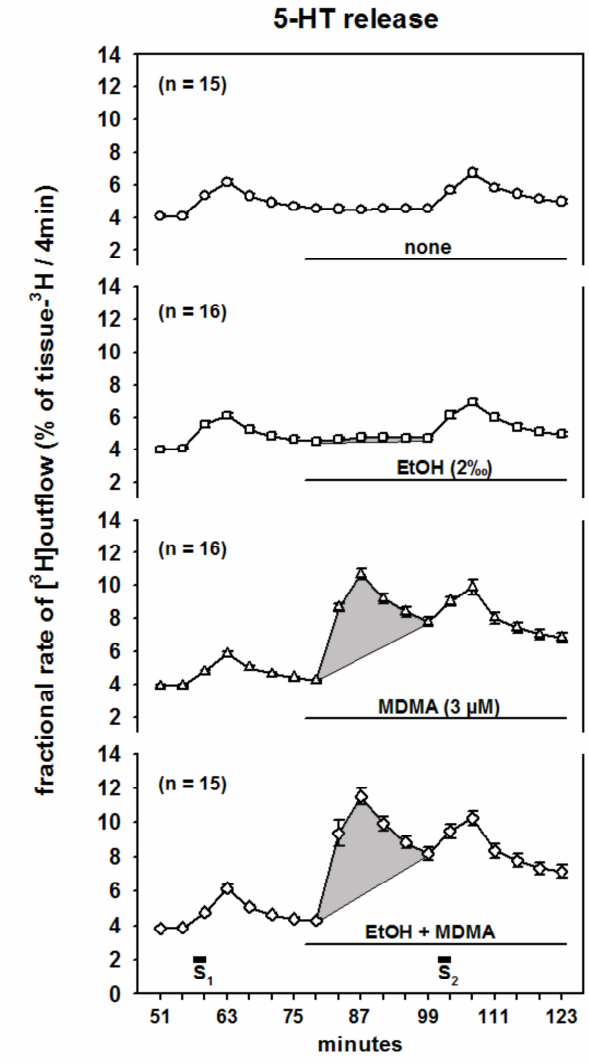

Figure 53. *Rat striatum (5-HT release); superfusion in the presence of nomifensine:* Time course of [^{3}H]-outflow from rat striatal slices incubated with [^{3}H]-5-HT. Following incubation with [^{3}H]-5-HT (0.1 µmol/L, in the presence of 1 µM nomifensine), the striatal slices were continuously superfused in the presence of nomifensine (1 µM) and stimulated electrically twice, as indicated by the short horizontal bars: S_1, S_2 (360 rectangular pulses at 3 Hz, 2 ms, 4 V/chamber, 26 – 28 mA). The outflow of [^{3}H] from the slices is shown as the fractional rate of [^{3}H]-outflow (in % of tissue-[^{3}H]/4min fraction). Ethanol (EtOH, 2‰), MDMA (3 µM), or the combination of both drugs were added to the medium from 24 min before S_2 onwards as indicated by the longer horizontal bars; the outflow of [^{3}H] induced by the latter drugs is represented by the shaded areas under the curves. All values are represented as means ± SEM, n = number of slices.

Figure 53 already suggests that EtOH (2‰) alone had only a small effect on basal and electrically-evoked [^{3}H]-outflow, whereas 3 µM MDMA, both alone and in combination with EtOH, significantly enhanced the basal [^{3}H]-efflux. In order to quantify the effect of drugs on the spontaneous outflow of [^{3}H] from striatal slices incubated with [^{3}H]5-HT, the shaded areas under the curves (see Figure 53) of all experiments were calculated and evaluated statistically using ANOVA, followed by Student-Newman-Keuls multiple comparisons test, when appropriate. This “drug-induced [^{3}H]-outflow” is depicted in Figure 54.

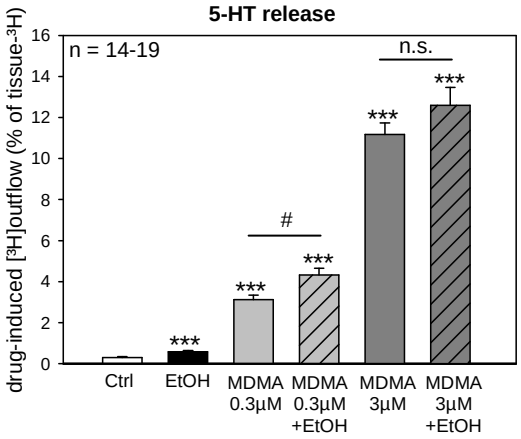

Figure 54. *Rat striatum (5-HT release); superfusion in the presence of nomifensine:* Effects of EtOH and MDMA (alone, or in combination) on the spontaneous outflow of [^{3}H] in rat striatal slices incubated with [^{3}H-]5-HT. Following incubation with [^{3}H]-5-HT (0.1 µmol/L, in the presence of 1 µM nomifensine), the striatal slices were continuously superfused in the presence of nomifensine (1 µM) and stimulated electrically twice as shown in Figure 53. EtOH (2‰), MDMA (0.3 or 3 µM), or the combination of both drugs were added to the medium from 24 minutes before S_2 onwards. Their effects on the spontaneous outflow of [^{3}H] ("drug-induced [^{3}H]-outflow") were calculated as the shaded areas under the curves (see Figure 53 and Methods) and are shown as a percentage of the tissue-[^{3}H] content before drug addition. Statistics: means ± SEM, n = number of slices; ***p < 0.001 significantly different from controls (Ctrl, no drug addition); $^{\#}$p < 0.05 significantly different from corresponding MDMA alone, n.s., not significant.

Figure 54 shows that the addition of EtOH (2‰) and MDMA (0.3 and 3 µM) or of both drugs to the superfusion buffer significantly increased the spontaneous outflow of tritium (given as a percentage of the [^{3}H]-content of the slices just before addition of drugs; $p < 0.001$ for all vs. controls). The magnitude (as compared to controls) of this drug-induced [^{3}H]-outflow was smallest with EtOH alone (93%) but much higher with MDMA 0.3 µM (924%) and 3 µM (3562%). With MDMA 0.3 µM + EtOH (2‰) it reached 1320% and with MDMA 3 µM + EtOH (2‰), it reached 4027% of the controls. Interestingly, the combination of MDMA at 0.3 µM with EtOH (2‰) led to a further significant enhancement of the MDMA-induced [^{3}H]-outflow as compared to MDMA 0.3 µM given alone (+39%; $p < 0.05$). When EtOH (2‰) was given together with MDMA 3 µM, it also enhanced the MDMA-induced [^{3}H]-outflow as compared to MDMA 3 µM given alone, (+13%), but this difference did not reach significance.

From the [^{3}H]-outflow curves depicted in Figure 53 the question arises whether MDMA alone and/or in combination with EtOH also changed the size and the time course of the electrically-evoked [^{3}H]-overflow at S_2 (although the still increased basal [^{3}H]-outflow makes it difficult to appreciate such effects). Evaluation of these effects showed however, that only the highest concentration of MDMA (3 µM) as well as its combination with EtOH significantly enhanced the electrically-evoked overflow of [^{3}H] (S_2/S_1 ratios in % of corresponding drug-free controls: EtOH 2‰: 106.68 ± 4.42 [n = 18;

n.s. vs. Ctrl.]; MDMA 0.3 µM: 79.86 ± 2.90 [n = 14; n.s. vs. Ctrl.]; MDMA 0.3 µM + EtOH: 84.19 ± 5.02 [n = 15; n.s. vs. Ctrl.]; MDMA 3 µM: 139.23 ± 7.67 [n = 20; $p < 0.001$ vs. Ctrl.]; MDMA 3 µM + EtOH: 128.45 ± 7.85 [n = 20; $p < 0.05$ vs. Ctrl.].

In order to check for a possible participation of endogenously released DA on the effects of MDMA and/or EtOH on the basal and electrically-evoked outflow of [^{3}H]-5-HT from striatal slices, experiments on striatal slices were also performed, in which the DA reuptake inhibitor nomifensine (1 µM) was present only during tissue accumulation of [^{3}H]-5-HT, but not during superfusion (Table 15).

Drug added 24 min before S_2	Concentration	Drug-induced [^{3}H]-outflow (in % of tissue-^{3}H)	Electrically-evoked [^{3}H]-overflow (S_2/S_1 in % of controls)	n
None - Controls	–	0.31 ± 0.05	100.00 ± 3.54	20
EtOH	2‰	0.73 ± 0.06	102.19 ± 4.59	20
MDMA	0.3 µM	**3.06 ± 0.24*** **	102.87 ± 3.74	18
EtOH+MDMA	2‰ + 0.3 µM	**3.87 ± 0.29*** **	101.82 ± 4.43	19
MDMA	3 µM	**11.26 ± 0.62*** **	**144.30 ± 5.84*** **	17
EtOH+MDMA	2‰ + 3 µM	**10.71 ± 0.91*** **	**133.40 ± 10.12***	19

Table 15. *Rat striatum (5-HT release); superfusion in the absence of nomifensine:* Effects of EtOH and MDMA alone, or in combination on spontaneous and electrically-evoked [^{3}H]-outflow in rat striatal slices incubated with [^{3}H]-5-HT. Following incubation with [^{3}H]-5-HT (0.1 µmol/L, in the presence of nomifensine), the slices were continuously superfused in the absence of nomifensine and stimulated electrically twice as shown in Figure 53. Tissue accumulation of [^{3}H]-5-HT amounted to 1.01 ± 0.02 pmol/slice (n = 114), the basal [^{3}H]-outflow b_1 to 3.90 ± 0.04 % of tissue-[^{3}H] (n = 114) and the electrically-evoked overflow at S_1 to 2.45 ± 0.07 % of tissue-[^{3}H] (n = 114). EtOH and MDMA, alone or in combination were added to the medium from 24 min before S_2 onwards. Their effects on the spontaneous outflow of [^{3}H] ("drug-induced [^{3}H]-outflow") are given as a percentage of the tissue-[^{3}H] content before drug addition. Their effects on the electrically-evoked overflow at S_2 are shown as S_2/S_1 ratios in % of the corresponding drug-free controls (no drug addition before S_2). All values are given as mean ± SEM, n = number of slices, *$p < 0.05$ and ***$p < 0.001$ as compared to the corresponding controls.

Statistical comparison of the data of Table 15 with those of Figure 54 showed that the absence of nomifensine throughout superfusion did not significantly change the MDMA- (or EtOH-) induced enhancement of spontaneous [^{3}H]-outflow. The electrically-evoked [^{3}H]-overflow at S_1 was significantly ($p < 0.001$) smaller in the absence than the presence of nomifensine, whereas the effects of MDMA on the electrically-evoked [^{3}H]-overflow at S_2 were relatively comparable.

3.3.2. [^{3}H]-5-HT overflow in hippocampal and cortical slices

MDMA and EtOH alone or in combination affected in a similar manner also the outflow of [^{3}H] in slices of the rat hippocampus and neocortex, especially by strongly increasing the basal [^{3}H]-outflow. Data from these experiments are summarized in Table 16 (Hippocampus) and Table 17 (Neocortex). However, the following experimental differences to the investigations on striatal slices (see above) should be noted: (1) Hippocampal and neocortical slices of the rats were incubated with [^{3}H]-5-HT in the absence of reuptake inhibitors. (2) Reuptake inhibitors were also absent during superfusion. (3) Lower concentrations of MDMA (0.1 or 1 µM) were added to the superfusion medium 24 min before S_2.

Drug added 24 min before S_2	Concentration	Drug-induced [^{3}H]-outflow (in % of tissue-^{3}H)	Electrically-evoked [^{3}H]-overflow (S_2/S_1 in % of controls)	n
None - Controls	–	0.58 ± 0.06	100.00 ± 2.41	16
EtOH	2‰	**1.30 ± 0.08*** **	102.21 ± 3.48	17
MDMA	0.3 µM	**2.89 ± 0.24*** **	108.62 ± 3.34	18
EtOH+MDMA	2‰ + 0.3 µM	**3.33 ± 0.23*** **	97.94 ± 3.89	20
MDMA	3 µM	**16.87 ± 1.04*** **	96.59 ± 3.76	13
EtOH+MDMA	2‰ + 3 µM	**18.35 ± 1.10*** **	100.89 ± 5.92	16

Table 16. *Rat hippocampus (5-HT release):* Effects of EtOH ± MDMA on spontaneous and electrically-evoked [^{3}H]-outflow in rat hippocampal slices incubated with [^{3}H]-5-HT. Tissue accumulation of [^{3}H]-5-HT amounted to 0.58 ± 0.01 pmol/slice (n = 105), the basal [^{3}H]-outflow b_1 to 3.80 ± 0.04 % of tissue-[^{3}H] (n = 105) and the electrically-evoked overflow at S_1 to 3.62 ± 0.07 % of tissue-[^{3}H] (n = 105). Effects of EtOH and/or MDMA on the spontaneous outflow of [^{3}H] ("drug-induced [^{3}H]-outflow") are given as a percentage of the tissue-[^{3}H] content before drug addition. Their effects on the electrically-evoked overflow at S_2 are shown as S_2/S_1 ratios in % of the corresponding drug-free controls (no drug addition before S_2). All values are given as mean ± SEM, n = number of slices, ***p < 0.001 as compared to the corresponding controls.

Drug added 24 min before S_2	Concentration	Drug-induced [^{3}H]-outflow (in % of tissue-^{3}H)	Electrically-evoked [^{3}H]-overflow (S_2/S_1 in % of controls)	n
None - Controls	–	1.03 ± 0.09	100.00 ± 3.21	18
EtOH	2‰	**1.68 ± 0.13*** **	91.64 ± 4.09	17
MDMA	0.3 µM	**4.25 ± 0.22*** **	101.26 ± 4.09	18
EtOH+MDMA	2‰ + 0.3 µM	**4.65 ± 0.22*** **	97.66 ± 3.95	19
MDMA	3 µM	**23.90 ± 1.06*** **	95.11 ± 7.23	15
EtOH+MDMA	2‰ + 3 µM	**21.14 ± 1.03*** **	84.92 ± 5.02	16

Table 17. *Rat neocortex (5-HT release):* Effects of EtOH ± MDMA on spontaneous and electrically-evoked [^{3}H]-outflow in rat neocortical slices incubated with [^{3}H]-5-HT. Tissue accumulation of [^{3}H]-5-HT amounted to 0.51 ± 0.01 pmol/slice (n = 107), the basal [^{3}H]-outflow b_1 to 4.11 ± 0.05 % of tissue-[^{3}H] (n = 107) and the electrically-evoked overflow at S_1 to 3.18 ± 0.06 % of tissue-[^{3}H] (n = 107). Effects of EtOH and/or MDMA on the spontaneous outflow of [^{3}H] ("drug-induced [^{3}H]-outflow") are given as a percentage of the tissue-[^{3}H] content before drug addition. Their effects on the electrically-evoked overflow at S_2 are shown as S_2/S_1 ratios in % of the corresponding drug-free controls (no drug addition before S_2). All values are given as mean ± SEM, n = number of slices, ***p < 0.001 as compared to the corresponding controls.

ANOVA of the data in Table 16 and Table 17 shows that also in rat hippocampal or neocortical slices, respectively, EtOH and especially MDMA increased the spontaneous outflow of [^{3}H]; the combination of EtOH with MDMA, however, produced no additional effects. The electrically-evoked overflow of [^{3}H] on the other hand was completely unaffected by MDMA, EtOH or their combination.

3.3.3. [^{3}H]-Dopamine overflow in striatal slices

Incubation of striatal slices with [^{3}H]-DA (0.1 µM, in the presence of 1 µM fluvoxamine), led to the accumulation of 2.83 ± 0.06 pmoles/slice [^{3}H]-DA (n = 99). Subsequently the slices were superfused in the presence of fluvoxamine (1 µM). The basal outflow of [^{3}H] in the fraction (b_1) before the first electrical field stimulation period (S_1) amounted to 1.77 ± 0.03 % of tissue-^{3}H (n = 99), whereas the electrically-evoked [^{3}H]-overflow at S_1 amounted to 6.08 ± 0.16 % of tissue-^{3}H (n = 99). Figure 55 illustrates the time course of tritium outflow from striatal slices incubated with [^{3}H]-DA (given as fractional rates of [^{3}H]-outflow [mean ± SEM, n = 8-16]) under the influence of drugs added 24 min before the second stimulation period (S_2).

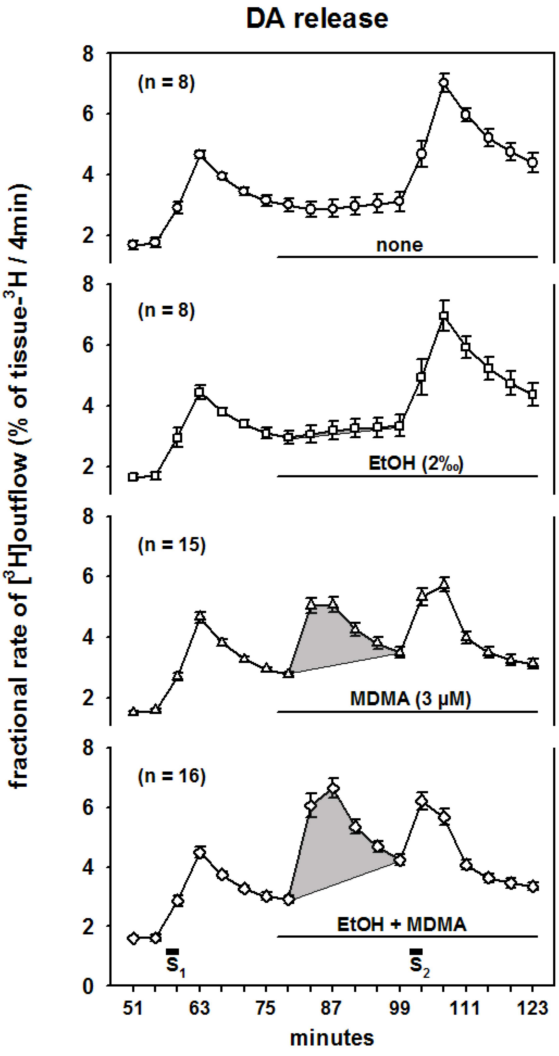

Figure 55. *Rat striatum (DA release); superfusion in the presence of fluvoxamine*: Time course of [^{3}H]-outflow from rat striatal slices incubated with [^{3}H]-DA. Following incubation with [^{3}H]-DA (0.1 µmol/L, in the presence of 1 µM fluvoxamine), the striatal slices were continuously superfused in the presence of fluvoxamine (1 µM) and stimulated electrically twice, as indicated by the short horizontal bars: S_1, S_2 (360 rectangular pulses at 3 Hz, 2 ms, 4 V/chamber, 26 – 28 mA). The outflow of [^{3}H] from the slices is shown as the fractional rate of [^{3}H]-outflow (in % of tissue-|^{3}H]/4min fraction). Ethanol (EtOH, 2‰), MDMA (3 µM), or the combination of both drugs were added to the medium from 24 minutes before S_2 onwards as indicated by the longer horizontal bars; the outflow of [^{3}H] induced by the latter drugs is represented by the shaded areas under the curves. All values are given as means ± SEM, n = number of slices.

Evidently, EtOH (2‰) alone had only a small effect on basal [^{3}H]-outflow, whereas 3 µM MDMA, both alone and in combination with EtOH, significantly enhanced the basal [^{3}H]-efflux. Moreover, MDMA alone and in combination visibly also changed the size and the time course of the stimulation-evoked [^{3}H]-outflow at S_2 (see below).

In order to quantify the effect of drugs on the spontaneous outflow of [^{3}H] from striatal slices, the shaded areas under the curves (in Figure 55) of all experiments were calculated and statistically analyzed using ANOVA, followed by Student-Newman-

Keuls multiple comparisons test when appropriate. This “drug-induced [^{3}H]-outflow” is depicted in Figure 56.

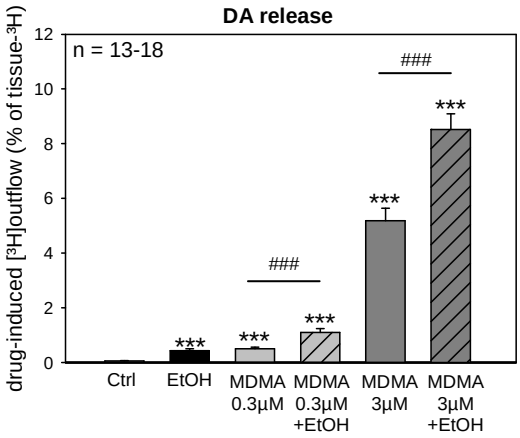

Figure 56. *Rat striatum (DA release); superfusion in the presence of fluvoxamine:* Effects of EtOH and MDMA (alone or in combination) on the spontaneous outflow of [^{3}H] in rat striatal slices incubated with [^{3}H]-DA. Following incubation with [^{3}H]-DA (0.1 µmol/L; in the presence of 1 µM fluvoxamine), the striatal slices were continuously superfused in the presence of fluvoxamine (1 µM) and stimulated electrically twice as shown in Figure 55. EtOH (2‰), MDMA (0.3 or 3 µM), or their combination were added to the medium from 24 minutes before S_2 onwards. Their effects on the spontaneous outflow of [^{3}H] (“drug-induced [^{3}H]-outflow”) were calculated as the shaded areas under the curves and are shown as a percentage of the tissue-[^{3}H] content before drug addition. All values are shown as means ± SEM, n = number of slices; ***p<0.001 vs. controls (Ctrl, no drug addition); $^{###}$p<0.001 vs. corresponding MDMA concentration alone.

It is evident from Figure 56 that the addition of EtOH (2‰) and MDMA (0.3 and 3 µM) or of both drugs to the superfusion buffer significantly increased the spontaneous outflow of tritium (shown as a percentage of the [^{3}H]-content of the slices just before addition of drugs). The magnitude (as compared to controls) of this drug-induced [^{3}H]-outflow was smallest with EtOH alone (+766%) or with MDMA 0.3 µM (+898%) and much higher following MDMA 3 µM (+2118%). Following treatment of the slices with MDMA 0.3 µM + EtOH (2‰) and MDMA 3 µM + EtOH, the magnitude of this increase reached, respectively, +10254% and +16942% of the controls, respectively ($p < 0.001$ for all as compared to controls). Interestingly, the combination of MDMA (both 0.3 or 3 µM) with EtOH (2‰) led to a further significant enhancement of the MDMA-induced [^{3}H]-outflow. Thus, the increase was of +122% when EtOH was given together with MDMA 0.3 µM ($p < 0.001$ as compared to MDMA 0.3 µM given alone) and of +65% when EtOH was given together with MDMA 3 µM ($p < 0.001$ as compared to MDMA 3 µM given alone).

The [^{3}H]-outflow curves depicted in Figure 55 suggests that MDMA alone and in combination with EtOH not only affected the basal outflow of [^{3}H], but also changed the

size and the time course of the electrically-evoked [^{3}H]-overflow at S_2 (although the still increased basal [^{3}H]-outflow makes it difficult to appreciate such effects). In fact, MDMA both alone and in combination with EtOH significantly reduced the electrically-evoked [^{3}H]-overflow in rat striatal slices incubated with [^{3}H]DA. The following data (given as S_2/S_1 ratios in % of corresponding drug-free controls) were observed: MDMA 0.3 µM: 82.42 ± 3.89 (n = 18; $p < 0.05$ vs. Ctrl.); MDMA 0.3 µM + EtOH: 77.64 ± 3.24 (n = 20; $p < 0.001$ vs. Ctrl.); MDMA 3 µM: 59.89 ± 3.69 (n =15; $p < 0.001$ vs. Ctrl.); MDMA 3 µM + EtOH: 55.86 ± 5.07 (n = 16; $p < 0.001$ vs. Ctrl.). Addition of EtOH (2‰) alone did not significantly change the electrically-evoked overflow at S_2 (95.71 ± 4.82 [n = 18; n.s. vs. Ctrl.]).

In order to check for a participation of endogenously released 5-HT on the effects of MDMA and/or EtOH on the basal and electrically-evoked outflow of [^{3}H]-DA from rat striatal slices, the experiments described above were also performed on striatal slices, with the 5-HT reuptake inhibitor fluvoxamine (1 µM) being only present during tissue accumulation of [^{3}H]-DA, but not during superfusion. The data of these experiments are summarized in Table 18.

Drug added 24 min before S_2	Concentration	Drug-induced [^{3}H]-outflow (in % of tissue-^{3}H)	Electrically-evoked [^{3}H]-overflow (S_2/S_1 in % of controls)	n
None - Controls	–	0.133 ± 0.03	100.00 ± 2.26	17
EtOH	2‰	0.74 ± 0.07***	106.80 ± 2.95	17
MDMA	0.3 µM	1.37 ± 0.15***	92.23 ± 4.03	15
EtOH+MDMA	2‰ + 0.3 µM	2.28 ± 0.23***$^{\#\#}$	85.49 ± 4.32*	14
MDMA	3 µM	8.94 ± 0.57***	97.03 ± 3.54	14
EtOH+MDMA	2‰ + 3 µM	9.70 ± 0.55***	92.42 ± 3.96	18

Table 18. *Rat striatum (DA release), superfusion in the absence of fluvoxamine:* Effects of EtOH and MDMA (alone or in combination) on spontaneous and electrically-evoked [^{3}H]-outflow in rat striatal slices incubated with [^{3}H]-DA. Following incubation with [^{3}H]-DA (0.1 µmol/L), the slices were continuously superfused in the absence of further drugs and stimulated electrically twice as shown in Figure 55. Tissue accumulation of [^{3}H]-DA amounted to 2.72 ± 0.06 pmol/slice (n = 102), the basal [^{3}H]-outflow b_1 to 2.21 ± 0.04 % of tissue-[^{3}H] (n = 102) and the electrically-evoked overflow at S_1 to 3.70 ± 0.12 % of tissue-[^{3}H] (n = 102). EtOH and MDMA, alone or in combination were added to the medium from 24 min before S_2 onwards. Their effects on the spontaneous outflow of [^{3}H] ("drug-induced [^{3}H]-outflow") are given as a percentage of the tissue-[^{3}H] content before drug addition. Their effects on the electrically-evoked overflow at S_2 are shown as S_2/S_1 ratios in % of the corresponding drug-free controls (no drug addition before S_2). All values are given as mean ± SEM, n = number of slices, *$p < 0.05$ and ***$p < 0.001$ as compared to the corresponding controls; $^{\#\#}p < 0.01$ as compared to MDMA (0.3 µM).

Table 18 shows that EtOH and MDMA, or their combination significantly increased the basal [^{3}H]-outflow from striatal slices also in the absence of fluvoxamine throughout superfusion. Moreover, statistical comparison of the data of Table 18 with those of Figure 56 revealed that in the absence of fluvoxamine, the MDMA- (or EtOH-) induced

[^{3}H]-outflow was significantly more pronounced ($p < 0.001$, except for 3 µM MDMA + EtOH: n.s.). On the other hand, both the electrically-evoked [^{3}H]-overflow at S_1 and the basal [^{3}H]-outflow (b_1) were significantly ($p < 0.001$) smaller in the absence of fluvoxamine throughout superfusion and the inhibitory effects of 3 µM MDMA ± EtOH on the electrically-evoked [^{3}H]-overflow (S_2/S_1 in % of controls, see above) almost disappeared in the absence of fluvoxamine.

3.4. INCREASED EXPRESSION OF 5-HT$_{1B}$ AUTORECEPTORS IN THE RAT BRAIN: LOCOMOTOR EFFECTS OF MDMA +/- ETOH ADMINISTRATION (PART 4)

The first part of this thesis (see section 3.1 of the Results), demonstrated the possibility to use HSV-1 as a tool to increase the expresssion of the 5-HT$_{1B}$ receptor in *non-serotonergic* (cholinergic) neurons, i.e., as a *heteroreceptor*. This technique had already been validated to transfect serotonergic neurons in the raphé.

Thus, the goal of this last part of the present work was to use the same technique to induce an enhanced expression of the 5-HT$_{1B}$ receptor in *serotonergic* neurons of the dorsal raphé, in which it is an *autoreceptor.* Subsequently, we wanted to study the effects of this manipulation on a more integrated, behavioural level. Since behavioural effects of MDMA alone or in combination with EtOH formed the framework of Parts 2 and 3 of the present thesis, we decided to study (part of) these behavioural effects to investigate the consequences of an enhanced expression of 5-HT$_{1B}$ autoreceptors. Interestingly,the 5-HT$_{1B}$ receptor has been implicated in the locomotor effects of MDMA and the additional presence of EtOH potentiates the MDMA-induced locomotor effect and alters the functionality of this receptor.

Thus, to get further insight in the possible role of this 5-HT receptor type in the locomotor effects of MDMA alone or in combination with EtOH, we used virally-mediated gene tranfer to increase the expression of the 5-HT$_{1B}$ receptor in serotonergic neurons from the dorsal raphé nucleus (DRN). Subsequently, the locomotor activity of rats treated with MDMA, EtOH, or the combination of both drugs was evaluated. As the effects of such transfection have been described in details (see 3.1.), no further release experiments was performed before the transfection of the 5-HT neurons and the assessment of its possible effects on MDMA-induced locomotion. These experiments are nevertheless necessary and will be done in future experiments.

3.4.1. Immunocytochemical verification of transfection

50 male Long-Evans rats sustained a unilateral stereotaxic implantation of a guide cannula into the dorsal raphé nucleus. Approximately 11 days later they were transfected with 1 µl of either GFP- or HA1B/GFP vector. Three days after the transfection they were treated by intraperitoneal injection with MDMA, EtOH or the

combination of both drugs. The locomotor effects of these treatments were then monitored during the following four hours.

Subsequent to behavioural testing, the rats were killed by decapitation, their brain were quickly removed and fixed in a solution of PFA 4%. 40-µm brain sections of the raphe region were prepared from these brains using a vibratome. All sections were inspected under a fluorescence microscope and all rats for which the cannula was not implanted in the improper zone or for which no GFP-positive cells could be detected were discarded from further statistical analysis.

Figure 57 shows pictures from brain sections of rats from both the GFP and the HA1B/GFP groups. GFP-positive cells were detected in the dorsal raphé region mainly in a restricted zone around the tip of the injection cannula. All cells had a relatively homogeneous morphology and size and several neurites were also visible on these sections.

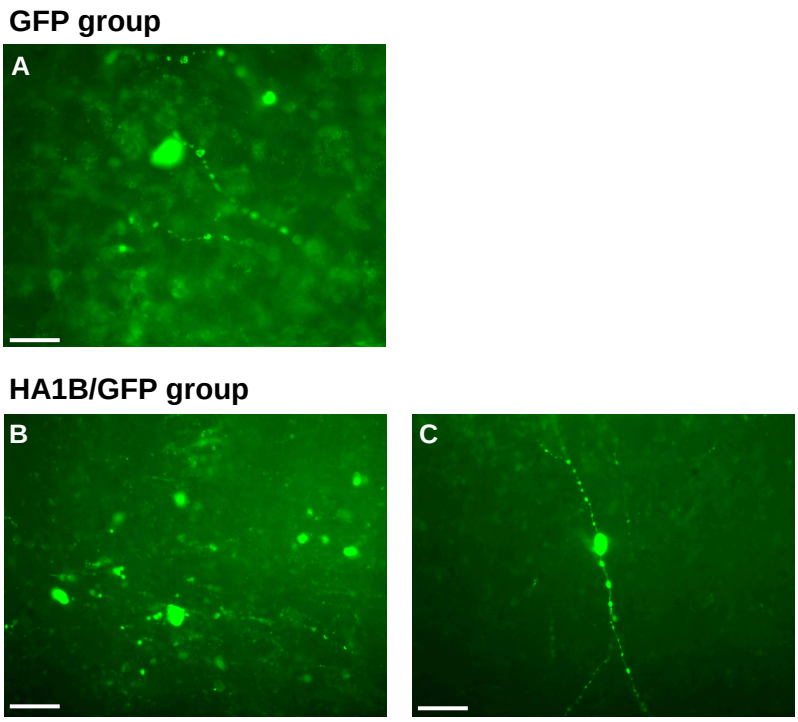

Figure 57. Microscopic observation of GFP-positive cells in brain sections from the dorsal raphe nucleus of rats previously transfected with the GFP- (upper panel) and HA1B/GFP (lower panel) vectors. Scale bar in A: 30 µm; scale bar in B & C: 20 µm.

3.4.2. Locomotor activity of these rats

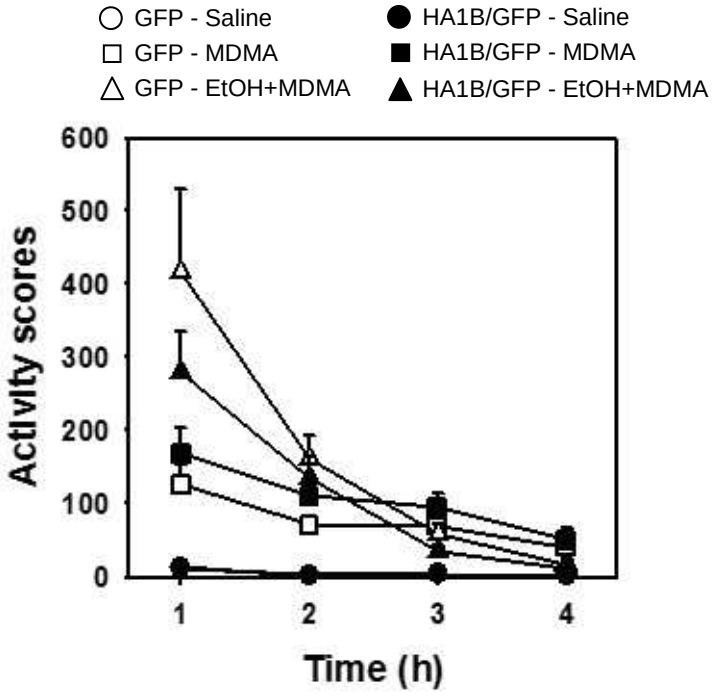

Figure 58. Activity scores of rats transfected with the GFP and the HA1B/GFP vectors and further injected with Saline, MDMA or EtOH+MDMA. After injection of the drugs, locomotor activity of the rats was monitored for 4 consecutive hours. See text for statistics.

Following administration of MDMA, EtOH or their combination to rats, their locomotor activity was monitored for 4 hours. A first analysis of Variance (ANOVA) was performed on these 4 hours with the following factors: Drug (Saline, MDMA or EtOH+MDMA), Vector (GFP or HA1B/GFP) and Hour (H1, H2, H3 and H4). ANOVA showed that there was an overall effect of Drug ($F[2,38] = 21.7$; $p < 0.001$) and of Hour ($F[3,114] = 27.0$; $p < 0.001$), as well as a significative interaction between these two factors ($F[6,114] = 12.25$; $p < 0.001$). This same analysis showed that there was no effect of the Vector ($F[1,38] = 0.32$; n.s.), no interaction between the Drug and Vector factors ($F[2,38] = 1.64$; n.s.), as well as no interaction between the Hour and Vector factors ($F[3,114] = 0.40$; n.s.). Finally, there was no significant interaction between the three factors considered ($F[6,114] = 0.88$; n.s.). As shown on Figure 58, the Hour effect was due to activity scores that were significantly different between the first and the second hour (H1 vs. H2: $p < 0.001$), between the first and the third hour (H1 vs. H3: $p < 0.001$) and also between the first and the fourth hour (H1 vs. H4: $p < 0.001$). The Drug effect was due to significant differences in the activity scores of rats to which MDMA or

EtOH+MDMA were administered. Thus, we could show that Saline had no effect on the activity scores of these rats. On the contrary, MDMA increased the locomotor activity of rats, whether transfected with the GFP ($p < 0.05$) or the HA1B/GFP vector ($p < 0.05$) as compared to rats injected with Saline. In addition, the combination of EtOH+MDMA also increased the locomotor activity of those rats ($p < 0.001$ for those transfected with the GFP vector and $p < 0.01$ for those transfected with the HA1B/GFP vector) as compared to rats injected with Saline. Moreover, when considering the first hour of monitoring, but without distinction between the GFP and the HA1B/GFP vectors, we could show that the administration of EtOH+MDMA increased the locomotor activity to a greater extent than MDMA alone ($p < 0.001$). More interestingly, when considering the GFP vector, the latter effect could also be shown. Thus, in this group, the combination of EtOH and MDMA potentiated the locomotor effect of MDMA ($p < 0.05$). On the contrary, when considering the rats transfected with the HA1B/GFP vector, this effect was no more noticeable. Indeed, the combination of EtOH with MDMA, did not potentiate the MDMA-induced locomotor activity in this group ($p = 0.49$; n.s.).

In this respect, the Drug × Hour interaction showed that the effects described above where only present in the first hour of recording of the locomotor activity.

These effects were confirmed when statistical analysis was performed on the activity scores of the first hour, splitted in three 20-min blocks, as shown in Figure 59.

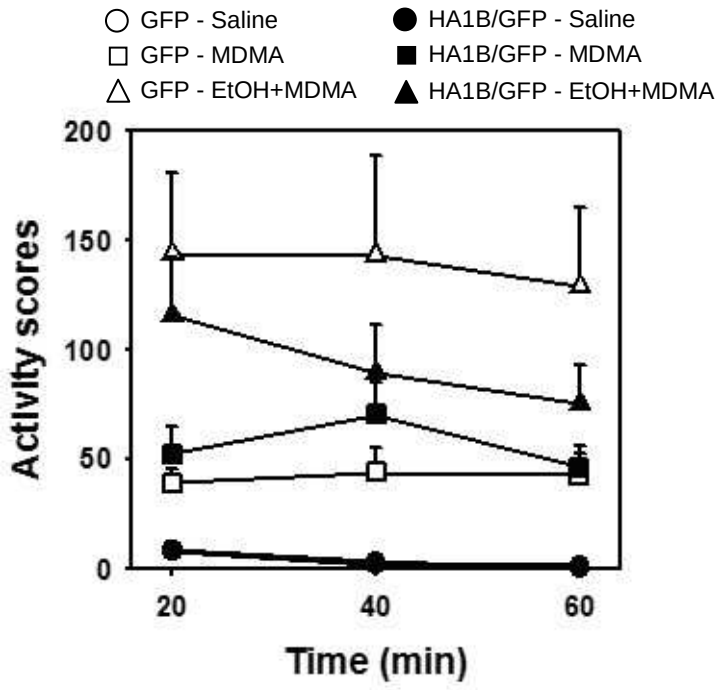

Figure 59. Activity scores of rats transfected with the GFP and the HA1B/GFP vectors and further injected with Saline, MDMA or EtOH+MDMA during the first hour of recording. See text for statistics.

4. DISCUSSION

4.1. INCREASED EXPRESSION OF 5-HT_{1B} RECEPTORS *IN VITRO* AND *IN VIVO* (PART 1)

In the following paragraphs, the experiments described in section 3.1. will be discussed, in which we used virus-mediated gene transfer (1) in primary septal cell cultures and (2) in sterotaxically-injected rats, to increase the expression of 5-HT_{1B} receptors in cholinergic neurons.

In the present thesis Herpes simplex viral particles were used as vectors for the expression of both GFP and the 5-HT_{1B} receptor, which were transfected either alone or together ["GFP vector", expressing only GFP, or "HA1B/GFP vector", expressing HA-tagged 5-HT_{1B} receptor and GFP, respectively; see (Clark et al., 2002)]. To analyse the ability of these vectors to express the proteins in question, the study was performed in two steps. The first step consisted in an *in vitro* approach, in which the growth medium of primary neuronal cultures prepared from the fetal septal region (Ehret et al., 2001; Ehret et al., 2007b) was infected with the viral vectors to allow an analysis of the functional effects of an increased expression of the 5-HT_{1B} receptor at a more cellular level. The second step relied upon stereotaxic injections of the same viral particles into the septal region of the rat basal forebrain, in order to enhance the expression of the 5-HT_{1B} receptor in the target region of cholinergic neurons of the medial septum/diagonal band of Broca, namely the hippocampus. In each of these approaches, increased expression of the 5-HT_{1B} receptor was verified by immunocytochemical techniques, whereas its functional consequences were assessed by measuring the modulation of the electrically-evoked ACh release. For the latter purpose, septal cell cultures or hippocampal slices, respectively, were incubated with [^{3}H]-choline, superfused and electrically stimulated. Since electrically-evoked [^{3}H]-overflow from septal cell cultures (Ehret et al., 2001) or brain slices (Molenaar et al., 1973; Richardson and Szerb, 1974; Hertting et al., 1980) incubated with [^{3}H]-choline has been shown to reflect action-potential-induced, exocytotic release of acetylcholine (ACh), mainly the expression "evoked release of ACh" will be used hereafter.

Properties of non-infected septal cell cultures

After 14 days *in vitro* (DIV), immunostaining for the specific cholinergic marker choline acetyltransferase (ChAT) of non-infected cell cultures showed the presence of many cholinergic neurons which were organized in aggregates and extended their neurites so that all aggregates seemed connected to each other (Figure 19).

As previously shown, such septal cultures consisted of a mixture of non-neuronal (mainly astroglial, see Figure 20B) and neuronal cells (see Figure 20A). The present study extends the observations of (Ehret et al., 2001) by showing, that also GAD_{67}-positive GABAergic neurons (Figure 22) were detectable in such primary septal cell cultures.

Besides an increase in ChAT-positive neurons during growth, the study of Ehret and co-workers (Ehret et al., 2001), also showed that following electrical field stimulation of such cultures, an action potential-induced and exocytotic release of ACh was easily detectable. Moreover, this evoked release of ACh was modulated by presynaptic muscarinic autoreceptors as well as by adenosine A_1 and μ-opioid heteroreceptors (Ehret et al., 2001). The present study extends this list of presynaptic receptors: the significant inhibitory effects of the selective 5-HT_{1B} agonist CP-93,129 [see (Hoyer et al., 1994)] suggests that also presynaptic 5-HT_{1B} receptors are present on cholinergic neurons in cultured septal cells. Indeed, the study of non-infected septal cell cultures showed a concentration-dependent inhibitory influence of the selective 5-HT_{1B} receptor agonist CP-93,129 (Figure 32) on the evoked release of ACh. Moreover, the selective 5-HT_{1B} receptor antagonist GR-55,562 reversed the inhibitory action of CP-93,129. These data confirm that functional 5-HT_{1B} receptors are present on cholinergic neurons in the primary septal cell cultures.

Increased expression of 5-HT_{1B} receptors in primary septal cell cultures: characterization of transfected cells

In the past, different approaches were used to deliver DNA into cells such as microinjection of frog oocytes (Noda et al., 1983), transgenic mice (Palmiter et al., 1983), transfection of DNA into cells (Graham and van der Eb, 1973b, 1973a) or the use of retroviral vectors (Mann et al., 1983). Unfortunately, however, none of these methods allowed delivery of a gene directly into postmitotic cells (see also Introduction). For this reason, the group of Geller A.I. and Freese A. developed a defective Herpes simplex virus type 1 (HSV-1) to introduce genes into postmitotic cells such as neurons. Many attractive features of this virus such as its wide host range including neurons in adult animals, its capability to be maintained in neurons indefinitely in a latent state as well as its large genome suggesting a possibility to transfer several genes at ones (see Introduction) led researchers to study the possibility to use HSV-1 as a viral vector. It was shown that infection with pHSVlac virus (HSV-1 vector containing the *Escherichia coli LacZ* gene under the control of the

HSV-1 immediate early 4/5 promoter) of neurons in primary culture derived from areas throughout the rat CNS resulted in expression of ß-galactosidase without causing cell death (Geller and Freese, 1990). Another study published by the same group in 1993 showed that it was possible to express a constitutively active adenylate cyclase from a HSV-1 vector in neuronal cells, and that this expression led to long-term increase in neurotransmitter release. These results offer the opportunity to correlate molecular changes in neurons with altered behavioural responses in learning paradigms (Geller et al., 1993). Moreover Farkas and co-workers, who expressed *Escherichia coli* ß-galactosidase using HSV-1 vector in rat cholinergic or dopaminergic neurons in culture, showed that the electrophysiological properties of the infected neurons were unchanged. Indeed the neurons remained electrically excitable and responsive to neurotransmitters (Farkas et al., 1994).

In the present work, we confirmed the selectivity of the viral vector described by (Clark et al., 2002) for neurons, since astroglial cells visibly did not express GFP [see Figure 24 and also (Barot et al., 2007)]. Moreover, as substantiated by the present data, some but not all of the GFP-positive neuronal cells in the septal culture were also positive for the cholinergic marker ChAT (Figure 26); in addition, following infection with the vector HA1B/GFP, the same neurons were also positive for the hemagglutinin-tag (Figure 25). Taken together, these observations suggest that (at least some of) the cholinergic cells in the culture have been transfected with the gene coding for the 5-HT_{1B} receptor. It should be noted, however, that in addition to cholinergic neurons in the culture, also GABAergic neurons might exhibit an increased expression of the 5-HT_{1B} receptor (Figure 27) although we did not check for the colocalization of the HA-tag with cells positive for GAD_{67}.

Increased expression of 5-HT_{1B} receptors in primary septal cell cultures: functional changes in cholinergic neurons

General remarks on ACh release from cultured neurons

As discussed above, primary cell cultures of the fetal rat brain allow to study the modulation of neurotransmitter release by presynaptic receptors (Ehret et al., 2001; Birthelmer et al., 2007; Ehret et al., 2007b) and thus should be useful to check the functional consequences of an enhanced expression of presynaptic receptors.

Nevertheless, it should be emphasized that release experiments on cultured neurons have the drawback of a relatively high variability of the release data, making their statistical analysis somehow difficult. In this context, one has to keep in mind the

difficulty to prepare such cultures in a reproducible manner, especially during dissection of “septal pieces” from the embryonic brain. Moreover, subsequently to the preparation of the cell suspension, the growth of each cell culture depends on a high number of factors, despite all efforts to routinely use a standardized procedure. Altogether, such variabilities in both preparation and culturing of primary neuronal cells also seem to affect the *functional* tests, i.e. by variabilities in the amount of the released transmitter and in its presynaptic modulation. Therefore, it is always difficult to compare data that are not directly obtained from the same cell culture set. For instance, in the present study values for the electrically-evoked ACh release at the first stimulation (S_1) were observed, which could be twice as high as in another septal cell culture. For all these reasons, cells that were used in the present thesis to compare the functional effects of transfection with GFP and HA1B/GFP viruses always originated from the same fetal septal cell suspension. These cells were then grown together and treated with the viral vectors exactly at the same day and time. For instance, at the day of infection (3 days before the functional tests), half of such septal cell cultures was treated with the GFP vector, while the other half was exposed to the HA1B/GFP vector. Results from several cell cultures were finally pooled to obtain mean values for normalization vs. controls. Using this strategy, culture to culture variabilities were reduced to a minimum.

Basal and evoked release of acetylcholine

Septal cell cultures, that were transfected with the viral vectors for 3 days (from DIV 11 to DIV 14), washed and incubated with [^{3}H]-choline, exhibited a [^{3}H]-outflow pattern during the superfusion experiments which was quite similar to that of untreated septal cell cultures at DIV 14. The observation (Figure 33), that both the basal and the evoked release of [^{3}H]-ACh was unaffected by an increased expression of the 5-HT_{1B} heteroreceptor in HA1B/GFP treated cultures is not surprising since these cultures, due to their origin - i.e., the fetal septal area which is free of serotonergic cell bodies (Jakab and Leranth, 1995; Risold, 2004) - should also be devoid of serotonergic neurons. Hence, due to the absence of endogenously released 5-HT in the culture, a decrease in the basal and evoked release of ACh should not be expected despite an increased expression of the 5-HT_{1B} heteroreceptor. Nevertheless Figure 33 also shows that the expression of the 5-HT_{1B} receptor in addition to GFP did not change the excitability and basic properties of those cholinergic neurons, although we cannot completely rule out the possibility that, due to an insufficient number of cells overexpressing these proteins, such effects might have been too small to be detected. Moreover, as in non-infected

cells (see above), the presence of functional 5-HT_{1B} receptors is confirmed also for cells transfected with the GFP vector (Figure 34): the exogenously added agonist CP-93,129 significantly inhibited the evoked release of ACh. This inhibition was, however, lower than that observed in non-infected cells. As tests on non-infected cultures were not performed directly in parallel, however, this observation might as well be attributable to the variability in cell culture experiments discussed above.

Presynaptic modulation of acetylcholine release via 5-HT_{1B} receptors

The first main observation of the present thesis is that septal cells treated with the HA1B/GFP viral vector show an increased expression of functional 5-HT_{1B} receptors as compared to cultures treated with the GFP vector. This conclusion is supported by Figure 34, which shows that the inhibitory effect of the 5-HT_{1B} agonist CP-93,129 was significantly more pronounced in HA1B/GFP-treated cells as compared to those infected with the GFP virus only, and this for the three concentrations of the agonist tested.

As concerns this first main finding, the following points have to be discussed:

(1) One has to keep in mind that HSV-1 is an episomal vector and therefore not integrated into the host genome. Thus it does not replicate along with the cellular chromosomal DNA and consequently, the percentage of infected cells in a population may decrease during further division of the infected cells (Neve et al., 2005). In the present study, septal cells were used for neurotransmitter release experiments at DIV 14, three days after infection of the growth medium with viral particles. It has been shown previously that following infection of primary neuronal cultures with HSV-1 vectors, expression of the transgene was detectable already within 2 hours (Bursztajn et al., 1998) and it did not diminish for up to 48 hours post-infection (Bahr et al., 1994). Thus, one might assume that 3 days after the infection, no decrease in the transgene expression should occur. On the other hand we have previously shown that there was an increase of ChAT activity in primary septal cell cultures of about 25% from DIV 11 to DIV 14 (Ehret et al., 2001). Although this value may not exactly reflect the increase in the number of cholinergic cells, it indicates that there is still an ongoing development of cholinergic neurons in the cultures over these 3 days. Therefore, it cannot be excluded that this development has contributed to dilute the expression of the transgene not replicated together with the chromosomal DNA.

(2) As evident from Figure 27, also GABAergic neurons in the culture might exhibit an increased expression of the 5-HT_{1B} receptor following treatment with the viral vectors. Since GABA release has been shown to be inhibited via presynaptic 5-HT_{1B} receptors in several brain regions (Bagdy et al., 2000; Chadha et al., 2000; Yan and Yan, 2001a; Bramley et al., 2005), it may be assumed that in HA1B/GFP-treated cultures, the presence of CP-93,129 more potently inhibits GABA release than in GFP-treated cultures. Since GABA, on the other hand, has been shown to inhibit the release of ACh in various CNS regions via presynaptic $GABA_B$ receptors (Moor et al., 1998a; Moor et al., 1998b; Vizi and Kiss, 1998; Nava et al., 2001), a decrease in the release of GABA should be equivalent to a disinhibition of ACh release, thereby counterbalancing the inhibitory effect of the 5-HT_{1B} receptor agonist CP-93,129.

In order to check this possibility, we reinvestigated the effects of CP-93,129 on septal cell cultures infected with GFP- and HA1B/GFP viral vectors, with the addition of $GABA_{A/B}$ antagonists to the superfusion medium. Thus, these experiments aimed at blocking the influence of GABA on cholinergic neurotransmission. Hence, it should be possible to study the effects of the increased expression of the 5-HT_{1B} receptor on cholinergic neurons only, i.e., without any GABAergic influence on ACh release. Interestingly, when these $GABA_{A/B}$ antagonists were present in the superfusion medium, we noticed that the septal cell cultures accumulated significantly more tritiated precursor (see Figure 33 and Figure 35). As it is known that the amount of accumulated [^{3}H]-choline depends on the rate of spontaneous firing of cultured cholinergic neurons, this observation suggests that this spontaneous firing rate is reduced by the presence of GABA released from neighbouring GABAergic neurons in the culture, an inhibition abolished by the presence of the $GABA_{A/B}$ antagonists.

Moreover, it was observed in presence of $GABA_{A/B}$ antagonists throughout superfusion, that in cultures treated with the HA1B/GFP vector the evoked [^{3}H]-ACh release at the first stimulation (S_1) was significantly smaller than in the absence of the $GABA_{A/B}$ antagonists from such cultures. This finding, however, is not in line with the hypothesis (see above) that a possible enhanced expression of 5-HT_{1B} receptors on GABAergic neurons in the culture leads to a disinhibition of cholinergic transmission; it rather points to more complicated neuronal interactions.

Finally, in the presence of $GABA_{A/B}$ antagonists, the inhibitory effect of the 5-HT_{1B} receptor agonist CP-93,129 on the evoked [^{3}H]-ACh release appeared to be abolished in septal cell cultures infected with the HA1B/GFP vector, but was unchanged in cultures with the GFP vector alone (Figure 36). Also this finding, which is again not in agreement with the hypothesis of an enhanced expression of 5-HT_{1B} receptors on

GABAergic neurons, suggests additional neuronal interactions involving both 5-HT_{1B} receptors and GABergic neurons.

Nevertheless, even if questions on the exact location of the 5-HT_{1B} receptors involved remain to be answered, these in vitro experiments showed that, using a HSV-1 vector, it was possible to induce functional changes of the 5-HT_{1B} heteroreceptors in septal cell cultures that contained transfected cholinergic neurons.

Increased expression of 5-HT_{1B} receptors in septohippocampal cholinergic neurons in vivo

General remarks on in vivo gene transfer

HSV-1 is currently the most extensively used herpes virus for purposes of gene transfer *in vivo* (Burton et al., 2001a; Kay et al., 2001; Burton et al., 2002) since it allows a reliable transfer of specific cellular properties to defined brain structures. Moreover, targeted gene transfer avoids the developmental compensations often seen in non-inducible knock-out (KO) mice (see Introduction for more details).

Immunocytochemical verification of viral transfections

The microscopic observation of septal sections of non-injected rat brains immunostained for cholinergic and GABAergic neurons (Figure 28) confirms the organization of these cells in the medial septal area (Risold, 2004): GABAergic cells are more grouped along the midline whereas cholinergic neurons occupy a more lateral position.

(1) Following injection of both viral vectors (GFP or HA1B/GFP, respectively) into the medial septum/diagonal band of Broca, a sphere of virus-infected, GFP-positive cells around the injection site was observed due to their bright green fluorescence. In addition, a small but non-negligible gliosis or inflammatory response (showing up as autofluorescence, see Figure 29) appeared at the place were the guide cannulae were lowered into this brain region.

(2) Using immunostaining for HA, the epitope-tag of the transfected 5-HT_{1B} receptor (Figure 30), it was also possible to demonstrate that following injection of the HA1B/GFP vector, some of the GFP-positive cells were also labelled for HA and thus

seemed to express both GFP and the 5-HT_{1B} receptor. In contrast, cells transfected with the GFP vector alone were never stained for HA.

(3) Finally, it was verified using confocal microscopy and immunocytochemistry for the cholinergic marker enzyme ChAT that in the medial septum/diagonal band of Broca infected with the HA1B/GFP vector, several GFP-positive cells were also ChAT-positive (Figure 31).

Taken together, it may be concluded from these observations that injection of the HA1B/GFP vector into the medial septum/diagonal band of Broca led to an additional expression of (GFP and) 5-HT_{1B} receptors in (at least some of the) cholinergic neurones of this brain region.

In support of this conclusion, Neumaier's group recently showed [see Figure 1 in (Barot et al., 2007)] that stereotaxical injection of the same viral vectors into the shell of the nucleus accumbens led to an expression of the transgene mostly in medium spiny neurons of this region and subsequently – as confirmed by western blots - to an overexpression of the HA-5-HT_{1B} protein in the projection field of these medium spiny neurons, namely the ventral tegmental area. There is no reason to believe that it was different for transfected neurons of the septal region.

However, as regards colocalization of GFP fluorescence with ChAT staining in the present study (see (3) above), we noticed by careful inspection of many brain sections that apparently not all cholinergic neurons underwent transfection. Therefore, one may wonder whether the number of injected viral particles used was high enough. Recently, targeted gene transfer into the ventral tegmental area (VTA) was studied using different combinations of viral concentrations and injection volumes. It was concluded that, in the VTA, the sphere of transgene-expressing neurons was substantially larger with a 2 µl than with a 1 µl microinjection volume, independent of the vector titer; in addition, it was underlined that an increase in the vector titer would simply cause more infections per cell rather than increasing the number of infected cells (Carlezon and Neve, 2003). In the present study, the titer of the vector was of 1-2×10^8 I.U./ml (I.U. infective units) and a total of 4 µl was injected at two depths of the medial septum/diagonal band of Broca.

Cholinergic specifity of the transfection?

Although the HSV-1 mediated gene transfer seems to be neuron-specific, one of the most important limitations of this technique is that it is difficult to design vectors that target specific subtypes of neurons, although this problem is less important when the

vector is injected in more homogeneous structures. As the medial septum/diagonal band of Broca is the site of origin of both cholinergic and GABAergic fibers projecting to the hippocampus (Jakab and Leranth, 1995; Risold, 2004), we cannot exclude that some of the septal GABAergic projection neurons were also infected. This possibility, which seems to occur following injection of the viral vector into the Nucleus accumbens (Neumaier et al., 2002; Hoplight et al., 2006), was not tested by immunocytochemical techniques in the present study (but see discussion on functional aspects of this point below), but in our cell cultures we found that the transfection of GABAergic neurons is possible.

Functional consequences of an increase in 5-HT$_{1B}$ receptor expression in septohippocampal cholinergic neurons

5-HT$_{1B}$ receptor-mediated inhibition of acetylcholine release in the hippocampus of non-injected rats

In order to gain further knowledge about 5-HT$_{1B}$ receptor-mediated modulation of hippocampal ACh release, this presynaptic mechanism was first studied in non-injected rats, using the selective 5-HT$_{1B}$ receptor agonist CP-93,129 alone or in combination with the corresponding antagonist GR-55,562.

When, before the second stimulation, the selective 5-HT$_{1B}$ receptor agonist was added to the superfusion medium, the electrically-evoked ACh release was significantly diminished, and this diminution was concentration-dependent (Figure 38). The concentration-effect curve was shifted to the right in a competitive manner in the presence of the antagonist GR-55,562 (1 µM) throughout superfusion. These observations further confirm the presence of 5-HT$_{1B}$ receptors on cholinergic axon terminals in the hippocampus [e.g. (Maura and Raiteri, 1986; Vizi and Kiss, 1998)].

Interestingly, the presence of GR-55,562 throughout superfusion significantly increased the tissue accumulation of [^{3}H], but decreased the evoked [^{3}H]-ACh release at S_1. Both effects are difficult to explain but may involve effects of endogenous 5-HT via interneuronal peptidergic loops in the hippocampal formation (e.g. (Feuerstein et al., 1996c; Feuerstein et al., 1996b)

Effects of transfection surgery on hippocampal acetylcholine release

In order to check whether the intraseptal injection procedure *itself* affected cholinergic transmission in the hippocampus, ACh release data from hippocampal slices of the GFP group were compared to those of rats that were not subjected to surgery (group

CON; see Table 12). Surprisingly it was observed that both the spontaneous [^{3}H]-outflow (b_1-values) as well as the electrically-evoked [^{3}H]-overflow (S_1-values), the latter corresponding to the evoked release of ACh, were significantly lower in GFP vector-injected as compared to CON rats. These differences suggest that the lesion resulting from our surgical procedures, perhaps more particularly from the guide cannula implantation, has damaged some septohippocampal cholinergic afferents.
On the other hand, the inhibitory effects of the 5-HT_{1B} agonist CP-93,129 did not differ among GFP and CON groups, suggesting, that the 5-HT_{1B} heteroreceptor mediated modulation of hippocampal ACh release was unaffected by the surgery. Taken together, these observations clearly attest that the GFP group is the most appropriate control for the rats that received the HA1B/GFP vector.

Effects of intraseptal gene transfer on the modulation of hippocampal acetylcholine release

Three days following intraseptal injection with GFP or HA1B/GFP viral vectors, hippocampal slices accumulated similar amounts of [^{3}H]-choline, whatever be the vector, suggesting that the density of cholinergic afferents to the hippocampus was relatively similar.
On the other hand, it was observed that both the spontaneous [^{3}H]-ouflow (b_1-values) as well as the electrically-evoked [^{3}H]-overflow (S_1-values), which corresponds to the evoked release of ACh, were significantly lower in HA1B/GFP vector-treated as compared to GFP vector-treated rats (Figure 40). This observation clearly suggests, that endogenously released 5-HT arising from raphé projections to the hippocampus inhibits the evoked release of ACh more effectively in rats with increased 5-HT_{1B} receptor expression on its septohippocampal cholinergic axon terminals (HA1B/GFP rats) than in rats of the GFP group.
This is the second main observation of this thesis, an observation which is further supported by the higher potency of the selective, exogenously added 5-HT_{1B} receptor agonist CP-93,129 (Figure 41) on the evoked release of ACh (an effect, which is already visible on the fractional rate plots depicted in Figure 39). Our data thus confirm that an intraseptal injection of the HA1B/GFP vector not only resulted in transfection of septal cholinergic neurons, as demonstrated by the immunocytochemical changes described above, but also affected the modulation of ACh release in the hippocampus. Thus it has to be assumed that the density of presynaptic 5-HT_{1B} receptors on hippocampal cholinergic afferents of the HA1B/GFP group was higher than in the GFP group. Since the concentration-response curve of CP-93,129 was shifted to the left but

reached the same maximal inhibitory effect, the number of spare receptors (the receptor reserve) appears to be increased by the transfection. Thus, lower concentrations of the 5-HT_{1B} receptor agonist resulted in higher levels of inhibition of hippocampal ACh release.

Finally in additional rats, the selective 5-HT_{1B} receptor antagonist (GR-55,562) was used to further evaluate the effects mentioned above. For that purpose, this compound was either present in the superfusion medium throughout the experiment whereas the selective agonist CP-93,129 was given before the second stimulation **(1)**, or the antagonist was given alone before the second stimulation **(2)**. When GR 55,562 was present throughout superfusion, the inhibition of the evoked release of ACh mediated by CP-93,129 (Figure 43) was completely antagonized in both HA1B/GFP- and GFP-treated rats, confirming once more that the inhibitory effect of CP-93,129 on evoked ACh release in the hippocampus was specifically mediated by 5-HT_{1B} receptors. The experiments designed to study the effects of GR-55,562 alone on hippocampal release of ACh, revealed two interesting results. Firstly, they were able to confirm once more (Figure 44) that the electrically-evoked ACh release elicited by the first stimulation S_1 (i.e. before addition of GR-55,562) was significantly lower in slices of rats injected with the HA1B/GFP vector than in those injected with the GFP vector. The second main finding of this part of the thesis, showing an increased expression of functional 5-HT_{1B} heteroreceptors on cholinergic terminals following injection of viral vectors into the medial septum/diagonal band of Broca, was replicated in this study.

Finally, when the specific 5-HT_{1B} receptor antagonist GR-55,562 was given as a drug just before the second stimulation (S_2) (Figure 45), no drug effect on the evoked ACh release was observed. However, since GR-55,562 should antagonize the effects of endogenously released 5-HT at the 5-HT_{1B} heteroreceptor on cholinergic neurons, a facilitatory effect was expected, which - due to equal levels of endogenous 5-HT - should be similar in both virus treated groups. We do not know why an enhancement of the evoked ACh by GR-55,562 was not observed, but a similar lack of facilitatory effects of 5-HT_1 antagonists, like methiotepine, on the evoked ACh release in hippocampal slices had been observed previously (Birthelmer et al., 2003a; Rutz et al., 2006b).

Enhanced 5-HT_{1B} receptor expression in septohippocampal GABAergic neurons?

Although the HSV-1-mediated gene transfer seems to be neuron specific, it may affect several types of neurons and hence also the important septohippocampal GABAergic

projection neurons (Jakab and Leranth, 1995; Risold, 2004). Concerning the functional aspects of a possible transfection of GABergic neurons with the HA1B/GFP vector (which we cannot exclude), the following points may be emphasized: (1) Whereas several studies have shown that presynaptic 5-HT_{1B} receptors inhibit the release of GABA in various other brain regions (Bagdy et al., 2000; Chadha et al., 2000; Yan and Yan, 2001a; Bramley et al., 2005), direct evidence is lacking for their presence on GABAergic terminals in the hippocampus (Vizi and Kiss, 1998). (2) Although the main effect of GABA on septohippocampal cholinergic projection neurons seems to take place in the septal nuclei themselves, there is also evidence for the presence of inhibitory $GABA_B$ receptors on cholinergic axon terminals in the hippocampus (Moor et al., 1998a; Vizi and Kiss, 1998; Nava et al., 2001). (3) Consequently, an increased expression of 5-HT_{1B} receptors on septohippocampal GABAergic projection neurons (if these receptors really occur on the axon terminals of these neurons) might lead to a decrease in hippocampal GABA release and, in turn, to a disinhibition, i.e. a facilitation of hippocampal ACh release. (4) In the present study, however, a decrease rather than an increase of ACh release was observed (Figure 40), suggesting that the enhanced expression of 5-HT_{1B} receptor in cholinergic projection neurons from the septum overruled a (still possible) increased expression of the 5-HT_{1B} receptor in GABAergic projection neurons. In any event, the targeted expression of HA1B/GFP transgene expression in septal neurons makes it very unlikely that 5-HT_{1B} receptors arising from elsewhere (e.g. hippocampal or dorsal raphé neurons) accounted for the increased potency of CP-93,129 on the electrically-evoked [^{3}H]-ACh release from hippocampal slices.

4.2. LONG-TERM EFFECTS OF MDMA +/- ETOH ADMINISTRATION IN RATS (PART 2)

Experiments described in section 3.2 of the Results were performed in order to get further insights in the effects of the combination of EtOH and MDMA (3,4-methylenedioxymethamphetamine or ecstasy) on several behavioural, neuropharmacological and neurochemical parameters. As described in the Introduction, the combination of these two drugs is widespread within MDMA abusers and it appears that the combination of such compounds enhances the subjective effects of MDMA (Lora-Tamayo et al., 2004; Schifano, 2004). Moreover, special interest was given on the effects of the combination of these drugs on the 5-HT_{1B} receptor-mediated modulation of 5-HT release in hippocampal and cortical slices, the ultimate goal there being to study the effects of MDMA ± ethanol after gene transfer targeting various relevant brain regions.

Acute Effects of MDMA or EtOH alone or in combination

Our group recently reported that the hyperactivity and hyperthermia induced by MDMA did not change in magnitude when the treatment was repeated at three other occasions, 24h apart (Cassel et al., 2004). Moreover, EtOH treatment had no effect on locomotor activity scores, but resulted in a small but significant hypothermia (about -0.5℃). Co-administration of EtOH with MDMA potenti ated the locomotor response and protected against hyperthermia due to MDMA. Prevention of hyperthermia, however, was observed only after the first treatment, as in the experiment shown in this part of the thesis (Figure 46). This limited prevention might have resulted from: (1) tolerance to the hyperthermic effects of MDMA (Marston et al., 1999) or (2) tolerance to the effect of EtOH, perhaps specifically in the presence of MDMA. In this respect, it was shown that prevention of the MDMA-induced hyperthermia by EtOH was preserved even following prior repeated EtOH administration. Indeed, rats were daily treated with only EtOH for 4 days before being challenged with MDMA and no tolerance due to this EtOH pre-treatment was observable on body temperature and locomotor activity (Hamida et al., 2006), suggesting that *EtOH-MDMA combination has unique pharmacological effects, which are not altered by prior experience of EtOH*.

Long-Term Effects of EtOH and/or MDMA on Monoaminergic Markers

Since we have shown that EtOH modulates the acute effects of MDMA, long-lasting effects of the combination of EtOH with MDMA are of obvious interest, particularly in terms of toxicity. Moreover, as the objective of this second part is was to study the possible effects of the combination of EtOH and MDMA on the modulation of 5-HT release, it seemed of particular interest to previously checked the effects of our drug regimen on monoaminergic markers.

As concerns long-term effects of short periods of EtOH treatment, the literature is rather scanty. A few reports show that brief periods of alcohol intoxication (binge exposure) may result in damage in the olfactory bulbs, the entorhinal cortex, and the dentate gyrus (Zou et al., 1996; Crews et al., 2000). Recently, Vasconcelos et al., reported that, in rats, EtOH administered daily for 7 days did not alter striatal 5-HT concentration 48h after the last treatment (Vasconcelos et al., 2003). In the present study, we do not know yet how to account for the significant increase in 5-HT concentration in the prefrontal cortex of rats given only EtOH, but it is interesting to note that in the EtOH+MDMA group, this increase was not observed. EtOH may interfere with the metabolism of tryptophan (Badawy, 1999), as well as increase the sensitivity of presynaptic 5-HT_{1A} receptors modulating 5-HT synthesis (Esteban et al., 2002).

Although the serotonergic toxicity of MDMA may vary as a matter of species, strain, and other factors (Green et al., 2003), serotonergic alterations are found in rats already one week after intoxication (Schmidt et al., 1987). These effects persist for several months, despite protracted recovery in all brain structures affected, although at a structure-dependent speed (Schmidt et al., 1987; Scanzello et al., 1993; Sabol et al., 1996). As our rats were killed 3 weeks after the last drug treatment, recovery of neurochemical parameters was probably limited. Keeping in mind that neurochemical markers are indirect markers of neurotoxicity (Green et al., 2003), our data are in line with reports showing that MDMA reduced 5-HT and 5-HIAA concentrations in several brain regions (Sabol et al., 1996). As serotonergic toxicity depends on MDMA-induced hyperthermia [but see (McGregor et al., 2003)] and EtOH has been shown to attenuate MDMA-induced hyperthermia (Cassel et al., 2004; Johnson et al., 2004), it might seem surprising that neurochemical serotonergic parameters were similar for MDMA and EtOH+MDMA-treated rats. One explanation might be that, as the MDMA-induced hyperthermia was prevented only by the first injection of EtOH, thus the still hypothetic protective effect of EtOH on MDMA-induced serotonergic neurotoxicity might not have

developed enough to protect 5-HT contents. Further studies are needed to understand this protective effect of EtOH on MDMA-induced hyperthermia and to determine a possible also protective effect of EtOH on MDMA-induced serotonergic toxicity.

Long-Term Effects of EtOH and/or MDMA on Behaviour

In the long-term, chronic EtOH treatment may alter cognitive functions (Beracochea and Jaffard, 1991), even after withdrawal (Arendt, 1994), and withdrawal from EtOH produces anxiogenic effects (File et al., 1993).

MDMA intoxication may produce changes in anxiety-related (Morley et al., 2001; McGregor et al., 2003) and, to some extent, cognitive (Marston et al., 1999) behaviours; however, there are no data on long-term effects of both drugs in combination.

The data presented in this part of the thesis show a deficit of rats pretreated with MDMA, EtOH or their combination only in the beam-walking test, which was performed 10 days after the last injections. This task is extremely sensitive to alterations in balance or sensory-motor coordination. For instance, rats with partial lesions of Purkinje cells (Thach et al., 1992) show impaired beam walking. One possible reason for the persistence of effect is neuronal loss. Owing to the dose of EtOH used, however, we believe that this explanation is unlikely. Repeated EtOH treatment also induces lasting dysfunction of cerebellar neurons. This possibility would deserve further investigation, but appears compatible with findings showing EtOH-induced dysfunction of Purkinje cells (Gruol et al., 1997; Wang et al., 1999). Rats given MDMA also showed impaired beam-walking performance. Serotonergic depletion may alter balance or sensory-motor coordination [(Lehmann et al., 2000), but see (Lehmann et al., 2002)]. MDMA might also directly affect cerebellar (for instance, granule or Purkinje) cells or perturb their interactions with serotonergic terminals. Thus, it is possible that beam-walking deficits in MDMA-treated rats reflected a long-term alteration of such interactions. Future studies relying upon morphological approaches should contribute to progress on this issue.

MDMA was found to induce anxiety after prolonged treatment (Morley et al., 2001), an anxiety syndrome that was presumably linked to serotonergic toxicity (Gurtman et al., 2002). Since the present results give clear evidence for serotonergic depletion, the lack of MDMA-induced anxiety in the elevated plus maze was not due to lack of serotonergic alterations. It is possible, however, that our serotonergic effects were less pronounced than in the study of Morley et al., in which effects on serotonergic

parameters were not reported. Despite different testing conditions (red light vs. white light), both test situations yielded comparable percent time spent in the open arms in controls (about 33%). A further difference in the experimental design was the shorter post-injection delay in our experiments, which was 19 days herein, but 3 months in the study by Morley et al (2001) and 9 weeks in the study by Gurtman et al. (2002). Thus, it could be that some of the alterations induced by MDMA require some delay before anxiety-related behaviours appear. This speculation seems in line with observations from the literature: long-term anxiogenic effects of MDMA were found only at post-intoxication delays of more than 4 weeks (Morley et al., 2001; Gurtman et al., 2002; McGregor et al., 2003; Bull et al., 2004) against no or small effects at shorter delays (Ho et al., 2004; Sumnall et al., 2004). Nevertheless, data on anxiety-related behaviours subsequent to MDMA intoxication are still controversal. For instance, even anxiolytic effects were reported, 80 days after a unique administration of MDMA (12.5 mg/kg) (Mechan et al., 2002a).

Long-Term Effects of EtOH +/- MDMA on Evoked 5-HT Release and Its Modulation by 5-HT$_{1B}$ Autoreceptors

The long-term effects of a short period of repeated EtOH intoxication on 5-HT release are unknown. Several findings pointing towards a reduction of the release of 5-HT after MDMA treatment contrast with our present results (Series et al., 1994; Gartside et al., 1996; Shankaran and Gudelsky, 1999; Matuszewich et al., 2002; Green et al., 2003). Indeed, in rats given MDMA alone, the 5-HT and 5-HIAA concentrations were reduced in various brain regions, but accumulation of [^{3}H]-5-HT in cortical and hippocampal slices, baseline outflow, and electrically-evoked overflow of [^{3}H]-5-HT were close to normal (Table 14). This is a *first important result* of these release experiments. If one excepts our observations in the frontal cortex, our data agree with those of (Gartside et al., 1996). These authors showed that, 2 weeks after intensive treatment with MDMA, (i) the firing activity of dorsal raphé neurons was normal, (ii) the basal release of 5-HT assessed by means of *in vivo* microdialysis was normal in the hippocampus, and (iii) the stimulation of the dorsal or the median raphé induced an increased 5-HT release in the hippocampus. Interestingly, this stimulated increase was not different between MDMA and saline-treated rats. Thus, despite marked 5-HT depletion in various brain regions, and particularly in the regions in which evoked 5-HT release has been studied, it appears that normal serotonergic functions can be detected. These authors attributed this to a capability of unaltered serotonergic terminals to increase their releasable 5-HT

pool. This interpretation is compatible with enhanced neurotransmitter release properties described in other lesion models (Suhr et al., 1999b).

Also the modulation of 5-HT release via autoreceptors, which are of the 5-HT_{1B} subtype, was found to be normal in MDMA-treated rats (Figure 52). Indeed, the functional characteristics of 5-HT_{1B} autoreceptors seem to be normal despite long-term alterations of tissue-5-HT and 5-HIAA concentrations. The functional characteristics of 5-HT_{1B} heteroreceptors were not tested in this work but as regards autoreceptors, it has been shown that the sensitivity towards 5-HT agonists of autoreceptors is higher than that of heteroreceptors (Sarhan and Fillion, 1999). Thus, it could be that despite long-term reduction in 5-HT contents in the brain, the functional properties of 5-HT_{1B} autoreceptors are preserved, at least to some extent.

The *second important finding* from the release experiments is the apparent change in the modulation of 5-HT release in the hippocampus of rats given EtOH and MDMA in combination (Figure 52). Our data clearly show that the evoked overflow of 5-HT (in percent of tissue-[^{3}H]) in the hippocampus was slightly but significantly increased in the EtOH+MDMA group as compared to the rats treated with saline, EtOH or MDMA alone (Table 14). This increase in the relative amount of the evoked 5-HT release was observed despite a decrease in hippocampal tissue concentrations of both 5-HT and 5-HIAA (Figure 50). Taken together, these two observations suggest changes in the modulation of 5-HT release at the serotonergic axon terminals, changes that appear to lead to a greater amount of transmitter release per individual axon terminal. Such alterations might either reflect a reduction of inhibitory control mechanisms or an enhancement of facilitatory influences due to the combined treatment with MDMA and EtOH. Interestingly, however, in the hippocampus of these rats, the main presynaptic inhibitory receptor, the 5-HT_{1B} autoreceptor, appeared to be not less, but even significantly more sensitive. In that concern, it is noteworthy that also in previous studies using rats with fimbria-fornix lesions of hippocampal afferent fibers, an increase in the sensitivity of the 5-HT_{1B} autoreceptor was observed (Jackisch et al., 1999a). Similar lesions cause, however, a significant serotonergic denervation and lead to a decrease of hippocampal 5-HT content and 5-HT release during ongoing stimulation. Therefore, it was possible to show (Jackisch et al., 1999a) that the higher potency of the 5-HT_{1B} autoreceptor agonist was only apparent and was most probably caused by the diminished competition with the endogenous agonist, i.e., 5-HT, in the vicinity of the autoreceptor (“biophase concentration of 5-HT”). Although a similar interpretation for the present data is further supported by the decrease of the facilitatory effect of the nonselective 5-HT receptor antagonist methiotepin, it contrasts with the relative

increase of 5-HT release at the first stimulation (S_1), an observation that was, however, also made in rats with fimbria-fornix lesions (Jackisch et al., 1999a). In addition, if true, this hypothesis would suppose that changes found in EtOH+MDMA rats should also be present in MDMA rats: this was not the case. One possibility to account for the apparently paradoxical findings with CP-93,129 and methiotepin would be that methiotepin may alter the release of another transmitter that (i) is not influenced by a drug acting selectively on 5-HT_{1B} receptors, (ii) might interfere with the serotonergic terminal in a way that would oppose to the facilitatory effects of methiotepin on evoked 5-HT release, and (iii) would activate an inhibitory heteroreceptor present on the serotonergic terminal, and which is upregulated after combined EtOH and MDMA treatment. Based on our current state of knowledge, it is not possible to propose a particular receptor. Possible candidates include $GABA_A$, $GABA_B$, and NMDA receptors (Vizi and Kiss, 1998). It could also be that EtOH+MDMA treatment has resulted in an increase of presynaptic facilitatory influences on 5-HT release, which might involve AMPA or 5-HT_3 receptors (Vizi and Kiss, 1998).

4.3. INTERACTIONS OF MDMA AND ETOH ON NEUROTRANSMITTER RELEASE *IN VITRO* (PART 3)

As already mentioned, electrically-evoked overflow of [^{3}H] from brain slices incubated with the corresponding tritiated neurotransmitter or precursor is a valuable model for the study of the presynaptic modulation of action potential-induced, exocytotic neurotransmitter release (Hertting et al., 1980; Jackisch et al., 1980; Birthelmer et al., 2003d; Birthelmer et al., 2003b). Conversely, the spontaneous [^{3}H]-outflow and the [^{3}H]-outflow induced by direct drug application to such slices consists in a mixture of the efflux of both the [^{3}H]-transmitter itself and its tritiated metabolites (Starke et al., 1981; Zumstein et al., 1981; Steppeler and Starke, 1982; Ehret et al., 2001).

The present part of our work investigated the effects of MDMA and EtOH, given alone or in combination, on the spontaneous outflow and the electrically-evoked overflow of [^{3}H] from slices of the rat striatum, previously incubated with [^{3}H]-5-HT, [^{3}H]-DA or [^{3}H]-choline (vs. the hippocampus and neocortex for 5-HT release). As concerns the locomotor effects of EtOH+MDMA, it seemed reasonable to hypothesize that the mesolimbic dopaminergic system may be a target for the EtOH × MDMA interactions, although the mechanisms of the aforementioned effects are still unknown. These mechanisms could non-exclusively involve pharmacokinetic and pharmacodynamic components (Oesterheld et al., 2004). Concerning pharmacodynamics, two perhaps complementary hypotheses might be that **(i)** EtOH and MDMA modify the functional properties within complex multi-synaptic circuitries, or that **(ii)** EtOH and MDMA act more locally on presynaptic neuropharmacological substrates participating in the regulation of neurotransmitter release. In the present part of this thesis, we focused on this second possibility, again by using a slice superfusion technique.

Serotonin release in rat striatum, hippocampus and neocortex

As shown in section 3.3 of the Results, MDMA, but less effectively also EtOH, enhanced the spontaneous outflow of [^{3}H] in slices of the rat striatum (Figure 54), hippocampus (Table 16) and neocortex (Table 17) previously incubated with [^{3}H]-5-HT. Also, the electrically-evoked overflow of tritium was increased, but only by the highest concentration of MDMA and only in striatal slices. In striatal slices, these effects were almost independent on whether the DA reuptake carrier (DAT) was blocked or not with

nomifensine. EtOH also potentiated the MDMA-induced release of [^{3}H], but only at the lower concentration of MDMA (0.3 µM) and only in striatal slices.

As shown in earlier studies, EtOH, given intraperitoneally (i.p.) or applied directly to the ventral tegmental area (VTA) is able to stimulate the release of 5-HT (Yan et al., 1996; Yan, 1999). Moreover, in the caudate-putamen, EtOH increases 5-HT release despite its ability to decrease the firing rate of 5-HT neurons in the dorsal raphé, suggesting that this release of 5-HT could in fact mainly depend on local action of EtOH (Thielen et al., 2001). Our results with EtOH confirm the latter findings. This effect was not due to modifications of neuronal electrical properties as EtOH did not modify the electrically-evoked overflow of [^{3}H]-5-HT in these same slices.

Also the application of 0.3 or 3 µM of MDMA significantly increased the spontaneous release of 5-HT from striatal slices, which is in line with the literature. Indeed, several studies using *in vivo* microdialysis reported an acute and rapid release of 5-HT in the striatum and a decreased 5-HT concentration following MDMA administration (Gudelsky and Nash, 1996; Sabol and Seiden, 1998; Mechan et al., 2002b). This enhanced release of 5-HT both involves a carrier-mediated mechanism and depends on vesicular stores of 5-HT (Wichems et al., 1995). Moreover, and as shown in this work, MDMA triggers an acute release of 5-HT following its application on brain slices and, in particular, on striatal slices (Schmidt et al., 1987; Crespi et al., 1997; Koch and Galloway, 1997).

After pre-treatment of the slices with EtOH+MDMA (at 0.3 µM), the drug-induced 5-HT release was even larger than that elicited by MDMA alone, which is our first main finding of this investigation, as it points towards a synergistic effect of EtOH and MDMA in the striatum. It also appears that this synergism in releasing 5-HT undergoes saturation as it was not found with 3 µM of MDMA (associated to EtOH). Moreover this effect seems to be affected by DA, as it was significant in the presence but not in the absence of the preferential DA-reuptake inhibitor nomifensine throughout superfusion. One possibility to explain this potentiated 5-HT release after combined EtOH-MDMA treatment could be related to an EtOH-mediated change in the availability of MDMA within (or the penetration into) the striatal slices: the higher the availability (the better the penetration), the larger the release. In fact, it was shown in the mouse striatum, that combining MDMA with EtOH increased striatal MDMA levels by 4- to 7-fold (Johnson et al., 2004). This EtOH-mediated increase in tissue MDMA concentrations could then lead to an increase in MDMA-induced 5-HT release. However, one should keep in mind that in our experiment, MDMA and EtOH were directly applied to striatal slices *in vitro* whereas the effects in mice were observed after systemic administration (15.0 mg/kg

MDMA s.c. every 2 hours × 4), which raises the possibility that EtOH simply facilitated the penetration of MDMA into the brain when it is given systemically. Thus, the mechanism accounting for the increased 5-HT release after local application of MDMA and EtOH on striatal slices, remains to be identified.
It is nevertheless noteworthy that in the presence of nomifensine during the superfusion, the effect of MDMA on DA release should be markedly weakened, if not abolished, suggesting that the potentiation by EtOH of MDMA-induced 5-HT release may appear under the condition of a lower dopaminergic tonus, or when the 5-HT/DA balance is largely in favor of 5-HT.

Concerning the effects of EtOH, MDMA, or their combination in the hippocampus or the neocortex, our results showed that both drugs and their combination increased 5-HT release in these structures (Table 16 & Table 17). Concerning EtOH, these observations are in line with previous results (Thielen et al., 2002). It is also well-known from the literature that MDMA stimulates this release (Esteban et al., 2001) by an action on both the 5-HT transporter (SERT) and intraneuronal vesicular stores of 5-HT (Mlinar and Corradetti, 2003). It was also reported that MDMA is also able to induce the release of 5-HT from cortical synaptosomes (Kramer et al., 1994). Finally, intra-venous injected MDMA was shown to trigger the release of 5-HT in both the hippocampus and the frontal cortex (Gartside et al., 1997). As such, our results with MDMA alone are in line with the literature. But in neither of these two structures, and in contrast to striatal 5-HT release, the combination of MDMA with EtOH led to a modification of 5-HT release as compared to MDMA given alone, suggesting a region-specific effect of EtOH+MDMA interactions.

Dopamine release in rat striatum

The DA releasing effect of MDMA is well known from the literature, as is also that of the participation of an enhanced 5-HT release in this effect (Yamamoto et al., 1995; Gudelsky and Nash, 1996; Koch and Galloway, 1997; Goni-Allo et al., 2006). In order to avoid an influence of 5-HT on DA release, part of the experiments were performed in presence of the selective SERT inhibitor fluvoxamine. It has been shown that SERT is one of the main targets of MDMA (Rudnick and Wall, 1992) and that selective SERT inhibitors prevent at least part of the 5-HT releasing effect of MDMA (Berger et al., 1992; Wichems et al., 1995). Hence, in support of the findings mentioned above, also in the present study the MDMA-induced release of DA was significantly higher in the

absence (i.e. when MDMA-induced 5-HT release was high) than in the presence of fluvoxamine (i.e. when MDMA-induced 5-HT release was weaker).

MDMA (0.3 and 3 µM), and also EtOH (2‰) enhanced the spontaneous outflow of [^{3}H] in slices of the rat striatum previously incubated with [^{3}H]-DA (Figure 56), whereas the electrically-evoked DA release was decreased in the presence of MDMA. In the absence of the SERT inhibitor fluvoxamine throughout superfusion, however, the inhibitory effects of MDMA (3 µM) on the electrically-evoked [^{3}H]-DA release disappeared (Table 18). In the absence of fluvoxamine during the superfusion, the combination of MDMA with EtOH caused a significantly higher facilitatory effect of MDMA on drug-induced release only at the low concentration of MDMA (0.3 µM: +66%). But in the presence of fluvoxamine throughout superfusion, the drug-induced DA release was facilitated at both the low and high concentrations of MDMA (+122% and +65% respectively, (Figure 56), thus under conditions for which the effects of MDMA on the serotonergic terminals were most probably weaker than in its absence (Gudelsky and Nash, 1996; Mechan et al., 2002b). One has to keep in mind however, that fluvoxamine was given throughout the superfusion, and thus may have contributed to a substantial increase of the 5-HT tonus before MDMA was applied. In the striatum, 5-HT has an inhibitory influence on DA release (Bankson and Cunningham, 2001; De Deurwaerdere et al., 2004), which could be reflected by the fact that the release of DA induced by 0.3 µM MDMA in the presence of fluvoxamine was by more than twice weaker than in the absence of the SERT blocker. The same observation was made using 3 µM MDMA, but only in the absence of EtOH. This observation is interesting as it indicates that one of the possible targets for EtOH-mediated effects in MDMA-treated rats could be the level of inhibition that DA exerts on 5-HT terminals. How can these findings be used to explain effects of MDMA and EtOH observed *in vivo*?

In vivo microdialysis studies have shown that MDMA induces maximal effects on striatal 5-HT efflux, but weaker effects on that of DA. Thus, it is possible that the presynaptic inhibition exerted by 5-HT on DA terminals could be rather high after MDMA alone treatment. Thus, it may be speculated, that the administration of EtOH together with MDMA could contribute to attenuate this inhibition, resulting in a larger efflux of DA and thus an increased locomotor activity. This possibility, which is not in contradiction with our findings on 5-HT release (see above), from which we speculated on the possibility that EtOH can potentiate the MDMA-induced locomotor effects of MDMA when the 5-HT/DA balance is in favor of 5-HT, must be tested in future experiments using intrastriatal microdialysis.

4.4. INCREASED EXPRESSION OF 5-HT_{1B} AUTORECEPTORS IN THE RAT BRAIN: LOCOMOTOR EFFECTS OF MDMA +/- ETOH ADMINISTRATION (PART 4)

As a consequence of the results obtained in the previous sections following administration of MDMA, EtOH or their combination on locomotor activity, as well as on the modulation of neurotransmitter systems, especially in the striatum, it appeared extremely important to further test the hypothesis of an implication of the 5-HT_{1B} receptor in these processes. In the first part of this thesis we showed that it is possible to increase the expression of the 5-HT_{1B} receptor in cholinergic neurons (i.e., as a *heteroreceptor*) of the medial septum/diagonal band of Broca via HSV-1-mediated gene transfer. The functionality of this increased receptor density was assessed by measuring the modulation of the release of ACh in the hippocampus.
In 2002, Clark and co-workers had already shown that a functionally-relevant overexpression of 5-HT_{1B} receptors could be induced by viral transfection in serotonergic neurons of the dorsal raphé (Clark et al., 2002).
Therefore, the goal of this last part of the thesis was to use the same technique in order to investigate the possible involvement of 5-HT_{1B} receptors in the locomotor effects of MDMA, as well as of its combination with EtOH. To that end, the viral vectors characterized in the first part of this work were stereotaxically injected into the rat dorsal raphé nucleus (DRN) as described in Methods. As outlined in the Introduction, the 5-HT-containing fibers originating in the DRN project to dopaminergic cells bodies in the ventral tegmental area (VTA) and substantia nigra (SN), but also to the prefrontal cortex, the nucleus accumbens (Nac) and the striatum (Steinbusch, 1981). Since the stereotaxic gene transfer is performed in the DRN, we assume that only the expression of 5-HT_{1B} *autoreceptors* present on serotonergic nerve terminals is increased, thereby changing the presynaptic modulation of the release of 5-HT in these projection zones.

Results of this part of the thesis were presented in section 3.4. Briefly, following stereotaxic injection into the DRN of the GFP or HA1B/GFP viral vectors, GFP-positive cells were detected in brain sections containing the dorsal raphé nucleus, indicating the presence of the viral vectors in this transfected structure (Figure 57). MDMA, EtOH or their combination were then administered to those transfected rats. We showed that, as compared to rats treated with saline, MDMA increased the locomotor activity in both groups tested. Moreover, in the GFP group, EtOH potentiated this MDMA-induced

activity. Finally, and more interestingly, in the HA1B/GFP transfected rats, this potentiation of MDMA-induced locomotion was not detectable (Figure 58).

Among others, the serotonergic 5-HT_{1B} receptor has been shown to participate in the hyperlocomotor effect of MDMA. Firstly, 5-HT_{1B} agonists were shown to elicit a behavioural profile similar to that of low doses of MDMA (Rempel et al., 1993). For instance, both RU-24,969 and CGS-12,066B increased locomotor activity in rodents (Cheetham and Heal, 1993). Furthermore, this 5-HT_{1B} receptor agonist-induced hyperactivity was prevented by selective 5-HT_{1B} receptor antagonists (McCreary et al., 1999). Moreover, it was demonstrated that transgenic mice lacking the 5-HT_{1B} receptor do not exhibit MDMA-induced hyperkinetic effects (Scearce-Levie et al., 1999a). These data strongly support a critical role for 5-HT_{1B} receptors in hyperlocomotion subsequent to MDMA application.

In addition it was shown that MDMA acts on both serotonergic and dopaminergic transmissions (even with greater affinity for SERT, the serotonin transporter) creating a unique neurochemical profile. Thus, in the case of MDMA and its psychostimulant effect, the interaction between 5-HT and DA systems appears to be of high importance (Bankson and Cunningham, 2001). This aspect was also illustrated in the previous experiment (Part 3) of this thesis.

Finally, the involvement of 5-HT_{1B} receptors in MDMA-induced hyperlocomotion is further supported by its modulatory role on dopaminergic transmission in nigrostriatal and mesolimbic pathways (see next paragraph).

The implication of the 5-HT_{1B} receptor in the modulation of DA release in several brain regions has been shown *in vitro* and *in vivo*. For instance, it was shown, mainly using *in vivo* microdialysis studies, that striatal 5-HT_{1B} receptors facilitate the release of nigrostriatal DA (Benloucif and Galloway, 1991; Benloucif et al., 1993; Galloway et al., 1993; Ng et al., 1999). Whereas the latter experiments all went in the direction of a permissive role of the 5-HT_{1B} receptor on DA release, investigations on synaptosomes suggested an inhibitory role for this receptor (Sarhan et al., 1999; Sarhan et al., 2000). It was suggested, however, that this inhibitory effect can be overshadowed *in vivo* by an overall facilitation or would require feedback loops in the substantia nigra that are not observable *in vitro* (Alex and Pehek, 2007). Thus, as it is widely accepted that the 5-HT_{1B} receptor is negatively coupled to adenylate cyclase (Bouhelal et al., 1988) and thus inhibits the release of neurotransmitters (both as auto- or heteroreceptor), it was proposed that it could be present on the terminals of striatonigral GABAergic neurons

and thus indirectly modulate nigrostriatal DA release (Waeber et al., 1989; Bruinvels et al., 1994; Sari et al., 1999).
On the other hand, several studies also showed a facilitatory influence of 5-HT_{1B} receptors on DA release in the mesolimbic pathway. For instance, the infusion of CP-93,129 directly into the nucleus accumbens, led to a local increase in DA content (Yan and Yan, 2001b). This effect does not represent a tonic modulation of DA release as infusion of the selective 5-HT_{1B} antagonist GR-127,935 was without effect on basal mesolimbic DA levels (Hallbus et al., 1997). On the other hand, the mRNA for the 5-HT_{1B} receptor was not detected in the cell bodies of DA neurons projecting to the nucleus accumbens (Boschert et al., 1994; Bruinvels et al., 1994) so that it seems unlikely that the relevant 5-HT_{1B} receptors reside on DA terminals in the nucleus accumbens.

More is known about the regulation of dopaminergic transmission by 5-HT_{1B} receptors located in the VTA. Thus it was reported that administration of CP-93,129 into the VTA led to increased DA levels in the nucleus accumbens, whereas the release of GABA was decreased in the VTA (Yan and Yan, 2001b; O'Dell and Parsons, 2004; Yan et al., 2004a). Systemically applied agonists also decreased GABA levels in the VTA (Harrison et al., 1999). These studies are in favor of a regulation of mesolimbic DA activity via 5-HT_{1B}-mediated inhibition of GABA release in the VTA. In support of this hypothesis, it was shown that a 5-HT_{1B} selective agonist inhibited high-K^+-induced [^{3}H]-GABA release from VTA slices (Yan and Yan, 2001a). Moreover, application of 5-HT or 5-HT_{1B} agonists on VTA slices decreased the amplitude of $GABA_B$-mediated IPSPs in DA neurons (Johnson et al., 1992b), effects, which were blocked by co-administration of the 5-HT_{1B} antagonist cyanopindolol. From all these informations, it was assumed that the 5-HT_{1B} heteroreceptors concerned are located on the axon terminals of GABAergic projection neurons from the nucleus accumbens. Activation of these receptors would thus decrease an inhibitory influence on DA neurons, i.e. increase the release of DA in the terminal fields of these projections neurons.
As already shown in previous experiments of our group, EtOH is able to potentiate the MDMA-induced hyperlocomotor activity (Cassel et al., 2004). In Part 3 of this thesis (see section 3.3 and 4.3), we showed that local synergistic effects, relying on pharmacodynamic interactions, contribute to increase both the release of 5-HT and DA in the striatum and could thus be responsible, at least in part, for this potentiation. This last experiment gives some more details about the possible role of the 5-HT_{1B} autoreceptors in this phenomenon.

An increased expression of 5-HT_{1B} autoreceptors in the axon terminals of serotonergic neurons (in HA1B/GFP transfected rats) should thus decrease the amounts of 5-HT released in the target regions of serotonergic fibers originating in the DRN. As a consequence, the influence of 5-HT on the surrounding nerve terminals and neuronal cell bodies bearing various 5-HT receptors (including also 5-HT_{1B} heteroreceptors) will be reduced. For instance, the facilitatory effects of 5-HT on the release of DA in the nucleus accumbens and the striatum, i.e. in regions that seem to be key components in the hyperlocomotor effects of MDMA (see above), will also be diminished as observed in the present experiment. Indeed, in the VTA, the increased number of 5-HT_{1B} autoreceptors on serotonergic fibers originating in the DRN leads to a decreased 5-HT release. This effect thus tends to reduce the influence of 5-HT on GABAergic nerve terminals which in turn leads to larger amounts of released GABA. This GABA was then shown to inhibit the release of DA in the target structure of the VTA, i.e., the nucleus accumbens. Thus, the results of the present experiment suggest that 5-HT_{1B} autoreceptors may take part in the potentiating effect of EtOH on hyperlocomotion induced by MDMA administration.

Thus, even if the last experiment of this thesis was only preliminary and certainly needs further investigations, it allowed us to suspect that 5-HT_{1B} autoreceptors, on serotonergic nerve terminals from the DRN, might play a regulatory role in the hyperlocomotor effects of MDMA as well as in that of its combination to EtOH. The data also suggest that not only action potential-evoked release of 5-HT, but also the outflow induced by a direct application of MDMA might be regulated via the 5-HT_{1B} autoreceptor mechanism.

General conclusion and perspectives

Conclusion of Part 1 of this thesis

The present investigation shows for the first time some functional consequences of an increased expression of 5-HT_{1B} heteroreceptors on septohippocampal cholinergic projection neurons. In view of the suggested cholinergic-serotonergic interactions in learning and memory (see Introduction), future experiments will now have to examine if an increased expression of 5-HT_{1B} heteroreceptors on septohippocampal cholinergic neurons is accompanied by behavioural modifications, for instance in cognitive tests. However, especially with regard to behavioural tests of cognition, which are always time consuming and often require experiments extending over weeks and months, the present transfection technique, despite its regional selectivity, may cause technical problems, because the increased expression is only transitory. However, it is of importance to emphasize that transient expression of the viral transfection vector has also clear-cut advantages: for instance, it may sensitize animals to subsequent treatments with drugs of abuse, and, more generally, enable a powerful within-subject approach of various integrated effects of an increased expression of 5-HT_{1B} receptors, as a control can be used before the transfection, and another one once the overexpression has vanished.

In relation with the present data, it is noteworthy that changes in the level of 5-HT_{1B} receptor expression may also be relevant to pathophysiological phenomena, given the plasticity of 5-HT_{1B} mRNA expression levels that has been detected in various brain regions following behavioural stress exposure (Hoplight et al., 2007). Moreover, septal 5-HT_{1B} mRNA levels may also be altered by various environmental factors; indeed, an about 50% reduction in septal 5-HT_{1B} mRNA in old (24 months) vs. young (3 months) rats has been detected recently (J.F. Neumaier, personal unpublished data).

Conclusion of Part 2

The results depicted in Part 2 of this thesis, show that repeated treatment with EtOH or/and a neurotoxic dose of MDMA produces lasting effects that are manifest in behaviour and neurochemistry. Some of these effects may be attributed **(i)** to MDMA alone, that is, reduced concentrations of 5-HT and 5-HIAA in various brain regions, although 5-HT release capabilities appear normal, **(ii)** to MDMA alone or to EtOH alone, perhaps by the way of different mechanisms leading to comparable consequences, which seems to be the case for the reduced sensory-motor coordination capabilities, or **(iii)** specifically to the combination of both drugs, that is,

alteration of mechanisms involved in the modulation of 5-HT release via 5-HT_{1B} receptors in the hippocampus. They also demonstrated that EtOH neither attenuates nor exacerbates effects of MDMA on levels of 5-HT and 5-HIAA in the cortex and the hippocampus. This is the first study to address delayed effects of MDMA and EtOH, singly and in combination. We conclude that the mechanisms involved in presynaptic modulation of 5-HT release in the hippocampus may be particularly sensitive to this combination. In view of the results of Part 1, it would be of particular ineterest to study the responsivness of 5-HT_{1B} receptors in such animals, but after transfection of 5-HT neurons of the dorsal raphe.

Our findings also suggest that when recreational use of ecstasy in combined with EtOH, it is possible that the long-term psychopathological problems reported by ecstasy users – which are usually attributed to the 5-HT depleting effect of MDMA – may not be caused solely by the consumption of MDMA. Indeed, we have shown that the combination of MDMA with EtOH may have some long-term consequences on serotonergic functions that MDMA alone does not account for.

Conclusion of Part 3

This part of the thesis brings to light several new informations regarding the complex mechanisms behind the effects of MDMA and/or EtOH on the modulation of striatal transmission in the rat. Even if the effects mediating the action of these drugs on striatal ACh release need further investigations, the use of specific antagonists allowed us to show that several receptors seem to be implicated in these mechanisms. Moreover, this work shows, for the first time, a local synergistic interaction of these two drugs on the spontaneous outflow of [^{3}H]-DA and [^{3}H]-5-HT. Indeed, when applied together, MDMA and EtOH increased the spontaneous outflow of both DA and 5-HT with a higher potency than did MDMA alone. In no case, however, should the current findings be considered as demonstrating an exclusive mechanism accounting for the synergistic effects of EtOH-MDMA co-administration on physiological or behavioural parameters such as hyperthermia or hyperactivity. In fact, our present result clearly suggest that one or more local mechanisms may participate in these interactions, but they neither exclude an additional *in vivo* action via more complex polysynaptic loops that could involve also extra-striatal neurons, nor do they discard the possibility of an additional involvement of pharmacokinetic factors. Obviously, the two latter issues need further investigation.

Conclusion of Part 4

In view of the previously cited results, several new informations were given through this work regarding the possibility to use a gene transfer technique to overexpress 5-HT_{1B} receptors in neurons. Moreover, various aspects of the effects of the combination of MDMA and EtOH, especially on neurotransmitters release in several brain regions were investigated. In an attempt to study the effects of this drug combination at a more integrated level, the behavioural effects of the combination of MDMA and EtOH on the locomotor activity of rats was studied. The results of this part of the thesis suggest that an increased expression of 5-HT_{1B} autoreceptors, after transfection of neurons of the DRN with the GFP and HA1B/GFP viral vectors, tends to reduce the hyperlocomotor effect of MDMA as well as that of its combination with EtOH. Thus it appeared that 5-HT_{1B} autoreceptors may also take part in the potentiating effect of EtOH on hyperlocomotion induced by MDMA intoxication. Even if serotonergic neurons from the raphé nuclei are not so numerous, the serotonergic system in the CNS appears to be one of the most widespread due to important arborisation of the axons of its neurons. Thus, this technique, allowing to study specifically 5-HT_{1B} auto- **or** heretoreceptors is of great interest. Moreover, serotonergic neurons and receptors are implicated in a great variety of neurochemical processes and behaviours and the technique studied here was shown to be useful, also when studying behaviour.

5. APPENDICES

APPENDIX 1

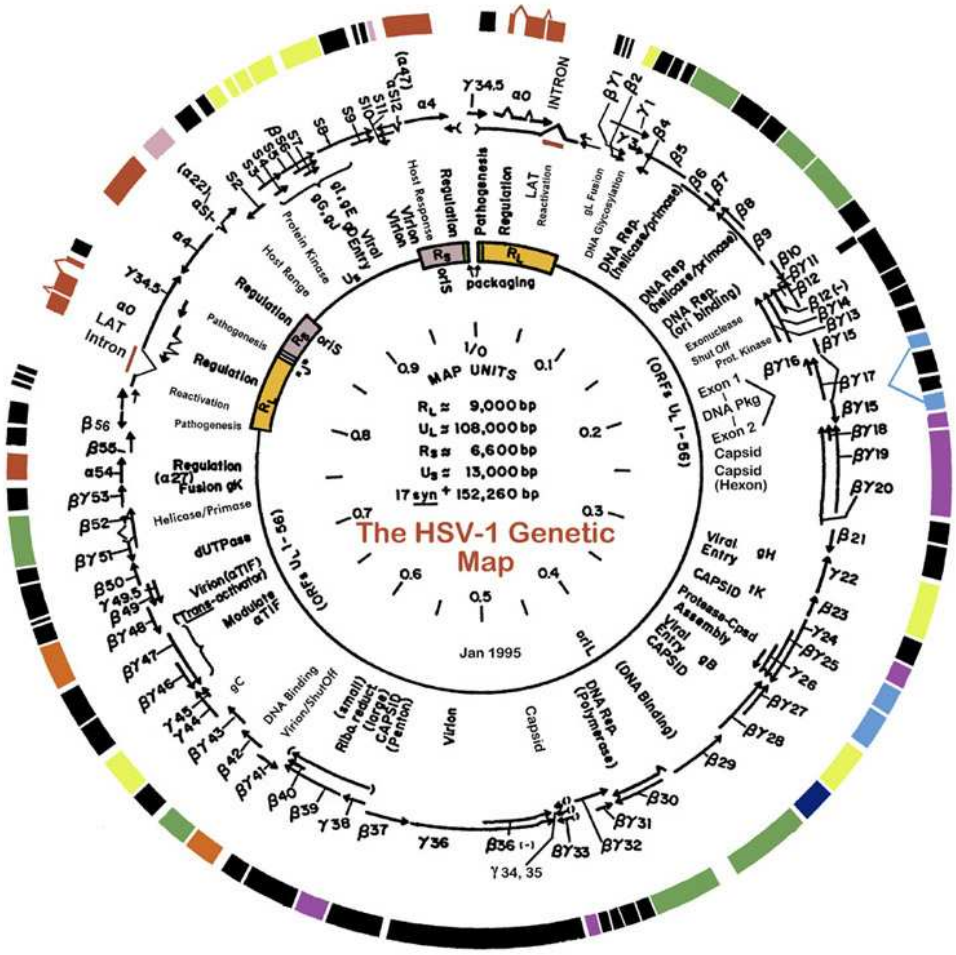

The HSV-1 genetic map. As during the life cycle of HSV, the DNA circularises, this circular map was chosen. One may also find linear representations of the HSV genome.

http://darwin.bio.uci.edu/~faculty/wagner/table.html gives some functions encoded by HSV-1.

APPENDIX 2

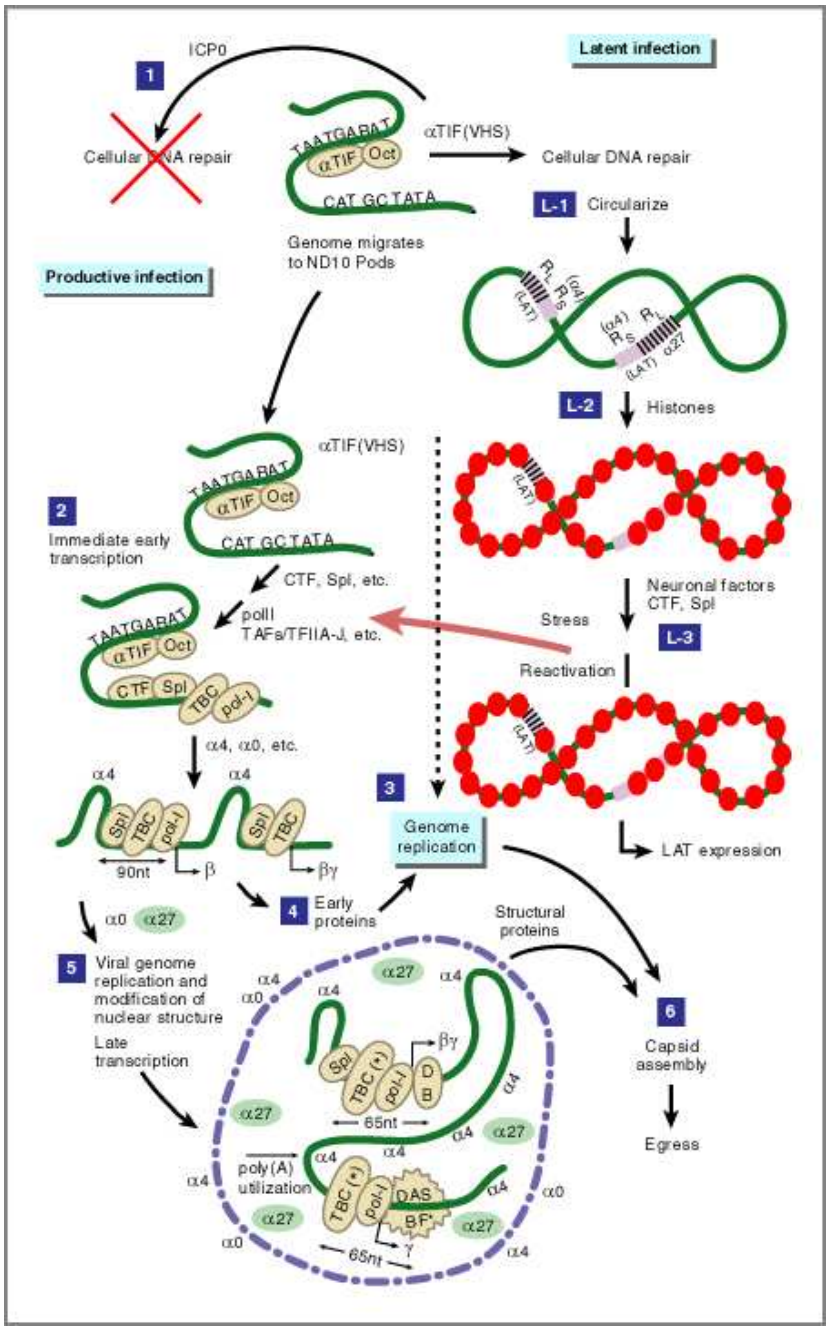

Replication steps in the life cycle of HSV. The replication cycle of HSV lasts less than 10 hours and invariably results in cell death (left panel). When entering neurons, the virus can also initiate latent infection than can end in reactivation (right panel) and achievement of the cell cycle (Frampton et al., 2005). In the case of replication cycle, the first genes expressed are the immediate-early (α) genes that “prime” the cell for further viral gene expression and mobilize the host transcriptional machinery. This

activation results in the expression of early or β genes encoding proteins implicated in viral DNA replication. Some of these proteins are involved in increasing the deoxyribonucleotide pool of the cell while others appears to act as repair enzymes of the newly synthesized DNA. Following the start of DNA replication, early expression is significantly reduced and late (γ) genes begin to be expressed at high levels. These γ genes are primarily encoding structural components of the virion such as the capsid forming proteins. Capsids are produced in the host cell nucleus where they are packaged with the viral DNA before being release into the cytoplasm. Subsequently, capsids will be enveloped to form mature virions (Homa and Brown, 1997).

6. REFERENCES

Adell A, Celada P, Artigas F (2001) The role of 5-HT1B receptors in the regulation of serotonin cell firing and release in the rat brain. J Neurochem 79:172-182.

Adham N, Romanienko P, Hartig P, Weinshank RL, Branchek T (1992) The rat 5-hydroxytryptamine1B receptor is the species homologue of the human 5-hydroxytryptamine1D beta receptor. Mol Pharmacol 41:1-7.

Aguirre N, Galbete JL, Lasheras B, Del Rio J (1995) Methylenedioxymethamphetamine induces opposite changes in central pre- and postsynaptic 5-HT1A receptors in rats. Eur J Pharmacol 281:101-105.

Albrecht C, Bloss HG, Jackisch R, Feuerstein TJ (1999) Evaluation of autoreceptor-mediated control of [(3)H]acetylcholine release in rat and human neocortex. Exp Brain Research 128:383-389.

Alex KD, Pehek EA (2007) Pharmacologic mechanisms of serotonergic regulation of dopamine neurotransmission. Pharmacol Ther 113:296-320.

Alonso A, Kohler C (1982) Evidence for separate projections of hippocampal pyramidal and non-pyramidal neurons to different parts of the septum in the rat brain. Neurosci Lett 31:209-214.

Alonso A, Kohler C (1984) A study of the reciprocal connections between the septum and the entorhinal area using anterograde and retrograde axonal transport methods in the rat brain. J Comp Neurol 225:327-343.

Amaral DG, Kurz J (1985) An analysis of the origins of the cholinergic and noncholinergic septal projections to the hippocampal formation of the rat. J Comp Neurol 240:37-59.

Amaral DG, Witter MP (1995) Hippocampal formation. New York: Academic Press.

Ando RD, Benko A, Ferrington L, Kirilly E, Kelly PA, Bagdy G (2006) Partial lesion of the serotonergic system by a single dose of MDMA results in behavioural disinhibition and enhances acute MDMA-induced social behaviour on the social interaction test. Neuropharmacology 50:884-896.

Arduino PG, Porter SR (2006) Oral and perioral herpes simplex virus type 1 (HSV-1) infection: review of its management. Oral Dis 12:254-270.

Arendt T (1994) Impairment in memory function and neurodegenerative changes in the cholinergic basal forebrain system induced by chronic intake of ethanol. J Neural Transm Suppl 44:173-187.

Arrue A, Ruiz-Ortega JA, Ugedo L, Giralt MT (2003) Short-term effects of 3,4-methylenedioximethamphetamine on noradrenergic activity in locus coeruleus and hippocampus of the rat. Neurosci Lett 337:123-126.

Badawy AA (1999) Tryptophan metabolism in alcoholism. Adv Exp Med Biol 467:265-274.

Bagdy E, Kiraly I, Harsing LG, Jr. (2000) Reciprocal innervation between serotonergic and GABAergic neurons in raphe nuclei of the rat. Neurochem Res 25:1465-1473.

Bahr BA, Neve RL, Sharp J, Geller AI, Lynch G (1994) Rapid and stable gene expression in hippocampal slice cultures from a defective HSV-1 vector. Brain Res Mol Brain Res 26:277-285.

Bankiewicz KS, Eberling JL, Kohutnicka M, Jagust W, Pivirotto P, Bringas J, Cunningham J, Budinger TF, Harvey-White J (2000) Convection-enhanced delivery of AAV vector in parkinsonian monkeys; in vivo detection of gene expression and restoration of dopaminergic function using pro-drug approach. Exp Neurol 164:2-14.

Bankson MG, Cunningham KA (2001) 3,4-Methylenedioxymethamphetamine (MDMA) as a unique model of serotonin receptor function and serotonin-dopamine interactions. J Pharmacol Exp Ther 297:846-852.

Bankson MG, Cunningham KA (2002) Pharmacological studies of the acute effects of (+)-3,4-methylenedioxymethamphetamine on locomotor activity: role of 5-HT(1B/1D) and 5-HT(2) receptors. Neuropsychopharmacology 26:40-52.

Barnes NM, Sharp T (1999) A review of central 5-HT receptors and their function. Neuropharmacology 38:1083-1152.

Barot SK, Ferguson SM, Neumaier JF (2007) 5-HT(1b) receptors in nucleus accumbens efferents enhance both rewarding and aversive effects of cocaine. Eur J Neurosci 25:3125-3131.

Battaglia G, Yeh SY, De Souza EB (1988a) MDMA-induced neurotoxicity: parameters of degeneration and recovery of brain serotonin neurons. Pharmacol Biochem Behav 29:269-274.

Battaglia G, Brooks BP, Kulsakdinun C, De Souza EB (1988b) Pharmacologic profile of MDMA (3,4-methylenedioxymethamphetamine) at various brain recognition sites. Eur J Pharmacol 149:159-163.

Battaglia G, Sharkey J, Kuhar MJ, de Souza EB (1991) Neuroanatomic specificity and time course of alterations in rat brain serotonergic pathways induced by MDMA (3,4-methylenedioxymethamphetamine): assessment using quantitative autoradiography. Synapse 8:249-260.

Battaglia G, Yeh SY, O'Hearn E, Molliver ME, Kuhar MJ, De Souza EB (1987) 3,4-Methylenedioxymethamphetamine and 3,4-methylenedioxyamphetamine destroy serotonin terminals in rat brain: quantification of neurodegeneration by measurement of [3H]paroxetine-labeled serotonin uptake sites. J Pharmacol Exp Ther 242:911-916.

Baumann MH, Wang X, Rothman RB (2007) 3,4-Methylenedioxymethamphetamine (MDMA) neurotoxicity in rats: a reappraisal of past and present findings. Psychopharmacology (Berl) 189:407-424.

Benloucif S, Galloway MP (1991) Facilitation of dopamine release in vivo by serotonin agonists: studies with microdialysis. Eur J Pharmacol 200:1-8.

Benloucif S, Keegan MJ, Galloway MP (1993) Serotonin-facilitated dopamine release in vivo: pharmacological characterization. J Pharmacol Exp Ther 265:373-377.

Bennett MK (1997) Ca2+ and the regulation of neurotransmitter secretion. Curr Opin Neurobiol 7:316-322.

Beracochea D, Jaffard R (1991) Effects of chronic ethanol consumption associated or not with experimental anterior thalamic lesions on spontaneous sequential alternation in mice. Neurosci Lett 134:45-48.

Berger UV, Gu XF, Azmitia EC (1992) The substituted amphetamines 3,4-methylenedioxymethamphetamine, methamphetamine, p-chloroamphetamine and fenfluramine induce 5-hydroxytryptamine release via a common mechanism blocked by fluoxetine and cocaine. Eur J Pharmacol 215:153-160.

Berridge MJ (1998) Neuronal calcium signaling. Neuron 21:13-26.

Birthelmer A, Stemmelin J, Jackisch R, Cassel JC (2003a) Presynaptic modulation of acetylcholine, noradrenaline, and serotonin release in the hippocampus of aged rats with various levels of memory impairments. Brain Res Bull 60:283-296.

Birthelmer A, Stemmelin J, Jackisch R, Cassel JC (2003b) Presynaptic modulation of acetylcholine, noradrenaline, and serotonin release in the hippocampus of aged rats with various levels of memory impairments. Brain Res Bull 60:283-296.

Birthelmer A, Schweizer T, Jeltsch H, Jackisch R, Cassel JC (2002) 5,7-Dihydroxytryptamine lesions enhance and serotonergic grafts normalize the evoked overflow of acetylcholine in rat hippocampal slices. Eur J Neurosci 16:1839-1849.

Birthelmer A, Lazaris A, Schweizer T, Jackisch R, Cassel JC (2003c) Presynaptic regulation of neurotransmitter release in the cortex of aged rats with differential memory impairments. Pharmacol Biochem Behav 75:147-162.

Birthelmer A, Lazaris A, Schweizer T, Jackisch R, Cassel JC (2003d) Presynaptic regulation of neurotransmitter release in the cortex of aged rats with differential memory impairments. Pharmacol Biochem Behav 75:147-162.

Birthelmer A, Ehret A, Riegert C, Rothmaier AK, Leemhuis J, Jackisch R (2007) Modulation of electrically evoked serotonin release in cultured rat raphe neurons. J Neurochem 100:1613-1625.

Birthelmer A, Ehret A, Amtage F, Forster S, Lehmann O, Jeltsch H, Cassel JC, Jackisch R (2003e) Neurotransmitter release and its presynaptic modulation in the rat hippocampus after selective damage to cholinergic or/and serotonergic afferents. Brain Res Bull 59:371-381.

Birthelmer A, Ehret A, Amtage F, Forster S, Lehmann O, Jeltsch H, Cassel JC, Jackisch R (2003f) Neurotransmitter release and its presynaptic modulation in the rat hippocampus after selective damage to cholinergic or/and serotonergic afferents. Brain Res Bull 59:371-381.

Blesch A, Lu P, Tuszynski MH (2002) Neurotrophic factors, gene therapy, and neural stem cells for spinal cord repair. Brain Res Bull 57:833-838.

Blessing WW, Seaman B (2003) 5-hydroxytryptamine(2A) receptors regulate sympathetic nerves constricting the cutaneous vascular bed in rabbits and rats. Neuroscience 117:939-948.

Blier P, Pineyro G, el Mansari M, Bergeron R, de Montigny C (1998) Role of somatodendritic 5-HT autoreceptors in modulating 5-HT neurotransmission. Ann N Y Acad Sci 861:204-216.

Bobker DH, Williams JT (1989) Serotonin agonists inhibit synaptic potentials in the rat locus ceruleus in vitro via 5-hydroxytryptamine1A and 5-hydroxytryptamine1B receptors. J Pharmacol Exp Ther 250:37-43.

Boehm S, Kubista H (2002) Fine tuning of sympathetic transmitter release via ionotropic and metabotropic presynaptic receptors. Pharmacol Rev 54:43-99.

Boehm SL, 2nd, Schafer GL, Phillips TJ, Browman KE, Crabbe JC (2000) Sensitivity to ethanol-induced motor incoordination in 5-HT(1B) receptor null mutant mice is task-dependent: implications for behavioral assessment of genetically altered mice. Behav Neurosci 114:401-409.

Boeijinga PH, Boddeke HW (1993) Serotonergic modulation of neurotransmission in the rat subicular cortex in vitro: a role for 5-HT_{1B} receptors. Naunyn Schmiedebergs Arch Pharmacol 348:553-557.

Boess FG, Martin IL (1994) Molecular biology of 5-HT receptors. Neuropharmacology 33:275-317.

Bolanos-Jimenez F, de Castro RM, Fillion G (1993) Antagonism by citalopram and tianeptine of presynaptic 5-HT1B heteroreceptors inhibiting acetylcholine release. Eur J Pharmacol 242:1-6.

Bolanos-Jimenez F, Manhaes de Castro R, Fillion G (1994) Effect of chronic antidepressant treatment on 5-HT1B presynaptic heteroreceptors inhibiting acetylcholine release. Neuropharmacology 33:77-81.

Bolanos F, Fillion G (1989) Minaprine antagonises the serotonergic inhibitory effect of trifluoromethylphenylpiperazine (TFMPP) on acetylcholine release. Eur J Pharmacol 168:87-92.

Bolla KI, McCann UD, Ricaurte GA (1998) Memory impairment in abstinent MDMA ("Ecstasy") users. Neurology 51:1532-1537.

Bommert K, Charlton MP, DeBello WM, Chin GJ, Betz H, Augustine GJ (1993) Inhibition of neurotransmitter release by C2-domain peptides implicates synaptotagmin in exocytosis. Nature 363:163-165.

Bonner TI, Buckley NJ, Young AC, Brann MR (1987) Identification of a family of muscarinic acetylcholine receptor genes. Science 237:527-532.

Boschert U, Amara DA, Segu L, Hen R (1994) The mouse 5-hydroxytryptamine1B receptor is localized predominantly on axon terminals. Neuroscience 58:167-182.

Bouhelal R, Smounya L, Bockaert J (1988) 5-HT1B receptors are negatively coupled with adenylate cyclase in rat substantia nigra. Eur J Pharmacol 151:189-196.

Bouwknecht JA, Hijzen TH, van der Gugten J, Maes RA, Hen R, Olivier B (2000) Ethanol intake is not elevated in male 5-HT(1B) receptor knockout mice. Eur J Pharmacol 403:95-98.

Bramley JR, Sollars PJ, Pickard GE, Dudek FE (2005) 5-HT1B receptor-mediated presynaptic inhibition of GABA release in the suprachiasmatic nucleus. J Neurophysiol 93:3157-3164.

Brauer K, Schober A, Wolff JR, Winkelmann E, Luppa H, Luth HJ, Bottcher H (1991) Morphology of neurons in the rat basal forebrain nuclei: comparison between NADPH-diaphorase histochemistry and immunohistochemistry of glutamic acid decarboxylase, choline acetyltransferase, somatostatin and parvalbumin. J Hirnforsch 32:1-17.

Brazell MP, Marsden CA, Nisbet AP, Routledge C (1985) The 5-HT1 receptor agonist RU-24969 decreases 5-hydroxytryptamine (5-HT) release and metabolism in the rat frontal cortex in vitro and in vivo. Br J Pharmacol 86:209-216.

Breckpot K, Aerts JL, Thielemans K (2007) Lentiviral vectors for cancer immunotherapy: transforming infectious particles into therapeutics. Gene Ther 14:847-862.

Brodie MS, Shefner SA, Dunwiddie TV (1990) Ethanol increases the firing rate of dopamine neurons of the rat ventral tegmental area in vitro. Brain Res 508:65-69.

Brodie MS, Trifunovic RD, Shefner SA (1995) Serotonin potentiates ethanol-induced excitation of ventral tegmental area neurons in brain slices from three different rat strains. J Pharmacol Exp Ther 273:1139-1146.

Brodie MS, Pesold C, Appel SB (1999) Ethanol directly excites dopaminergic ventral tegmental area reward neurons. Alcohol Clin Exp Res 23:1848-1852.

Broening HW, Morford LL, Inman-Wood SL, Fukumura M, Vorhees CV (2001) 3,4-methylenedioxymethamphetamine (ecstasy)-induced learning and memory impairments depend on the age of exposure during early development. J Neurosci 21:3228-3235.

Brooks AI, Stein CS, Hughes SM, Heth J, McCray PM, Jr., Sauter SL, Johnston JC, Cory-Slechta DA, Federoff HJ, Davidson BL (2002) Functional correction of established central nervous system deficits in an animal model of lysosomal storage disease with feline immunodeficiency virus-based vectors. Proc Natl Acad Sci U S A 99:6216-6221.

Brown L, Amedro J, Williams G, Smith D (1988) A pharmacological analysis of the rat spinal cord serotonin (5-HT) autoreceptor. Eur J Pharmacol 145:163-171.

Bruinvels AT, Landwehrmeyer B, Gustafson EL, Durkin MM, Mengod G, Branchek TA, Hoyer D, Palacios JM (1994) Localization of 5-HT1B, 5-HT1D alpha, 5-HT1E and 5-HT1F receptor messenger RNA in rodent and primate brain. Neuropharmacology 33:367-386.

Bubar MJ, Pack KM, Frankel PS, Cunningham KA (2004) Effects of dopamine D1- or D2-like receptor antagonists on the hypermotive and discriminative stimulus effects of (+)-MDMA. Psychopharmacology (Berl) 173:326-336.

Buhot M, Wolff M, Savova M, Malleret G, Hen R, Segu L (2003a) Protective effect of 5-HT1B receptor gene deletion on the age-related decline in spatial learning abilities in mice. Behav Brain Res 142:135-142.

Buhot MC (1997) Serotonin receptors in cognitive behaviors. Curr Opin Neurobiol 7:243-254.

Buhot MC, Martin S, Segu L (2000) Role of serotonin in memory impairment. Ann Med 32:210-221.

Buhot MC, Wolff M, Benhassine N, Costet P, Hen R, Segu L (2003b) Spatial learning in the 5-HT1B receptor knockout mouse: selective facilitation/impairment depending on the cognitive demand. Learn Mem 10:466-477.

Bull EJ, Hutson PH, Fone KC (2004) Decreased social behaviour following 3,4-methylenedioxymethamphetamine (MDMA) is accompanied by changes in 5-HT2A receptor responsivity. Neuropharmacology 46:202-210.

Bunney EB, Appel SB, Brodie MS (2000) Cocaine potentiates ethanol-induced excitation of dopaminergic reward neurons in the ventral tegmental area. J Pharmacol Exp Ther 293:383-389.

Bursztajn S, DeSouza R, McPhie DL, Berman SA, Shioi J, Robakis NK, Neve RL (1998) Overexpression in neurons of human presenilin-1 or a presenilin-1 familial Alzheimer disease mutant does not enhance apoptosis. J Neurosci 18:9790-9799.

Burton EA, Fink DJ, Glorioso JC (2002) Gene delivery using herpes simplex virus vectors. DNA Cell Biol 21:915-936.

Burton EA, Fink DJ, Glorioso JC (2005) Replication-defective genomic HSV gene therapy vectors: design, production and CNS applications. Curr Opin Mol Ther 7:326-336.

Burton EA, Bai Q, Goins WF, Glorioso JC (2001a) Targeting gene expression using HSV vectors. Adv Drug Deliv Rev 53:155-170.

Burton EA, Wechuck JB, Wendell SK, Goins WF, Fink DJ, Glorioso JC (2001b) Multiple applications for replication-defective herpes simplex virus vectors. Stem Cells 19:358-377.

Butler GK, Montgomery AM (2004) Impulsivity, risk taking and recreational 'ecstasy' (MDMA) use. Drug Alcohol Depend 76:55-62.

Callaway CW, Wing LL, Geyer MA (1990) Serotonin release contributes to the locomotor stimulant effects of 3,4-methylenedioxymethamphetamine in rats. J Pharmacol Exp Ther 254:456-464.

Cambridge GW, Holgate JA (1955) Superfusion as a method for the study of drug antagonism. Br J Pharmacol Chemother 10:326-335.

Cao YJ, Surowy CS, Puttfarcken PS (2005) Nicotinic acetylcholine receptor-mediated [3H]dopamine release from hippocampus. J Pharmacol Exp Ther 312:1298-1304.

Carlezon WA, Jr., Neve RL (2003) Viral-mediated gene transfer to study the behavioral correlates of CREB function in the nucleus accumbens of rats. Methods Mol Med 79:331-350.

Carlezon WA, Jr., Nestler EJ, Neve RL (2000) Herpes simplex virus-mediated gene transfer as a tool for neuropsychiatric research. Crit Rev Neurobiol 14:47-67.

Cassel JC, Jeltsch H (1995) Serotonergic modulation of cholinergic function in the central nervous system: cognitive implications. Neuroscience 69:1-41.

Cassel JC, Jeltsch H, Koenig J, Jones BC (2004) Locomotor and pyretic effects of MDMA-ethanol associations in rats. Alcohol 34:285-289.

Cassel JC, Jeltsch H, Neufang B, Lauth D, Szabo B, Jackisch R (1995a) Downregulation of muscarinic- and 5-HT1B-mediated modulation of [3H]acetylcholine release in hippocampal slices of rats with fimbria-fornix lesions and intrahippocampal grafts of septal origin. Brain Res 704:153-166.

Cassel JC, Jeltsch H, Neufang B, Lauth D, Szabo B, Jackisch R (1995b) Downregulation of muscarinic- and 5-HT_{1B}-mediated modulation of [^{3}H]acetylcholine release in hippocampal slices of rats with fimbria- fornix lesions and intrahippocampal grafts of septal origin. Brain Res 704:153-166.

Cassel JC, Riegert C, Rutz S, Koenig J, Rothmaier K, Cosquer B, Lazarus C, Birthelmer A, Jeltsch H, Jones BC, Jackisch R (2005) Ethanol, 3,4-methylenedioxymethamphetamine (ecstasy) and their combination: long-term behavioral, neurochemical and neuropharmacological effects in the rat. Neuropsychopharmacology 30:1870-1882.

Chadha A, Sur C, Atack J, Duty S (2000) The 5HT(1B) receptor agonist, CP-93129, inhibits [(3)H]-GABA release from rat globus pallidus slices and reverses akinesia following intrapallidal injection in the reserpine-treated rat. Br J Pharmacol 130:1927-1932.

Che S, Johnson M, Hanson GR, Gibb JW (1995) Body temperature effect on methylenedioxymethamphetamine-induced acute decrease in tryptophan hydroxylase activity. Eur J Pharmacol 293:447-453.

Cheetham SC, Heal DJ (1993) Evidence that RU 24969-induced locomotor activity in C57/B1/6 mice is specifically mediated by the 5-HT1B receptor. Br J Pharmacol 110:1621-1629.

Chuck TL, McLaughlin PJ, Arizzi-LaFrance MN, Salamone JD, Correa M (2006) Comparison between multiple behavioral effects of peripheral ethanol administration in rats: sedation, ataxia, and bradykinesia. Life Sci 79:154-161.

Clark MS, Neumaier JF (2001) The 5-HT1B receptor: behavioral implications. Psychopharmacol Bull 35:170-185.

Clark MS, Vincow ES, Sexton TJ, Neumaier JF (2004) Increased expression of 5-HT1B receptor in dorsal raphe nucleus decreases fear-potentiated startle in a stress dependent manner. Brain Res 1007:86-97.

Clark MS, Sexton TJ, McClain M, Root D, Kohen R, Neumaier JF (2002) Overexpression of 5-HT1B receptor in dorsal raphe nucleus using Herpes Simplex Virus gene transfer increases anxiety behavior after inescapable stress. J Neurosci 22:4550-4562.

Colado MI, Green AR (1994) A study of the mechanism of MDMA ('ecstasy')-induced neurotoxicity of 5-HT neurones using chlormethiazole, dizocilpine and other protective compounds. Br J Pharmacol 111:131-136.

Colado MI, Murray TK, Green AR (1993) 5-HT loss in rat brain following 3,4-methylenedioxymethamphetamine (MDMA), p-chloroamphetamine and fenfluramine administration and effects of chlormethiazole and dizocilpine. Br J Pharmacol 108:583-589.

Colado MI, O'Shea E, Granados R, Murray TK, Green AR (1997) In vivo evidence for free radical involvement in the degeneration of rat brain 5-HT following administration of MDMA ('ecstasy') and p-chloroamphetamine but not the degeneration following fenfluramine. Br J Pharmacol 121:889-900.

Colado MI, Granados R, O'Shea E, Esteban B, Green AR (1998) Role of hyperthermia in the protective action of clomethiazole against MDMA ('ecstasy')-induced neurodegeneration, comparison with the novel NMDA channel blocker AR-R15896AR. Br J Pharmacol 124:479-484.

Colado MI, O'Shea E, Esteban B, Granados R, Green AR (1999a) In vivo evidence against clomethiazole being neuroprotective against MDMA ('ecstasy')-induced degeneration of rat brain 5-HT nerve terminals by a free radical scavenging mechanism. Neuropharmacology 38:307-314.

Colado MI, O'Shea E, Granados R, Esteban B, Martin AB, Green AR (1999b) Studies on the role of dopamine in the degeneration of 5-HT nerve endings in the brain of Dark Agouti rats following 3,4-methylenedioxymethamphetamine (MDMA or 'ecstasy') administration. Br J Pharmacol 126:911-924.

Conner JM, Darracq MA, Roberts J, Tuszynski MH (2001) Nontropic actions of neurotrophins: subcortical nerve growth factor gene delivery reverses age-related degeneration of primate cortical cholinergic innervation. Proc Natl Acad Sci U S A 98:1941-1946.

Connor TJ, McNamara MG, Finn D, Currid A, O'Malley M, Redmond AM, Kelly JP, Leonard BE (1998) Acute 3,4-methylenedioxymethamphetamine(MDMA) administration produces a rapid and sustained suppression of immune function in the rat. Immunopharmacology 38:253-260.

Conrad LC, Leonard CM, Pfaff DW (1974) Connections of the median and dorsal raphe nuclei in the rat: an autoradiographic and degeneration study. J Comp Neurol 156:179-205.

Consolo S, Arnaboldi S, Giorgi S, Russi G, Ladinsky H (1994a) 5-HT4 receptor stimulation facilitates acetylcholine release in rat frontal cortex. Neuroreport 5:1230-1232.

Consolo S, Bertorelli R, Russi G, Zambelli M, Ladinsky H (1994b) Serotonergic facilitation of acetylcholine release in vivo from rat dorsal hippocampus via serotonin 5-HT3 receptors. J Neurochem 62:2254-2261.

Consolo S, Arnaboldi S, Ramponi S, Nannini L, Ladinsky H, Baldi G (1996) Endogenous serotonin facilitates in vivo acetylcholine release in rat frontal cortex through 5-HT 1B receptors. J Pharmacol Exp Ther 277:823-830.

Crabbe JC, Wahlsten D, Dudek BC (1999) Genetics of mouse behavior: interactions with laboratory environment. Science 284:1670-1672.

Crabbe JC, Phillips TJ, Feller DJ, Hen R, Wenger CD, Lessov CN, Schafer GL (1996) Elevated alcohol consumption in null mutant mice lacking 5-HT1B serotonin receptors. Nat Genet 14:98-101.

Crespi D, Mennini T, Gobbi M (1997) Carrier-dependent and Ca(2+)-dependent 5-HT and dopamine release induced by (+)-amphetamine, 3,4-methylendioxymethamphetamine, p-chloroamphetamine and (+)-fenfluramine. Br J Pharmacol 121:1735-1743.

Crews FT, Braun CJ, Hoplight B, Switzer RC, 3rd, Knapp DJ (2000) Binge ethanol consumption causes differential brain damage in young adolescent rats compared with adult rats. Alcohol Clin Exp Res 24:1712-1723.

Cullinan WE, Zaborszky L (1991) Organization of ascending hypothalamic projections to the rostral forebrain with special reference to the innervation of cholinergic projection neurons. J Comp Neurol 306:631-667.

Dafters RI (1994) Effect of ambient temperature on hyperthermia and hyperkinesis induced by 3,4-methylenedioxymethamphetamine (MDMA or "ecstasy") in rats. Psychopharmacology (Berl) 114:505-508.

Dafters RI, Lynch E (1998) Persistent loss of thermoregulation in the rat induced by 3,4-methylenedioxymethamphetamine (MDMA or "Ecstasy") but not by fenfluramine. Psychopharmacology (Berl) 138:207-212.

Darstein M, Albrecht C, Lopez-Francos L, Knorle R, Holter SM, Spanagel R, Feuerstein TJ (1998) Release and accumulation of neurotransmitters in the rat brain: acute effects of ethanol in vitro and effects of long-term voluntary ethanol intake. Alcohol Clin Exp Res 22:704-709.

Davidson BL, Breakefield XO (2003) Viral vectors for gene delivery to the nervous system. Nat Rev Neurosci 4:353-364.

Daws LC, Irvine RJ, Callaghan PD, Toop NP, White JM, Bochner F (2000) Differential behavioural and neurochemical effects of para-methoxyamphetamine and 3,4-methylenedioxymethamphetamine in the rat. Prog Neuropsychopharmacol Biol Psychiatry 24:955-977.

De Deurwaerdere P, Navailles S, Berg KA, Clarke WP, Spampinato U (2004) Constitutive activity of the serotonin2C receptor inhibits in vivo dopamine release in the rat striatum and nucleus accumbens. J Neurosci 24:3235-3241.

de la Torre R, Farre M (2004) Neurotoxicity of MDMA (ecstasy): the limitations of scaling from animals to humans. Trends Pharmacol Sci 25:505-508.

De Waard M, Liu H, Walker D, Scott VE, Gurnett CA, Campbell KP (1997) Direct binding of G-protein betagamma complex to voltage-dependent calcium channels. Nature 385:446-450.

Devroe E, Silver PA (2002) Retrovirus-delivered siRNA. BMC Biotechnol 2:15.

Di Chiara G, Imperato A (1988) Drugs abused by humans preferentially increase synaptic dopamine concentrations in the mesolimbic system of freely moving rats. Proc Natl Acad Sci U S A 85:5274-5278.

Divito S, Cherpes TL, Hendricks RL (2006) A triple entente: virus, neurons, and CD8+ T cells maintain HSV-1 latency. Immunol Res 36:119-126.

Dohner K, Radtke K, Schmidt S, Sodeik B (2006) Eclipse phase of herpes simplex virus type 1 infection: Efficient dynein-mediated capsid transport without the small capsid protein VP26. J Virol 80:8211-8224.

Dotti CG, Simons K (1990) Polarized sorting of viral glycoproteins to the axon and dendrites of hippocampal neurons in culture. Cell 62:63-72.

Dunnett SB, Björklund A (1992) Staging and dissection of rat embryos. In: Neural transplantation. A practical approach. (Dunnett SB, Björklund A, eds), pp 1-19. Oxford: IRL Press.

Dutar P, Lamour Y, Jobert A (1985) Activation of identified septo-hippocampal neurons by noxious peripheral stimulation. Brain Res 328:15-21.

Easton N, Marsden CA (2006) Ecstasy: are animal data consistent between species and can they translate to humans? J Psychopharmacol 20:194-210.

Ehret A, Haaf A, Jeltsch H, Heimrich B, Feuerstein TJ, Jackisch R (2001) Modulation of electrically evoked acetylcholine release in cultured rat septal neurones. J Neurochem 76:555-564.

Ehret A, Birthelmer A, Rutz S, Riegert C, Rothmaier AK, Jackisch R (2007a) Agonist-mediated regulation of presynaptic receptor function during development of rat septal neurons in culture. J Neurochem.

Ehret A, Birthelmer A, Rutz S, Riegert C, Rothmaier AK, Jackisch R (2007b) Agonist-mediated regulation of presynaptic receptor function during development of rat septal neurons in culture. J Neurochem 102:1071-1082.

Elliger SS, Elliger CA, Aguilar CP, Raju NR, Watson GL (1999) Elimination of lysosomal storage in brains of MPS VII mice treated by intrathecal administration of an adeno-associated virus vector. Gene Ther 6:1175-1178.

Engel G, Gothert M, Hoyer D, Schlicker E, Hillenbrand K (1986) Identity of inhibitory presynaptic 5-hydroxytryptamine (5-HT) autoreceptors in the rat brain cortex with 5-HT1B binding sites. Naunyn Schmiedebergs Arch Pharmacol 332:1-7.

Erb C, Klein J, Koppen A, Loffelholz K, Jeltsch H, Cassel JC (1997) Modulation of hippocampal acetylcholine release after fimbria-fornix lesions and septal transplantation in rats. Neurosci Lett 231:5-8.

Esteban B, O'Shea E, Camarero J, Sanchez V, Green AR, Colado MI (2001) 3,4-Methylenedioxymethamphetamine induces monoamine release, but not toxicity, when administered centrally at a concentration occurring following a peripherally injected neurotoxic dose. Psychopharmacology (Berl) 154:251-260.

Esteban S, Moranta D, Sastre-Coll A, Miralles A, Garcia-Sevilla JA (2002) Withdrawal from chronic ethanol increases the sensitivity of presynaptic 5-HT(1A) receptors modulating serotonin and dopamine synthesis in rat brain in vivo. Neurosci Lett 326:121-124.

Evrard A, Laporte AM, Chastanet M, Hen R, Hamon M, Adrien J (1999) 5-HT1A and 5-HT1B receptors control the firing of serotoninergic neurons in the dorsal raphe nucleus of the mouse: studies in 5-HT1B knock-out mice. Eur J Neurosci 11:3823-3831.

Farkas RH, Nakajima S, Nakajima Y (1994) Cultured neurons infected with an HSV-1-derived vector remain electrically excitable and responsive to neurotransmitter. Neurosci Lett 165:153-156.

Farnebo LO, Hamberger B (1971) Drug-induced changes in the release of 3 H-monoamines from field stimulated rat brain slices. Acta Physiol Scand Suppl 371:35-44.

Feuerstein TJ, Gleichauf O, Landwehrmeyer GB (1996a) Modulation of cortical acetylcholine release by serotonin: the role of substance P interneurons. Naunyn Schmiedebergs Arch Pharmacol 354:618-626.

Feuerstein TJ, Gleichauf O, Landwehrmeyer GB (1996b) Modulation of cortical acetylcholine release by serotonin: the role of substance P interneurons. Naunyn-Schmiedbergs Arch Pharmacol 354:618-626.

Feuerstein TJ, Gleichauf O, Landwehrmeyer BG (1996c) Dual control by 5-HT terminals and by SP interneurons of neocortical acetylcholine release.

Feuerstein TJ, Lehmann J, Sauermann W, van Velthoven V, Jackisch R (1992) The autoinhibitory feedback control of acetylcholine release in human neocortex tissue. Brain Research 572:64-71.

Feuerstein TJ, Gleichauf O, Peckys D, Landwehrmeyer GB, Scheremet R, Jackisch R (1996d) Opioid receptor-mediated control of acetylcholine release in human neocortex tissue. Naunyn Schmiedebergs Arch Pharmacol 354:586-592.

File SE, Andrews N, al-Farhan M (1993) Anxiogenic responses of rats on withdrawal from chronic ethanol treatment: effects of tianeptine. Alcohol Alcohol 28:281-286.

Fillion G, Beaudoin D, Rousselle JC, Deniau JM, Fillion MP, Dray F, Jacob J (1979) Decrease of [3H]5-HT high affinity binding and 5-HT adenylate cyclase activation after kainic acic lesion in rat brain striatum. J Neurochem 33:567-570.

Fink DJ, DeLuca NA, Goins WF, Glorioso JC (1996) Gene transfer to neurons using herpes simplex virus-based vectors. Annu Rev Neurosci 19:265-287.

Fitzgerald JL, Reid JJ (1990) Effects of methylenedioxymethamphetamine on the release of monoamines from rat brain slices. Eur J Pharmacol 191:217-220.

Fletcher PJ, Sinyard J, Higgins GA (2006) The effects of the 5-HT(2C) receptor antagonist SB242084 on locomotor activity induced by selective, or mixed, indirect serotonergic and dopaminergic agonists. Psychopharmacology (Berl) 187:515-525.

Fletcher PJ, Korth KM, Robinson SR, Baker GB (2002) Multiple 5-HT receptors are involved in the effects of acute MDMA treatment: studies on locomotor activity and responding for conditioned reinforcement. Psychopharmacology (Berl) 162:282-291.

Fraefel C, Song S, Lim F, Lang P, Yu L, Wang Y, Wild P, Geller AI (1996) Helper virus-free transfer of herpes simplex virus type 1 plasmid vectors into neural cells. J Virol 70:7190-7197.

Frampton AR, Jr., Goins WF, Nakano K, Burton EA, Glorioso JC (2005) HSV trafficking and development of gene therapy vectors with applications in the nervous system. Gene Ther 12:891-901.

Freedman RR, Johanson CE, Tancer ME (2005) Thermoregulatory effects of 3,4-methylenedioxymethamphetamine (MDMA) in humans. Psychopharmacology (Berl) 183:248-256.

Frei E, Gamma A, Pascual-Marqui R, Lehmann D, Hell D, Vollenweider FX (2001) Localization of MDMA-induced brain activity in healthy volunteers using low resolution brain electromagnetic tomography (LORETA). Hum Brain Mapp 14:152-165.

Freund TF (1989) GABAergic septohippocampal neurons contain parvalbumin. Brain Res 478:375-381.

Freund TF (1992) GABAergic septal and serotonergic median raphe afferents preferentially innervate inhibitory interneurons in the hippocampus and dentate gyrus. Epilepsy Res Suppl 7:79-91.

Freund TF, Antal M (1988) GABA-containing neurons in the septum control inhibitory interneurons in the hippocampus. Nature 336:170-173.

Freund TF, Buzsaki G (1996) Interneurons of the hippocampus. Hippocampus 6:347-470.

Freund TF, Gulyas AI, Acsady L, Gorcs T, Toth K (1990) Serotonergic control of the hippocampus via local inhibitory interneurons. Proc Natl Acad Sci U S A 87:8501-8505.

Friedman E, Wang HY (1988) Effect of chronic lithium treatment on 5-hydroxytryptamine autoreceptors and release of 5-[3H]hydroxytryptamine from rat brain cortical, hippocampal, and hypothalamic slices [published erratum appears in J Neurochem 1990 Apr;54(4)):1456]. J Neurochem 50:195-201.

Frotscher M, Leranth C (1985) Cholinergic innervation of the rat hippocampus as revealed by choline acetyltransferase immunocytochemistry: a combined light and electron microscopic study. J Comp Neurol 239:237-246.

Fujii T, Yoshizawa M, Nakai K, Fujimoto K, Suzuki T, Kawashima K (1997) Demonstration of the facilitatory role of 8-OH-DPAT on cholinergic transmission in the rat hippocampus using in vivo microdialysis. Brain Res 761:244-249.

Gaddum JH (1953) The technique of superfusion. Br J Pharmacol Chemother 8:321-326.

Gage FH, Bjorklund A, Stenevi U (1983) Reinnervation of the partially deafferented hippocampus by compensatory collateral sprouting from spared cholinergic and noradrenergic afferents. Brain Res 268:27-37.

Gall C, Moore RY (1984) Distribution of enkephalin, substance P, tyrosine hydroxylase, and 5-hydroxytryptamine immunoreactivity in the septal region of the rat. J Comp Neurol 225:212-227.

Gallate JE, Morley KC, Ambermoon P, McGregor IS (2003) The consequences of beer consumption in rats: acute anxiolytic and ataxic effects and withdrawal-induced anxiety. Psychopharmacology (Berl) 166:51-60.

Galloway MP, Suchowski CS, Keegan MJ, Hjorth S (1993) Local infusion of the selective 5HT-1b agonist CP-93,129 facilitates striatal dopamine release in vivo. Synapse 15:90-92.

Gamma A, Buck A, Berthold T, Liechti ME, Vollenweider FX (2000) 3,4-Methylenedioxymethamphetamine (MDMA) modulates cortical and limbic brain activity as measured by [H(2)(15)O]-PET in healthy humans. Neuropsychopharmacology 23:388-395.

Gandhi SP, Stevens CF (2003) Three modes of synaptic vesicular recycling revealed by single-vesicle imaging. Nature 423:607-613.

Gardier AM, Gruwez B, Trillat AC, Jacquot C, Hen R, Bourin M (2001) Interaction between 5-HT(1A) and 5-HT(1B) receptors: effects of 8-OH-DPAT-induced hypothermia in 5-HT(1B) receptor knockout mice. Eur J Pharmacol 421:171-175.

Gartside SE, McQuade R, Sharp T (1996) Effects of repeated administration of 3,4-methylenedioxymethamphetamine on 5-hydroxytryptamine neuronal activity and release in the rat brain in vivo. J Pharmacol Exp Ther 279:277-283.

Gartside SE, McQuade R, Sharp T (1997) Acute effects of 3,4-methylenedioxymethamphetamine (MDMA) on 5-HT cell firing and release: comparison between dorsal and median raphe 5-HT systems. Neuropharmacology 36:1697-1703.

Gaspar P, Cases O, Maroteaux L (2003) The developmental role of serotonin: news from mouse molecular genetics. Nat Rev Neurosci 4:1002-1012.

Gaykema RP, Luiten PG, Nyakas C, Traber J (1990) Cortical projection patterns of the medial septum-diagonal band complex. J Comp Neurol 293:103-124.

Gaykema RP, van der Kuil J, Hersh LB, Luiten PG (1991) Patterns of direct projections from the hippocampus to the medial septum-diagonal band complex: anterograde tracing with Phaseolus vulgaris leucoagglutinin combined with immunohistochemistry of choline acetyltransferase. Neuroscience 43:349-360.

Gazyakan E, Hennegriff M, Haaf A, Landwehrmeyer GB, Feuerstein TJ, Jackisch R (2000) Characterization of opioid receptor types modulating acetylcholine release in septal regions of the rat brain. Naunyn Schmiedebergs Arch Pharmacol 362:32-40.

Geller AI, Freese A (1990) Infection of cultured central nervous system neurons with a defective herpes simplex virus 1 vector results in stable expression of Escherichia coli beta-galactosidase. Proc Natl Acad Sci U S A 87:1149-1153.

Geller AI, During MJ, Haycock JW, Freese A, Neve R (1993) Long-term increases in neurotransmitter release from neuronal cells expressing a constitutively active adenylate cyclase from a herpes simplex virus type 1 vector. Proc Natl Acad Sci U S A 90:7603-7607.

Georgievska B, Kirik D, Bjorklund A (2002) Aberrant sprouting and downregulation of tyrosine hydroxylase in lesioned nigrostriatal dopamine neurons induced by long-lasting overexpression of glial cell line derived neurotrophic factor in the striatum by lentiviral gene transfer. Exp Neurol 177:461-474.

Geppert M, Goda Y, Hammer RE, Li C, Rosahl TW, Stevens CF, Sudhof TC (1994) Synaptotagmin I: a major Ca2+ sensor for transmitter release at a central synapse. Cell 79:717-727.

Geraghty RJ, Krummenacher C, Cohen GH, Eisenberg RJ, Spear PG (1998) Entry of alphaherpesviruses mediated by poliovirus receptor-related protein 1 and poliovirus receptor. Science 280:1618-1620.

Gerra G, Zaimovic A, Giucastro G, Maestri D, Monica C, Sartori R, Caccavari R, Delsignore R (1998) Serotonergic function after (+/-)3,4-methylene-dioxymethamphetamine ('Ecstasy') in humans. Int Clin Psychopharmacol 13:1-9.

Gerra G, Zaimovic A, Ferri M, Zambelli U, Timpano M, Neri E, Marzocchi GF, Delsignore R, Brambilla F (2000) Long-lasting effects of (+/-)3,4-methylenedioxymethamphetamine (ecstasy) on serotonin system function in humans. Biol Psychiatry 47:127-136.

Gessa GL, Muntoni F, Collu M, Vargiu L, Mereu G (1985) Low doses of ethanol activate dopaminergic neurons in the ventral tegmental area. Brain Res 348:201-203.

Geula C, Schatz CR, Mesulam MM (1993) Differential localization of NADPH-diaphorase and calbindin-D28k within the cholinergic neurons of the basal forebrain, striatum and brainstem in the rat, monkey, baboon and human. Neuroscience 54:461-476.

Ghavami A, Stark KL, Jareb M, Ramboz S, Segu L, Hen R (1999) Differential addressing of 5-HT1A and 5-HT1B receptors in epithelial cells and neurons. J Cell Sci 112 (Pt 6):967-976.

Ghodsi A, Stein C, Derksen T, Martins I, Anderson RD, Davidson BL (1999) Systemic hyperosmolality improves beta-glucuronidase distribution and pathology in murine MPS VII brain following intraventricular gene transfer. Exp Neurol 160:109-116.

Gingrich JA, Hen R (2001) Dissecting the role of the serotonin system in neuropsychiatric disorders using knockout mice. Psychopharmacology (Berl) 155:1-10.

Givens B (1995) Low doses of ethanol impair spatial working memory and reduce hippocampal theta activity. Alcohol Clin Exp Res 19:763-767.

Glorioso JC, Fink DJ (2004) Herpes vector-mediated gene transfer in treatment of diseases of the nervous system. Annu Rev Microbiol 58:253-271.

Glorioso JC, DeLuca NA, Fink DJ (1995) Development and application of herpes simplex virus vectors for human gene therapy. Annu Rev Microbiol 49:675-710.

Gobert A, Rivet JM, Audinot V, Newman-Tancredi A, Cistarelli L, Millan MJ (1998) Simultaneous quantification of serotonin, dopamine and noradrenaline levels in single frontal cortex dialysates of freely-moving rats reveals a complex pattern of reciprocal auto- and heteroreceptor-mediated control of release. Neuroscience 84:413-429.

Goins WF, Wolfe D, Krisky DM, Bai Q, Burton EA, Fink DJ, Glorioso JC (2004) Delivery using herpes simplex virus: an overview. Methods Mol Biol 246:257-299.

Gold LH, Hubner CB, Koob GF (1989) A role for the mesolimbic dopamine system in the psychostimulant actions of MDMA. Psychopharmacology (Berl) 99:40-47.

Goni-Allo B, Ramos M, Herv'as I, Lasheras B, Aguirre N (2006) Studies on striatal neurotoxicity caused by the 3,4-methylenedioxymethamphetamine/ malonate combination: implications for serotonin/dopamine interactions. J Psychopharmacol 20:245-256.

Gorwood P, Aissi F, Batel P, Ades J, Cohen-Salmon C, Hamon M, Boni C, Lanfumey L (2002) Reappraisal of the serotonin 5-HT(1B) receptor gene in alcoholism: of mice and men. Brain Res Bull 57:103-107.

Göthert M (1986) Presynaptic 5-HT autoreceptors and the modulation of the release of 5- HT. Clin Neuropharmacol 9:308-310.

Göthert M (1990) Presynaptic serotonin receptors in the central nervous system. Ann N Y Acad Sci 604:102-112.

Göthert M, Weinheimer G (1979) Extracellular 5-hydroxytryptamine inhibits 5-hydroxytryptamine release from rat brain cortex slices. Naunyn Schmiedebergs Arch Pharmacol 310:93-96.

Göthert M, Schlicker E (1993) Relevance of 5-HT autoreceptors for psychotropic drug action. Psychopharmacol Ser 10:38-51.

Göthert M, Schlicker E, Kollecker P (1986) Receptor-mediated effects of serotonin and 5-methoxytryptamine on noradrenaline release in the rat vena cava and in the heart of the pithed rat. Naunyn Schmiedebergs Arch Pharmacol 332:124-130.

Göthert M, Schlicker E, Fink K, Classen K (1987) Effects of RU 24969 on serotonin release in rat brain cortex: further support for the identity of serotonin autoreceptors with 5-HT1B sites. Arch Int Pharmacodyn Ther 288:31-42.

Gouzoulis-Mayfrank E, Daumann J (2006) The confounding problem of polydrug use in recreational ecstasy/MDMA users: a brief overview. J Psychopharmacol 20:188-193.

Graat HC, Carette JE, Schagen FH, Vassilev LT, Gerritsen WR, Kaspers GJ, Wuisman PI, van Beusechem VW (2007) Enhanced tumor cell kill by combined treatment with a small-molecule antagonist of mouse double minute 2 and adenoviruses encoding p53. Mol Cancer Ther 6:1552-1561.

Grady S, Marks MJ, Wonnacott S, Collins AC (1992) Characterization of nicotinic receptor-mediated [3H]dopamine release from synaptosomes prepared from mouse striatum. J Neurochem 59:848-856.

Grady SR, Marks MJ, Collins AC (1994) Desensitization of nicotine-stimulated [3H]dopamine release from mouse striatal synaptosomes. J Neurochem 62:1390-1398.

Grady SR, Murphy KL, Cao J, Marks MJ, McIntosh JM, Collins AC (2002) Characterization of nicotinic agonist-induced [(3)H]dopamine release from synaptosomes prepared from four mouse brain regions. J Pharmacol Exp Ther 301:651-660.

Graham FL, van der Eb AJ (1973a) A new technique for the assay of infectivity of human adenovirus 5 DNA. Virology 52:456-467.

Graham FL, van der Eb AJ (1973b) Transformation of rat cells by DNA of human adenovirus 5. Virology 54:536-539.

Grant KA, Colombo G (1993) Substitution of the 5-HT1 agonist trifluoromethylphenylpiperazine (TFMPP) for the discriminative stimulus effects of ethanol: effect of training dose. Psychopharmacology (Berl) 113:26-30.

Grant KA, Colombo G, Gatto GJ (1997) Characterization of the ethanol-like discriminative stimulus effects of 5-HT receptor agonists as a function of ethanol training dose. Psychopharmacology (Berl) 133:133-141.

Grant RT (1963) Vasodilation and body warming in the rat. J Physiol 167:311-317.

Greco A, Diaz JJ, Thouvenot D, Morfin F (2007) Novel targets for the development of anti-herpes compounds. Infect Disord Drug Targets 7:11-18.

Green AR, Cross AJ, Goodwin GM (1995) Review of the pharmacology and clinical pharmacology of 3,4-methylenedioxymethamphetamine (MDMA or "Ecstasy"). Psychopharmacology (Berl) 119:247-260.

Green AR, O'Shea E, Colado MI (2004) A review of the mechanisms involved in the acute MDMA (ecstasy)-induced hyperthermic response. Eur J Pharmacol 500:3-13.

Green AR, Mechan AO, Elliott JM, O'Shea E, Colado MI (2003) The pharmacology and clinical pharmacology of 3,4-methylenedioxymethamphetamine (MDMA, "ecstasy"). Pharmacol Rev 55:463-508.

Green AR, O'Shea E, Saadat KS, Elliott JM, Colado MI (2005) Studies on the effect of MDMA ('ecstasy') on the body temperature of rats housed at different ambient room temperatures. Br J Pharmacol 146:306-312.

Gritti I, Mainville L, Jones BE (1993) Codistribution of GABA- with acetylcholine-synthesizing neurons in the basal forebrain of the rat. J Comp Neurol 329:438-457.

Groenink L, van Bogaert MJ, van der Gugten J, Oosting RS, Olivier B (2003) 5-HT1A receptor and 5-HT1B receptor knockout mice in stress and anxiety paradigms. Behav Pharmacol 14:369-383.

Gruol DL, Parsons KL, DiJulio N (1997) Acute ethanol alters calcium signals elicited by glutamate receptor agonists and K+ depolarization in cultured cerebellar Purkinje neurons. Brain Res 773:82-89.

Gudelsky GA, Nash JF (1996) Carrier-mediated release of serotonin by 3,4-methylenedioxymethamphetamine: implications for serotonin-dopamine interactions. J Neurochem 66:243-249.

Gudelsky GA, Yamamoto BK, Nash JF (1994) Potentiation of 3,4-methylenedioxymethamphetamine-induced dopamine release and serotonin neurotoxicity by 5-HT2 receptor agonists. Eur J Pharmacol 264:325-330.

Gurtman CG, Morley KC, Li KM, Hunt GE, McGregor IS (2002) Increased anxiety in rats after 3,4-methylenedioxymethamphetamine: association with serotonin depletion. Eur J Pharmacol 446:89-96.

Hallbus M, Magnusson T, Magnusson O (1997) Influence of 5-HT1B/1D receptors on dopamine release in the guinea pig nucleus accumbens: a microdialysis study. Neurosci Lett 225:57-60.

Hamida SB, Bach S, Plute E, Jones BC, Kelche C, Cassel JC (2006) Ethanol-ecstasy (MDMA) interactions in rats: preserved attenuation of hyperthermia and potentiation of hyperactivity by ethanol despite prior ethanol treatment. Pharmacol Biochem Behav 84:162-168.

Harris DS, Baggott M, Mendelson JH, Mendelson JE, Jones RT (2002) Subjective and hormonal effects of 3,4-methylenedioxymethamphetamine (MDMA) in humans. Psychopharmacology (Berl) 162:396-405.

Harrison AA, Parsons LH, Koob GF, Markou A (1999) RU 24969, a 5-HT1A/1B agonist, elevates brain stimulation reward thresholds: an effect reversed by GR 127935, a 5-HT1B/1D antagonist. Psychopharmacology (Berl) 141:242-250.

Hemminki A, Zinn KR, Liu B, Chaudhuri TR, Desmond RA, Rogers BE, Barnes MN, Alvarez RD, Curiel DT (2002) In vivo molecular chemotherapy and noninvasive imaging with an infectivity-enhanced adenovirus. J Natl Cancer Inst 94:741-749.

Hernandez-Lopez C, Farre M, Roset PN, Menoyo E, Pizarro N, Ortuno J, Torrens M, Cami J, de La Torre R (2002) 3,4-Methylenedioxymethamphetamine (ecstasy) and alcohol interactions in humans: psychomotor performance, subjective effects, and pharmacokinetics. J Pharmacol Exp Ther 300:236-244.

Hertting G, Zumstein A, Jackisch R, Hoffmann I, Starke K (1980) Modulation by endogenous dopamine of the release of acetylcholine in the caudate nucleus of the rabbit. Naunyn Schmiedebergs Arch Pharmacol 315:111-117.

Hiatt ES, Brunetta PG, Seiler GR, Barney SA, Selles WD, Wooledge KH, King JC (1992) Subgroups of luteinizing hormone-releasing hormone perikarya defined by computer analyses in the basal forebrain of intact female rats. Endocrinology 130:1030-1043.

Higgins GA, Tomkins DM, Fletcher PJ, Sellers EM (1992) Effect of drugs influencing 5-HT function on ethanol drinking and feeding behaviour in rats: studies using a drinkometer system. Neurosci Biobehav Rev 16:535-552.

Ho YJ, Pawlak CR, Guo L, Schwarting RK (2004) Acute and long-term consequences of single MDMA administration in relation to individual anxiety levels in the rat. Behav Brain Res 149:135-144.

Homa FL, Brown JC (1997) Capsid assembly and DNA packaging in herpes simplex virus. Rev Med Virol 7:107-122.

Honess RW, Roizman B (1974) Regulation of herpesvirus macromolecular synthesis. I. Cascade regulation of the synthesis of three groups of viral proteins. J Virol 14:8-19.

Hoplight BJ, Sandygren NA, Neumaier JF (2006) Increased expression of 5-HT1B receptors in rat nucleus accumbens via virally mediated gene transfer increases voluntary alcohol consumption. Alcohol 38:73-79.

Hoplight BJ, Vincow ES, Neumaier JF (2007) Cocaine increases 5-HT(1B) mRNA in rat nucleus accumbens shell neurons. Neuropharmacology 52:444-449.

Hopwood SE, Stamford JA (2001) Multiple 5-HT(1) autoreceptor subtypes govern serotonin release in dorsal and median raphe nuclei. Neuropharmacology 40:508-519.

Hoyer D, Clarke DE, Fozard JR, Hartig PR, Martin GR, Mylecharane EJ, Saxena PR, Humphrey PP (1994) International Union of Pharmacology classification of receptors for 5-hydroxytryptamine (Serotonin). Pharmacol Rev 46:157-203.

Ikeda SR, Lovinger DM, McCool BA, Lewis DL (1995) Heterologous expression of metabotropic glutamate receptors in adult rat sympathetic neurons: subtype-specific coupling to ion channels. Neuron 14:1029-1038.

Inoue T, Krumlauf R (2001) An impulse to the brain--using in vivo electroporation. Nat Neurosci 4 Suppl:1156-1158.

Iyer RN, Bradberry CW (1996) Serotonin-mediated increase in prefrontal cortex dopamine release: pharmacological characterization. J Pharmacol Exp Ther 277:40-47.

Izumi J, Washizuka M, Miura N, Hiraga Y, Ikeda Y (1994) Hippocampal serotonin 5-HT1A receptor enhances acetylcholine release in conscious rats. J Neurochem 62:1804-1808.

Jackisch R, Zumstein A, Hertting G, Starke K (1980) Interneurones are probably not involved in the presynaptic dopaminergic control of dopamine release in rabbit caudate nucleus. Naunyn-Schmiedeberg's Archives of Pharmacology 314:129-133.

Jackisch R, Haaf A, Jeltsch H, Lazarus C, Kelche C, Cassel JC (1999a) Modulation of 5-hydroxytryptamine release in hippocampal slices of rats: effects of fimbria-fornix lesions on 5-HT1B-autoreceptor and alpha2-heteroreceptor function. Brain Research Bulletin 48:49-59.

Jackisch R, Haaf A, Jeltsch H, Lazarus C, Kelche C, Cassel JC (1999b) Modulation of 5-hydroxytryptamine release in hippocampal slices of rats: effects of fimbria-fornix lesions on 5-HT_{1B}-autoreceptor and $alpha_2$-heteroreceptor function. Brain Res Bull 48:49-59.

Jackisch R, Stemmelin J, Neufang B, Lauth D, Neughebauer B, Kelche C, Cassel JC (1999c) Sympathetic sprouting: no evidence for muscarinic modulation of noradrenaline release in hippocampal slices of rats with fimbria-fornix lesions. Experimental Brain Research 124:17-24.

Jackson D, Stachowiak MK, Bruno JP, Zigmond MJ (1988) Inhibition of striatal acetylcholine release by endogenous serotonin. Brain Res 457:259-266.

Jacobs BL, Azmitia EC (1992) Structure and function of the brain serotonin system. Physiol Rev 72:165-229.

Jahn R, Lang T, Sudhof TC (2003) Membrane fusion. Cell 112:519-533.

Jakab RL, Leranth C (1995) Septum. In: The Rat Nervous System (Paxinos G, ed), pp 405-442. San Diego: Academic Press.

Jin Y, Fischer I, Tessler A, Houle JD (2002) Transplants of fibroblasts genetically modified to express BDNF promote axonal regeneration from supraspinal neurons following chronic spinal cord injury. Exp Neurol 177:265-275.

Johnson EA, O'Callaghan JP, Miller DB (2004) Brain concentrations of d-MDMA are increased after stress. Psychopharmacology (Berl) 173:278-286.

Johnson M, Mitros K, Stone DM, Zobrist R, Hanson GR, Gibb JW (1992a) Effect of flunarizine and nimodipine on the decrease in tryptophan hydroxylase activity induced by methamphetamine and 3,4-methylenedioxymethamphetamine. J Pharmacol Exp Ther 261:586-591.

Johnson SW, Mercuri NB, North RA (1992b) 5-hydroxytryptamine1B receptors block the GABAB synaptic potential in rat dopamine neurons. J Neurosci 12:2000-2006.

Jolimay N, Franck L, Langlois X, Hamon M, Darmon M (2000) Dominant role of the cytosolic C-terminal domain of the rat 5-HT1B receptor in axonal-apical targeting. J Neurosci 20:9111-9118.

Kang Y, Liao WM, Yuan ZH, Sheng PY, Zhang LJ, Yuan XW, Lei L (2007) In vitro and in vivo induction of bone formation based on adeno-associated virus-mediated BMP-7 gene therapy using human adipose-derived mesenchymal stem cells. Acta Pharmacol Sin 28:839-849.

Kay MA, Glorioso JC, Naldini L (2001) Viral vectors for gene therapy: the art of turning infectious agents into vehicles of therapeutics. Nat Med 7:33-40.

Kehne JH, Ketteler HJ, McCloskey TC, Sullivan CK, Dudley MW, Schmidt CJ (1996) Effects of the selective 5-HT2A receptor antagonist MDL 100,907 on MDMA-induced locomotor stimulation in rats. Neuropsychopharmacology 15:116-124.

Kish SJ, Furukawa Y, Ang L, Vorce SP, Kalasinsky KS (2000) Striatal serotonin is depleted in brain of a human MDMA (Ecstasy) user. Neurology 55:294-296.

Kiss J, Patel AJ, Baimbridge KG, Freund TF (1990) Topographical localization of neurons containing parvalbumin and choline acetyltransferase in the medial septum-diagonal band region of the rat. Neuroscience 36:61-72.

Klein RL, Meyer EM, Peel AL, Zolotukhin S, Meyers C, Muzyczka N, King MA (1998) Neuron-specific transduction in the rat septohippocampal or nigrostriatal pathway by recombinant adeno-associated virus vectors. Exp Neurol 150:183-194.

Koch S, Galloway MP (1997) MDMA induced dopamine release in vivo: role of endogenous serotonin. J Neural Transm 104:135-146.

Köhler C, Eriksson LG (1984) An immunohistochemical study of somatostatin and neurotensin positive neurons in the septal nuclei of the rat brain. Anat Embryol (Berl) 170:1-10.

Köhler C, Chan-Palay V, Wu JY (1984) Septal neurons containing glutamic acid decarboxylase immunoreactivity project to the hippocampal region in the rat brain. Anat Embryol (Berl) 169:41-44.

Kordower JH, Emborg ME, Bloch J, Ma SY, Chu Y, Leventhal L, McBride J, Chen EY, Palfi S, Roitberg BZ, Brown WD, Holden JE, Pyzalski R, Taylor MD, Carvey P, Ling Z, Trono D, Hantraye P, Deglon N, Aebischer P (2000) Neurodegeneration prevented by lentiviral vector delivery of GDNF in primate models of Parkinson's disease. Science 290:767-773.

Kramer K, Azmitia EC, Whitaker-Azmitia PM (1994) In vitro release of [3H]5-hydroxytryptamine from fetal and maternal brain by drugs of abuse. Brain Res Dev Brain Res 78:142-146.

Krejci A, Michal P, Jakubik J, Ricny J, Dolezal V (2004) Regulation of signal transduction at M2 muscarinic receptor. Physiol Res 53 Suppl 1:S131-140.

Kubista H, Boehm S (2006) Molecular mechanisms underlying the modulation of exocytotic noradrenaline release via presynaptic receptors. Pharmacol Ther 112:213-242.

Langen B, Dietze S, Fink H (2002) Acute effect of ethanol on anxiety and 5-HT in the prefrontal cortex of rats. Alcohol 27:135-141.

Lappalainen J, Long JC, Eggert M, Ozaki N, Robin RW, Brown GL, Naukkarinen H, Virkkunen M, Linnoila M, Goldman D (1998) Linkage of antisocial alcoholism to the serotonin 5-HT1B receptor gene in 2 populations. Arch Gen Psychiatry 55:989-994.

Lauterborn JC, Bizon JL, Tran TM, Gall CM (1995) NGF mRNA is expressed by GABAergic but not cholinergic neurons in rat basal forebrain. J Comp Neurol 360:454-462.

Le Grand B, Panissie A, Pauwels PJ, John GW (1998) Activation of recombinant h 5-HT1B and h 5-HT1D receptors stably expressed in C6 glioma cells produces increases in Ca2+-dependent K+ current. Naunyn Schmiedebergs Arch Pharmacol 358:608-615.

Lehmann O, Jeltsch H, Lehnardt O, Pain L, Lazarus C, Cassel JC (2000) Combined lesions of cholinergic and serotonergic neurons in the rat brain using 192 IgG-saporin and 5,7-dihydroxytryptamine: neurochemical and behavioural characterization. Eur J Neurosci 12:67-79.

Lehmann O, Jeltsch H, Lazarus C, Tritschler L, Bertrand F, Cassel JC (2002) Combined 192 IgG-saporin and 5,7-dihydroxytryptamine lesions in the male rat brain: a neurochemical and behavioral study. Pharmacol Biochem Behav 72:899-912.

Leonardi ET, Azmitia EC (1994) MDMA (ecstasy) inhibition of MAO type A and type B: comparisons with fenfluramine and fluoxetine (Prozac). Neuropsychopharmacology 10:231-238.

Leranth C, Frotscher M (1987) Cholinergic innervation of hippocampal GAD- and somatostatin-immunoreactive commissural neurons. J Comp Neurol 261:33-47.

Levey AI, Armstrong DM, Atweh SF, Terry RD, Wainer BH (1983) Monoclonal antibodies to choline acetyltransferase: production, specificity, and immunohistochemistry. J Neurosci 3:1-9.

Lew R, Sabol KE, Chou C, Vosmer GL, Richards J, Seiden LS (1996) Methylenedioxymethamphetamine-induced serotonin deficits are followed by partial recovery over a 52-week period. Part II: Radioligand binding and autoradiography studies. J Pharmacol Exp Ther 276:855-865.

Lewis PR, Shute CC (1967) The cholinergic limbic system: projections to hippocampal formation, medial cortex, nuclei of the ascending cholinergic reticular system, and the subfornical organ and supra-optic crest. Brain 90:521-540.

Liechti ME, Vollenweider FX (2000a) The serotonin uptake inhibitor citalopram reduces acute cardiovascular and vegetative effects of 3,4-methylenedioxymethamphetamine ('Ecstasy') in healthy volunteers. J Psychopharmacol 14:269-274.

Liechti ME, Vollenweider FX (2000b) Acute psychological and physiological effects of MDMA ("Ecstasy") after haloperidol pretreatment in healthy humans. Eur Neuropsychopharmacol 10:289-295.

Liechti ME, Kunz I, Kupferschmidt H (2005) Acute medical problems due to Ecstasy use. Case-series of emergency department visits. Swiss Med Wkly 135:652-657.

Liechti ME, Baumann C, Gamma A, Vollenweider FX (2000a) Acute psychological effects of 3,4-methylenedioxymethamphetamine (MDMA, "Ecstasy") are attenuated by the serotonin uptake inhibitor citalopram. Neuropsychopharmacology 22:513-521.

Liechti ME, Saur MR, Gamma A, Hell D, Vollenweider FX (2000b) Psychological and physiological effects of MDMA ("Ecstasy") after pretreatment with the 5-HT(2) antagonist ketanserin in healthy humans. Neuropsychopharmacology 23:396-404.

Limberger N, Deicher R, Starke K (1991) Species differences in presynaptic serotonin autoreceptors: mainly 5- HT1B but possibly in addition 5-HT1D in the rat, 5-HT1D in the rabbit and guinea-pig brain cortex. Naunyn-Schmiedeberg's Archives of Pharmacology 343:353-364.

Lin SL, Setya S, Johnson-Farley NN, Cowen DS (2002) Differential coupling of 5-HT(1) receptors to G proteins of the G(i) family. Br J Pharmacol 136:1072-1078.

Loewi O (1921) Über humorale Übertragbarkeit der Herznervenwirkung. Pflugers Archiv 189:239-242.

Lof E, Ericson M, Stomberg R, Soderpalm B (2007) Characterization of ethanol-induced dopamine elevation in the rat nucleus accumbens. Eur J Pharmacol 555:148-155.

Lora-Tamayo C, Tena T, Rodriguez A, Moreno D, Sancho JR, Ensenat P, Muela F (2004) The designer drug situation in Ibiza. Forensic Sci Int 140:195-206.

Lotze MT, Kost TA (2002) Viruses as gene delivery vectors: application to gene function, target validation, and assay development. Cancer Gene Ther 9:692-699.

Luiten PG, Wouterlood FG, Matsuyama T, Strosberg AD, Buwalda B, Gaykema RP (1988) Immunocytochemical applications in neuroanatomy. Demonstration of connections, transmitters and receptors. Histochemistry 90:85-97.

Luo X, Persico AM, Lauder JM (2003) Serotonergic regulation of somatosensory cortical development: lessons from genetic mouse models. Dev Neurosci 25:173-183.

Macor JE, Burkhart CA, Heym JH, Ives JL, Lebel LA, Newman ME, Nielsen JA, Ryan K, Schulz DW, Torgersen LK, et al. (1990) 3-(1,2,5,6-Tetrahydropyrid-4-yl)pyrrolo[3,2-b]pyrid-5-one: a potent and selective serotonin (5-HT1B) agonist and rotationally restricted phenolic analogue of 5-methoxy-3-(1,2,5,6-tetrahydropyrid-4-yl)indole. J Med Chem 33:2087-2093.

Maiya R, Buck KJ, Harris RA, Mayfield RD (2002) Ethanol-sensitive sites on the human dopamine transporter. J Biol Chem 277:30724-30729.

Malleret G, Hen R, Guillou JL, Segu L, Buhot MC (1999) 5-HT1B receptor knock-out mice exhibit increased exploratory activity and enhanced spatial memory performance in the Morris water maze. J Neurosci 19:6157-6168.

Mann R, Mulligan RC, Baltimore D (1983) Construction of a retrovirus packaging mutant and its use to produce helper-free defective retrovirus. Cell 33:153-159.

Maroteaux L, Saudou F, Amlaiky N, Boschert U, Plassat JL, Hen R (1992) Mouse 5HT1B serotonin receptor: cloning, functional expression, and localization in motor control centers. Proc Natl Acad Sci U S A 89:3020-3024.

Marston HM, Reid ME, Lawrence JA, Olverman HJ, Butcher SP (1999) Behavioural analysis of the acute and chronic effects of MDMA treatment in the rat. Psychopharmacology (Berl) 144:67-76.

Martin-Moutot N, Charvin N, Leveque C, Sato K, Nishiki T, Kozaki S, Takahashi M, Seagar M (1996) Interaction of SNARE complexes with P/Q-type calcium channels in rat cerebellar synaptosomes. J Biol Chem 271:6567-6570.

Martinou I, Fernandez PA, Missotten M, White E, Allet B, Sadoul R, Martinou JC (1995) Viral proteins E1B19K and p35 protect sympathetic neurons from cell death induced by NGF deprivation. J Cell Biol 128:201-208.

Mas M, Farre M, de la Torre R, Roset PN, Ortuno J, Segura J, Cami J (1999) Cardiovascular and neuroendocrine effects and pharmacokinetics of 3, 4-methylenedioxymethamphetamine in humans. J Pharmacol Exp Ther 290:136-145.

Mata M, Glorioso JC, Fink DJ (2002) Targeted gene delivery to the nervous system using herpes simplex virus vectors. Physiol Behav 77:483-488.

Mata M, Zhang M, Hu X, Fink DJ (2001) HveC (nectin-1) is expressed at high levels in sensory neurons, but not in motor neurons, of the rat peripheral nervous system. J Neurovirol 7:476-480.

Matuszewich L, Filon ME, Finn DA, Yamamoto BK (2002) Altered forebrain neurotransmitter responses to immobilization stress following 3,4-methylenedioxymethamphetamine. Neuroscience 110:41-48.

Maura G, Raiteri M (1986) Cholinergic terminals in rat hippocampus possess 5-HT1B receptors mediating inhibition of acetylcholine release. Eur J Pharmacol 129:333-337.

Maura G, Roccatagliata E, Raiteri M (1986) Serotonin autoreceptor in rat hippocampus: pharmacological characterization as a subtype of the 5-HT1 receptor. Naunyn Schmiedebergs Arch Pharmacol 334:323-326.

Maura G, Fedele E, Raiteri M (1989) Acetylcholine release from rat hippocampal slices is modulated by 5-hydroxytryptamine. Eur J Pharmacol 165:173-179.

McAllister AK, Katz LC, Lo DC (1997) Opposing roles for endogenous BDNF and NT-3 in regulating cortical dendritic growth. Neuron 18:767-778.

McBride WJ, Murphy JM, Gatto GJ, Levy AD, Yoshimoto K, Lumeng L, Li TK (1993) CNS mechanisms of alcohol self-administration. Alcohol Alcohol Suppl 2:463-467.

McBride WJ, Chernet E, Russell RN, Wong DT, Guan XM, Lumeng L, Li TK (1997) Regional CNS densities of monoamine receptors in alcohol-naive alcohol-preferring P and -nonpreferring NP rats. Alcohol 14:141-148.

McCann UD, Slate SO, Ricaurte GA (1996) Adverse reactions with 3,4-methylenedioxymethamphetamine (MDMA; 'ecstasy'). Drug Saf 15:107-115.

McCann UD, Ridenour A, Shaham Y, Ricaurte GA (1994) Serotonin neurotoxicity after (+/-)3,4-methylenedioxymethamphetamine (MDMA; "Ecstasy"): a controlled study in humans. Neuropsychopharmacology 10:129-138.

McCann UD, Mertl M, Eligulashvili V, Ricaurte GA (1999) Cognitive performance in (+/-) 3,4-methylenedioxymethamphetamine (MDMA, "ecstasy") users: a controlled study. Psychopharmacology (Berl) 143:417-425.

McCann UD, Szabo Z, Scheffel U, Dannals RF, Ricaurte GA (1998) Positron emission tomographic evidence of toxic effect of MDMA ("Ecstasy") on brain serotonin neurons in human beings. Lancet 352:1433-1437.

McCreary AC, Bankson MG, Cunningham KA (1999) Pharmacological studies of the acute and chronic effects of (+)-3, 4-methylenedioxymethamphetamine on locomotor activity: role of 5-hydroxytryptamine(1A) and 5-hydroxytryptamine(1B/1D) receptors. J Pharmacol Exp Ther 290:965-973.

McGehee DS, Role LW (1996) Presynaptic ionotropic receptors. Curr Opin Neurobiol 6:342-349.

McGregor IS, Clemens KJ, Van der Plasse G, Li KM, Hunt GE, Chen F, Lawrence AJ (2003) Increased anxiety 3 months after brief exposure to MDMA ("Ecstasy") in rats: association with altered 5-HT transporter and receptor density. Neuropsychopharmacology 28:1472-1484.

McNamara MG, Kelly JP, Leonard BE (1995) Some behavioural and neurochemical aspects of subacute (+/-)3,4-methylenedioxymethamphetamine administration in rats. Pharmacol Biochem Behav 52:479-484.

McQuade R, Sharp T (1997) Functional mapping of dorsal and median raphe 5-hydroxytryptamine pathways in forebrain of the rat using microdialysis. J Neurochem 69:791-796.

Mechan AO, O'Shea E, Elliott JM, Colado MI, Green AR (2001) A neurotoxic dose of 3,4-methylenedioxymethamphetamine (MDMA; ecstasy) to rats results in a long-term defect in thermoregulation. Psychopharmacology (Berl) 155:413-418.

Mechan AO, Moran PM, Elliott M, Young AJ, Joseph MH, Green R (2002a) A study of the effect of a single neurotoxic dose of 3,4-methylenedioxymethamphetamine (MDMA; "ecstasy") on the subsequent long-term behaviour of rats in the plus maze and open field. Psychopharmacology (Berl) 159:167-175.

Mechan AO, Esteban B, O'Shea E, Elliott JM, Colado MI, Green AR (2002b) The pharmacology of the acute hyperthermic response that follows administration of 3,4-methylenedioxymethamphetamine (MDMA, 'ecstasy') to rats. Br J Pharmacol 135:170-180.

Melander T, Staines WA, Hokfelt T, Rokaeus A, Eckenstein F, Salvaterra PM, Wainer BH (1985) Galanin-like immunoreactivity in cholinergic neurons of the septum-basal forebrain complex projecting to the hippocampus of the rat. Brain Res 360:130-138.

Meneses A (1999) 5-HT system and cognition. Neurosci Biobehav Rev 23:1111-1125.

Meneses A (2001) Could the 5-HT1B receptor inverse agonism affect learning consolidation? Neurosci Biobehav Rev 25:193-201.

Mesulam MM, Mufson EJ, Wainer BH, Levey AI (1983) Central cholinergic pathways in the rat: an overview based on an alternative nomenclature (Ch1-Ch6). Neuroscience 10:1185-1201.

Metz GA, Gonzalez CL, Piecharka DM, Whishaw IQ (2003) Acute alcohol administration improves skilled reaching success in intact but not 6-OHDA dopamine depleted rats: a subsystems analysis of the motoric and anxiolytic effects of alcohol. Behav Brain Res 142:167-174.

Miller RJ (1990) Receptor-mediated regulation of calcium channels and neurotransmitter release. Faseb J 4:3291-3299.

Miller RJ (1998) Presynaptic receptors. Annu Rev Pharmacol Toxicol 38:201-227.

Mlinar B, Corradetti R (2003) Endogenous 5-HT, released by MDMA through serotonin transporter- and secretory vesicle-dependent mechanisms, reduces hippocampal excitatory synaptic transmission by preferential activation of 5-HT1B receptors located on CA1 pyramidal neurons. Eur J Neurosci 18:1559-1571.

Mohajeri MH, Figlewicz DA, Bohn MC (1999) Intramuscular grafts of myoblasts genetically modified to secrete glial cell line-derived neurotrophic factor prevent motoneuron loss and disease progression in a mouse model of familial amyotrophic lateral sclerosis. Hum Gene Ther 10:1853-1866.

Molenaar PC, Nickolson VJ, Polak RL (1973) Preferential release of newly synthesized 3 H-acetylcholine from rat cerebral cortex slices in vitro. Br J Pharmacol 47:97-108.

Moor E, DeBoer P, Westerink BH (1998a) GABA receptors and benzodiazepine binding sites modulate hippocampal acetylcholine release in vivo. Eur J Pharmacol 359:119-126.

Moor E, Schirm E, Jacso J, Westerink BH (1998b) Involvement of medial septal glutamate and GABAA receptors in behaviour-induced acetylcholine release in the hippocampus: a dual probe microdialysis study. Brain Res 789:1-8.

Morgan MJ, McFie L, Fleetwood H, Robinson JA (2002) Ecstasy (MDMA): are the psychological problems associated with its use reversed by prolonged abstinence? Psychopharmacology (Berl) 159:294-303.

Morikawa H, Manzoni OJ, Crabbe JC, Williams JT (2000) Regulation of central synaptic transmission by 5-HT(1B) auto- and heteroreceptors. Mol Pharmacol 58:1271-1278.

Morley KC, McGregor IS (2000) (+/-)-3,4-methylenedioxymethamphetamine (MDMA, 'Ecstasy') increases social interaction in rats. Eur J Pharmacol 408:41-49.

Morley KC, Gallate JE, Hunt GE, Mallet PE, McGregor IS (2001) Increased anxiety and impaired memory in rats 3 months after administration of 3,4-methylenedioxymethamphetamine ("ecstasy"). Eur J Pharmacol 433:91-99.

Muramatsu M, Lapiz MD, Tanaka E, Grenhoff J (1998) Serotonin inhibits synaptic glutamate currents in rat nucleus accumbens neurons via presynaptic 5-HT1B receptors. Eur J Neurosci 10:2371-2379.

Nash JF, Brodkin J (1991) Microdialysis studies on 3,4-methylenedioxymethamphetamine-induced dopamine release: effect of dopamine uptake inhibitors. J Pharmacol Exp Ther 259:820-825.

Nash JF, Yamamoto BK (1992) Methamphetamine neurotoxicity and striatal glutamate release: comparison to 3,4-methylenedioxymethamphetamine. Brain Res 581:237-243.

Nash JF, Meltzer HY, Gudelsky GA (1988) Antagonism of serotonin receptor mediated neuroendocrine and temperature responses by atypical neuroleptics in the rat. Eur J Pharmacol 151:463-469.

Nava F, Carta G, Bortolato M, Gessa GL (2001) gamma-Hydroxybutyric acid and baclofen decrease extracellular acetylcholine levels in the hippocampus via GABA(B) receptors. Eur J Pharmacol 430:261-263.

Neumaier JF, Vincow ES, Arvanitogiannis A, Wise RA, Carlezon WA, Jr. (2002) Elevated expression of 5-HT1B receptors in nucleus accumbens efferents sensitizes animals to cocaine. J Neurosci 22:10856-10863.

Neve RL, Neve KA, Nestler EJ, Carlezon WA, Jr. (2005) Use of herpes virus amplicon vectors to study brain disorders. Biotechniques 39:381-391.

Ng NK, Lee HS, Wong PT (1999) Regulation of striatal dopamine release through 5-HT1 and 5-HT2 receptors. J Neurosci Res 55:600-607.

Nisijima K, Shioda K, Yoshino T, Takano K, Kato S (2004) Memantine, an NMDA antagonist, prevents the development of hyperthermia in an animal model for serotonin syndrome. Pharmacopsychiatry 37:57-62.

Noda M, Furutani Y, Takahashi H, Toyosato M, Tanabe T, Shimizu S, Kikyotani S, Kayano T, Hirose T, Inayama S, et al. (1983) Cloning and sequence analysis of calf cDNA and human genomic DNA encoding alpha-subunit precursor of muscle acetylcholine receptor. Nature 305:818-823.

O'Dell LE, Parsons LH (2004) Serotonin1B receptors in the ventral tegmental area modulate cocaine-induced increases in nucleus accumbens dopamine levels. J Pharmacol Exp Ther 311:711-719.

O'Hearn E, Battaglia G, De Souza EB, Kuhar MJ, Molliver ME (1988) Methylenedioxyamphetamine (MDA) and methylenedioxymethamphetamine (MDMA) cause selective ablation of serotonergic axon terminals in forebrain: immunocytochemical evidence for neurotoxicity. J Neurosci 8:2788-2803.

O'Loinsigh ED, Boland G, Kelly JP, O'Boyle KM (2001) Behavioural, hyperthermic and neurotoxic effects of 3,4-methylenedioxymethamphetamine analogues in the Wistar rat. Prog Neuropsychopharmacol Biol Psychiatry 25:621-638.

O'Shea E, Granados R, Esteban B, Colado MI, Green AR (1998) The relationship between the degree of neurodegeneration of rat brain 5-HT nerve terminals and the dose and frequency of administration of MDMA ('ecstasy'). Neuropharmacology 37:919-926.

O'Shea E, Esteban B, Camarero J, Green AR, Colado MI (2001) Effect of GBR 12909 and fluoxetine on the acute and long term changes induced by MDMA ('ecstasy') on the 5-HT and dopamine concentrations in mouse brain. Neuropharmacology 40:65-74.

Oesterheld JR, Armstrong SC, Cozza KL (2004) Ecstasy: pharmacodynamic and pharmacokinetic interactions. Psychosomatics 45:84-87.

Oksenberg D, Marsters SA, O'Dowd BF, Jin H, Havlik S, Peroutka SJ, Ashkenazi A (1992) A single amino-acid difference confers major pharmacological variation between human and rodent 5-HT1B receptors. Nature 360:161-163.

Oleskevich S, Descarries L, Lacaille JC (1989) Quantified distribution of the noradrenaline innervation in the hippocampus of adult rat. J Neurosci 9:3803-3815.

Pacifici R, Zuccaro P, Hernandez Lopez C, Pichini S, Di Carlo S, Farre M, Roset PN, Ortuno J, Segura J, Torre RL (2001) Acute effects of 3,4-methylenedioxymethamphetamine alone and in combination with ethanol on the immune system in humans. J Pharmacol Exp Ther 296:207-215.

Palfi S, Leventhal L, Chu Y, Ma SY, Emborg M, Bakay R, Deglon N, Hantraye P, Aebischer P, Kordower JH (2002) Lentivirally delivered glial cell line-derived neurotrophic factor increases the number of striatal dopaminergic neurons in primate models of nigrostriatal degeneration. J Neurosci 22:4942-4954.

Palmiter RD, Norstedt G, Gelinas RE, Hammer RE, Brinster RL (1983) Metallothionein-human GH fusion genes stimulate growth of mice. Science 222:809-814.

Parrott AC (2001) Human psychopharmacology of Ecstasy (MDMA): a review of 15 years of empirical research. Hum Psychopharmacol 16:557-577.

Parrott AC (2004) MDMA (3,4-Methylenedioxymethamphetamine) or ecstasy: the neuropsychobiological implications of taking it at dances and raves. Neuropsychobiology 50:329-335.

Parrott AC, Lasky J (1998) Ecstasy (MDMA) effects upon mood and cognition: before, during and after a Saturday night dance. Psychopharmacology (Berl) 139:261-268.

Parrott AC, Sisk E, Turner JJ (2000) Psychobiological problems in heavy 'ecstasy' (MDMA) polydrug users. Drug Alcohol Depend 60:105-110.

Passini MA, Wolfe JH (2001) Widespread gene delivery and structure-specific patterns of expression in the brain after intraventricular injections of neonatal mice with an adeno-associated virus vector. J Virol 75:12382-12392.

Paxinos G, Watson C (1998) The rat brain in stereotaxic coordinates, 4th Edition. San Diego: Academic Press.

Pedersen W, Skrondal A (1999) Ecstasy and new patterns of drug use: a normal population study. Addiction 94:1695-1706.

Pedigo NW, Yamamura HI, Nelson DL (1981) Discrimination of multiple [3H]5-hydroxytryptamine binding sites by the neuroleptic spiperone in rat brain. J Neurochem 36:220-226.

Peroutka SJ, Newman H, Harris H (1988) Subjective effects of 3,4-methylenedioxymethamphetamine in recreational users. Neuropsychopharmacology 1:273-277.

Porcu P, Grant KA (2004) Discriminative stimulus effects of ethanol in rats using a three-choice ethanol-midazolam-water discrimination. Behav Pharmacol 15:555-567.

Qin N, Platano D, Olcese R, Stefani E, Birnbaumer L (1997) Direct interaction of gbetagamma with a C-terminal gbetagamma-binding domain of the Ca2+ channel alpha1 subunit is responsible for channel inhibition by G protein-coupled receptors. Proc Natl Acad Sci U S A 94:8866-8871.

Quik M, Sum JD, Whiteaker P, McCallum SE, Marks MJ, Musachio J, McIntosh JM, Collins AC, Grady SR (2003) Differential declines in striatal nicotinic receptor subtype function after nigrostriatal damage in mice. Mol Pharmacol 63:1169-1179.

Quirion R, Richard J (1987) Differential effects of selective lesions of cholinergic and dopaminergic neurons on serotonin-type 1 receptors in rat brain. Synapse 1:124-130.

Rada PV, Mark GP, Hoebel BG (1993) In vivo modulation of acetylcholine in the nucleus accumbens of freely moving rats: I. Inhibition by serotonin. Brain Res 619:98-104.

Raiteri M, Maura G, Bonanno G, Pittaluga A (1986) Differential pharmacology and function of two 5-HT1 receptors modulating transmitter release in rat cerebellum. Journal of Pharmacology and Experimental Therapeutics 237:644-648.

Ramaekers JG, Kuypers KP (2006) Acute effects of 3,4-methylenedioxymethamphetamine (MDMA) on behavioral measures of impulsivity: alone and in combination with alcohol. Neuropsychopharmacology 31:1048-1055.

Rempel NL, Callaway CW, Geyer MA (1993) Serotonin1B receptor activation mimics behavioral effects of presynaptic serotonin release. Neuropsychopharmacology 8:201-211.

Rettig J, Neher E (2002) Emerging roles of presynaptic proteins in Ca++-triggered exocytosis. Science 298:781-785.

Ricaurte GA, McCann UD, Szabo Z, Scheffel U (2000) Toxicodynamics and long-term toxicity of the recreational drug, 3, 4-methylenedioxymethamphetamine (MDMA, 'Ecstasy'). Toxicol Lett 112-113:143-146.

Richardson IW, Szerb JC (1974) The release of labelled acetylcholine and choline from cerebral cortical slices stimulated electrically. Br J Pharmacol 52:499-507.

Risinger FO, Bormann NM, Oakes RA (1996) Reduced sensitivity to ethanol reward, but not ethanol aversion, in mice lacking 5-HT1B receptors. Alcohol Clin Exp Res 20:1401-1405.

Risold PY (2004) The Septal Region. In: The Rat Nervous System, 3rd Edition (Paxinos G, ed), pp 605-632. San Diego: Academic Press.

Risold PY, Swanson LW (1997) Connections of the rat lateral septal complex. Brain Res Brain Res Rev 24:115-195.

Rizzoli SO, Betz WJ (2003) Neurobiology: All change at the synapse. Nature 423:591-592.

Roberts C, Price GW, Jones BJ (1997) The role of 5-HT(1B/1D) receptors in the modulation of 5-hydroxytryptamine levels in the frontal cortex of the conscious guinea pig. Eur J Pharmacol 326:23-30.

Roberts C, Price GW, Middlemiss DN (2001) Ligands for the investigation of 5-HT autoreceptor function. Brain Res Bull 56:463-469.

Roberts C, Watson J, Burton M, Price GW, Jones BJ (1996) Functional characterization of the 5-HT terminal autoreceptor in the guinea-pig brain cortex. Br J Pharmacol 117:384-388.

Rocha BA, Scearce-Levie K, Lucas JJ, Hiroi N, Castanon N, Crabbe JC, Nestler EJ, Hen R (1998) Increased vulnerability to cocaine in mice lacking the serotonin-1B receptor. Nature 393:175-178.

Roghani A, Feldman J, Kohan SA, Shirzadi A, Gundersen CB, Brecha N, Edwards RH (1994) Molecular cloning of a putative vesicular transporter for acetylcholine. Proc Natl Acad Sci U S A 91:10620-10624.

Roizman B (1996) The function of herpes simplex virus genes: a primer for genetic engineering of novel vectors. Proc Natl Acad Sci U S A 93:11307-11312.

Rosenberg MB, Friedmann T, Robertson RC, Tuszynski M, Wolff JA, Breakefield XO, Gage FH (1988) Grafting genetically modified cells to the damaged brain: restorative effects of NGF expression. Science 242:1575-1578.

Rothman RB, Baumann MH, Dersch CM, Romero DV, Rice KC, Carroll FI, Partilla JS (2001) Amphetamine-type central nervous system stimulants release norepinephrine more potently than they release dopamine and serotonin. Synapse 39:32-41.

Rudnick G, Wall SC (1992) The molecular mechanism of "ecstasy" [3,4-methylenedioxy-methamphetamine (MDMA)]: serotonin transporters are targets for MDMA-induced serotonin release. Proc Natl Acad Sci U S A 89:1817-1821.

Ruotsalainen S, Miettinen R, MacDonald E, Riekkinen M, Sirvio J (1998) The role of the dorsal raphe-serotonergic system and cholinergic receptors in the modulation of working memory. Neurosci Biobehav Rev 22:21-31.

Rutz S, Riegert C, Rothmaier AK, Buhot MC, Cassel JC, Jackisch R (2006a) Presynaptic serotonergic modulation of 5-HT and acetylcholine release in the hippocampus and the cortex of 5-HT1B-receptor knockout mice. Brain Res Bull 70:81-93.

Rutz S, Riegert C, Rothmaier AK, Buhot MC, Cassel JC, Jackisch R (2006b) Presynaptic serotonergic modulation of 5-HT and acetylcholine release in the hippocampus and the cortex of 5-HT(1B)-receptor knockout mice. Brain Res Bull 70:81-93.

Ryabinin AE (1998) Role of hippocampus in alcohol-induced memory impairment: implications from behavioral and immediate early gene studies. Psychopharmacology (Berl) 139:34-43.

Rye DB, Wainer BH, Mesulam MM, Mufson EJ, Saper CB (1984) Cortical projections arising from the basal forebrain: a study of cholinergic and noncholinergic components employing combined retrograde tracing and immunohistochemical localization of choline acetyltransferase. Neuroscience 13:627-643.

Sabol KE, Seiden LS (1998) Reserpine attenuates D-amphetamine and MDMA-induced transmitter release in vivo: a consideration of dose, core temperature and dopamine synthesis. Brain Res 806:69-78.

Sabol KE, Lew R, Richards JB, Vosmer GL, Seiden LS (1996) Methylenedioxymethamphetamine-induced serotonin deficits are followed by partial recovery over a 52-week period. Part I: Synaptosomal uptake and tissue concentrations. J Pharmacol Exp Ther 276:846-854.

Sapolsky RM (2003) Neuroprotective gene therapy against acute neurological insults. Nat Rev Neurosci 4:61-69.

Sarhan H, Fillion G (1999) Differential sensitivity of 5-HT1B auto and heteroreceptors. Naunyn Schmiedebergs Arch Pharmacol 360:382-390.

Sarhan H, Grimaldi B, Hen R, Fillion G (2000) 5-HT1B receptors modulate release of [3H]dopamine from rat striatal synaptosomes: further evidence using 5-HT moduline, polyclonal 5-HT1B receptor antibodies and 5-HT1B receptor knock-out mice. Naunyn Schmiedebergs Arch Pharmacol 361:12-18.

Sarhan H, Cloez-Tayarani I, Massot O, Fillion MP, Fillion G (1999) 5-HT1B receptors modulate release of [3H]dopamine from rat striatal synaptosomes. Naunyn Schmiedebergs Arch Pharmacol 359:40-47.

Sari Y (2004) Serotonin1B receptors: from protein to physiological function and behavior. Neurosci Biobehav Rev 28:565-582.

Sari Y, Miquel MC, Brisorgueil MJ, Ruiz G, Doucet E, Hamon M, Verge D (1999) Cellular and subcellular localization of 5-hydroxytryptamine1B receptors in the rat central nervous system: immunocytochemical, autoradiographic and lesion studies. Neuroscience 88:899-915.

Sari Y, Lefevre K, Bancila M, Quignon M, Miquel MC, Langlois X, Hamon M, Verge D (1997) Light and electron microscopic immunocytochemical visualization of 5-HT1B receptors in the rat brain. Brain Res 760:281-286.

Saudou F, Amara DA, Dierich A, LeMeur M, Ramboz S, Segu L, Buhot MC, Hen R (1994) Enhanced aggressive behavior in mice lacking 5-HT1B receptor. Science 265:1875-1878.

Scanzello CR, Hatzidimitriou G, Martello AL, Katz JL, Ricaurte GA (1993) Serotonergic recovery after (+/-)3,4-(methylenedioxy) methamphetamine injury: observations in rats. J Pharmacol Exp Ther 264:1484-1491.

Scanziani M, Gahwiler BH, Thompson SM (1995) Presynaptic inhibition of excitatory synaptic transmission by muscarinic and metabotropic glutamate receptor activation in the hippocampus: are Ca2+ channels involved? Neuropharmacology 34:1549-1557.

Scearce-Levie K, Viswanathan SS, Hen R (1999a) Locomotor response to MDMA is attenuated in knockout mice lacking the 5-HT1B receptor. Psychopharmacology (Berl) 141:154-161.

Scearce-Levie K, Chen JP, Gardner E, Hen R (1999b) 5-HT receptor knockout mice: pharmacological tools or models of psychiatric disorders. Ann N Y Acad Sci 868:701-715.

Schifano F (2004) A bitter pill. Overview of ecstasy (MDMA, MDA) related fatalities. Psychopharmacology (Berl) 173:242-248.

Schifano F, Oyefeso A, Webb L, Pollard M, Corkery J, Ghodse AH (2003) Review of deaths related to taking ecstasy, England and Wales, 1997-2000. Bmj 326:80-81.

Schmidt CJ (1987a) Neurotoxicity of the psychedelic amphetamine, methylenedioxymethamphetamine. J Pharmacol Exp Ther 240:1-7.

Schmidt CJ (1987b) Acute administration of methylenedioxymethamphetamine: comparison with the neurochemical effects of its N-desmethyl and N-ethyl analogs. Eur J Pharmacol 136:81-88.

Schmidt CJ, Taylor VL (1988) Direct central effects of acute methylenedioxymethamphetamine on serotonergic neurons. Eur J Pharmacol 156:121-131.

Schmidt CJ, Levin JA, Lovenberg W (1987) In vitro and in vivo neurochemical effects of methylenedioxymethamphetamine on striatal monoaminergic systems in the rat brain. Biochem Pharmacol 36:747-755.

Schmidt CJ, Black CK, Abbate GM, Taylor VL (1990) Methylenedioxymethamphetamine-induced hyperthermia and neurotoxicity are independently mediated by 5-HT2 receptors. Brain Res 529:85-90.

Schmued LC (2003) Demonstration and localization of neuronal degeneration in the rat forebrain following a single exposure to MDMA. Brain Res 974:127-133.

Scholey AB, Parrott AC, Buchanan T, Heffernan TM, Ling J, Rodgers J (2004) Increased intensity of Ecstasy and polydrug usage in the more experienced recreational Ecstasy/MDMA users: a WWW study. Addict Behav 29:743-752.

Schwerdtfeger WK, Buhl E (1986) Various types of non-pyramidal hippocampal neurons project to the septum and contralateral hippocampus. Brain Res 386:146-154.

Semba K (2000) Multiple output pathways of the basal forebrain: organization, chemical heterogeneity, and roles in vigilance. Behav Brain Res 115:117-141.

Semba K, Fibiger HC (1988) Time of origin of cholinergic neurons in the rat basal forebrain. J Comp Neurol 269:87-95.

Semba K, Reiner PB, McGeer EG, Fibiger HC (1989) Brainstem projecting neurons in the rat basal forebrain: neurochemical, topographical, and physiological distinctions from cortically projecting cholinergic neurons. Brain Res Bull 22:501-509.

Sena-Esteves M, Saeki Y, Fraefel C, Breakefield XO (2000) HSV-1 amplicon vectors--simplicity and versatility. Mol Ther 2:9-15.

Senut MC, Menetrey D, Lamour Y (1989) Cholinergic and peptidergic projections from the medial septum and the nucleus of the diagonal band of Broca to dorsal hippocampus, cingulate cortex and olfactory bulb: a combined wheatgerm agglutinin-apohorseradish peroxidase-gold immunohistochemical study. Neuroscience 30:385-403.

Series HG, Cowen PJ, Sharp T (1994) p-Chloroamphetamine (PCA), 3,4-methylenedioxy-methamphetamine (MDMA) and d-fenfluramine pretreatment attenuates d-fenfluramine-evoked release of 5-HT in vivo. Psychopharmacology (Berl) 116:508-514.

Seuwen K, Magnaldo I, Pouyssegur J (1988) Serotonin stimulates DNA synthesis in fibroblasts acting through 5-HT1B receptors coupled to a Gi-protein. Nature 335:254-256.

Shankaran M, Gudelsky GA (1999) A neurotoxic regimen of MDMA suppresses behavioral, thermal and neurochemical responses to subsequent MDMA administration. Psychopharmacology (Berl) 147:66-72.

Shankaran M, Yamamoto BK, Gudelsky GA (1999) Involvement of the serotonin transporter in the formation of hydroxyl radicals induced by 3,4-methylenedioxymethamphetamine. Eur J Pharmacol 385:103-110.

Shankaran M, Yamamoto BK, Gudelsky GA (2001) Ascorbic acid prevents 3,4-methylenedioxymethamphetamine (MDMA)-induced hydroxyl radical formation and the behavioral and neurochemical consequences of the depletion of brain 5-HT. Synapse 40:55-64.

Shieh MT, WuDunn D, Montgomery RI, Esko JD, Spear PG (1992) Cell surface receptors for herpes simplex virus are heparan sulfate proteoglycans. J Cell Biol 116:1273-1281.

Shippenberg TS, Hen R, He M (2000) Region-specific enhancement of basal extracellular and cocaine-evoked dopamine levels following constitutive deletion of the Serotonin(1B) receptor. J Neurochem 75:258-265.

Smith ML, Hale BD, Booze RM (1994) Calbindin-D28k immunoreactivity within the cholinergic and GABAergic projection neurons of the basal forebrain. Exp Neurol 130:230-236.

Sodhi MS, Sanders-Bush E (2004) Serotonin and brain development. Int Rev Neurobiol 59:111-174.

Solowij N, Hall W, Lee N (1992) Recreational MDMA use in Sydney: a profile of 'Ecstacy' users and their experiences with the drug. Br J Addict 87:1161-1172.

Sotelo C, Cholley B, El Mestikawy S, Gozlan H, Hamon M (1990) Direct Immunohistochemical Evidence of the Existence of 5-HT1A Autoreceptors on Serotoninergic Neurons in the Midbrain Raphe Nuclei. Eur J Neurosci 2:1144-1154.

Spaete RR, Frenkel N (1982) The herpes simplex virus amplicon: a new eucaryotic defective-virus cloning-amplifying vector. Cell 30:295-304.

Spear PG (2004) Herpes simplex virus: receptors and ligands for cell entry. Cell Microbiol 6:401-410.

Sprouse JS, Aghajanian GK (1987) Electrophysiological responses of serotoninergic dorsal raphe neurons to 5-HT1A and 5-HT1B agonists. Synapse 1:3-9.

Starke K (2005) Zwölf wichtige Transmitter. In: Allgemeine und spezielle Pharmakologie und Toxikologie (Aktories K, Förstermann U, Hofmann F, Starke K, eds), pp 124-140. München: Elsevier.

Starke K, Hedler L, Steppeler A (1981) Metabolism of endogenous and exogenous noradrenaline in guinea-pig atria. Naunyn Schmiedebergs Arch Pharmacol 317:193-198.

Starke K, Göthert M, Kilbinger H (1989a) Modulation of neurotransmitter release by presynaptic autoreceptors. Physiol Rev 69:864-989.

Starke K, Gothert M, Kilbinger H (1989b) Modulation of neurotransmitter release by presynaptic autoreceptors. Physiol Rev 69:864-989.

Steckler T, Sahgal A (1995) The role of serotonergic-cholinergic interactions in the mediation of cognitive behaviour. Behav Brain Res 67:165-199.

Steele TD, Nichols DE, Yim GK (1987) Stereochemical effects of 3,4-methylenedioxymethamphetamine (MDMA) and related amphetamine derivatives on inhibition of uptake of [3H]monoamines into synaptosomes from different regions of rat brain. Biochem Pharmacol 36:2297-2303.

Steinbusch HW (1981) Distribution of serotonin-immunoreactivity in the central nervous system of the rat-cell bodies and terminals. Neuroscience 6:557-618.

Steppeler A, Starke K (1982) Fate of [3H]amezinium in sympathetically innervated rabbit tissues. Biochem Pharmacol 31:1075-1080.

Stone DM, Hanson GR, Gibb JW (1987a) Differences in the central serotonergic effects of methylenedioxymethamphetamine (MDMA) in mice and rats. Neuropharmacology 26:1657-1661.

Stone DM, Merchant KM, Hanson GR, Gibb JW (1987b) Immediate and long-term effects of 3,4-methylenedioxymethamphetamine on serotonin pathways in brain of rat. Neuropharmacology 26:1677-1683.

Stone DM, Johnson M, Hanson GR, Gibb JW (1988) Role of endogenous dopamine in the central serotonergic deficits induced by 3,4-methylenedioxymethamphetamine. J Pharmacol Exp Ther 247:79-87.

Strauss BE, Costanzi-Strauss E (2007) Combating oncogene activation associated with retrovirus-mediated gene therapy of X-linked severe combined immunodeficiency. Braz J Med Biol Res 40:601-613.

Strote J, Lee JE, Wechsler H (2002) Increasing MDMA use among college students: results of a national survey. J Adolesc Health 30:64-72.

Sudhof TC (2004) The synaptic vesicle cycle. Annu Rev Neurosci 27:509-547.

Sugimoto Y, Ohkura M, Inoue K, Yamada J (2001) Involvement of serotonergic and dopaminergic mechanisms in hyperthermia induced by a serotonin-releasing drug, p-chloroamphetamine in mice. Eur J Pharmacol 430:265-268.

Suhr R, Balse E, Haaf A, Kelche C, Cassel JC, Jackisch R (1999a) Modulation of acetylcholine and 5-hydroxytryptamine release in hippocampal slices of rats with fimbria-fornix lesions and intrahippocampal grafts containing cholinergic and/or serotonergic neurons. Brain Res Bull 50:15-25.

Suhr R, Balse E, Haaf A, Kelche C, Cassel JC, Jackisch R (1999b) Modulation of acetylcholine and 5-hydroxytryptamine release in hippocampal slices of rats with fimbria-fornix lesions and intrahippocampal grafts containing cholinergic and/or serotonergic neurons. Brain Res Bull 50:15-25.

Sumnall HR, O'Shea E, Marsden CA, Cole JC (2004) The effects of MDMA pretreatment on the behavioural effects of other drugs of abuse in the rat elevated plus-maze test. Pharmacol Biochem Behav 77:805-814.

Swanson LW, Cowan WM (1979) The connections of the septal region in the rat. J Comp Neurol 186:621-655.

Tabbaa S, Corso TD, Jenkins L, Tran RK, Bloom DC, Stachowiak MK (2005) In vivo gene transfer to the brain cortex using a single injection of HSV-1 vector into the medial septum. Folia Morphol (Warsz) 64:273-281.

Tanaka E, North RA (1993) Actions of 5-hydroxytryptamine on neurons of the rat cingulate cortex. J Neurophysiol 69:1749-1757.

Tancer M, Johanson CE (2007) The effects of fluoxetine on the subjective and physiological effects of 3,4-methylenedioxymethamphetamine (MDMA) in humans. Psychopharmacology (Berl) 189:565-573.

Thach WT, Goodkin HP, Keating JG (1992) The cerebellum and the adaptive coordination of movement. Annu Rev Neurosci 15:403-442.

Thielen RJ, Morzorati SL, McBride WJ (2001) Effects of ethanol on the dorsal raphe nucleus and its projections to the caudate putamen. Alcohol 23:131-139.

Thielen RJ, Bare DJ, McBride WJ, Lumeng L, Li TK (2002) Ethanol-stimulated serotonin release in the ventral hippocampus: an absence of rapid tolerance for the alcohol-preferring P rat and insensitivity in the alcohol-nonpreferring NP rat. Pharmacol Biochem Behav 71:111-117.

Tomkins DM, O'Neill MF (2000) Effect of 5-HT(1B) receptor ligands on self-administration of ethanol in an operant procedure in rats. Pharmacol Biochem Behav 66:129-136.

Topp L, Hando J, Dillon P, Roche A, Solowij N (1999) Ecstasy use in Australia: patterns of use and associated harm. Drug Alcohol Depend 55:105-115.

Turunen MP, Puhakka HL, Koponen JK, Hiltunen MO, Rutanen J, Leppanen O, Turunen AM, Narvanen A, Newby AC, Baker AH, Yla-Herttuala S (2002) Peptide-retargeted adenovirus encoding a tissue inhibitor of metalloproteinase-1 decreases restenosis after intravascular gene transfer. Mol Ther 6:306-312.

Umbriaco D, Garcia S, Beaulieu C, Descarries L (1995) Relational features of acetylcholine, noradrenaline, serotonin and GABA axon terminals in the stratum radiatum of adult rat hippocampus (CA1). Hippocampus 5:605-620.

Vallet PG, Charnay Y, Bouras C (1990) Distribution and colocalization of delta sleep-inducing peptide and luteinizing hormone-releasing hormone in the aged human brain: an immunohistochemical study. J Chem Neuroanat 3:207-214.

Vasconcelos SM, Macedo DS, Lima LO, Sousa FC, Fonteles MM, Viana GS (2003) Effect of one-week ethanol treatment on monoamine levels and dopaminergic receptors in rat striatum. Braz J Med Biol Res 36:503-509.

Verge D, Daval G, Marcinkiewicz M, Patey A, el Mestikawy S, Gozlan H, Hamon M (1986) Quantitative autoradiography of multiple 5-HT1 receptor subtypes in the brain of control or 5,7-dihydroxytryptamine-treated rats. J Neurosci 6:3474-3482.

Vertes RP (1988) Brainstem afferents to the basal forebrain in the rat. Neuroscience 24:907-935.

Vizi ES, Kiss JP (1998) Neurochemistry and pharmacology of the major hippocampal transmitter systems: synaptic and nonsynaptic interactions [see comments]. Hippocampus 8:566-607.

Vlazny DA, Kwong A, Frenkel N (1982) Site-specific cleavage/packaging of herpes simplex virus DNA and the selective maturation of nucleocapsids containing full-length viral DNA. Proc Natl Acad Sci U S A 79:1423-1427.

Vollenweider FX, Liechti ME, Gamma A, Greer G, Geyer M (2002) Acute psychological and neurophysiological effects of MDMA in humans. J Psychoactive Drugs 34:171-184.

Waeber C, Dietl MM, Hoyer D, Palacios JM (1989) 5-HT1 receptors in the vertebrate brain: regional distribution examined by autoradiography. Naunyn-Schmiedeberg´s Archives of Pharmacology 340:486-494.

Wainer BH, Rye DB (1984) Retrograde horseradish peroxidase tracing combined with localization of choline acetyltransferase immunoreactivity. J Histochem Cytochem 32:439-443.

Wallace TL, Gudelsky GA, Vorhees CV (2001) Alterations in diurnal and nocturnal locomotor activity in rats treated with a monoamine-depleting regimen of methamphetamine or 3,4-methylenedioxymethamphetamine. Psychopharmacology (Berl) 153:321-326.

Walsh DM, Beattie DT, Connor HE (1995) The activity of 5-HT1D receptor ligands at cloned human 5-HT1D alpha and 5-HT1D beta receptors. Eur J Pharmacol 287:79-84.

Wang X, Baumann MH, Xu H, Rothman RB (2004) 3,4-methylenedioxymethamphetamine (MDMA) administration to rats decreases brain tissue serotonin but not serotonin transporter protein and glial fibrillary acidic protein. Synapse 53:240-248.

Wang Y, Freund RK, Palmer MR (1999) Potentiation of ethanol effects in cerebellum by activation of endogenous noradrenergic inputs. J Pharmacol Exp Ther 288:211-220.

Washbourne P, McAllister AK (2002) Techniques for gene transfer into neurons. Curr Opin Neurobiol 12:566-573.

Webb E, Ashton CH, Kelly P, Kamali F (1996) Alcohol and drug use in UK university students. Lancet 348:922-925.

Wichems CH, Hollingsworth CK, Bennett BA (1995) Release of serotonin induced by 3,4-methylenedioxymethamphetamine (MDMA) and other substituted amphetamines in cultured fetal raphe neurons: further evidence for calcium-independent mechanisms of release. Brain Res 695:10-18.

Wilkie GI, Hutson P, Sullivan JP, Wonnacott S (1996) Pharmacological characterization of a nicotinic autoreceptor in rat hippocampal synaptosomes. Neurochem Res 21:1141-1148.

Williamson S, Gossop M, Powis B, Griffiths P, Fountain J, Strang J (1997) Adverse effects of stimulant drugs in a community sample of drug users. Drug Alcohol Depend 44:87-94.

Wilson AW, Costall B, Neill JC (2000) Manipulation of operant responding for an ethanol-paired conditioned stimulus in the rat by pharmacological alteration of the serotonergic system. J Psychopharmacol 14:340-346.

Winer BJ (1971) Statistical principles in experimental design, 2nd ed Edition. New York ; London: McGraw-Hill.

Winstock AR, Griffiths P, Stewart D (2001) Drugs and the dance music scene: a survey of current drug use patterns among a sample of dance music enthusiasts in the UK. Drug Alcohol Depend 64:9-17.

Wolff M, Savova M, Malleret G, Hen R, Segu L, Buhot MC (2003) Serotonin 1B knockout mice exhibit a task-dependent selective learning facilitation. Neurosci Lett 338:1-4.

Wonnacott S (1997) Presynaptic nicotinic ACh receptors. Trends in Neurosciences 20:92-98.

Wonnacott S, Kaiser S, Mogg A, Soliakov L, Jones IW (2000) Presynaptic nicotinic receptors modulating dopamine release in the rat striatum. Eur J Pharmacol 393:51-58.

Wozniak KM, Pert A, Mele A, Linnoila M (1991) Focal application of alcohols elevates extracellular dopamine in rat brain: a microdialysis study. Brain Res 540:31-40.

Wu LG, Saggau P (1997) Presynaptic inhibition of elicited neurotransmitter release. Trends Neurosci 20:204-212.

Yamamoto BK, Nash JF, Gudelsky GA (1995) Modulation of methylenedioxymethamphetamine-induced striatal dopamine release by the interaction between serotonin and gamma-aminobutyric acid in the substantia nigra. J Pharmacol Exp Ther 273:1063-1070.

Yan QS (1999) Extracellular dopamine and serotonin after ethanol monitored with 5-minute microdialysis. Alcohol 19:1-7.

Yan QS, Yan SE (2001a) Serotonin-1B receptor-mediated inhibition of [(3)H]GABA release from rat ventral tegmental area slices. J Neurochem 79:914-922.

Yan QS, Yan SE (2001b) Activation of 5-HT(1B/1D) receptors in the mesolimbic dopamine system increases dopamine release from the nucleus accumbens: a microdialysis study. Eur J Pharmacol 418:55-64.

Yan QS, Zheng SZ, Yan SE (2004a) Involvement of 5-HT1B receptors within the ventral tegmental area in regulation of mesolimbic dopaminergic neuronal activity via GABA mechanisms: a study with dual-probe microdialysis. Brain Res 1021:82-91.

Yan QS, Zheng SZ, Yan SE (2004b) Prenatal cocaine exposure decreases brain-derived neurotrophic factor proteins in the rat brain. Brain Res 1009:228-233.

Yan QS, Reith ME, Jobe PC, Dailey JW (1996) Focal ethanol elevates extracellular dopamine and serotonin concentrations in the rat ventral tegmental area. Eur J Pharmacol 301:49-57.

Yan QS, Zheng SZ, Feng MJ, Yan SE (2005) Involvement of 5-HT1B receptors within the ventral tegmental area in ethanol-induced increases in mesolimbic dopaminergic transmission. Brain Res 1060:126-137.

Yim HJ, Schallert T, Randall PK, Gonzales RA (1998) Comparison of local and systemic ethanol effects on extracellular dopamine concentration in rat nucleus accumbens by microdialysis. Alcohol Clin Exp Res 22:367-374.

Yokoyama CT, Sheng ZH, Catterall WA (1997) Phosphorylation of the synaptic protein interaction site on N-type calcium channels inhibits interactions with SNARE proteins. J Neurosci 17:6929-6938.

Yoshimoto K, McBride WJ, Lumeng L, Li TK (1992) Alcohol stimulates the release of dopamine and serotonin in the nucleus accumbens. Alcohol 9:17-22.

Zamponi GW, Bourinet E, Nelson D, Nargeot J, Snutch TP (1997) Crosstalk between G proteins and protein kinase C mediated by the calcium channel alpha1 subunit. Nature 385:442-446.

Ziporyn T (1986) A growing industry and menace: makeshift laboratory's designer drugs. Jama 256:3061-3063.

Zou JY, Martinez DB, Neafsey EJ, Collins MA (1996) Binge ethanol-induced brain damage in rats: effect of inhibitors of nitric oxide synthase. Alcohol Clin Exp Res 20:1406-1411.

Zumstein A, Karduck W, Starke K (1981) Pathways of dopamine metabolism in the rabbit caudate nucleus in vitro. Naunyn Schmiedebergs Arch Pharmacol 316:205-217.

7. SUMMARY

ENGLISH SUMMARY

The work presented here had two main aspects, both of which are related to the understanding of the functional implications of the 5-HT_{1B} serotonergic receptor. The first aspect concerns the functional characterization of a virally-mediated gene transfer procedure to increase the expression of 5-HT_{1B} receptors in cholinergic neurons, in which this receptor acts as a heteroreceptor. Successful overexpression of 5-HT_{1B} receptors had already been demonstrated in transfected serotonergic neurons of the dorsal raphé. The second aspect is related to the physiological, behavioural, neurochemical and neuropharmacological effects of the combined administration of MDMA (3,4-methylenedioxymethamphetamine or "ecstasy") and ethanol (EtOH) to rats, effects which also suggest an involvement of 5-HT_{1B} receptors. Moreover, as these compounds were assumed to have local actions on neuronal circuitry, their effects were also assessed *in vitro* on brain slices, especially of the striatum. Finally, as the combined treatment was shown to have specific effects on the locomotor activity of rats in their home cage and to result in functional alterations of 5-HT_{1B} receptors on serotonergic terminals, the implication of the 5-HT_{1B} autoreceptor in MDMA-induced hyperlocomotion was studied after its viral vector-induced overexpression in neurons originating in the dorsal raphé. Thus, this last experiment was performed by using the gene transfer technique investigated in the first part of my work, although not in cholinergic neurons.

(1) In the *first part* of my doctoral work, Herpes simplex viral type 1 (HSV-1) particles were used as vectors for the expression of GFP (*Green Fluorescent protein*) or of the 5-HT_{1B} receptor, which were transfected either alone ("GFP vector" expressing only GFP) or together ("HA1B/GFP vector", expressing hemagglutinin-tagged 5-HT_{1B} receptor and GFP) (Clark et al., 2002). As we wanted to study the functional consequences of an increased expression of the 5-HT_{1B} receptor in the axon terminals of the septo-hippocampal cholinergic pathway, primary cell cultures were prepared from the embryonic septal region at ED17 (Embryonic Day) for the *in vitro* study (Ehret et al., 2001). Immunocytochemically, we confirmed that the primary septal cell cultures consisted of a mixture of glial and neuronal cells, the latter being mostly of the cholinergic and GABAergic types. We also confirmed the neurotropism of the viral vector as no infection of glial cell was detected. Most importantly, we showed that some of the GFP-positive cells (i.e. infected by viral particles) were also positive for ChAT, the catabolic enzyme of acetylcholine and therefore a highly specific marker of cholinergic neurons. Additionally, following infection of cell cultures with the HA1B/GFP

vector, some GFP-positive neurons were also positive for the hemagglutinin tag, which shows that these cells contained the transfected 5-HT_{1B} receptor.

In order to detect functional consequences of such an increased expression of the 5-HT_{1B} receptor in cholinergic cells, the primary cell cultures were incubated with [^{3}H]-choline, superfused and electrically-stimulated. The basal and the electrically-evoked release of acetylcholine (ACh) were not affected by the increased expression of the 5-HT_{1B} heteroreceptor, which is not surprising as, due to their origin, these cultures are devoid of serotonergic cell bodies. On the contrary, when cell cultures were treated with the specific 5-HT_{1B} agonist, CP-93,129, the inhibitory effect of this compound was significantly more pronounced in cells infected with the HA1B/GFP vector as compared to those infected with the GFP vector.

Since we wanted to study such virally-mediated gene transfer also at a more integrated level, both HSV-1 vectors were stereotaxically injected into the medial septal region of the rat (Risold, 2004). Immunocytochemical observation of the medial septum/diagonal band of Broca showed that some neurons of this region were GFP-positive (Barot et al., 2007). Moreover, we established that some of these GFP-positive cells were cholinergic neurons. Finally, in the HA1B/GFP group, GFP-positive cells were also positive for the hemagglutinin tag of the 5-HT_{1B} receptor. Thus, as in the primary septal cell cultures, we showed that it is also possible to transfect septal cholinergic neurons with the protein of interest *in vivo*. Hippocampal slices of virally transfected rat were then incubated with [^{3}H]-choline, superfused and electrically stimulated. Three days after the intraseptal injection of the viral particles, which corresponds to a delay of maximal effects of the virus, we observed that the electrically-evoked ACh release was lower in slices of the HA1B/GFP group as compared to those of the GFP group. This first result shows that the release of ACh was more potently inhibited by endogenous serotonin in these slices, most probably because of the increased expression of 5-HT_{1B} receptors. Moreover, the selective 5-HT_{1B} agonist (CP-93,129) also had a significantly higher inhibitory potency on evoked ACh release in the HA1B/GFP group as compared to the GFP one, an effect which was specific, as it could be antagonized by the application of the selective 5-HT_{1B} antagonist, GR-55,562. We thus confirmed that intraseptal injection of the HA1B/GFP vector results in transfection of septal cholinergic neurons and affects the modulation of ACh release in the target region of the septal projections, namely the hippocampus.

As already demonstrated in other reports, virally-mediated gene transfer is a valuable technique enabling the expression of exogenous proteins in target cells (Burton et al., 2002). This technique makes it possible to overcome some of the difficulties linked to

gene manipulations (knock-out/knock-in) or related to classical pharmacological approaches, such as compensatory phenomena or lack of compound specificity. Moreover, HSV-1 has been shown to be a useful tool, particularly because of its capacity to infect postmitotic cells such as neurons. In addition, our study demonstrated that this vector can also be used to increase the expression of the 5-HT_{1B} receptor in non-serotonergic neurons, where this receptor functions as a heteroreceptor. Thus, this technique is useful to study 5-HT_{1B} heteroreceptors without modifying the density of 5-HT_{1B} autoreceptors. Interestingly, manipulating the level of 5-HT_{1B} receptors expression may be relevant to pathophysiological phenomena, given the plasticity of 5-HT_{1B} mRNA expression levels that has been detected in various brain regions following behavioural stress exposure or in response to psychostimulant drugs such as cocaine. Moreover, septal 5-HT_{1B} mRNA levels may also be altered by various environmental factors. Indeed, an about 50% reduction in septal 5-HT_{1B} mRNA in old (24 months) vs. young (3 months) rats has been detected recently, and their overexpression could be one way to restore lost functions due to aging.

(2) As is the case for cocaine-induced effects, serotonin 5-HT_{1B} receptors seem also to play a role in the effects of ecstasy (MDMA) (Green et al., 2003). This is why in the *second part* of this work we focused our attention to the neuropharmacological effects of MDMA, with the ultimate aim to investigate behavioural effects of ecstasy in rats with viral vector-induced overexpression of 5-HT_{1B} receptors in serotonergic neurons. Since recent studies showed that ethanol (EtOH) produced a dramatic potentiation of ecstasy-induced hyperlocomotion (Cassel et al., 2004), we also assessed the effects of EtOH alone or combined with MDMA. Thus, rats were treated with a regimen of MDMA (10 mg/kg), EtOH (1.5 g/kg), or their combination, once per day over four consecutive days. Our study was based on reports on drug abuse in humans, showing that EtOH, due to its social role and easy availability, is frequently taken in combination with other drugs, and in particular with MDMA. Measured at short-term delays, besides its effects on locomotion, it was shown previously that EtOH also attenuated the MDMA-induced hyperthermia, but only on the first day. As shown in my doctoral work, in the long-term, MDMA reduced 5-HT content (and that of its metabolite 5-HIAA) in several brain regions, accounting for serotonergic toxicity, without any interaction with EtOH. Besides alterations in the beam-walking test, which accounts for reduced motor coordination, we also showed that in hippocampal (not cortical) slices of rats pre-treated only with the combination of MDMA and EtOH, the CP-93,129 (selective 5-HT_{1B} agonist)-induced inhibition and the methiotepin (5-HT_1 antagonist)-induced facilitation of serotonin

release were stronger and weaker, respectively, after a combined EtOH plus MDMA treatment, as compared to the other groups. Thus, we show that even three weeks after the last treatment, the combination of both compounds has specific consequences on the presynaptic modulation of the release of serotonin via the 5-HT_{1B} autoreceptor and that these consequences do not appear when each drug is given alone (Cassel et al., 2005).

(3) Even if the substrates of the EtOH-induced potentiation of the effects of MDMA on activity levels are still unknown, it seems reasonable to hypothesize that an action on the nigrostriatal dopaminergic system could be involved in the potentiation. In this system, EtOH taken in addition to MDMA could enhance activity levels of dopaminergic and/or serotonergic terminals. The mechanisms of such interaction could non-exclusively involve pharmacokinetic and pharmacodynamic components (Oesterheld et al., 2004). Thus the *third part* of my work tested the hypothesis of possible pharmacodynamic interactions of EtOH with MDMA at a more cellular level. For this purpose the spontaneous and electrically-evoked release of serotonin (5-HT) and dopamine (DA) were measured in striatal slices previously superfused with saline, EtOH, MDMA or the combination of both drugs. These experiments brought to light several new informations regarding the complex mechanisms behind the effects of MDMA and/or EtOH on the modulation of striatal transmission in the rat. This study showed, for the first time, a local synergistic interaction of these two drugs on the spontaneous outflow of DA and 5-HT. Indeed, when used together, MDMA and EtOH increased the spontaneous outflow of both DA and 5-HT with a higher potency than did MDMA alone. Even if these findings do not demonstrate an exclusive mechanism accounting for the synergistic effects of EtOH-MDMA co-intoxication on physiological or behavioural parameters, they clearly demonstrate that one or more local mechanisms may participate in these interactions. Nevertheless, we cannot exclude an additional *in vivo* action via more complex polysynaptic loops that could involve also extra-striatal neurons, nor can we discard the possibility of a conjoint involvement of pharmacokinetic factors.

(4) Finally, the last and *fourth part* of my doctoral work focused on the mechanisms underlying the potentiation of MDMA-induced hyperlocomotion by EtOH. To that end, we used the virally-mediated gene transfer technique, described in the first part, in order to increase the expression of 5-HT_{1B} autoreceptors in serotonergic neurons. The 5-HT-containing fibers originating in the dorsal raphe nucleus (DRN) project to

dopaminergic cell bodies in the ventral tegmental area (VTA), the substantia nigra and to their terminal fields in the prefrontal cortex, nucleus accumbens and striatum. According to the literature, it appeared that the psychostimulant effect of MDMA relies on interactions between the serotonergic and the dopaminergic systems (Bankson and Cunningham, 2001). In this respect, 5-HT was shown to modulate DA release in the VTA most probably via 5-HT_{1B} heteroreceptors located on GABAergic terminals. The present experiment was thus used to further test the possibility that 5-HT_{1B} autoreceptors also have a modulatory role in the psychostimulant effects of MDMA. Of course, as in the previous parts of this work, the effects of the combination of EtOH to MDMA were also explored. For this purpose, three days after stereotaxic injection of the viral vectors (GFP and HA1B/GFP) into the DRN, rats were intraperitoneally injected with saline, EtOH, MDMA or the combination of both (EtOH+MDMA) before their locomotor activity (in the home cage) was measured for five hours. Firstly, observation of the brain of these rats showed, in the DRN region, some GFP-positive cells indicating the presence of the virus. If not, rats were discarded from further statistical analysis. When considering the first hour of recording of the locomotor activity, we observed that, while EtOH had no effect, MDMA enhanced the activity scores of rats previously injected with the GFP and HA1B/GFP vectors. As already described, when combining EtOH and MDMA, the MDMA-induced hyperactivity was potentiated, also in both the GFP and HA1B/GFP groups. However, in the HA1B/GFP group, we observed a decrease of the hyperlocomotor effect under EtOH+MDMA as compared to the GFP group given the same treatment. In other word, the hyperlocomotor effect of MDMA was potentiated by the co-intoxication with EtOH, but to a lesser extent than in the GFP group. These results suggest that an increased expression of 5-HT_{1B} autoreceptors attenuates the potentiating effects of EtOH in MDMA-treated rats.

Taken together, the present thesis has shown **(1)** the functional consequences of a virally-mediated gene transfer of the 5-HT_{1B} heteroreceptor into cholinergic neurons both *in vitro* and *in vivo*, **(2)** that the function of the 5-HT_{1B} autoreceptor may be affected even several weeks following a combined treatment with MDMA *and* EtOH, **(3)** that the same combination of drugs of abuse shows serious pharmacodynamic interactions *in vitro*, i.e. in the release of striatal neurotransmitter systems, and finally, **(4)**, that an enhanced expression of the 5-HT_{1B} autoreceptor in the DRN significantly reduces the hyperlocomotor effects of MDMA and of its combination with EtOH.

FRENCH SUMMARY

Le travail présenté comporte deux approches principales en rapport avec notre volonté de mieux comprendre les implications fonctionnelles du récepteur sérotoninergique du type 5-HT_{1B}. La première approche a porté sur la caractérisation d'une procédure de transfert de gène assurée par le vecteur HSV-1 (*Herpes simplex* virus type 1). Dans la seconde approche, nous avons mené une série d'études sur les effets physiologiques, comportementaux, neurochimiques et neuropharmacologiques de l'administration combinée de MDMA (3,4-methylenedioxymethamphetamine ou "ecstasy") et d'alcool (éthanol ou EtOH) chez le Rat. Etant donné que ces composés, MDMA comme EtOH, peuvent avoir une action locale sur des circuits neuronaux, leurs effets ont également été étudiés *in vitro* sur des coupes de tissu frais. Enfin, il apparaît que la co-administration de ces deux drogues a des effets spécifiques sur l'activité locomotrice de rats dans leur cage d'élevage. De même, nous avons pu montrer que ce co-traitement conduit à des altérations fonctionnelles des récepteurs 5-HT_{1B} sur les terminaisons sérotoninergiques. De ce fait, l'implication du récepteur 5-HT_{1B} dans ces phénomènes a été étudiée à l'aide d'un modèle reposant sur la surexpression de ce récepteur, par transfection virale, dans le noyau du raphé dorsal. La technique de transfert de gène expérimentée dans la première partie de ce travail a été utilisée selon les mêmes modalités que dans notre première approche, sauf que les particules virales ont été injectées dans le raphé dorsal (au lieu du septum médian).

(1) Dans la première partie de mon travail de thèse, des particules virales issues de HSV-1 ont été utilisées comme vecteur pour l'expression de GFP (*Green Fluorescent protein*) ou du récepteur 5-HT_{1B}. En pratique, un vecteur nommé « vecteur GFP » permettait l'expression de la GFP seule et un vecteur nommé « vecteur HA1B/GFP » permettait l'expression simultanée de la GFP et de la protéine 5-HT_{1B}, cette dernière étant marquée d'un « tag », dans notre cas, l'hemagglutinin (Clark et al., 2002). Le but étant d'étudier les conséquences fonctionnelles d'une surexpression du récepteur 5-HT_{1B} dans les terminaisons axoniques de la voie cholinergique septo-hippocampique, des cultures de cellules primaires ont été préparées à partir de régions septales embryonnaires prélevées chez des rates au 17ème jour de gestation (Ehret et al., 2001). L'observation microscopique de marquages immunocytochimiques a confirmé que ces cultures étaient constituées d'un mélange de cellules gliales et neuronales, ces dernières étant principalement de type cholinergique et GABAergique. Nous avons également pu montrer que certaines cellules GFP-positives (c'est-à-dire ayant été infectées par des particules virales) étaient aussi immunopositives pour la CHAT,

l'enzyme catabolique de l'acetylcholine, qui constitue un marqueur très spécifique des neurones cholinergiques. De plus, suite à l'infection par le vecteur HA1B/GFP, certaines cellules positives pour la GFP, l'étaient également pour l'hemagglutinin, ce qui prouve que ces cellules contenaient le récepteur 5-HT_{1B} transfecté.

Afin d'évaluer les conséquences fonctionnelles d'une telle surexpression d'hétérorécepteurs 5-HT_{1B} dans les cellules cholinergiques, les cultures cellulaires ont été incubées avec de la choline tritiée, superfusées et stimulées électriquement. La libération basale d'acétylcholine (ACh), ainsi que sa libération électriquement évoquée n'ont pas été modifiées par la surexpression de l'hétérorécepteur 5-HT_{1B}. Ce résultat n'est pas surprenant car, de part leur origine, ces cultures ne contiennent pas de corps cellulaires sérotoninergiques. Au contraire, lorsque ces cellules ont été traitées avec l'agoniste spécifique du récepteur 5-HT_{1B}, (CP-93,129) l'effet inhibiteur de ce composé sur la libération évoquée d'ACh était significativement plus prononcé dans les cellules préalablement traitées avec le vecteur HA1B/GFP comparativement à celles infectées avec le vecteur GFP.

L'étape suivante ayant consisté à étudier cette technique de transfert de gène à un niveau plus intégré, les vecteurs GFP et HA1B/GFP ont été injectés dans la région septale du rat adulte (Risold, 2004). L'observation immunocytochimique du septum médian/bande diagonale de Broca a montré que certains neurones de cette région étaient positifs pour la GFP (Barot et al., 2007). De plus, nous avons pu établir que certaines de ces cellules positives pour la GFP étaient des neurones cholinergiques (ChAT-positifs). Finalement, dans le groupe HA1B/GFP, les cellules GFP-positives étaient également positives pour le marqueur du récepteur 5-HT_{1B}, l'hemagglutinin. Par conséquent, comme ce fut le cas pour les cultures de cellules, nous avons montré qu'il est possible de transfecter *in vivo* des neurones cholinergiques septaux avec une protéine d'intérêt. Qu'en est-il des effets fonctionnels de ces transfections ? Des coupes d'hippocampe, issues de rats préalablement injectés avec les particules virales, ont été incubées avec de la choline tritiée, superfusées et électriquement stimulées. Trois jours après la transfection, délai permettant d'obtenir le maximum d'expression virale, nous avons observé que la libération électriquement évoquée d'ACh était diminuée dans le groupe HA1B/GFP comparativement au groupe GFP. Ce premier résultat montre que l'inhibition de la libération évoquée d'ACh par la sérotonine endogène a été plus importante dans le groupe HA1B/GFP par rapport au groupe GFP. De plus, l'agoniste sélectif du récepteur 5-HT_{1B} (CP-93,129) a également inhibé la libération évoquée d'ACh de manière plus importante dans le groupe HA1B/GFP que dans le groupe GFP. En conclusion, cette expérience nous a permis de montrer

que l'injection intraseptale du vecteur HA1B/GFP permet de transfecter des neurones cholinergiques septaux et module la libération d'ACh dans la région cible des projections septales, c'est-à-dire l'hippocampe.
Comme d'autres études l'ont montré, le transfert de gène par vecteurs viraux est une technique efficace permettant l'expression de protéines exogènes dans des cellules cibles (Burton et al., 2002). Cette technique permet d'outrepasser certaines des difficultés et inconvénients liés à la manipulation de gènes (knock-out/knock-in) ou aux approches pharmacologiques, comme des phénomènes de compensation ou le manque de spécificité de certains composés pharmacologiques. De plus, HSV-1 représente un vecteur idéal grâce à sa capacité à infecter des cellules post-mitotiques comme les neurones. Complétant le travail de Clark et al. (2002) sur la transfection de neurones sérotoninergiques, notre étude a montré que ce vecteur peut aussi être utilisé pour accroître l'expression du récepteur 5-HT_{1B} dans des neurones non-sérotoninergiques, neurones dans lesquels ce récepteur a une fonction d'hétérorécepteur. De ce fait, cette technique permet d'étudier le récepteur 5-HT_{1B} sans modifier la densité de l'autorécepteur 5-HT_{1B}. De façon intéressante, la manipulation des niveaux d'expression du récepteur 5-HT_{1B} peut s'avérer pertinente au regard de phénomènes pathophysiologiques. Par exemple, des modifications de niveaux d'expression de l'ARNm du récepteur 5-HT_{1B} ont été détectées dans différentes régions cérébrales suite à l'exposition à un stress comportemental. Ces récepteurs interviennent aussi dans les effets de certains psychostimulants, comme la cocaïne ou la MDMA (ecstasy). De plus, les niveaux de l'ARNm dans le septum peuvent également être modifiés par des facteurs environnementaux. En effet, une réduction d'environ 50% de l'ARNm du récepteur 5-HT_{1B} chez des rats âgés (24 mois) a été observé par rapport à des rats dits jeunes (3 mois). Il apparaît alors qu'une surexpression de ce récepteur pourrait constituer un moyen de restaurer des pertes de fonctions liées à l'âge.

(2) Comme je viens de le mentionner, il semble que le récepteur 5-HT_{1B} joue également un rôle modulateur dans les effets de l'ecstasy (MDMA) (Green et al., 2003). C'est pour cette raison que nous avons décidé, dans la seconde partie de mon travail de thèse, de porter notre attention sur les effets neuropharmacologiques de la MDMA, dans l'optique d'aborder la question du rôle des récepteurs 5-HT_{1B} en utilisant *in fine* le modèle de transfection virale. Cette approche visait donc à poser les bases pour l'étude des effets comportementaux de l'ecstasy chez des rats préalablement injectés avec les vecteurs viraux décrits ci-dessus en vue d'obtenir une surexpression

des récepteurs 5-HT_{1B}, mais cette fois dans les neurones sérotoninergiques du raphé dorsal. Etant donné que l'éthanol (EtOH) produit une potentialisation importante de l'hyperlocomotion induite par la MDMA (Cassel et al., 2004), nous avons également étudié les effets de l'EtOH, seul ou co-administré avec la MDMA. De ce fait, les rats ont été traités avec de la MDMA (10 mg/kg), de l'EtOH (1.5 g/kg) ou leur combinaison, une fois par jour pendant 4 jours consécutifs. Notre étude était basée sur des rapports concernant les habitudes en matière de consommation de drogues chez l'Homme. Ceux-ci ont montré que l'EtOH, en raison de son « rôle social » et de sa facilité d'accès, était fréquemment consommé avec d'autres drogues, et en particulier avec la MDMA. A court terme, il a été montré, qu'en plus de son rôle sur la locomotion, l'EtOH atténue l'hyperthermie induite par la MDMA, et ce, uniquement à la première injection dans le cadre d'un protocole d'injections quotidiennes. A long terme, nous avons pu montrer que la MDMA réduit la concentration de sérotonine (5-HT ; ainsi que celle de son principal métabolite, le 5-HIAA) dans différentes structures cérébrales, attestant de sa toxicité pour les neurones sérotoninergiques, et ce, sans interaction avec l'EtOH. D'un point de vue comportemental, des altérations dans le test de la barre ont été notées ; elles reflètent une diminution de la coordination motrice dans les trois groupes d'animaux considérés. Cependant, il a également été montré que dans des coupes de tissu hippocampique frais (et non cortical), l'inhibition de la libération évoquée de 5-HT par le CP-93,129 (agoniste 5-HT_{1B} sélectif) ainsi que la facilitation de cette libération par la methiotépine (antagoniste 5-HT_1) ont été, respectivement, plus forte et plus faible dans le groupe EtOH+MDMA que dans les autres groupes. De ce fait, nous avons pu montrer que trois semaines après le dernier traitement, la combinaison de l'EtOH avec la MDMA a des effets spécifiques, à long terme, sur la modulation présynaptique de la libération de 5-HT via le récepteur 5-HT_{1B} et qu'aucun de ces effets n'a été observé après le traitement unique par l'une de ces drogues (Cassel et al., 2005).

(3) Même si les substrats neurobiologiques de la potentialisation de l'hyperactivité induite par la MDMA sont inconnus, il apparaît, au regard de la littérature, que la voie dopaminergique nigrostriatale pourrait être une cible d'action de la combinaison d'EtOH et de MDMA, où ces drogues pourraient contribuer à accroître les niveaux d'activité des terminaisons dopaminergiques et sérotoninergiques. Un rapport récent explique que les mécanismes sous-tendant l'interaction de drogues avec la MDMA peuvent impliquer des composantes pharmacocinétiques et/ou pharmacodynamiques (Oesterheld et al., 2004). Par conséquent, la troisième partie de mon travail a testé

l'hypothèse d'interactions pharmacodynamiques entre l'EtOH et la MDMA au niveau cellulaire. Nous avons donc mesuré la libération basale et évoquée de sérotonine (5-HT) et de dopamine (DA) dans des coupes de tissu frais de striatum préalablement superfusées avec de l'EtOH et de la MDMA, séparément ou en combinaison. Ces expériences ont mis en évidence une action synergique de l'EtOH et de la MDMA sur la libération de DA et de 5-HT dans le striatum. En effet, lorsque ces drogues sont appliquées concomitamment, la libération basale de DA et de 5-HT augmente bel et bien, comme on peut s'y attendre au vu des propriétés de la MDMA, mais elle le fait de façon plus importante que lorsque la MDMA est appliquée seule. Ces résultats montrent qu'un mécanisme local intervient dans les interactions de l'EtOH et de la MDMA. Néanmoins, cette expérience ne permet pas d'exclure des mécanismes additionnels comme, par exemple, l'activation de boucles polysynaptiques plus complexes pouvant impliquer des neurones extra-striataux ou encore l'action conjointe de facteurs pharmacocinétiques.

(4) Finalement, dans la quatrième et dernière partie de mon travail, nous nous sommes intéressés aux mécanismes sous-tendant la potentialisation de l'hyperlocomotion induite par la MDMA ou par le cocktail EtOH+MDMA. Pour cela, nous avons utilisé la technique de transfert de gène, décrite dans la première partie, dans le but de surexprimer les autorécepteurs 5-HT_{1B} dans les neurones sérotoninergiques [voir aussi (Clark et al., 2002)]. Les fibres contenant la 5-HT trouvent leur origine dans les noyaux du raphé dorsal et projettent sur les corps cellulaires dopaminergiques de l'aire tegmentale ventrale et de la substance noire, ainsi que dans leurs structures de projection, le cortex préfrontral, le noyau accumbens et le striatum. D'après la littérature, il apparaît que les effets psychostimulants de la MDMA font intervenir des interactions entre les systèmes dopaminergiques et sérotoninergiques (Bankson and Cunningham, 2001). Par exemple, il a été montré que la 5-HT inhibe la libération de DA dans l'aire tegmentale ventrale via des hétérorécepteurs 5-HT_{1B} situés sur des neurones GABAergiques. Notre dernière expérience avait donc pour but d'étudier si les autorécepteurs 5-HT_{1B} jouent également un rôle modulateur dans les effets psychostimulants de la MDMA. De plus, les effets de la co-intoxication par EtOH et MDMA ont également été évalués. Trois jours après l'injection intraseptale des vecteurs viraux (GFP ou HA1B/GFP), les rats ont subi une injection intrapéritonéale de solution saline, d'EtOH, de MDMA ou d'EtOH+MDMA, avant que leur activité locomotrice (en cage d'élevage) ne soit évaluée pendant 5 heures. L'observation de coupes de cerveau de ces rats, au niveau du raphé dorsal, a montré des cellules

positives pour la GFP, indiquant la transfection de ces cellules. L'analyse de la première heure d'enregistrement de l'activité locomotrice a montré un effet hyperlocomoteur de la MDMA, alors que l'EtOH administré seul n'a eu aucun effet sur cette activité. De plus, la potentialisation de l'effet hyperlocomoteur de la MDMA par l'EtOH a été vérifiée dans les deux groupes de rats. Cependant, cette potentialisation a été moins importante dans le groupe HA1B/GFP que dans le groupe GFP. Ces résultats nous permettent donc de conclure que la surexpression de l'autorécepteur 5-HT_{1B} dans les neurones sérotoninergiques a entraîné une réduction de l'effet hyperlocomoteur de la MDMA et de sa combinaison avec l'EtOH.

En conclusion, ce travail a montré **(1)** les conséquences fonctionnelles de la surexpression de l'hétérorécepteur 5-HT_{1B} dans les neurones cholinergiques septaux, *in vitro* et *in vivo* ; **(2)** que la fonction de l'autorécepteur 5-HT_{1B} peut être modifiée après une co-intoxication des rats par de l'EtOH et de la MDMA, même plusieurs semaines après l'administration ; **(3)** que la même combinaison de drogues entraîne des interactions pharmacodynamiques *in vitro*, sur la libération des neurotransmetteurs et, finalement, **(4)** qu'une surexpression de l'autorécepteur 5-HT_{1B} atténue l'effet hyperlocomoteur de la MDMA et de sa potentialisation par l'EtOH.

GERMAN SUMMARY

Die hier dargestellte Arbeit hatte zwei Haupt-Aspekte, die beide mit dem Verständnis der funktionellen Bedeutung des 5-HT_{1B} Serotonin Rezeptors verknüpft sind. Der erste Aspekt betrifft die funktionelle Charakterisierung eines virusvermittelten Gentransfer Verfahrens, welches das Ziel hatte die Expression des 5-HT_{1B} Rezeptors in cholinergen Neuronen, in denen dieser Rezeptor als Heterorezeptor agiert, zu erhöhen. Eine erfolgreiche Überexpresssion des 5-HT_{1B} Rezeptors wurde schon früher in transfizierten serotonergen Neuronen der dorsalen Raphé gezeigt. Der zweite Aspekt bezieht sich auf die physiologischen, neurochemischen, neuropharmakologischen und Verhaltens-Effekte der kombinierten Anwendung von MDMA (3,4-methylenedioxymethamphetamine, oder "Ecstasy") und Ethanol (EtOH) bei Ratten, Effekte die ebenfalls eine Beteiligung von 5-HT_{1B} Rezeptoren suggerieren. Da weiterhin vermutet wird, dass diese Stoffe lokale Wirkungen auf das neuronale Netzwerk haben, wurden ihre Effekte auch *in vitro* an Hirnschnitten untersucht, insbesondere an Striatum-Schnitten. Da auch gezeigt wurde, dass die kombinierte Behandlung spezifische Effekte auf die lokomotorische Aktivität von Ratten in ihrem „Heimat-Käfig" hat und zu funktionellen Veränderungen des 5-HT_{1B} Rezeptors an serotonergen Terminalen führt, wurde schließlich auch die Beteiligung des 5-HT_{1B} Autorezeptors bei der MDMA-induzierten Hyperlokomotion nach seiner durch einen viralen Vektor induzierten Überexpression in Neuronen der dorsalen Raphé untersucht. Somit wurde dieses letzte Experiment mit der Gentransfer Technik durchgeführt - allerdings nicht in cholinergen Neuronen - die im ersten Teil meiner Arbeit untersucht worden war

(1) Im *ersten Teil* meiner Doktorarbeit, wurden Herpes simplex Virus Typ 1 (HSV-1) Partikel als Vektoren für die Expression von GFP (*Green Fluorescent Protein*) oder des 5-HT_{1B} Rezeptors verwendet, welche entweder allein ("GFP Vektor", der nur GFP exprimiert) oder gemeinsam übertragen wurden ("HA1B/GFP Vektor", der sowohl den 5-HT_{1B} Rezeptor mit einem Hemagglutinin-‚tag' als auch GFP exprimiert) (Clark *et al* 2002). Da wir die funktionellen Konsequenzen einer gesteigerten 5-HT_{1B} Rezeptor-Expression in den Axonterminalen der septohippocampalen cholinergen Bahn untersuchen wollten, wurden primäre Zellkulturen aus der embryonalen Septum-Region bei ED17 (Embryonaler Tag 17) für die *in vitro* Untersuchungen hergestellt (Ehret *et al* 2001). Immunocytochemisch konnten wir bestätigen, dass die primären septalen Zellkulturen aus einer Mischung von glialen und neuronalen Zellen bestanden, wobei letztere meist zum cholinergen und GABAergen Typ gehörten. Wir

bestätigten auch den Neurotropismus des viralen Vektors, da keine Infektion von Gliazellen beobachtet wurde. Insbesondere konnten wir zeigen, dass einige der GFP-positiven (d.h. mit Viruspartikeln infizierten) Zellen auch positiv für ChAT waren: das Acetylcholin (ACh) synthetisierende Enzym und daher ein hoch-spezifischer Marker für cholinerge Neurone. Außerdem waren nach der Infektion der Zellkulturen mit dem HA1B/GFP Vektor einige der GFP-positiven Neurone auch positiv für den Hemagglutinin-‚tag', welches zeigt, dass diese Zellen auch den transfizierten 5-HT_{1B} Rezeptor enthielten.

Um die funktionellen Konsequenzen einer solchen gesteigerten Expression des 5-HT_{1B} Rezeptors in cholinergen Zellen zu ermitteln, wurden die primären Zellkulturen mit [^{3}H]-Cholin vorinkubiert, superfundiert und elektrisch stimuliert. Die basale und die elektrisch evozierte Freisetzung von ACh wurden durch die gesteigerte Expression des 5-HT_{1B} Heterorezeptors nicht verändert. Dies ist aber nicht überraschend, da aufgrund ihrer Ursprungsregion diese Kulturen frei von serotonergen Zellkörpern sind. Im Gegensatz dazu fanden wir, dass nach Behandlung der Kulturen mit dem spezifischen 5-HT_{1B} Rezeptor-Agonisten CP-93,129, der inhibitorische Effekt dieser Substanz in Zellen, die mit dem HA1B/GFP Vektor infiziert waren, signifikant stärker ausgeprägt war als in denjenigen, die mit dem GFP Vektor behandelt waren.

Da wir einen solchen Virus-Vermittelten Gentransfer auch auf einer höheren Organisationsebene untersuchen wollten, wurden beide HSV-1 Vektoren stereotaktisch in die mediale Septum-Region der Ratte injiziert (Risold, 2004). Immunocytochemische Beobachtung des medialen Septum/diagonalen Band von Broca zeigte, dass einige Neurone dieser Region GFP-positiv waren (Barot *et al* 2007). Weiterhin stellten wir fest, dass einige dieser GFP-positiven Zellen cholinerge Neurone waren. Schließlich waren in der HA1B/GFP Gruppe GFP-positive Zellen auch positiv für den Hemagglutinin-‚tag' des 5-HT_{1B} Rezeptors. Somit zeigten wir, wie in den primären Zellkulturen, dass es auch *in vivo* möglich ist, septale cholinerge Neurone mit dem interessierenden Protein zu transfizieren. Hippocampale Schnitte von viral transfizierten Ratten wurden dann mit [^{3}H]-Cholin inkubiert, superfundiert und elektrisch stimuliert. Drei Tage nach der intraseptalen Injektion der Viruspartikel, d.h. nach einer Zeit, die der Verzögerung der maximal Effekte des Virus entspricht, fanden wir, dass die elektrisch evozierte ACh Freisetzung in Schnitten der HA1B/GFP Gruppe niedriger war als in denjenigen der GFP Gruppe. Dieses erste Ergebnis zeigt, dass die Freisetzung von ACh in diesen Schnitten, sehr wahrscheinlich aufgrund der gesteigerten Expression des 5-HT_{1B} Rezeptors, stärker durch endogenes Serotonin (5-HT) gehemmt wurde. Weiterhin war auch der selektive 5-HT_{1B} Agonist (CP-93,129) in

der HA1B/GFP Gruppe signifikant stärker hemmend wirksam als in der GFP Gruppe. Dieser Effekt war spezifisch, da er durch den selektiven 5-HT_{1B} Antagonisten, GR-55,562, aufgehoben wurde. Somit bestätigten wir, dass eine intraseptale Injektion des HA1B/GFP Vektors zu einer Transfection des 5-HT_{1B} Rezeptors in septale cholinerge Neuronen führt und damit die Modulation der ACh Freisetzung in der Zielregion der septalen Projektionen, nämlich im Hippocampus beeinflusst.

Wie schon in anderen Arbeiten gezeigt, ist der virusvermittelte Gentransfer eine wertvolle Technik, die es ermöglicht, die Expression exogener Proteine in Zielzellen zu erreichen (Burton *et al* 2002). Diese Technik macht es möglich, einige der Schwierigkeiten von Genmanipulationen (z.B. knock-out/knock-in), oder von klassischen pharmakologischen Techniken, wie kompensatorische Phänomene oder fehlende Substanz-Spezifität, zu überwinden. Darüber hinaus hat sich HSV-1 aufgrund seiner Fähigkeit post-mitotische Zellen, wie Neurone, zu infizieren als besonders nützliches Werkzeug erwiesen. Weiterhin zeigte unsere Studie, dass dieser Vektor auch verwendet werden kann, um die Expression des 5-HT_{1B} Rezeptors in nicht-serotonergen Neuronen zu steigern wo dieser Rezeptor als Heterorezeptor fungiert. Daher ist diese Technik nützlich um den 5-HT_{1B} Heterorezeptor zu untersuchen ohne die Dichte des 5-HT_{1B} Autorezeptors zu verändern. Interessanterweise kann eine Manipulation der 5-HT_{1B} Rezeptor-Expression für pathophysiologische Phänomene bedeutsam sein, wie die Plastizität der 5-HT_{1B} mRNA Expression zeigt, die in verschiedenen Gehirnregionen nach Stress-Situationen oder als Antwort auf psychostimulierende Drogen, wie Cocain, gefunden wurde. Weiterhin können septale 5-HT_{1B} mRNA Spiegel auch durch verschiedene Umweltfaktoren verändert werden. Tatsächlich wurde eine etwa 50%ige Reduktion der septalen 5-HT_{1B} mRNA in alten (24 Monate) im Vergleich zu jungen (3 Monate) Ratten kürzlich bestimmt: 5-HT_{1B} Rezeptor Überexpression könnte daher ein Weg sein Funktionen zu restaurieren, die durch das Altern verloren gingen.

(2) Wie es für Cocain-induzierte Wirkungen der Fall ist, scheint der 5-HT_{1B} Rezeptor auch eine Rolle bei den Effekten von Ecstasy (MDMA) zu spielen (Green *et al* 2003). Daher konzentrierten wir unsere Aufmerksamkeit im *zweiten Teil* dieser Arbeit auf die neuropharmakologischen Effekte von MDMA, mit dem ultimativen Ziel, Verhaltenseffekte von Ecstasy in Ratten mit virusvermittelter Überexpression des 5-HT_{1B} Rezeptors in serotonergen Neuronen zu untersuchen. Da neuere Studien zeigten, dass Ethanol (EtOH) eine dramatische Verstärkung der durch MDMA induzierten Hyperlokomotion bewirkte (Cassel *et al* 2004), bestimmten wir auch die Effekte of

EtOH allein, oder kombiniert mit MDMA. Daher wurden Ratten einmal täglich über 4 aufeinanderfolgende Tage entweder mit MDMA (10 mg/kg), oder mit EtOH (1.5 g/kg), oder der Kombination von beiden Stoffen behandelt. Unsere Studie basierte dabei auf Berichte über den Drogenmissbrauch im Menschen, welche zeigen dass EtOH, aufgrund seiner sozialen Bedeutung und leichten Verfügbarkeit, häufig zusammen mit anderen Drogen eingenommen wird, insbesondere zusammen mit MDMA. Für Zeiten kurz nach der Anwendung wurde berichtet, dass EtOH neben seinen Effekten auf die Lokomotion, auch die durch MDMA induzierte Hyperthermie milderte, jedoch nur am 1. Tag. Wie in meiner Doktorarbeit gezeigt, verminderte MDMA aufgrund seiner serotonergen Toxizität noch lange Zeit nach der Anwendung den 5-HT Gehalt (und denjenigen seines Metaboliten 5-HIAA) in verschiedenen Hirnregionen, jedoch ohne jegliche Interaktion mit EtOH. Neben Veränderungen im sog. “beam-walking test”, was auf eine verminderte Koordination der Motorik hinweist, zeigten wir auch in hippocampalen (aber nicht in corticalen) Schnitten von Ratten, dass die durch CP-93,129 (selektiver 5-HT_{1B} Agonist) induzierte Hemmung, oder die durch Methiotepin (5-HT_1 Antagonist) induzierte Steigerung der 5-HT Freisetzung stärker, bzw. schwächer, in Ratten mit einer *kombinierten* EtOH plus MDMA Vorbehandlung ausgeprägt war, als in den anderen Gruppen. Wir fanden also, dass die Kombination der beiden Drogen sogar noch 3 Wochen nach der letzten Behandlung spezifische Konsequenzen auf die präsynaptische Modulation der 5-HT-Freisetzung über den 5-HT_{1B} Autorezeptor hat und dass diese Folgen nicht auftreten, wenn die beiden Substanzen allein gegeben werden (Cassel *et al* 2005).

(3) Selbst wenn die Substrate der durch EtOH induzierten Potenzierung der Effekte von MDMA auf die motorische Aktivität noch unbekannt sind, scheint es vernünftig anzunehmen, dass eine Wirkung auf das nigrostriatale dopaminerge System an dieser Potenzierung beteiligt sein könnte. In diesem System, könnte EtOH, zusätzlich zu MDMA, Aktivitätslevel von dopaminergen und/oder serotonergen Terminalen beeinflussen. Die Mechanismen solch einer Interaktion könnten, in nicht exklusiver Weise, sowohl pharmakokinetische als auch pharmakodynamische Komponenten beinhalten (Oesterheld *et al* 2004). Daher wurde im *dritten Teil* meiner Arbeit die Hypothese eventueller pharmakodynamischer Interaktionen von EtOH mit MDMA auf einer mehr zellulären Ebene untersucht. Für dieses Ziel wurde die spontane und die elektrisch-evozierte Freisetzung von 5-HAT und Dopamin (DA) in striatalen Schnitten gemessen, die mit Saline, EtOH, MDMA oder der Kombination beider Substanzen superfundiert wurden. Diese Experimente brachten mehrere neue Informationen zu

den komplexen Mechanismen zutage, die hinter den Wirkungen von MDMA und/oder EtOH auf die Modulation der striatalen Transmission in der Ratte stehen. Darüber hinaus berichtet diese Untersuchung zum ersten Mal über eine lokale synergistische Interaktion dieser beiden Substanzen auf die spontane Freisetzung von DA und 5-HT. So wurde die spontane Freisetzung von sowohl DA als auch 5-HT signifikant stärker gesteigert, wenn MDMA und EtOH gemeinsam zugesetzt wurden. Auch wenn diese Befunde keinen exklusiven Mechanismus für die synergistischen Effekte einer EtOH/MDMA Co-Intoxikation aufzeigen, demonstrieren sie eindeutig, dass ein oder mehrere lokale Mechanismus(en) beteiligt sein können. Trotzdem können wir weder eine zusätzliche *in vivo* Wirkung über komplexere polysynaptische Neuronenschleifen, die auch extrastriatale Neurone betreffen könnten, noch die Möglichkeit einer zusätzlichen Beteiligung pharmakokinetischer Faktoren ausschließen.

(4) Schließlich fokussiert sich der letzte und *vierte Teil* meiner Doktorarbeit auf die Mechanismen, die der Potenzierung der MDMA-induzierten Hyperlokomotion durch EtOH zugrunde liegen. Für dieses Ziel benutzten wir die virus-vermittelte Gentransfer Technik, die im ersten Teil der Arbeit beschrieben ist, um die Expression des 5-HT_{1B} Autorezeptors in serotonergen Neuronen zu steigern. Die 5-HT-enthaltenden Fasern, die im dorsalen Raphé-Kern (DRN) entspringen projizieren zu dopaminergen Zellkörpern in der ventralen tegmentalen Area (VTA), zur Substantia nigra sowie zu deren terminalen Feldern im präfrontalen Cortex, Nucleus accumbens und Striatum. Nach der Literatur, scheint der psychostimulierende Effekt von MDMA auf Interaktionen zwischen serotonergen und dopaminergen Systemen zu beruhen (Bankson and Cunningham, 2001). In diesem Zusammenhang wurde gezeigt, dass 5-HT die DA Freisetzung in der VTA moduliert und zwar wahrscheinlich über 5-HT_{1B} Heterorezeptoren auf GABAergen Terminalen. Das hier geschilderte Experiment sollte daher weiter die Möglichkeit testen, dass 5-HT_{1B} Autorezeptoren ebenfalls eine modulatorische Bedeutung bei den psychostimulierenden Effekten von MDMA haben. Natürlich, wie auch in den vorigen Teilen dieser Arbeit, wurde auch der Effekt der Kombination von EtOH mit MDMA untersucht. Für dieses Ziel wurden Ratten, drei Tage nach der stereotaktischen Injektion der viralen Vektoren (GFP und HA1B/GFP) in den DRN, intraperitoneal mit Saline, EtOH, MDMA oder der Kombination von beiden Stoffen (EtOH + MDMA) injiziert, bevor ihre lokomotorische Aktivität (im „Heimat-Käfig“) für 5 Stunden gemessen wurde. Zunächst zeigte eine Untersuchung der Gehirne dieser Ratten, als Hinweis auf die Anwesenheit des Virus, das Vorkommen GFP-positiver Zellen in der DRN Region. Wenn nicht, wurden die betr. Ratten von der

weiteren statistischen Analyse ausgeschlossen. Während der ersten Stunde der Aufzeichnung der lokomotorischen Aktivität beobachteten wir (während EtOH unwirksam war), dass MDMA die Aktivität von Ratten steigerte, die mit dem GFP oder dem HA1B/GFP Vektor injiziert waren. Wie schon beschrieben, wurde die durch MDMA induzierte Hyperaktivität potenziert, wenn EtOH mit MDMA kombiniert wurde und zwar sowohl in der GFP als auch der HA1B/GFP Gruppe. Dennoch beobachteten wir in der HA1B/GFP Gruppe eine Abnahme des hyperlokomotorischen Effekts nach EtOH + MDMA im Vergleich zur GFP Gruppe, die die gleiche Behandlung erhalten hatte. Mit anderen Worten: der hyperlokomotorische Effekt von MDMA wurde durch die Co-Intoxication mit EtOH potenziert, aber in einem geringerem Ausmaß als in der GFP Gruppe. Diese Ergebnisse suggerieren, dass eine gesteigerte Expression des 5-HT_{1B} Autorezeptors den potenzierenden Effekt von EtOH in mit MDMA behandelten Ratten abschwächt.

Zusammengenommen zeigte die vorliegende Dissertation: **(1)** die funktionellen Konsequenzen eines virus-vermittelten Gentransfers des 5-HT_{1B} Heterorezeptors in cholinerge Neurone sowohl *in vitro* als auch *in vivo*, **(2)** dass die Funktion des 5-HT_{1B} Autorezeptors noch mehrere Wochen nach einer kombinierten Vorbehandlung mit MDMA *und* EtOH verändert sein kann, **(3)** dass die gleiche Kombination von Missbrauchs-Drogen zu schwerwiegenden pharmakodynamischen Interaktionen *in vitro* führt, nämlich bei der Freisetzung striataler Neurotransmitter, und schließlich, **(4)**, dass eine gesteigerte Expression des 5-HT_{1B} Autorezeptors in der DRN die hyperlokomotorischen Effekte von MDMA und seiner Kombination mit EtOH signifikant reduziert.